P-261

NASA Contractor Report 180850

304596

Energy Efficient Engine

High-Pressure Compressor Test Hardware
Detailed Design Report

D.C. Howe and R.D. Marchant
UNITED TECHNOLOGIES CORPORATION
Pratt & Whitney

March 1988

NASA

National Aeronautics and
Space Administration

NASA
National Aeronautics and Space Administration

Report Documentation Page

1. Report No. NASA CR-180850	2. Government Accession No.	3. Recipient's Catalog No.
4. Title and Subtitle Energy Efficient Engine High-Pressure Compressor Test Hardware Detailed Design Report		5. Report Date March 1988
		6. Performing Organization Code
7. Author(s) D. C. Howe and R. D. Marchant		8. Performing Organization Report No. PWA-5594-287
		10. Work Unit No.
9. Performing Organization Name and Address UNITED TECHNOLOGIES CORPORATION Pratt & Whitney East Hartford, Connecticut 06108		11. Contract or Grant No. NAS3-20646
		13. Type of Report and Period Covered Technology Report
12. Sponsoring Agency Name and Address NATIONAL AERONAUTICS AND SPACE ADMINISTRATION Lewis Research Center 21000 Brookpark Road; Cleveland, Ohio 44135		
		14. Sponsoring Agency Code

15. Supplementary Notes

Project Manager, Mr. Werner R. Britsch
NASA-Lewis Research Center; Cleveland, Ohio 44135

16. Abstract

The objective of the National Aeronautics and Space Administration Energy Efficient Engine program is to identify and verify the technology required to achieve significant reductions in fuel consumption and operating cost for future commercial gas turbine engines. This report documents the design and analysis of the high-pressure compressor which was to be tested as part of the Pratt & Whitney effort under the Energy Efficient Engine program. This compressor was designed to produce a 14:1 pressure ratio in ten stages with an adiabatic efficiency of 88.2 percent in the flight propulsion system. The corresponding expected efficiency for the compressor component test rig is 86.5 percent. Other performance goals are a surge margin of 20 percent, a corrected flow rate of 35.2 kg/sec (77.5 lb/sec), and a life of 20,000 missions and 30,000 hours. Low loss, highly loaded airfoils are used to increase efficiency while reducing the parts count. Active clearance control and case trenches in abradable strips over the blade tips are included in the compressor component design to further increase the efficiency potential. The test rig incorporates variable geometry stator vanes in all stages to permit maximum flexibility in developing stage-to-stage matching. This provision precluded active clearance control on the rear case of the test rig. Both the component and rig designs meet or exceed design requirements with the exception of life goals, which will be achievable with planned advances in materials technology.

17. Key Words (Suggested by Author(s)) Energy Efficient Engine Variable Geometry Stator Vanes Active Clearance Control Drum Rotor Construction	18. Distribution Statement	
19. Security Classif. (of this report) UNCLASSIFIED	20. Security Classif. (of this page) UNCLASSIFIED	21. No. of pages 233	22. Price

NASA FORM 1626 OCT 86

FOREWORD

The Energy Efficient Engine Component Development and Integration Program is currently being conducted under parallel National Aeronautics and Space Administration contracts to Pratt & Whitney and General Electric Company. The overall project is under the direction of Mr. Carl C. Ciepluch. The Pratt & Whitney effort is under NASA Contract NAS3-20646, and Mr. W. R. Britsch is the NASA Project Engineer responsible for the portion of the project described in this report. Mr. D. E. Gray is manager of the Energy Efficient Engine Project at Pratt & Whitney. This report was prepared by Mr. D. C. Howe and Mr. R. D. Marchant of Pratt & Whitney.

TABLE OF CONTENTS

PAGE IV INTENTIONALLY BLANK

LIST OF ILLUSTRATIONS

LIST OF ILLUSTRATIONS (continued)

LIST OF ILLUSTRATIONS (continued)

LIST OF TABLES

LIST OF TABLES (continued)

SECTION 1.0

SUMMARY

This report documents the design of the high-pressure compressor which was tested as part of the Pratt & Whitney Energy Efficient Engine Program under NASA Contract NAS3-20646.

The Energy Efficient Engine high-pressure compressor is designed to produce a 14:1 pressure ratio in ten stages with an adiabatic efficiency of 88.2 percent in a fully-developed flight propulsion system. The corresponding expected efficiency for the component test rig is 86.5 percent. Low loss, highly loaded airfoils are used to raise the efficiency while reducing the parts count. Both clearance control and blade tip trenches are incorporated into the case design to further increase the efficiency potential. The latter incorporate rub strips over the tips.

In addition to the aerodynamic and mechanical design of the compressor component, features also documented in this report include the compressor intermediate case and the compressor to be tested in the component rig. The intermediate case design was included in the compressor design effort because of the strong interdependence between these two subassemblies.

The compressor component rig incorporates variable-stagger stator vanes in all stages to allow maximum flexibility in developing optimal stage-to-stage matching. This has precluded the use of active clearance control on the rear case of the rig assembly. The core section of the compressor intermediate case and the engine diffuser-combustor are simulated in the rig to provide accurate aerodynamic interface during testing. Provisions are included for extensive rotating and stationary instrumentation in the rig assembly.

With the exceptions noted above, the designs of the compressor component and component rig assemblies are identical. The design base for both is the flight propulsion system. Flight propulsion system aerodynamic design is directly duplicated. Material substitutions have been made on the basis of cost and/or availability where function was not impaired. Compressor component and component rig efforts are timed so that the component design gains the maximum benefits derived from rig test results.

Both the compressor component and component rig designs meet or exceed design requirements, with the exception of life, which is limited by the present state of materials development. However, life is adequate to meet the requirements of the component rig test program. Flight propulsion system life goals will be achievable with planned advances in materials technology.

SECTION 2.0

INTRODUCTION

The objective of the Energy Efficient Engine program is to develop, evaluate, and demonstrate the technology for achieving lower installed fuel consumption and lower operating costs in future commercial turbofan engines. NASA has set minimum goals of a 12 percent reduction in thrust specific fuel consumption, a 5 percent reduction in direct operating cost, and a 50 percent reduction in performance degradation for the Energy Efficient Engine (flight propulsion system) relative to the JT9D-7A reference engine. In addition, environmental goals on emissions (meet the proposed EPA 1981 regulation) and noise (meet FAR 36-1978 standards) have been established.

The Pratt & Whitney program effort is based on an engine concept defined under the NASA-sponsored Energy Efficient Engine Preliminary Design and Integration Studies Program, Contract NAS3-20628. This program was completed under an earlier low-energy-consumption-engine contract effort, and is discussed in detail in NASA Report CR-135396. The Pratt & Whitney engine is a twin-spool, direct drive, mixed-flow exhaust configuration, utilizing an integrated engine-nacelle structure. A short, stiff, high rotor and a single-stage high-pressure turbine are among the major features in providing for both performance retention and major reductions in maintenance and direct operating costs. Improved active clearance control in the high-pressure compressor and turbines, advanced single crystal materials in turbine blades and vanes, and shroudless fan blades are among the major features providing performance improvement.

To meet the program objectives, two technical tasks were established by the Pratt & Whitney Project Team:

Task 1   Propulsion System Analysis, Design, and Integration.

Task 2   Component Analysis, Design, and Development.

The work described in this report was conducted as part of the high-pressure compressor effort in Task 2. An overview of the high-pressure compressor design is presented in Part I. A detailed discussion of the component and rig analysis and design work performed and reported herein is provided in Part II. Part III presents the component and test rig design update, based on initial testing of the rig.

The high-pressure compressor program effort was scheduled (Figure 1) to provide timely interaction between component and rig activities culminating in: 1) the generation of test data for input to the final component design update, and 2) substantiation of performance goals for the Task 1 flight propulsion system high-pressure compressor component.
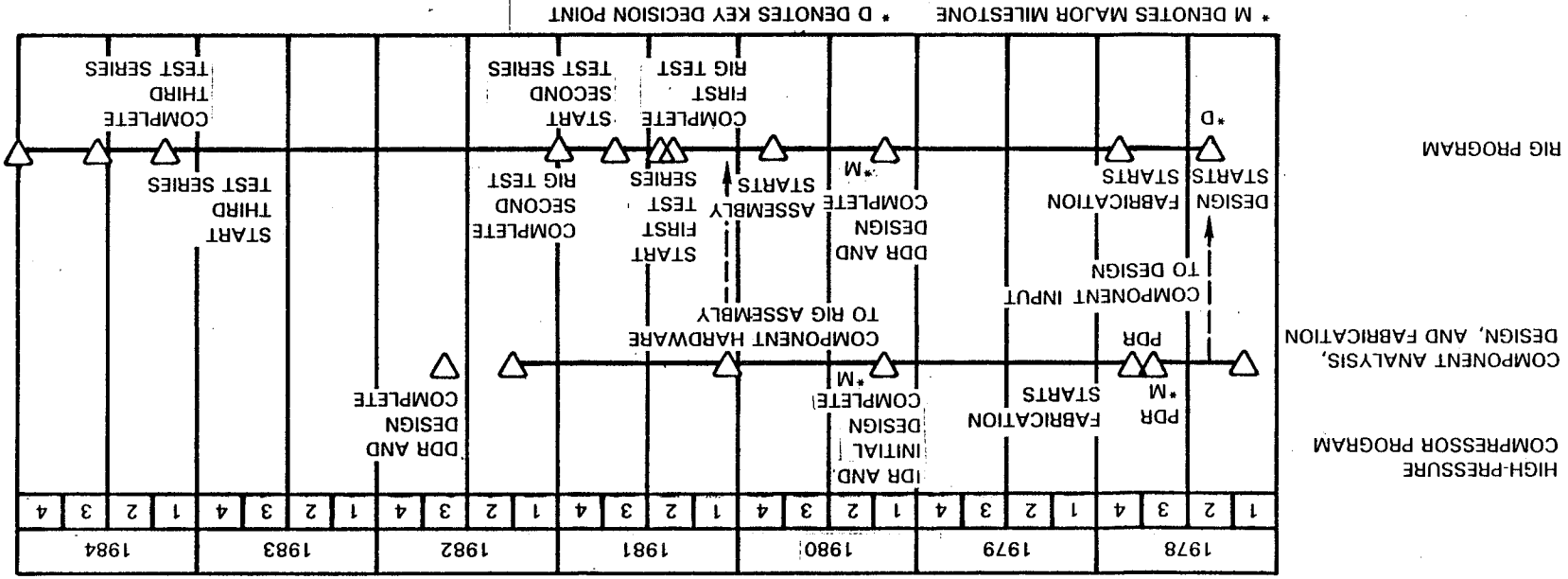
Figure 1   High-Pressure Compressor Program/Project Schedule

* M DENOTES MAJOR MILESTONE   * D DENOTES KEY DECISION POINT

	1978				1979				1980				1981				1982				1983				1984			
	1	2	3	4	1	2	3	4	1	2	3	4	1	2	3	4	1	2	3	4	1	2	3	4	1	2	3	4

HIGH-PRESSURE COMPRESSOR PROGRAM

COMPONENT ANALYSIS, DESIGN, AND FABRICATION

RIG PROGRAM

DESIGN STARTS

FABRICATION STARTS

COMPONENT INPUT TO DESIGN

*D

PDR STARTS

*M PDR

FABRICATION STARTS

IDR AND INITIAL DESIGN COMPLETE

*M

DDR AND DESIGN COMPLETE

*M

COMPONENT HARDWARE TO RIG ASSEMBLY

ASSEMBLY STARTS

START FIRST TEST

COMPLETE FIRST RIG TEST

START RIG TEST SECOND SERIES

COMPLETE SECOND RIG TEST SERIES

START SECOND TEST SERIES

DDR AND DESIGN COMPLETE

START THIRD TEST SERIES

COMPLETE THIRD TEST SERIES

PART I

HIGH-PRESSURE COMPRESSOR

COMPONENT AND TEST RIG DESIGN OVERVIEW

4

SECTION 1.0

INTRODUCTION

The objective of the High-Pressure Compressor Program is to design, fabricate, and test an advanced, ten-stage compression system that meets the following performance and design goals. Key performance goals include an adiabatic efficiency of 88.2 percent for the fully-developed flight propulsion system compressor and an efficiency of 86.5 percent for the compressor component rig test. Other performance goals are a pressure ratio of 14:1, a surge margin of 20 percent, and a corrected flow rate of 35.2 kg/sec (77.5 lb/sec). Component design goals for life are 20,000 missions and 30,000 hours.

The approach used to meet the program objective involved dividing the high-pressure compressor design effort into two major subtasks, including a component design subtask and a test rig design subtask.

The purpose of the component design subtask is to provide the design definition necessary for fabricating hardware to be used in the component rig test program. It included a design update of the component airfoils based on test results from the first two builds of the high-pressure compressor test rig. These updated airfoil designs were fabricated and tested in the third build of the component test rig.

The purpose of the test rig design subtask is to provide the design definition necessary for the fabrication of parts peculiar to the test rig. Parts such as inlet ducts, "dummy" diffuser case, rear compressor case with adjustable vanes, front and rear hubs, bearings, and instrumentation were designed under this subtask. Because of the mechanical complexity resulting from the adjustable vanes in all but the fifteenth-stage stator row, an active clearance control system was not incorporated into the rig design.

SECTION 2.0

HIGH-PRESSURE COMPRESSOR DESIGN DESCRIPTION

2.1 COMPRESSOR ASSEMBLY

The Energy Efficient Engine high-pressure compressor, shown in Figure 2, utilizes ten stages to produce the required 14:1 pressure ratio. This compressor features a drum rotor construction and significantly fewer airfoils than the JT9D-7A reference engine's high-pressure compressor. These concepts combine to make the compressor assembly lighter, less costly, and more easily maintained. The rear (or bleed) case is a single piece to accommodate active clearance control in the rear stages. Use of active clearance control increases compressor efficiency by minimizing blade tip clearance requirements.
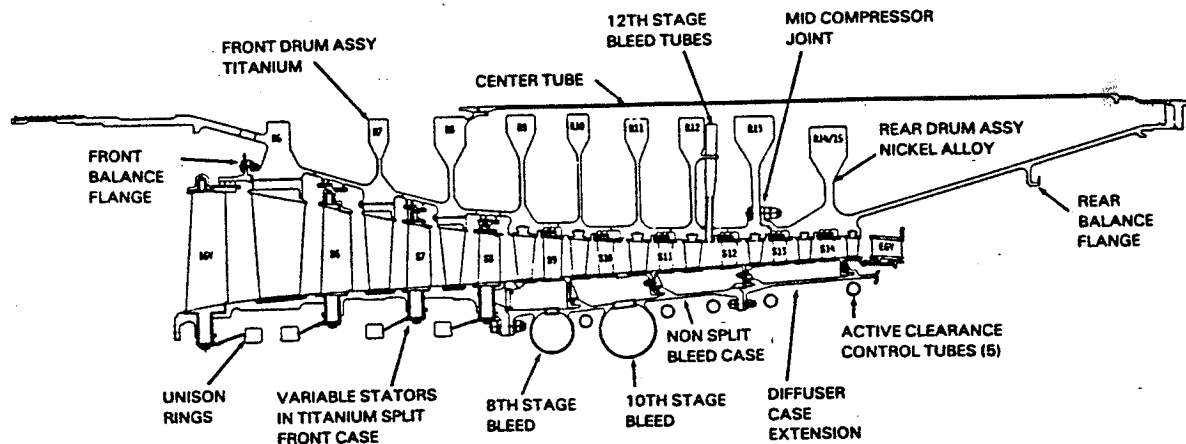
Figure 2   Energy Efficient Engine High-Pressure Compressor Assembly

The drum rotor construction features an electron beam-welded titanium front end bolted to a tandem disk of MERL 76 (PWA 1099) powdered nickel alloy. Axial blade attachments are used in the first three stages, and tangential attachments are used in the fourth through tenth stages. The compressor employs integral knife edge seals and low volume inner cavities to reduce recirculation losses. In addition, case trenches are employed above the rotors to reduce the performance sensitivity to tip clearance leakage. The variable geometry stators in the first four stages represent current state-of-the-art design, and the front case is a split configuration to accommodate the variable geometry stators.

The single-piece rear case does not have the axial split usually associated with a drum rotor design and therefore results in a lighter, less costly case. As a single-piece structure, the case is less susceptible to ovalization and more capable of providing improved control of blade tip clearances. The single-piece structure also accommodates the active clearance control system.

The rear stator and shroud configuration incorporates vane rows brazed into 90-degree shroud subassemblies. These subassemblies are attached to the case at locations selected to provide optimum blade tip clearance. This

6

construction also minimizes steps in the flowpath and allows the most effective use of active clearance control. The exit stator flowpath is canted outward 5 degrees to reduce the combustor/diffuser turning and risk of flow separation on the outer diameter wall.

The active clearance control system is an external design. This design eliminates a double wall construction, has fewer leaks, can be tailored to varied stage-to-stage active clearance control movement, and its characteristics are analytically more predictable than those of an internal design system.

Table I summarizes the compressor design parameters at the aerodynamic design point, following completion of detailed design activities. Table II compares the more significant parameters at several operating conditions. The adiabatic efficiency of 88.3 percent exceeds the 88.2 percent goal level established for the high-pressure compressor at the completion of the initial design. Detailed design results showed the capability to achieve a 0.030 cm (0.012 in) average rotor tip clearance for the flight propulsion system high-pressure compressor compared to the goal clearance of 0.033 cm (0.013 in). This 0.003 cm (0.001 in) tip clearance improvement was estimated to increase efficiency by an additional 0.1 percent.

TABLE I

HIGH-PRESSURE COMPRESSOR DESIGN SUMMARY AT AERODYNAMIC DESIGN POINT

Parameter	Design Value
Number of Stages	10
Pressure Ratio	14
Adiabatic Efficiency, %	88.3
Surge Margin, %	20
Corrected Flow, kg/sec (lb/sec)	35.2 (77.5)
Corrected Speed, rpm	12135
Inlet Corrected Tip Speed, m/sec (ft/sec)	379 (1245)
Inlet Specific Flow, kg/sec-m^2 (lb/sec-ft^2)	185 (38)
Inlet Hub/Tip Ratio	0.56
Exit Hub/Tip Ratio	0.924
Exit Mach Number (without blockage)	0.28
Average Aspect Ratio	1.52
Average Gap/Chord Ratio	0.89
Axial Velocity/Wheel Speed Ratio	0.56
Number of Variable Stator Rows	4
Number of Airfoils (without inlet guide vanes)	1266
Number of Inlet Guide Vanes	32
Flowpath Type	CMD*

*CMD - Constant Mean Diameter

7

TABLE II

EFFECT OF OPERATING CONDITIONS ON DESIGN PARAMETERS

Parameter	Operating Condition			
	Aero. Des. Point	Maximum Cruise	Maximum Climb	Takeoff
Pressure Ratio	14.0	13.8	14.2	13.0
Efficiency, %:				
(Adiabatic)	88.3	88.4	88.1	89.4
(Polytropic)	91.7	91.8	91.5	92.4
Inlet Corrected Airflow, kg/sec	35.2	34.9	35.5	33.6
(lb/sec)	(77.5)	(76.8)	(78.2)	(74.0)
Inlet Specific Airflow, kg/sec-m^2	185.5	184.0	187.5	177.2
(lb/sec-ft^2)	(38.0)	(37.7)	(38.4)	(36.3)
Inlet Corrected Tip Speed, m/sec	379	378	380	373
(ft/sec)	(1245)	(1242)	(1248)	(1225)
Actual Rotor Speed, rpm	13,177	13,092	13,586	13,968
Corrected Rotor Speed, rpm	12,135	12,110	12,130	11,975
Exit Temperature, °C	481	472	524	570
(°F)	(898)	(882)	(975)	(1058)

2.2 COMPRESSOR INTERMEDIATE CASE

The design of the intermediate case was included in the high-pressure compressor design effort because of its potentially strong interaction with compressor performance. It performs many functions in support of other engine parts and components, and has a very important effect on overall engine cost, weight, and performance.

The compressor intermediate case supports the fan and high-pressure compressor rotors, forms the low- to high-pressure compressor flowpath, and provides the front mount locations. In addition, it contains the provisions and plumbing for the towershaft and accessory drive components. The intermediate case, integrated between the low- and high-pressure compressors, is shown in Figure 3. The case assembly consists of three concentric annular cases with an array of both structural and nonstructural fan exit guide vanes.

NOTE: DIMENSIONS ARE IN INCHES
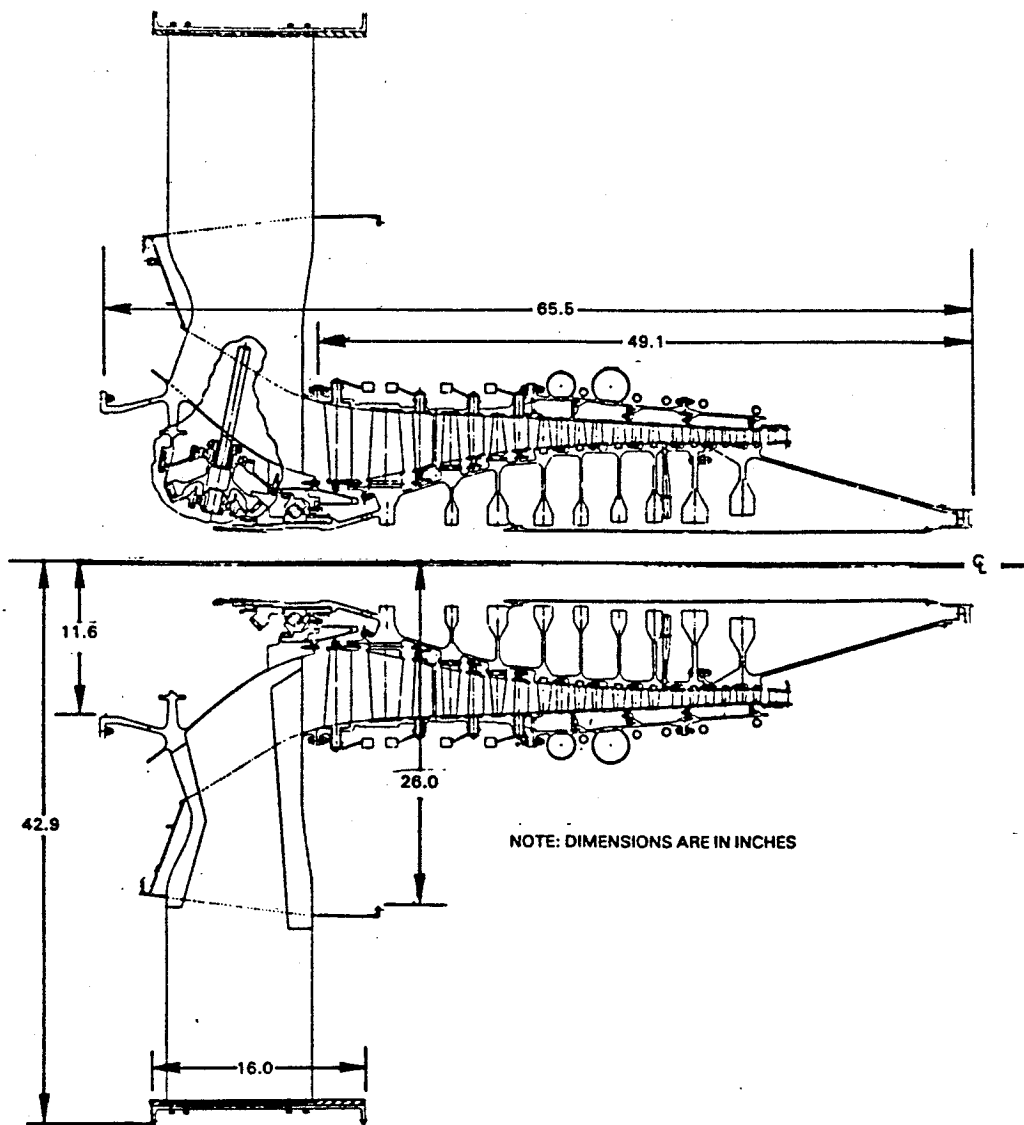
Figure 3   Intermediate Case Integrated with Compressor

9

SECTION 3.0

PREDICTED PERFORMANCE

3.1 SURGE MARGIN PREDICTION

The surge margin requirements for the high-pressure compressor are 20 percent at the aerodynamic design point and 15 percent at takeoff. A surge margin limit correlation, based on previous Pratt & Whitney compressor experience, is shown in Figure 4. As shown, surge margin requirements are satisfied at both conditions.

AERODYNAMIC
DESIGN POINT
20% SURGE MARGIN

SEA LEVEL TAKEOFF
15% SURGE MARGIN

AERODYNAMIC
DESIGN POINT LIMIT

SEA LEVEL TAKEOFF LIMIT

LOADING PARAMETER

SURGE CORRELATION PARAMETER
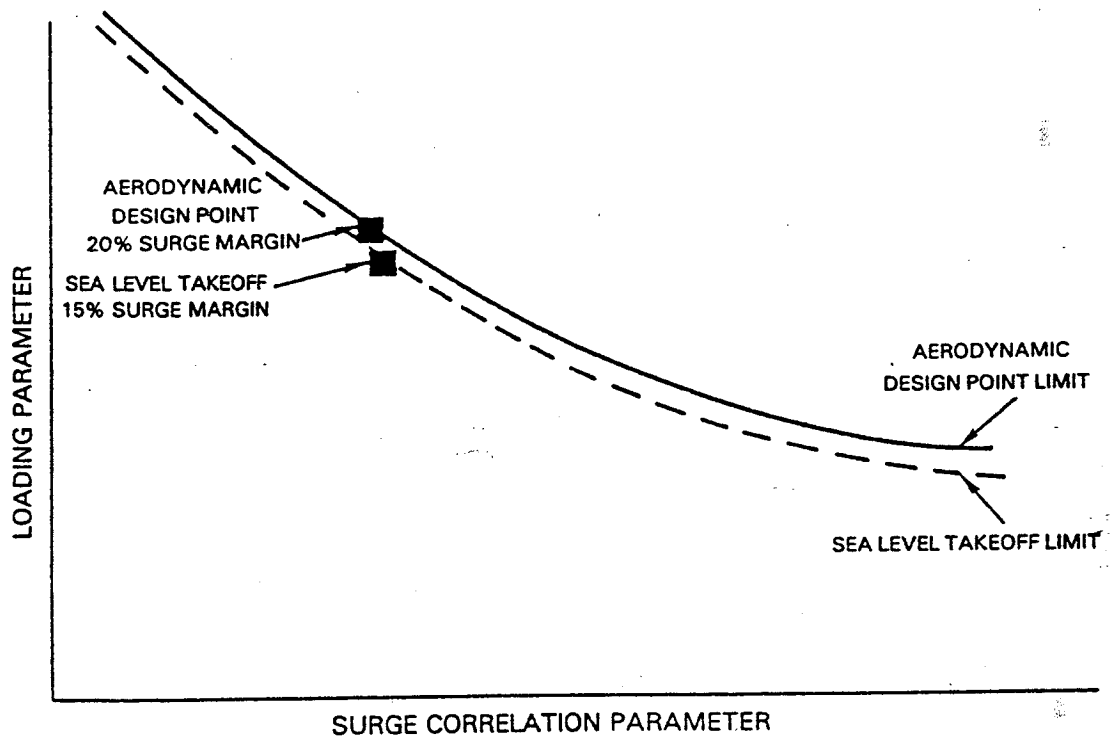
Figure 4   High-Pressure Compressor Surge Correlation Used in Estimating Surge Margin

3.2 EFFICIENCY PREDICTION

The design system efficiency prediction, along with the benefits from technology features summarized in Table III, indicate that the flight propulsion system goal of 88.2 percent compressor efficiency is achievable.

TABLE III

DESIGN SYSTEM PREDICTION AND TECHNOLOGY FEATURE BENEFITS

Design System Prediction   87.1%

The design system prediction includes the effects of:

    o   Average rotor tip clearance of 0.030 cm (0.012 in)

    o   Multiple circular arc airfoils

    o   Intermediate case pressure loss

    o   Small inner shroud cavities

    o   20 AA airfoil surface roughness

Additional Technology Features and Estimated Benefits:

    o   Trench rub strip benefit   +0.8%

    o   Controlled diffusion airfoil benefit   +0.4%

Estimated High-Pressure Compressor Efficiency   88.3%

3.3 OPERATING MAP PREDICTION

At the completion of the detailed design effort, the compressor operating characteristics were reviewed to determine the applicability of the map generated during the preliminary design and reported in Reference 1. The predicted operating map (Figure 5) remained unchanged from the earlier definition. The takeoff operating points, major altitude points, and operating line are shown.

OPERATING POINT	TAKEOFF	MAXIMUM CRUISE	MAXIMUM CLIMB	AERODYNAMIC DESIGN POINT
PRESSURE RATIO:	13.0	13.8	14.2	14.0
% INLET CORRECTED AIRFLOW	95.5	99.3	101.0	100.0
ADIABATIC EFFICIENCY:	0.894	0.884	0.881	0.883
SYMBOLS	◇	△	□	○
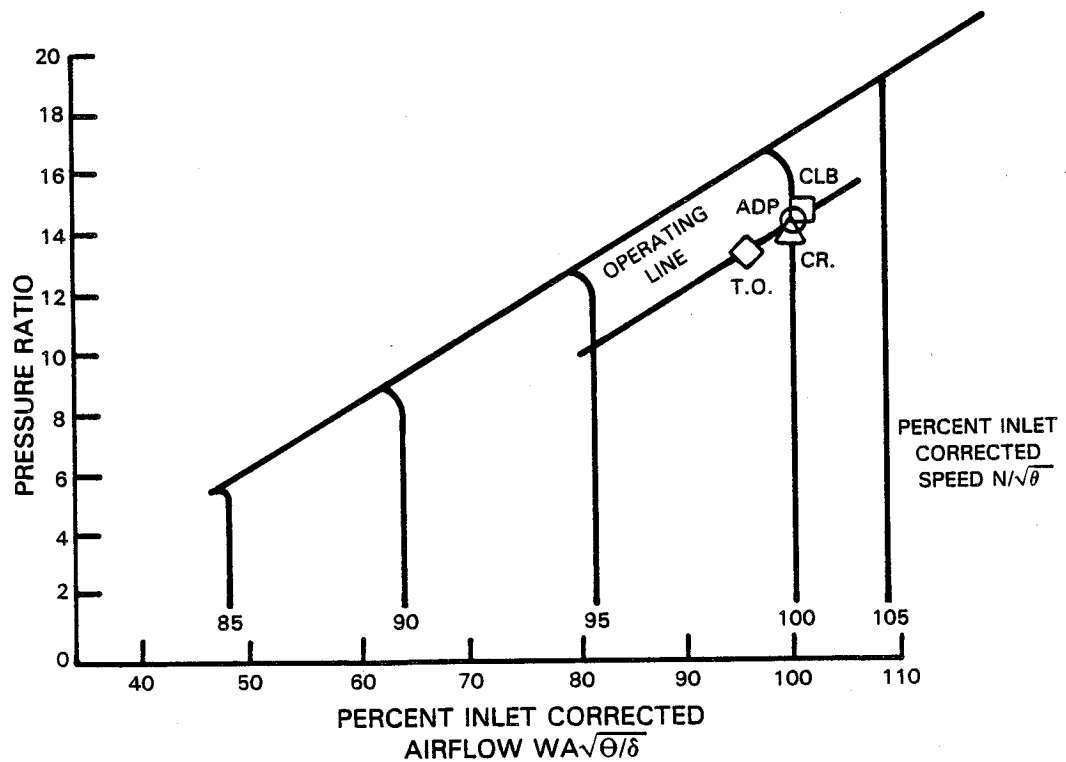
Figure 5   Predicted High-Pressure Compressor Operating Map. The data show the aerodynamic design, 10,668 m (35,000 ft) Mach 0.8 cruise/climb, and takeoff points.

PART II

HIGH-PRESSURE COMPRESSOR

COMPONENT BASE DESIGN

SECTION 1.0

INTRODUCTION

The compressor configuration for the Energy Efficient Engine was selected, as a result of an intensive study of the influence of the major compressor design features on the return on investment (ROI) for a subsonic commercial turbofan. Compressor efficiency was only one of the parameters considered. The engine weight, cost, maintainability, aircraft direct operating cost (DOC), and fuel burned for a typical flight mission were other items governing the final configuration choice.

The latest Pratt & Whitney engine compressor experience plus the results from research multistage compressor rigs and NASA-sponsored stages were used in the refinements of the final high-pressure compressor configuration. Advances in high-pressure turbine technology made it possible to drive the compressor of 14:1 pressure ratio with a single turbine stage and resulted in the optimum configuration. Other advanced technology items included in the design, to provide a high probability of meeting the efficiency and surge margin goals, are: 1) rotor tip trenching, 2) active clearance control (ACC), 3) improved drum rotor cavity design, 4) controlled diffusion airfoil (CDA) designs, and 5) hydraulically smooth airfoil surfaces.

SECTION 2.0

AERODYNAMIC DESIGN

2.1 OVERVIEW

To facilitate aerodynamic design and analysis, the compressor and intermediate case assembly was divided into three subelements: 1) intermediate case fan duct section, 2) intermediate case core section, and 3) high-pressure compressor module. The aerodynamic design of the intermediate case fan duct section was completed previously and is reported in Reference 2.

For the purpose of simulating engine performance, the high-pressure compressor component is defined as extending from the intermediate case leading edge to the trailing edge of the compressor exit guide vane. The design pressure ratio and efficiency, therefore, include the intermediate case core section losses. In addition, the corrected flow is defined at the inlet to the intermediate case core section.

The compressor aerodynamic design point is an altitude of 10,668 m (35,000 ft) and a flight Mach number of 0.8. The nominal aerodynamic design goals include:

o   14:1 pressure ratio in ten stages

o   Inlet corrected airflow of 35.2 kg/sec (77.5 lb/sec)

o   88.3 percent adiabatic efficiency

o   20 percent surge margin.

A summary of design parameters at the engine aerodynamic design point is given for the high-pressure compressor in Table IV. The values given are for the flight propulsion system (FPS), mature developed engine.

The number of stages was determined from performance and stability considerations. The inlet hub/tip ratio of 0.56 represents the smallest diameter that meets the mechanical constraints of the No. 3 bearing compartment. A specific flow of 185.5 kg/sec-m^2 (38.0 lb/sec-ft^2) into the first high-pressure compressor rotor gave the best trade-off between the compressor size and performance. This specific flow resulted in an axial Mach number of 0.52 prior to the addition of aerodynamic design blockage and swirl.

TABLE IV

HIGH-PRESSURE COMPRESSOR AERODYNAMIC DESIGN PARAMETERS
Aerodynamic Design Point; Altitude = 10,668 m (35,000 ft), Mach No. = 0.8

Parameter	Design Value
No. of Stages	10
Pressure Ratio	14:1
Surge Margin, %	20.0
Inlet Corrected Airflow, kg/sec (lb/sec)[1]	35.2 (77.5)
Inlet Corrected Tip Speed, m/sec (ft/sec)[1]	379.5 (1245)
Adiabatic Efficiency, %	88.3
Polytropic Efficiency, %	91.7
Flowpath Shape	Approx CMD *
Inlet Hub-to-Tip Radius Ratio[1]	0.56
Exit Hub-to-Tip Radius Ratio	0.924
Inlet Corrected Specific Airflow, kg/sec-m^2 (lb/sec-ft^2)	185.5 (38.0)
Exit Mach No. (Without Blockage)	0.28
Average Axial Velocity-to-Wheel Speed Ratio, C_x/U	0.559
Average Airfoil Aspect Ratio	1.52
Average Gap-to-Chord Ratio	0.89
Average Diffusion Factor	0.456
Average End-Wall Loading, P_s/P_0-P_s	0.413

(1) = Changed from preliminary design value.
* CMD = Constant Mean Diameter.

2.2 INTERMEDIATE CASE CORE SECTION AERODYNAMICS

The major consideration in the design of the intermediate case was static
pressure distribution on the walls. From the engine weight and length
considerations, a minimum-length nonseparated transition section between the
low- and high-pressure compressors was desired. Counterrotation of the low-
and high-pressure spools favored an axial flow through the intermediate case
with no turning required of the struts. The ten struts are axially oriented
airfoils of zero camber with a combination of thickness distributions: 1) 65
series airfoil thickness distribution about the meanline between the leading
edge and the tower shaft centerline, and 2) 400 series airfoil thickness
distribution from the tower shaft centerline to the trailing edge (Figure 6).
This combination airfoil provided a reduced blockage in the leading portion
and improved structural stiffness in the aft portion of the strut. Physical
and aerodynamic blockage was modeled after results from prior cold-flow rig
testing. Figure 7 shows the resultant inner diameter and outer diameter total
blockage distribution used in designing the intermediate case through the
strut section. The assumed spanwise loss distribution shown in Figure 8 was

derived from comparing both Pratt & Whitney and NASA results from similar configurations. The intermediate case wall contours were tailored to control the wall static pressure distribution so as to avoid excessive pressure gradients and the risk of wall boundary layer separation. Pressure and temperature spanwise profiles exiting the low-pressure compressor and assumed in the design of the intermediate case were based on Pratt & Whitney engine development experience and are shown in Figure 9. Figure 10 shows the design static pressure distribution on the inner and outer walls. The pressure rise on the inner wall is well within experience for separation-free flows.
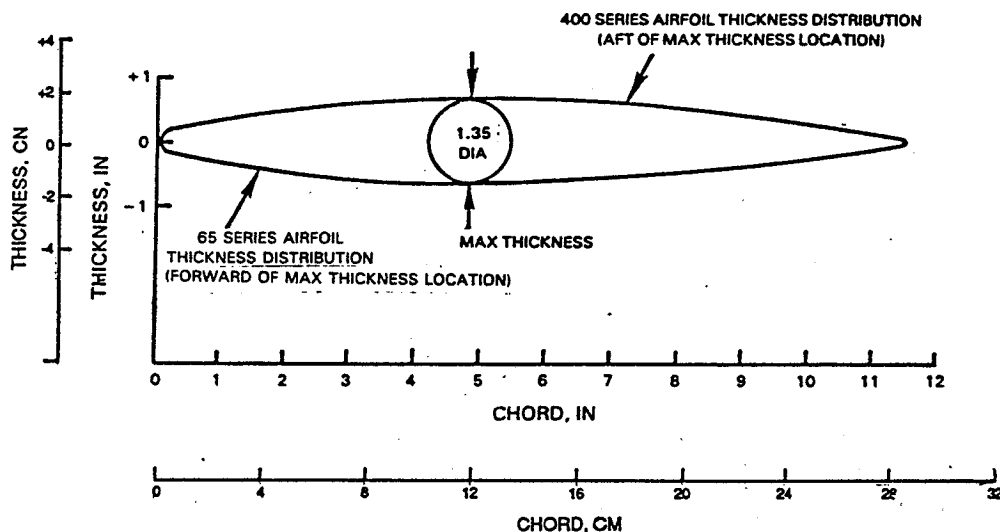
Figure 6   Thickness Distribution of Intermediate Case Strut
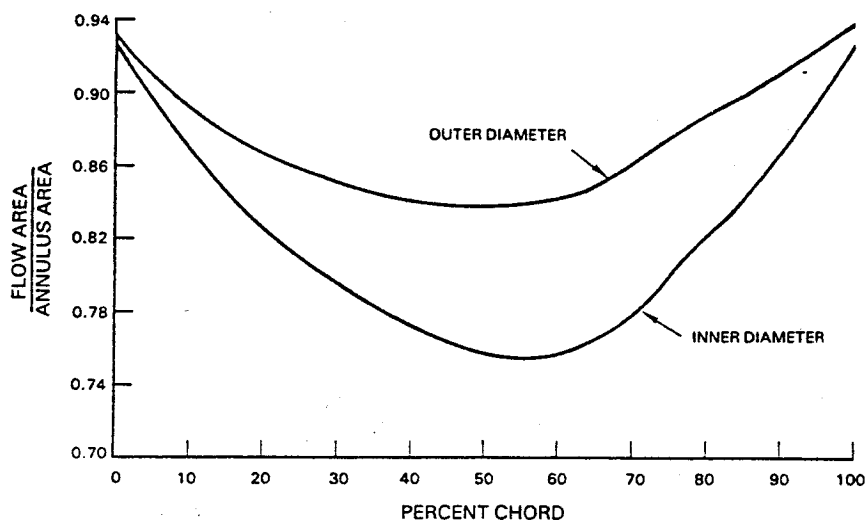
Figure 7   Intermediate Case Flowpath Blockage Distribution
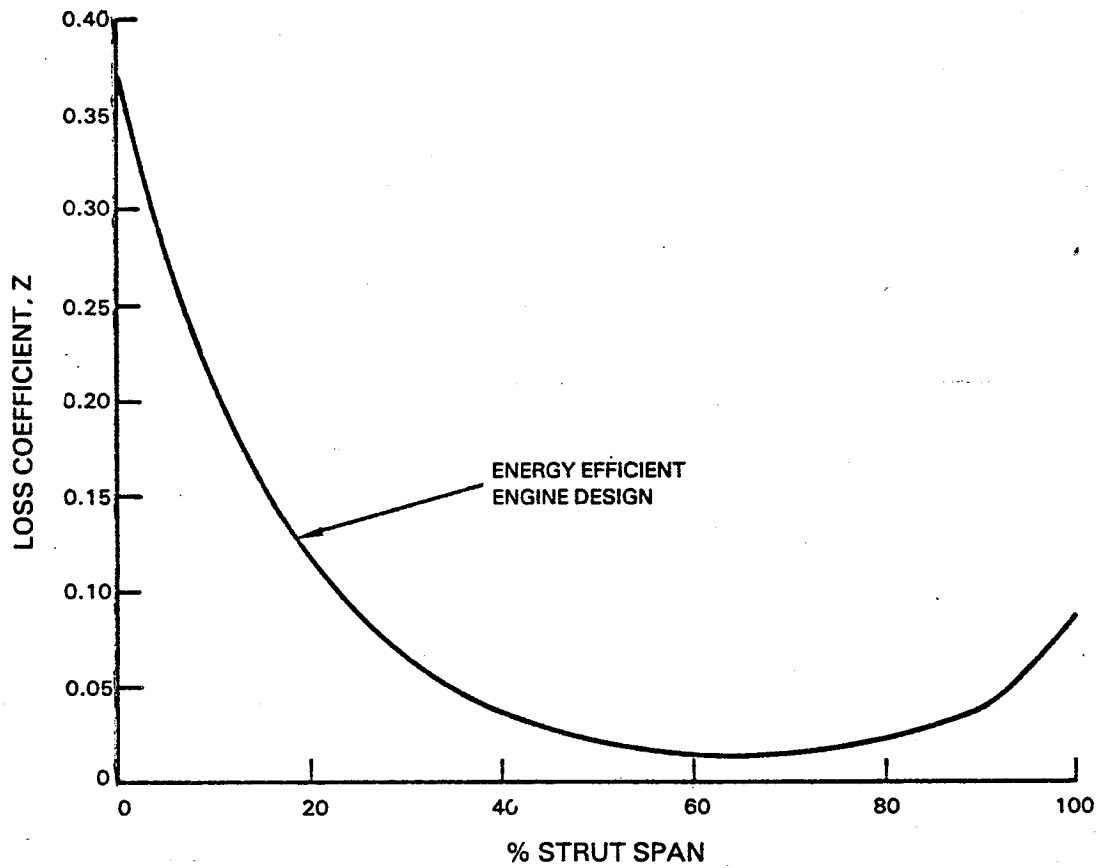
Figure 8   Spanwise Loss Distribution
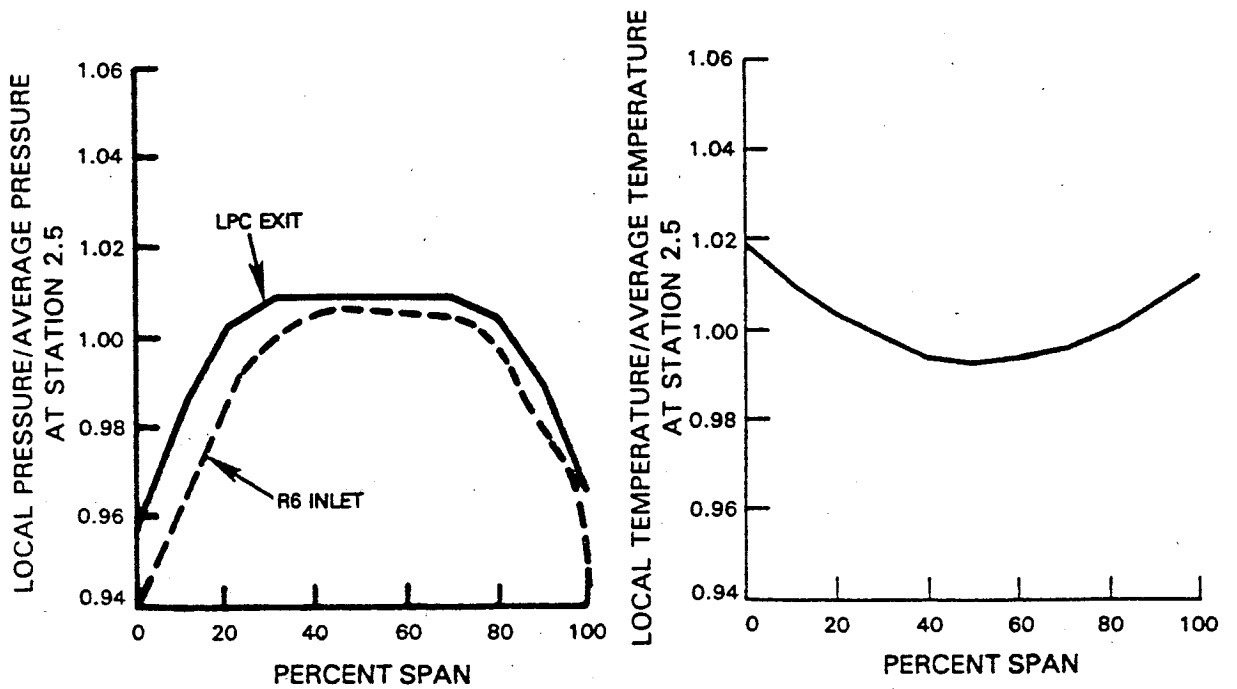
Figure 9   Assumed Low-Pressure Compressor Exit Pressure and Temperature
Profiles. High-pressure compressor inlet total pressure profile is
consistent with commercial experience.
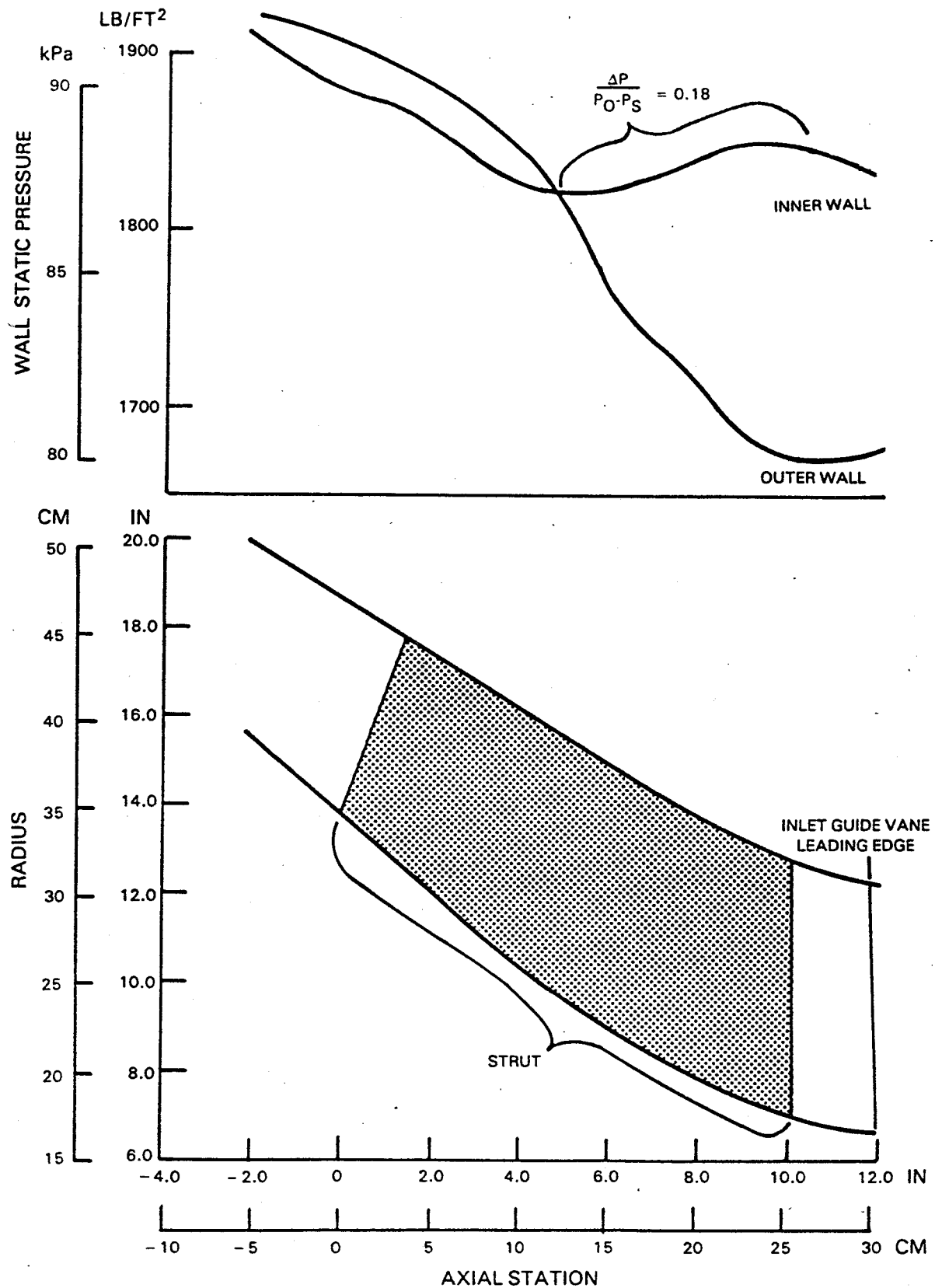
Figure 10 Compressor Intermediate Case Core Section Flowpath and Wall Static Pressure Distribution. Case design assures separation-free flow.

2.3 HIGH-PRESSURE COMPRESSOR MODULE AERODYNAMIC DESIGN

For the purpose of aerodynamic definition described in the following sections, the compressor module encompasses the flowpath from the inlet guide vane leading edge to the exit guide vane trailing edge.

2.3.1 Flowpath Definition

Desirable compressor design features were identified in the Advanced Multistage Axial Compressor (AMAC) studies which preceded the Energy Efficient Engine design. These features were not always consistent with the low-pressure compressor or combustor requirements and had to be modified to result in the optimum engine configuration. The final flowpath is shown in Figure 11. Low inlet hub/tip ratio was beneficial to performance through reduction in the first rotor tip Mach number. The performance benefit outweighed an increased diffusion across the intermediate case as well as an increase in length due to the larger first rotor chord required to eliminate 2E resonance from the operating range.

The exit stage flowpath is canted approximately 5 degrees outward from the centerline to improve the aerodynamic matching with the combustor-diffuser inlet section. The required elevation change across the diffuser and burner resulted in a strong static pressure (and velocity) gradient with a noncanted exit row. By turning the exit row flowpath (Figure 11) to mate with the diffuser flowpath, the static pressure gradient at the last stator exit was reduced and resulted in improved diffuser performance.

2.3.2 Inlet Guide Vanes

The non-turning intermediate case struts resulted in the requirement that the inlet guide vanes add 13° to 23° preswirl root to tip to match the Mach number and loading requirements of the high-pressure compressor front stage blades. A comparison of the selected gap/chord ratio (τ/b) and Zweiffel coefficients for the inlet guide vane with Pratt & Whitney experience is shown in Figure 12. As shown, both the loading and airfoil spacing are kept within prior experience.

A 400 series airfoil was chosen for the inlet guide vane design both for its large incidence range and choke margin capabilities. The pressure recovery profile assumed for this airfoil design is shown in Figure 13.

2.3.3 Mach Number Distribution

The meridional flow Mach number into the first rotor is 0.58. Midspan meridional Mach number decreases through the compressor as shown in Figure 14, which includes the effects of swirl on flow density, aerodynamic design blockage, and flow extraction through bleeds. Bleed flows extracted for turbine active clearance control and cooling are 1.4 percent at the stator 10 exit, 1.5 percent at the rotor 12 exit, and 3.5 percent at the rotor 15 exit.

IGV		R6		S6	R7	S7	R8	S8	R9	S9	R10	S10	R11	S11	R12	S12	R13	S13	R14	S14	R15	EGV
32		26		44	50	50	60	52	66	60	62	64	56	72	64	64	70	72	76	80	78	100

5°
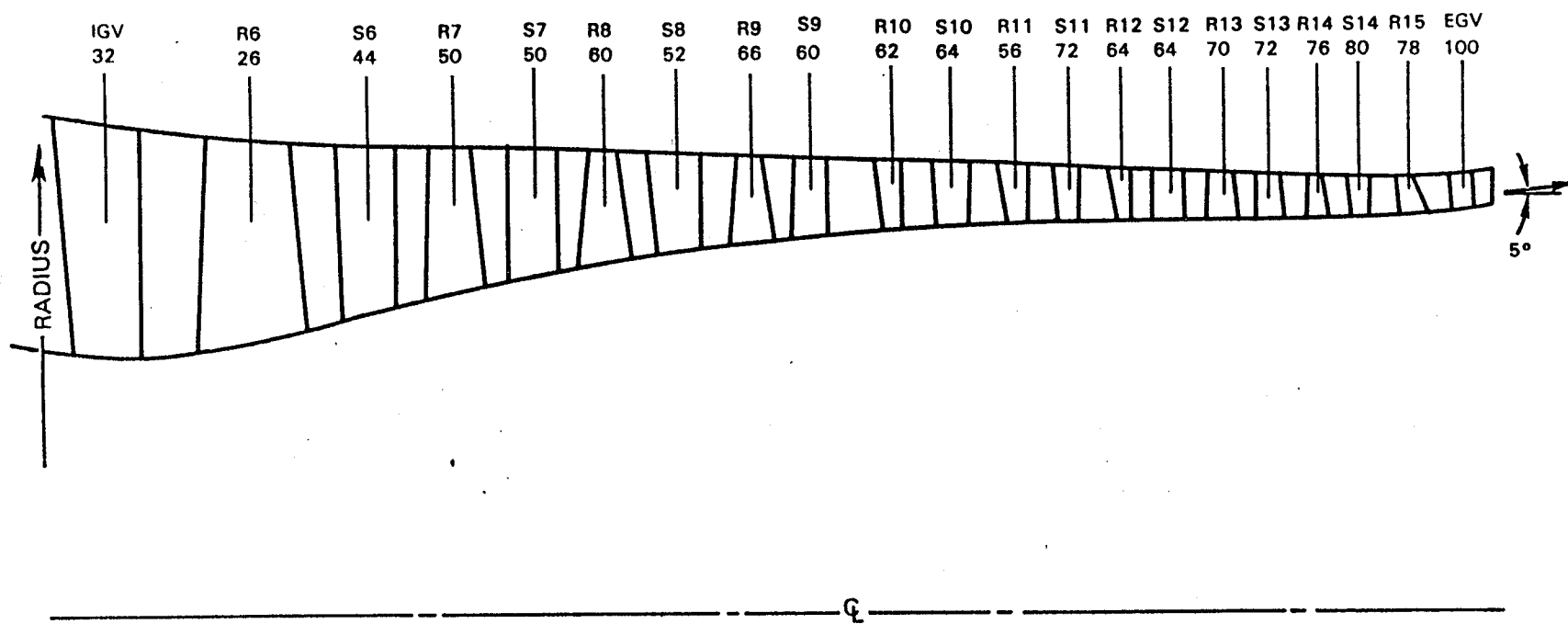
Figure 11   Flowpath of the High-Pressure Compressor Showing Airfoil Count and
Exit Cant Angle
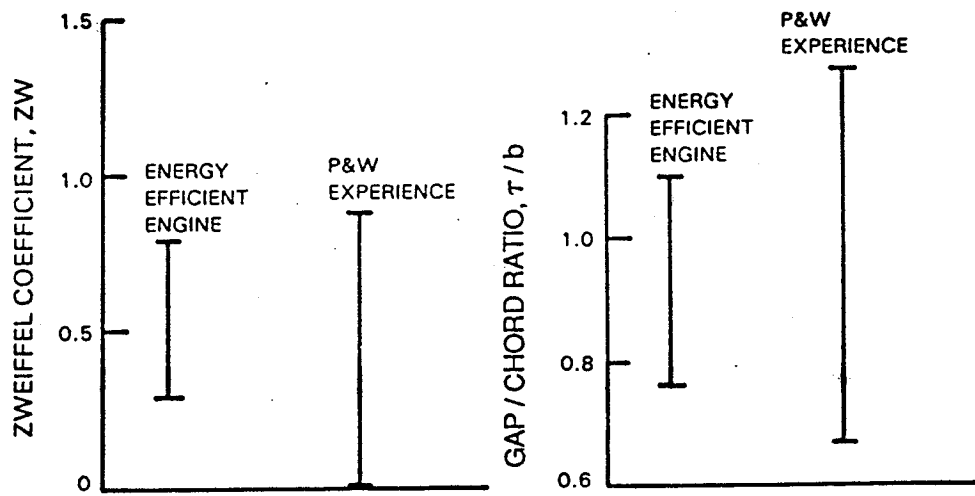
Figure 12 Zweiffel Coefficients and Airfoil Spacing Selected for the Inlet Guide Vane Design
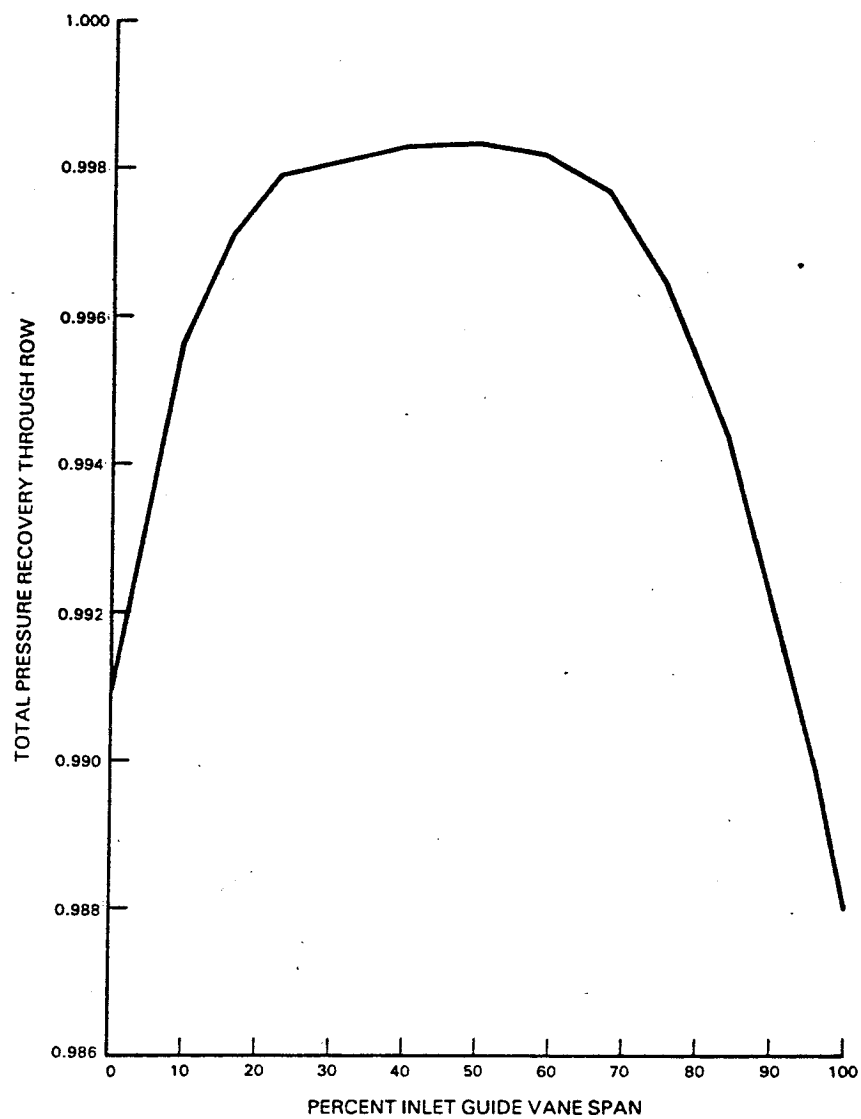
Figure 13 Spanwise Pressure Recovery Assumed for the Inlet Guide Vane
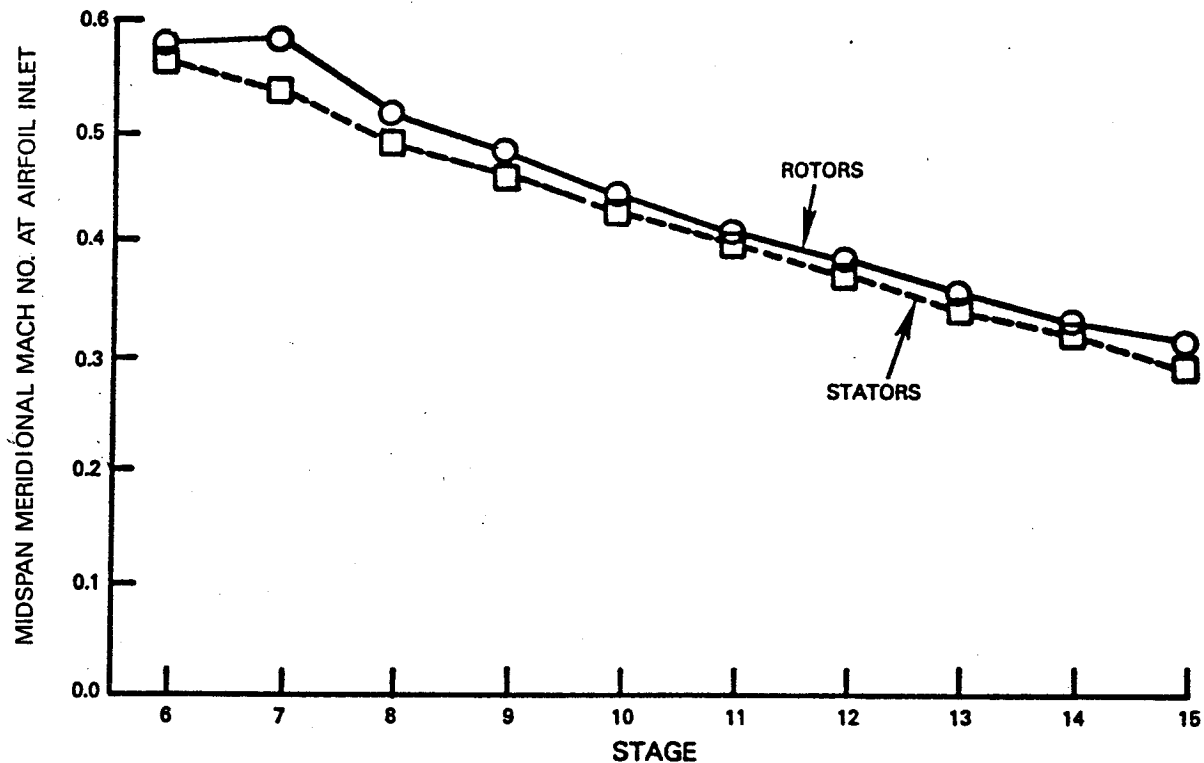
Figure 14 Midspan Meridional Mach Number Distribution. Effects of bleed flows extracted for turbine cooling and clearance control are included.

2.3.4 Pressure Ratio Distribution

The high-pressure compressor inlet conditions were based on a typical low-pressure compressor exit pressure distribution derived from Pratt & Whitney experience. The high-pressure compressor stage pressure ratio distribution was selected to balance the high speed surge loading requirements with the stage capabilities. This approach provided assurances of achieving the required stability for engine transient operations. Four variable stators (the inlet guide vanes and stators 6, 7, and 8) were required to provide adequate part-power stability. The final stage pressure ratio distribution for the high-pressure compressor is shown in Figure 15.

2.3.5 Pressure Profile Distribution

The assumed radial total pressure (Po) profile at the high-pressure compressor inlet, or low-pressure compressor exit, is basically flat with root and tip fall-off. The losses through the intermediate case struts and inlet guide vanes result in a somewhat different profile entering the first rotor of the high-pressure compressor (Figure 9). Positive radial total pressure slope at the inlet guide vane trailing edge is warped into a negative slope through the first few stages of the high-pressure compressor, reaching an approximate 2.5 percent negative slope at the twelfth stage. The slope is removed over the last three stages for a flat discharge profile. The negative Po slope helps to balance root and tip loadings and is consistent with Pratt & Whitney engine development experience. The radial pressure profile skew versus stage is shown in Figure 16.

23
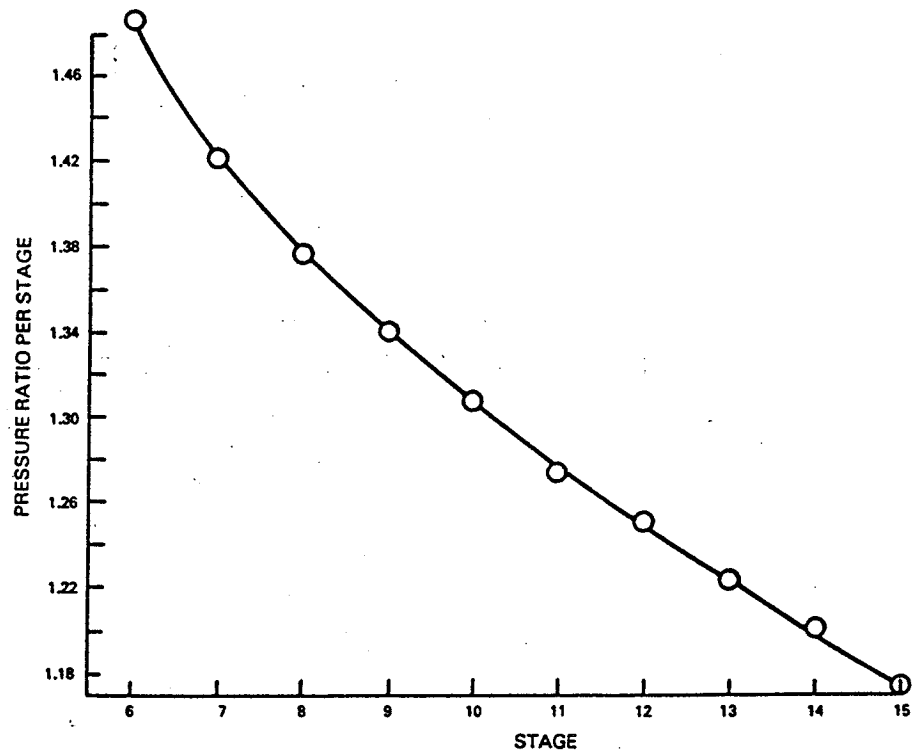
Figure 15 Stage Pressure Ratio. The stage pressure ratio distribution matches the surge loading requirements·with stage capability.
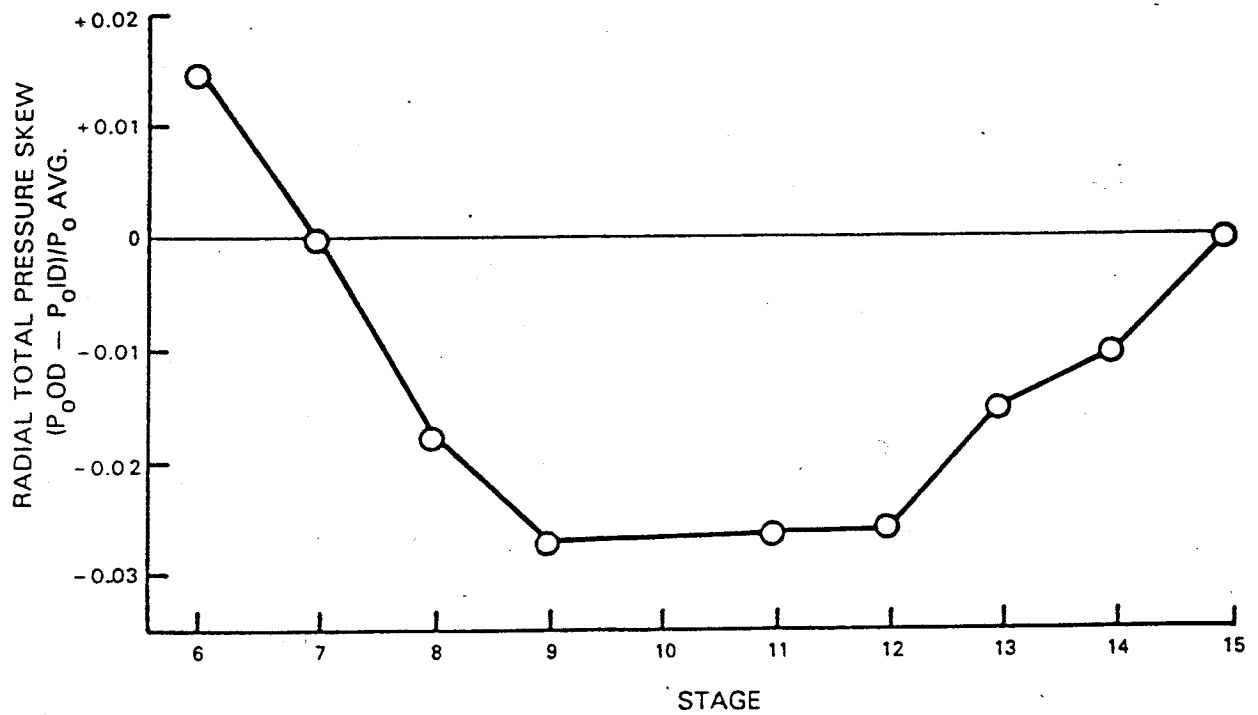
Figure 16 Radial Pressure-Profile Skew. The profile skew was used to balance root and tip loadings in front stages.

2.3.6 Aspect Ratio Distribution

The aspect ratio (average length/average chord) for the airfoils is shown in Figure 17. The selection of chords was based on aerodynamic surge loading requirements. Also, vibratory and structural criteria had to be met to ensure flutter- and resonance-free operation. The sixth rotor chord (first high-pressure compressor rotor) was chosen to move 2E resonance above the engine operating range. The exit guide vane represents a special case and is described separately.
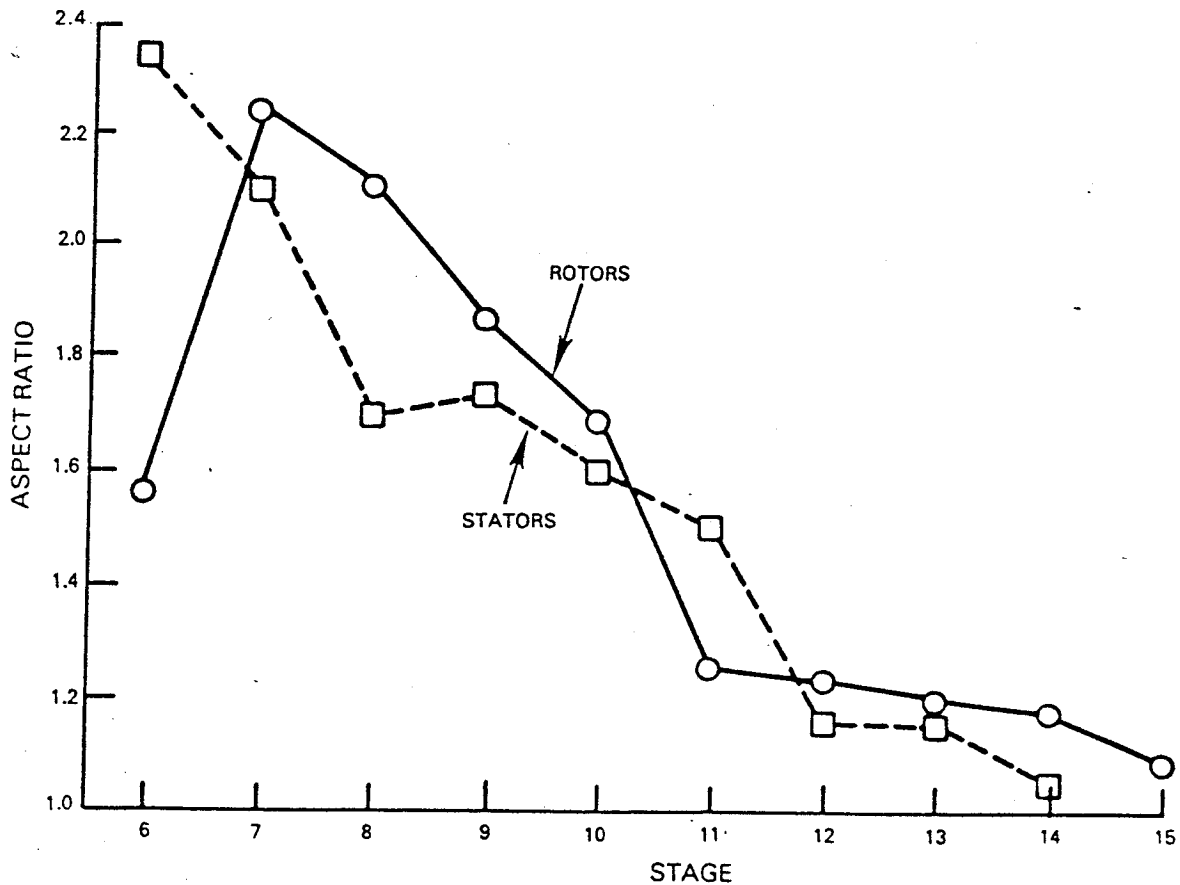
Figure 17 Stage Aspect Ratio. Selected aspect ratio reflects the requirement for flutter- and resonance-free operation.

2.3.7 Solidity Distribution

Configuration studies indicated that, in general, a relatively low solidity was best for operating line efficiency. Low solidity was the design goal for the back end of the compressor, but the solidity was also determined for some rows by the requirement to maintain goal surge margin. In the front stages, with higher inlet Mach numbers, increased solidity resulted in reduced los,ses. The stagewise solidity distribution is shown in Figure 18.
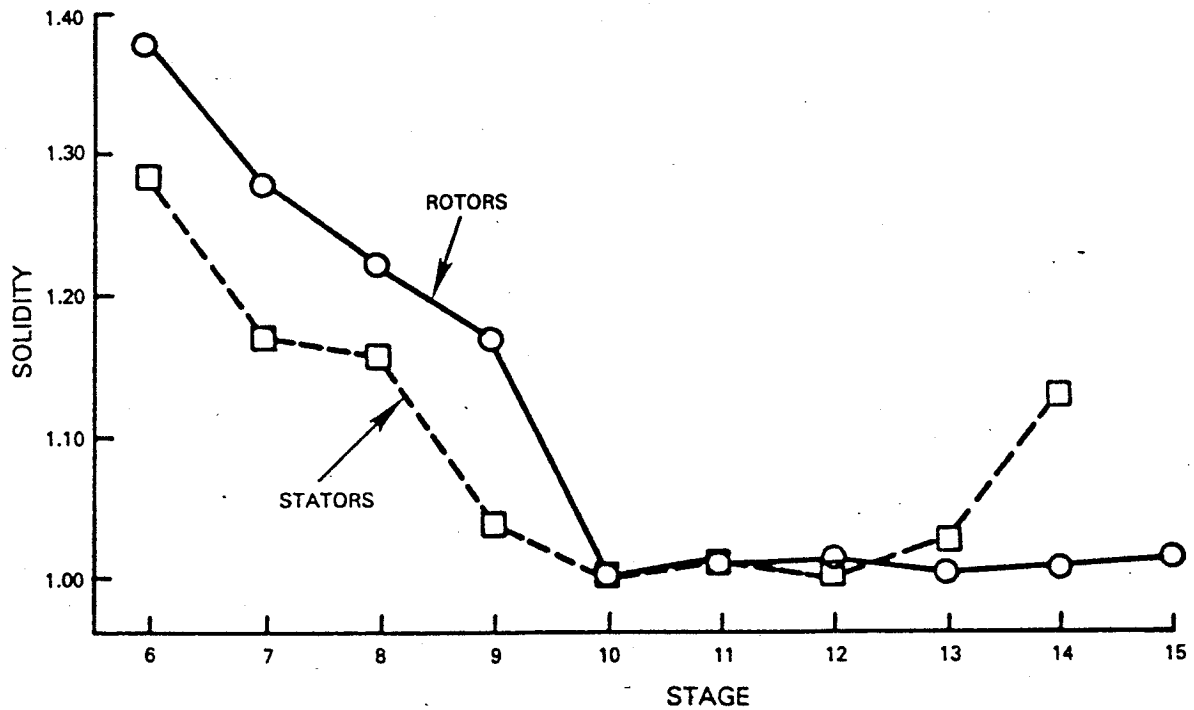
Figure 18   Solidity Distribution. Efficiency and surge margin requirements dictated the stagewise distribution.

2.3.8 Reaction

Efficiency optimization through meanline studies indicated that swirl angles resulting in approximately 50 percent reaction should be used in this compressor configuration. Detailed spanwise analysis led to somewhat increased reaction in the front stages so as to reduce stator root Mach numbers. The resulting stage reaction distribution is shown in Figure 19. This low reaction level resulted in lowering rotor Mach numbers and increasing stator Mach numbers. Figure 20 shows maximum inlet Mach numbers for all rows. The level is such that a maximum benefit could be derived from the controlled diffusion airfoils. Except for the inlet guide vane, which is a 400 series airfoil, and the first two rotors, which utilize transonic multiple circular arc airfoils, the compressor utilizes controlled diffusion airfoils for the lower loss and increased range demonstrated in several cascade tests.
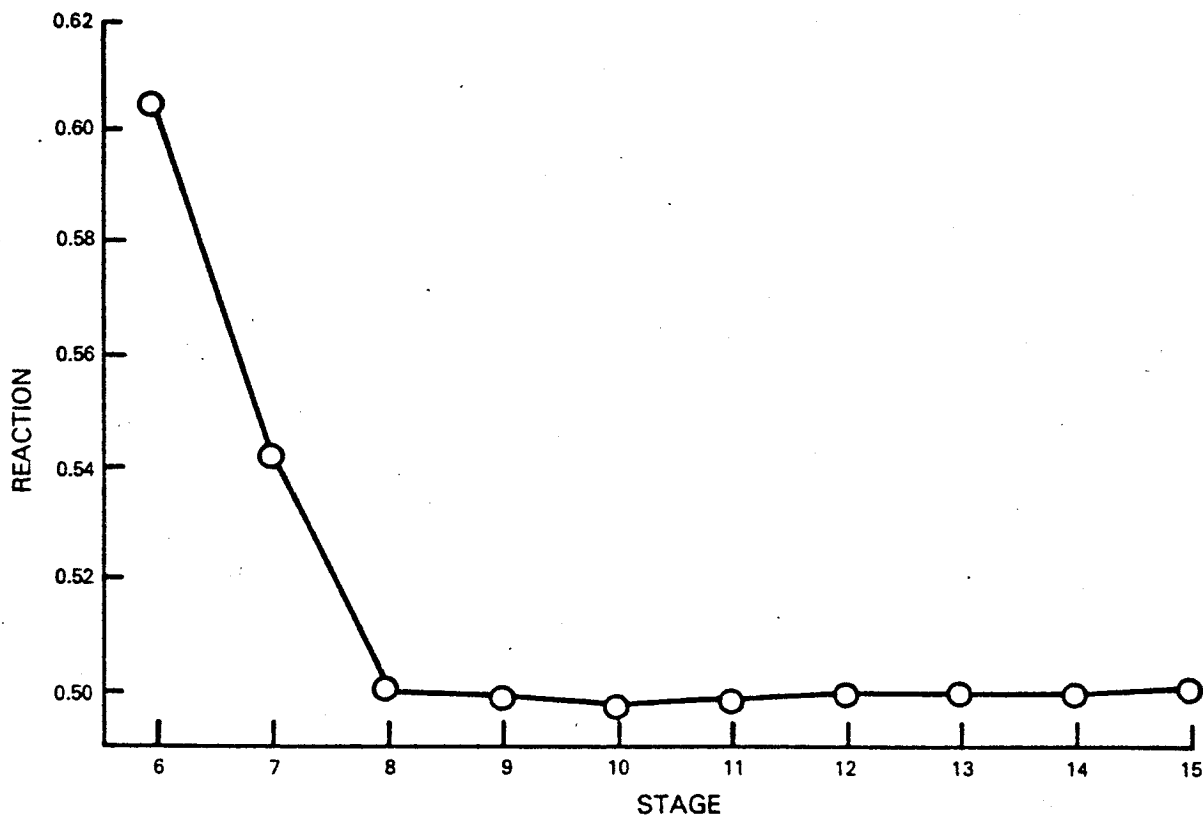
Figure 19   Stage Reaction. Selection is based on the predicted efficiency benefit.
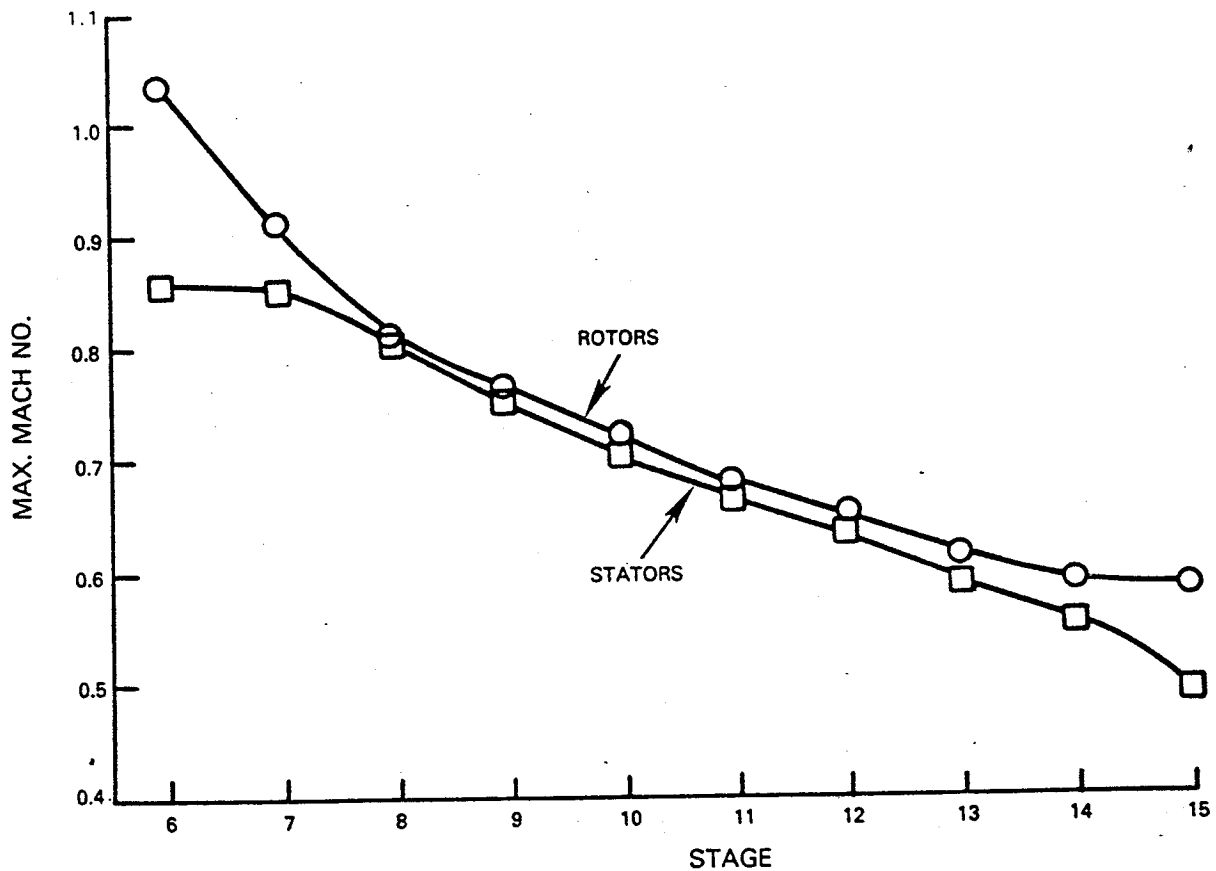
Figure 20   Airfoil Peak Mach Numbers. Reduced peak Mach numbers in front
            stators result in maximum benefit from controlled diffusion
            airfoils.

2.3.9 Stage Loading Distribution

Loading limit correlations based on Pratt & Whitney experience were used as a
guide in distributing stage loading throughout the compressor. The resultant
axial distribution of diffusion factor (D_f) and $\Delta P/P_0-P_s$ for root, mean
and tip sections are shown in Figure 21. Operating line and surge line levels
are based on surge loadings which were distributed smoothly in the axial
direction and balanced radially.

28
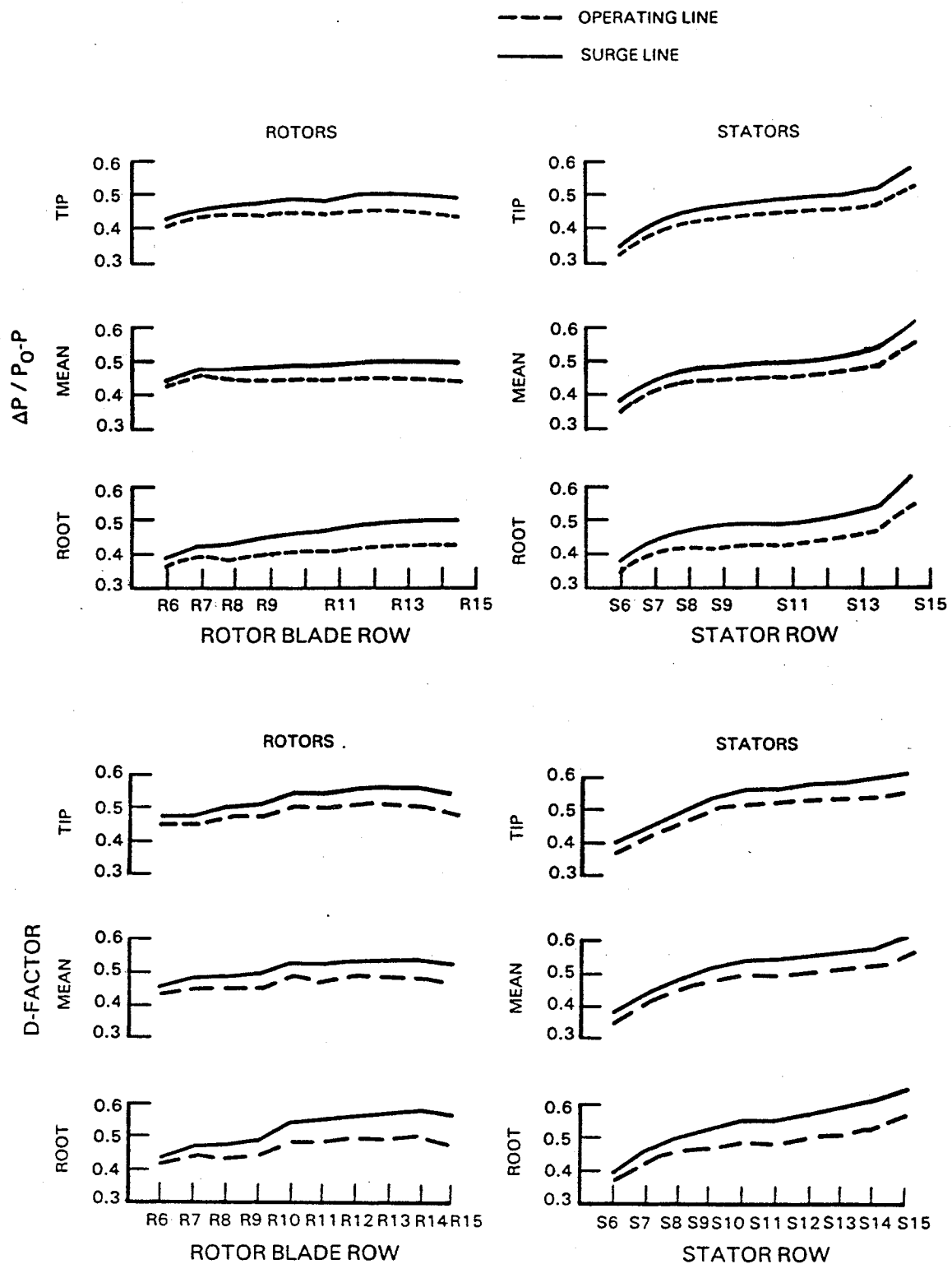
Figure 21   Stage Loading. Distribution is based on Pratt & Whitney experience.

2.3.10 Airfoil Selection

The selection of 400 series airfoils for the inlet guide vanes was based on Pratt & Whitney experience. In addition to low losses at the design point, 400 series airfoils also offer good off-design loss and turning characteristics which are important for part-power performance.

The Mach numbers on the first two rotors exceeded the range for controlled diffusion airfoils; therefore, multiple circular arc, transonic-type airfoils were selected for rotor 6 and rotor 7. The detailed design of the blading for choke margin and incidence was based on the experience derived from many transonic fans and from the NASA Low Aspect Ratio Front Stage.

The remaining 17 rows (from stator 7 rearward) incorporate controlled diffusion airfoils. The selection of low reaction resulted in Mach numbers which would be supercritical for conventional airfoils through stator 9 of the compressor. The controlled diffusion airfoils extended the low loss range beyond the design Mach number for these rows, resulting in a substantial performance advantage. The airfoils were designed in the core region for steady Mach number deceleration on the suction side. An incidence and deviation system developed from Pratt & Whitney cascade tests was used in establishing leading and trailing edge metal angles. In the end-wall region, the conventional Pratt & Whitney design approach was applied to set leading and trailing edge angles relative to the core. The resulting airfoils were analyzed and tuned as required for structural and vibratory characteristics to ensure satisfactory performance within the engine operating range. Airfoil design data are summarized in Appendix A.1.

2.3.11 Exit Guide Vanes

The low reaction design through the back stages resulted in a requirement to remove 52 degrees of swirl in the last stator in order to achieve an axial compressor discharge. This turning requirement was just beyond Pratt & Whitney experience for a single row (Figure 22). The more highly loaded single row configuration was selected for the engine with the intent of benefiting from lower cost for a single row exit vane configuration. However, provision was made to allow incorporation of double exit vanes if the performance of a single row exit vane did not meet expectations. The aspect ratio for the single row exit guide vane was set on the basis that enough axial flowpath space should be provided for a double row design if that became desirable. This provision resulted in an aspect ratio of 0.52. The gap/chord ratio was set at 0.4 to bring the diffusion-factor loading to the level comparable to the other back-end stators in the compressor.

2.3.12 Performance Prediction

The predicted performance of the high-pressure compressor is discussed earlier in Part I, Section 3.0 of this report.

Figure 22   Pratt & Whitney Exit Guide Vane Experience. Both single- and double-row systems are included.
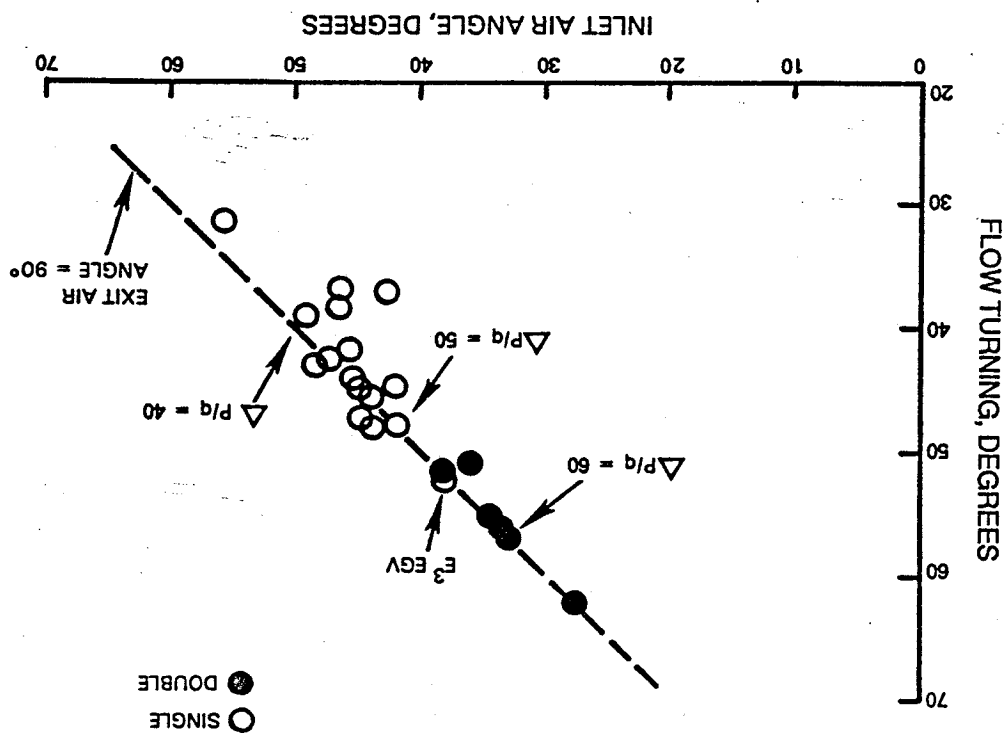
SECTION 3.0

MECHANICAL DESIGN

The mechanical design of the high-pressure compressor component included the compressor module and the intermediate case. The following sections describe the structural-mechanical design of these elements as well as the results of pertinent structural analyses used in the design substantiation process.

3.1 HIGH-PRESSURE COMPRESSOR MODULE DESIGN

The mechanical design of the high-pressure compressor evolved through an iterative process with the aerodynamic effort in order to arrive at a mechanical configuration that best achieves the design goals. A cross sectional view of the Energy Efficient Engine high-pressure compressor module is presented in Figure 23, illustrating many of the technology features. The major subassemblies of the compressor module are the rotor assembly, front case and stator assembly, and the rear case and stator assembly. These, along with the final flowpath gapping requirements, are discussed in the following sections.
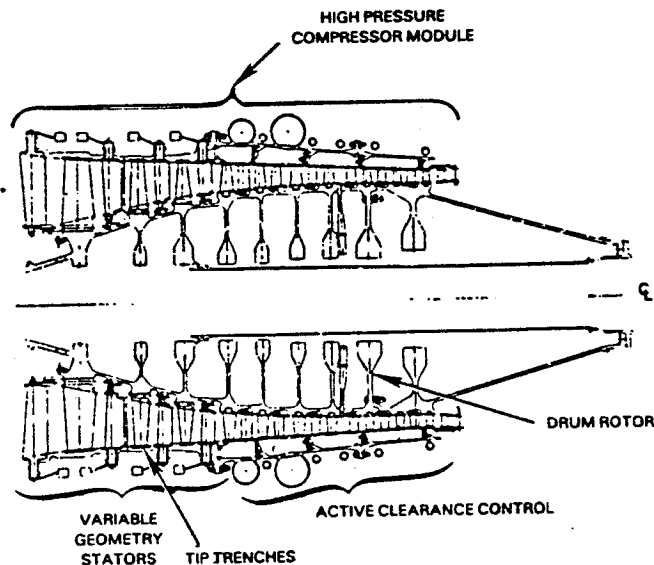
Figure 23   Energy Efficient Engine High-Pressure Compressor Showing Advanced Technology Features

3.1.1 Compressor Axial Gapping

Initial flowpath definition and preliminary gaps were established during the aerodynamic design effort. A final definition of these items was made during the mechanical design effort, consistent with constraints imposed by the actual configuration geometry. The resultant compressor configuration is illustrated in Figure 24.

Axial gaps were set to prevent rotor-to-stator rubs under conditions of the worst tolerance stack-up plus the worst combination of simultaneously occurring thrust, maneuver loads, surge, and thermal deflections during engine and rig operation. The gaps were set for each stage based on the limiting condition for the particular stage.
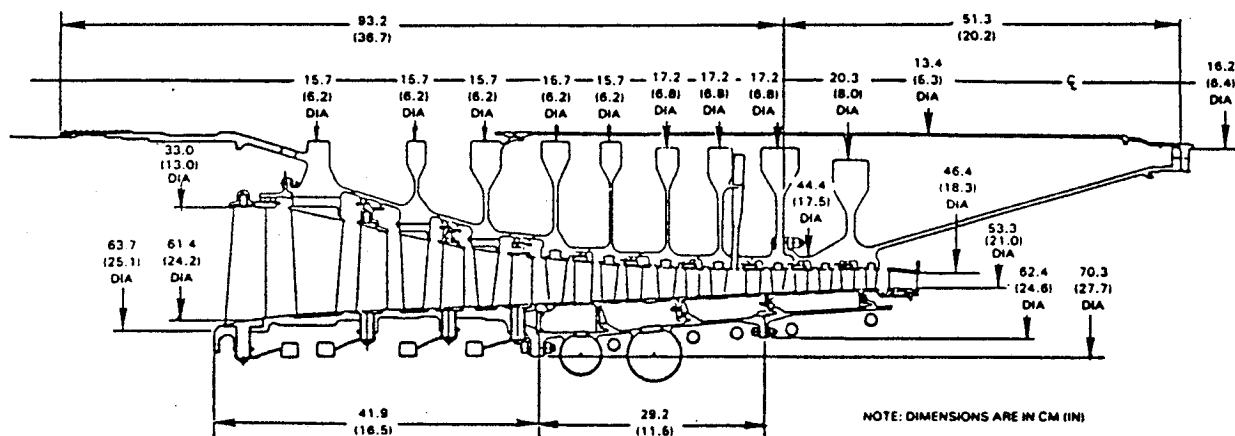
Figure 24 High-Pressure Compressor Configuration Resulting from Final
Flowpath Definition and Axial Gapping

The design philosophy for the high-pressure compressor was based on minimizing
program cost by using as much common hardware as possible in both the
integrated core/low spool (IC/LS) and the component test rig. This commonality
required a compromise in the length of the IC/LS compressor to account for the
use of variable stators in stages 9 through 14 of the test rig. A length
increase of 1.138 cm (0.448 in) resulted because the rig vane inner shrouds
are wider to accommodate the vane buttons.

The rotor was initially designed with flow guides on the inner diameter vane
platforms for stages 9 through 15 to improve performance. No additional length
increase is required to accommodate the ninth-stage flow guide, but a 0.25 cm
(0.100 in) overlap and an additional gap is required for the rear stages. Flow
guides add 1.77 cm (0.696 in) to the compressor length. Subsequent to
preliminary design activities, company-funded three-stage rig tests showed no
measurable benefit from the use of flow guides. They were, therefore, deleted
in the design of the component test rig hardware (Section 4.0). In a refined
flight propulsion system design, a high-pressure compressor length reduction
of 6.469 cm (2.547 in) would be possible if flow guides, rear variable vane
provisions, and excess gap are removed.

Table V summarizes the items requiring consideration when setting the gaps,
and Table VI presents the integrated core/low spool and high-pressure
compressor rig gaps that were established.

TABLE V

DESIGN CONSIDERATIONS USED TO ESTABLISH
ROTOR-TO-STATIC STRUCTURE AXIAL GAPS

Closure	Intermediate Case Deflection
Tolerance	Vane Surge
No. 3 Bearing Play	Vane Bending
No. 3 Bearing Deflection	Vane Deflection
Bearing Support Deflection	Bushing Wear
Maneuver Deflection	Vane Cocking

33

TABLE VI

INNER DIAMETER AXIAL GAPS
Integrated Core/Low Spool High-Pressure Compressor Component and Test Rig

GAPS BETWEEN:

IGV-R6	R6-S6	S6-R7	R7-S7	S7-R8	R8-S8	S8-R9	R9-S9	S9-R10	R10-S10	S10-R11	S11-R11	S11-R12	R12-S12	S12-R13	R13-S13	S13-R14	R14-S14	S14-R15	R15-EGV	Total	Units
Flight Engine / Test Rig Design Gaps:																					
1.498	1.415	1.237	0.927	0.775	0.749	0.848	0.483	0.587	0.505	0.587	0.447	0.612	0.455	0.602	0.445	0.572	0.455	0.579	0.925	14.703	cm
0.590	0.557	0.487	0.365	0.305	0.295	0.334	0.190	0.231	0.199	0.231	0.176	0.241	0.179	0.237	0.175	0.225	0.179	0.228	0.364	5.788	inch
Minimum Required Flight Engine Gaps:																					
1.250	1.204	1.143	0.828	0.732	0.597	0.569	0.465	0.404	0.421		0.378	0.378	0.340	0.333	0.361	0.353	0.386	0.328	0.363	0.305	11.138	cm
0.492	0.474	0.450	0.326	0.288	0.235	0.224	0.183	0.159	0.166		0.149	0.149	0.134	0.131	0.142	0.139	0.152	0.129	0.143	0.120	4.385	inch
Minimum Required Test Rig Gaps																					
0.881	0.955	0.780	0.696	0.566	0.617	0.373	0.429	0.368	0.394	0.363	0.394	0.394	0.381	0.427	0.394	0.457	0.384	0.465	0.282	10.000	cm
0.347	0.376	0.307	0.274	0.223	0.243	0.147	0.169	0.145	0.155	0.143	0.155	0.155	0.150	0.168	0.155	0.180	0.151	0.183	0.111	3.937	inch

3.1.2 Compressor Module Rotor Assembly

3.1.2.1 General Description

The rotor assembly is shown in Figure 25. It comprises a one-piece electron beam welded titanium drum front rotor, for stages 6 through 13 inclusive, bolted to a one-piece PWA 1099 (see Appendix B for material equivalency) nickel alloy tandem disk/rotor assembly, for stages 14 and 15, which is machined from a powdered metal compaction.

Ten rows of blades are attached to the rotor. The first three blade rows are attached to their respective disks by axial root attachments. The remaining seven rows have tangential attachments. Integral knife edge seals are used at interstage locations throughout the assembly, and a bolted-on knife edge seal is used at the sixth-stage inlet.

Bleed air for turbine cooling enters the inner rotor cavity via 22 bleed tubes which are installed in the rotor aft of the twelfth-stage disk.
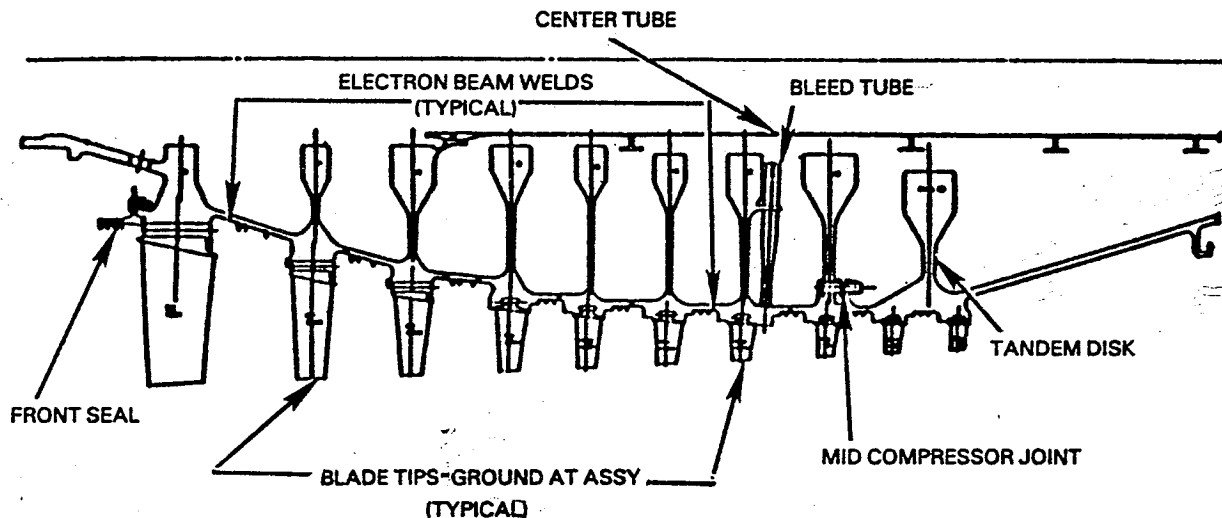
Figure 25   High-Pressure Compressor Rotor Assembly

3.1.2.2 Rotor Drum Design

Analysis of the drum portion of the module rotor assembly was conducted using the flight propulsion system flight cycle operating conditions. The procedure was initiated with a finite element analysis of the temperature distributions within the rotor structure. The resultant data were incorporated into a finite element (shell) structure analysis routine to establish rotor stresses and deflections. Spacer load was input into the structural analysis as a variable load. Figure 26 shows the thermal analysis model and Table VII indicates some typical temperature distributions at two of the operating conditions. Figure 27 shows the complementary structural analysis model.

Analysis focused on the following subelements: disks, drum rim spacer welds, blade tangential slots, oil weep and bore cooling air holes, solid body bleed tube, center tube, knife-edge seals, and rotor tie bolts. These subelements are discussed in the following sections.

The plastic growth limits, low cycle fatigue life, burst margin, radial stresses, creep life, and bore fracture mechanics are summarized in Tables VIII, IX, and X and Figures 28 and 29. The data show that the structural design is capable of meeting all of the life goals for the component rig and the integrated core/low spool. However, some improvements must be made to the low cycle fatigue life of certain components to meet the goals for the flight propulsion system.

3.1.2.2.1 Disk Design

In the integrated core/low spool, the disks in the sixth and seventh stages are titanium AMS 4928 material. The eighth through eleventh stage disks are PWA 1224, which is a form of 6-2-4-2 titanium with improved low-cycle fatigue and lower creep properties. In the twelfth and thirteenth stages, the disk material is PWA 1226 which is a high creep/lower low-cycle fatigue form of 6-2-4-2 titanium. The fourteenth/fifteenth stage tandem disk is PWA 1099, a nickel base alloy powder consolidation.

To meet the life requirements in the flight propulsion system, a beta-forged titanium (PWA 1225 6-2-4-2) is required in the twelfth and thirteenth stages. Also, MERL 80, an improved form of PWA 1099, is used for the tandem disk.

Analysis of disk structural characteristics indicates that the sixth through thirteenth disks are fracture mechanics limited at the bore. The thirteenth stage disk is also creep limited at the rim. The fourteenth/fifteenth stage tandem disk is low cycle fatigue limited at the bore. The characteristics are summarized in Table X.

36

TABLE VII

ROTOR THERMALS

MINIMUM TEMPERATURE REGIONS:

NODE NUMBER	FIG. 26 REF.	TEMP. AT ADP °F (°C)	TEMP. AT TAKEOFF °F (°C)
402	(A)	163 (72)	250 (121)
403		171 (77)	256 (124)
404		180 (82)	263 (128)
405	(B)	148 (64)	245 (118)
406		152 (66)	249 (120)
407		164 (73)	258 (125)
408		168 (75)	263 (128)
409		175 (79)	274 (134)
410		164 (73)	261 (127)
14	(C)	264 (128)	370 (187)
15		264 (128)	370 (187)
16		261 (127)	367 (186)
17		263 (128)	369 (187)
18	(D)	237 (113)	330 (165)
19		246 (118)	344 (173)
20		257 (125)	359 (181)

MAXIMUM TEMPERATURE REGIONS:

NODE NUMBER	FIG. 26 REF.	TEMP. AT ADP °F (°C)	TEMP. AT TAKEOFF °F (°C)
360	(E)	937 (502)	1102 (594)
361		923 (495)	1080 (582)
372		900 (482)	1058 (570)
501	(F)	950 (510)	1111 (599)
502		948 (508)	1110 (598)
503		945 (507)	1107 (597)
504		947 (508)	1108 (597)
505		947 (508)	1108 (597)
369	(G)	937 (502)	1078 (581)
364		938 (503)	1098 (592)
392		950 (510)	1109 (598)
393		951 (510)	1109 (598)
394		951 (510)	1109 (598)
395		950 (510)	1108 (597)
396		949 (509)	1106 (596)
397		948 (508)	1105 (596)

THERMAL MODEL —
HIGH PRESSURE COMPRESSOR ROTOR

ELEMENT INPUT

Y OR R AXIS

SCALE = 1.00

Ⓒ

16 14 15 17

407

Ⓑ

422

414

419

412

411

Ⓓ

410 409

406

405

408

407

Ⓐ

402   403   404

0.00   1.00   2.00   3.00   4.00   5.00   6.00   7.00   8.00   9.00
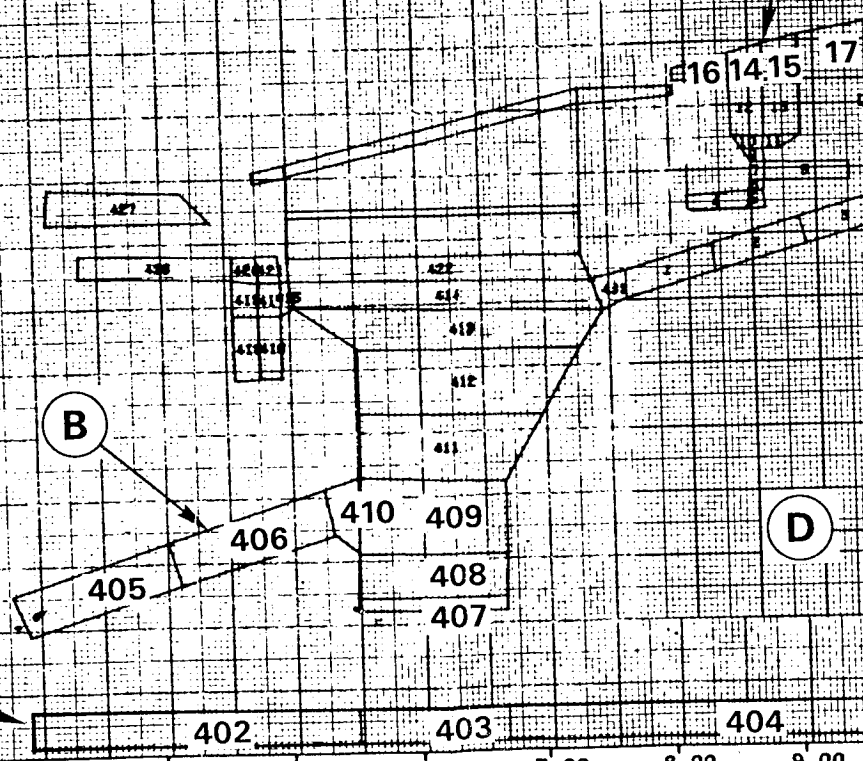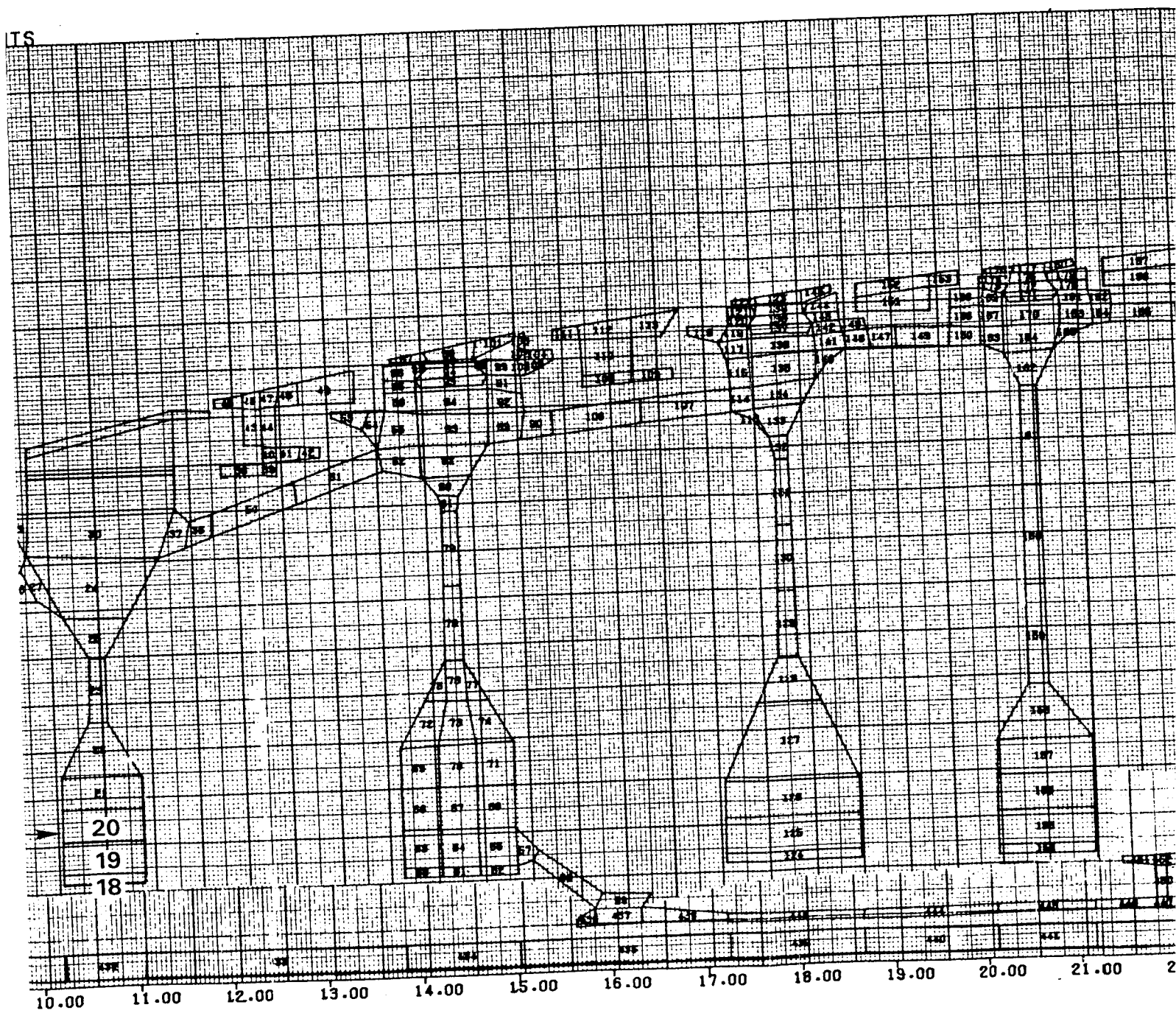
E

361 372
360
369
364

G

23.00 24.00 25.00 26.00 27.00 28.00 29.00 30.00 31.00 32.00 33.00 34.00
Y AXIS
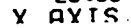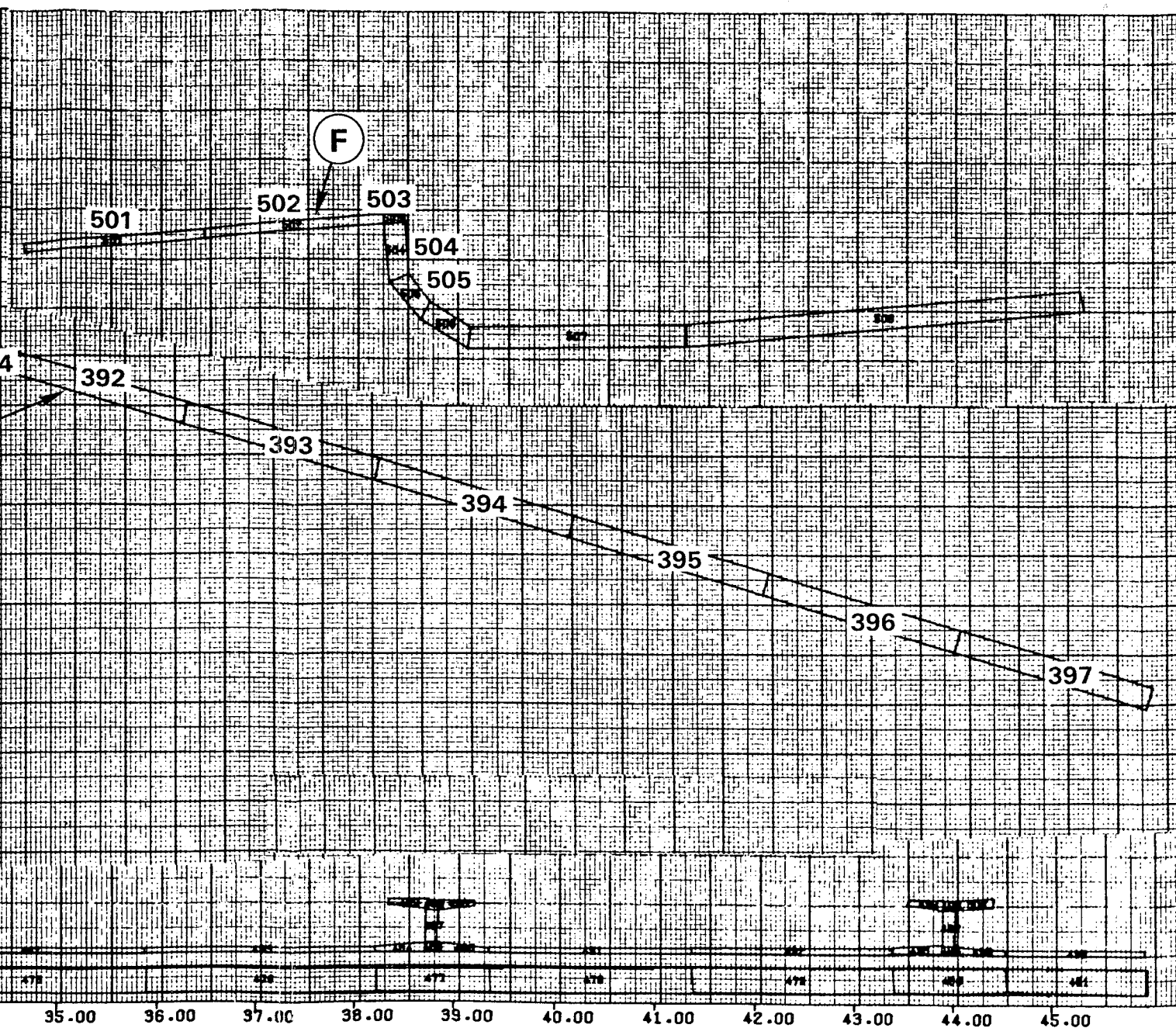
Figure 26   Thermal Model – High-Pressure Compressor Rotor

FOLDOUT FRAME

PAGE 38 INTENTIONALLY BLANK

E³ HIGH COMPRESSOR ROTOR ASSEMBLY
SHELL ANALYSIS MODEL
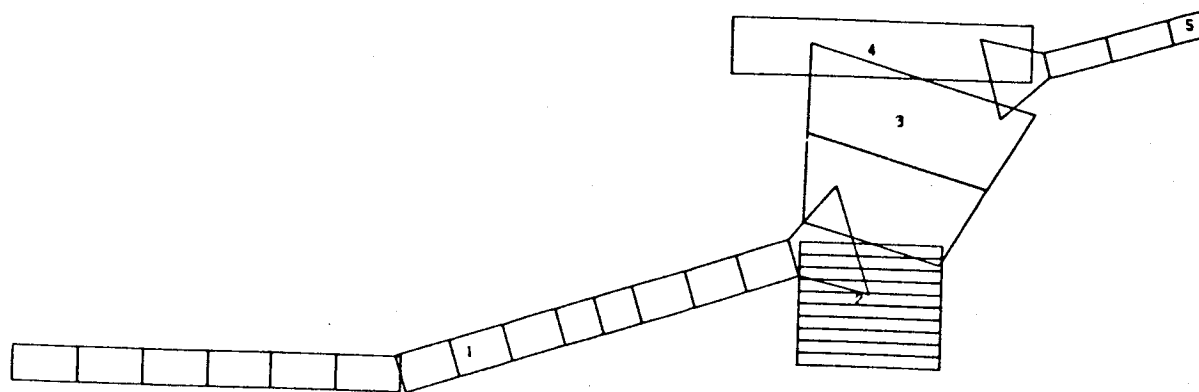
SCALE FACTOR = 0.9861
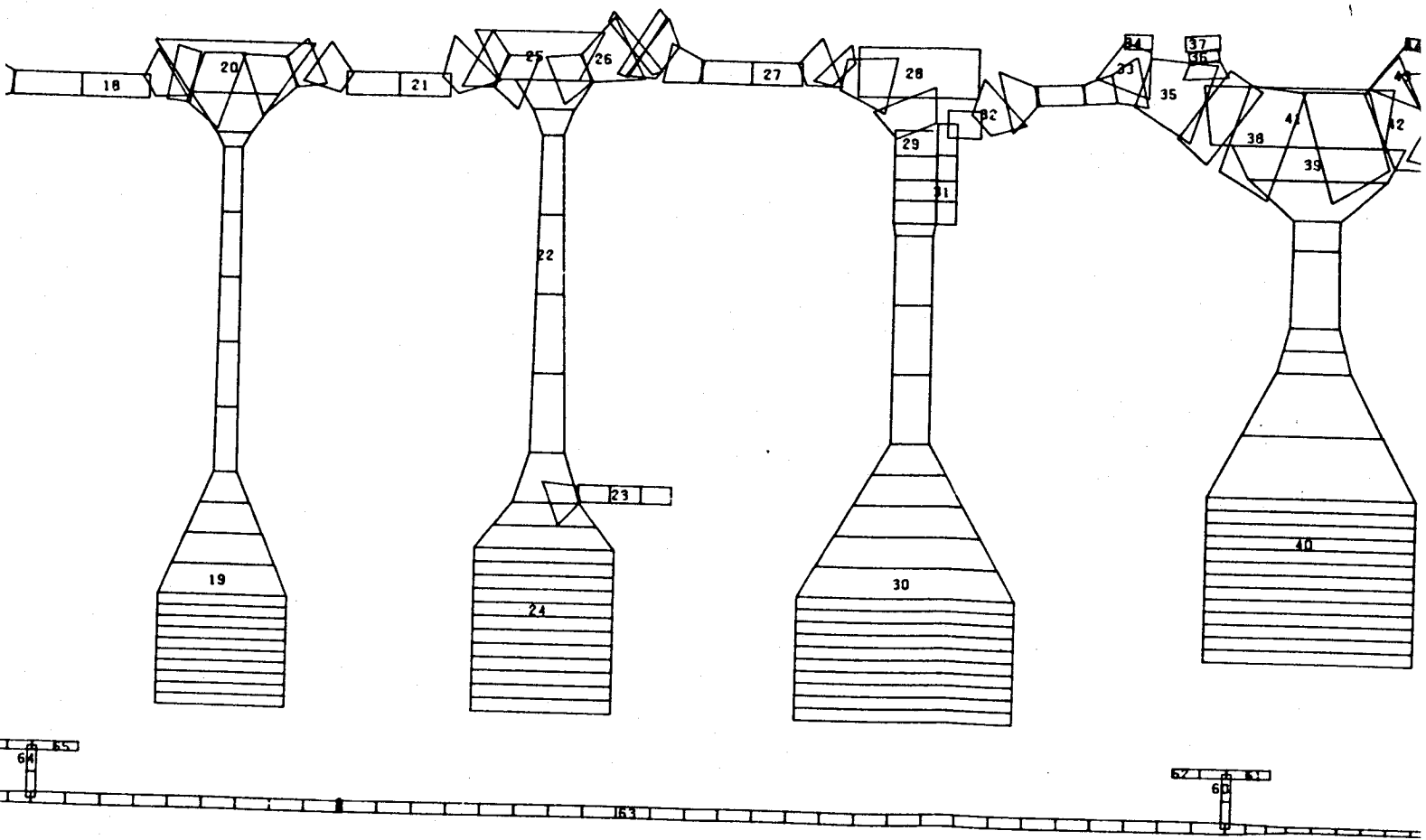
FOLDOUT FRAME
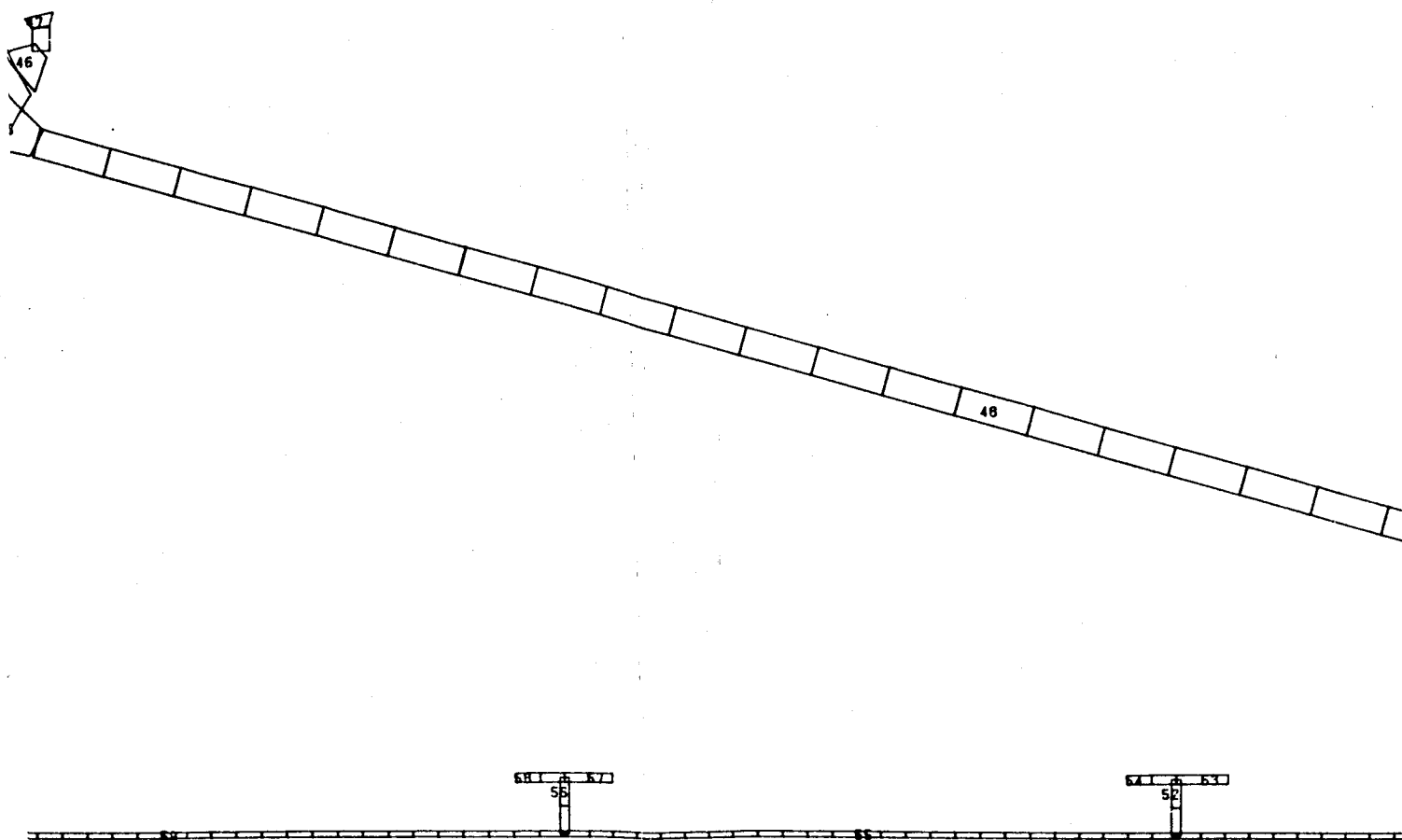
Figure 27   Energy Efficient Engine High Cor
            Analysis Model

50

49

tor Assembly Shell

FILMED

41
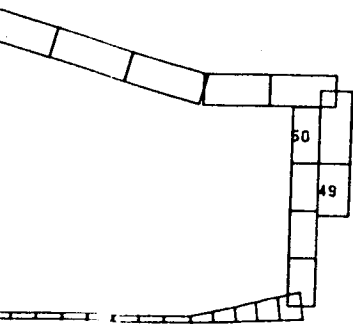
TABLE VIII

RIM LIFE ANALYSIS

Stage	6	6	7	8	12	12	14/15
Limiting Feature	Air Holes	Front Flange	Weep Hole	Weep Hole	Bleed Tube Inner	Bleed Tube Outer	Balance Flange
Max. Stress: (psi)	36,600	40,000	28,000	30,000	43,200	32,000	56,000
(MPa)	252.35	275.79	193.05	206.84	297.85	220.63	386.11
Temperature: (°F)	200	150	370	460	500	805	1050
(°C)	93.3	65.6	187.8	277.8	260	429.4	585.6
Low Cycle Fatigue Life (cycles x 10^3)	77,100	77,100	3.5	11	25	15	100

RIM WELD LIFE ANALYSIS

Spacer	6/7	7/8		8/9	9/10	10/11	11/12	12/13
Hoop Stress: (psi)	25,900	20,400	33,500	30,300	38,700	27,200	14,700	21,800	34,300
(MPa)	178.57	140.65	230.97	208.91	266.83	187.54	101.35	150.31	236.49
Hoop Life	All Lives Greater than 100,000 Cycles							
Axial Life (cycles x 10^3)	65	18	29	48	25	22	65	22.5	5.3

PRECEDING PAGE BLANK NOT FILMED

PAGE 42 INTENTIONALLY BLANK

43

TABLE IX

LOW CYCLE FATIGUE LIFE SUMMARY

Rotor	Location	Life (cycles)	Goal (cycles)
6	Bore	$>10^5$	20000
	Rim	$>10^5$	20000
	Bore Fracture Mech	21000	20000
7	Bore	$>10^5$	20000
	Rim	$>10^5$	20000
	Bore Fracture Mech	21000	20000
8	Bore	$>10^5$	20000
	Rim	$>10^5$	20000
	Bore Fracture Mech	20000	20000
9	Bore	$>10^5$	20000
	Rim	$>10^5$	20000
	Bore Fracture Mech	20000	20000
10	Bore	$>10^5$	20000
	Rim	$>10^5$	20000
	Bore Fracture Mech	20000	20000
11	Bore	$>10^5$	20000
	Rim	$>10^5$	20000
	Bore Fracture Mech	20000	20000
12	Bore	$>10^5$	20000
	Rim	$>10^5$	20000
	Bore Fracture Mech	20000	20000
13	Bore	$>10^5$	20000
	Rim	$>10^5$	20000
	Bore Fracture Mech	20000	20000
13	Bolt Circle Inner Diameter	$>10^5$	20000
	Bolt Circle Outer Diameter	$>10^5$	20000
	Bolt Circle Radial	31000	20000
14/15	Bore	25000 MERL 80	20000
		4000 MERL 76*	20000
	14th Rim	73000 MERL 80	20000
	15th Rim	16216 MERL 76	20000

* For -100 Mesh Powder

TABLE X

DISK DESIGN SUMMARY

Disk	6th	7th	8th	9th	10th	11th	12th	13th	14th	14/15 15th
Burst Margin	1.49	1.46	1.35	1.36	1.32	1.30	1.39	1.28	1.39	
Radial Web Stress:										
(psi)	22,300	88,000	104,600	103,500	103,500	102,900	85,900	99,000	182,800	
(MPa)	153.75	606.74	721.19	713.61	713.61	709.47	592.26	682.58	1260.36	
Disk 0.1% Creep										
Life (hours)	>1000	>1000	>1000	>1000	>1000	>1000	>1000	780	>1000	
Plastic Growth										
(inch)	<0.001	<0.001	<0.001	<0.001	<0.001	<0.001	<0.001	<0.001	<0.001	
(mm)	2.54	2.54	2.54	2.54	2.54	2.54	2.54	2.54	2.54	
Tangential Hoop Load at 13,921 rpm:										
(pounds)	750,000	403,000	660,000	267,500	219,000	214,000	171,520	152,000	112,000	102,200
(MN)	3.33617	1.79263	2.93583	1.18990	0.97416	0.95192	0.76296	0.67613	0.49820	0.45461
Radial Load at 13,921 rpm:										
(pounds)	611,000	321,000	547,000	267,500	219,000	214,000	171,520	152,000	112,000	102,200
(MN)	2.71786	1.42788	2.43318	1.18990	0.97416	0.95192	0.76296	0.67613	0.49820	0.45461
Max. Elastic Bore Stress During Take-Off: (psi)	66,600	66,800	67,000	67,000	66,500	66,900	66,800	66,700	146,000	
(MPa)	459.19	460.57	461.95	461.95	458.50	461.26	460.57	459.88	1006.63	

COOLING AIR HOLES
>10^5 CYCLES

BLEED TUBE INNER SUPPORT
25K CYCLES

TANDEM DISK BORE
4K CYCLES

BALANCE FLANGE
>100K CYCLES

FLANGE
>10^5 CYCLES

OIL WEEP HOLES
7TH — 3.5K CYCLES
8TH — 11K CYCLES
(THESE LIVES IMPROVED BY HOLE SURFACE
FINISH TO MEET FPS CRITERIA)

13TH STAGE BOLT CIRCLE
30K CYCLES

BLEED TUBE EXIT
15K CYCLES

- ALL OTHER IN-PLANE DISK LCF LIVES EXCEED 100K CYCLES
- ALL EB WELD TANGENTIAL LCF LIVES EXCEED 100K CYCLES
- ALL EB WELD AXIAL AND BENDING LCF LIVES EXCEED 20K CYCLES
  EXCEPT BETWEEN THE 12TH AND 13TH DISKS WHICH HAS 5.3 K CYCLES.
  THIS LIFE IS EASILY IMPROVED BY THICKNESS AND TAPERING

Figure 28   Low Cycle Fatigue Life Summary for the Integrated Core/Low Spool High-Pressure Compressor

ITEM	6 STAGE	9 STAGE	11 STAGE	13 STAGE	14/15 STAGE
AVG TANG MAX STRESS	312.33 MPa (45,300 PSI)	324.05 MPa (47,000 PSI)	326.81 MPa (47,400 PSI)	339.91 MPa (49,300 PSI)	599.15 MPa (86,900 PSI)
RIM TANG MAX STRESS	237.87 MPa (34,500 PSI)	207.53 MPa (30,100 PSI)	199.95 MPa (29,000 PSI)	168.92 MPa (24,500 PSI)	392.31 MPa (56,900 PSI)
DISK AVG TEMP	111°C (232°F)	262°C (504°F)	336°C (638°F)	413°C (776°F)	465°C (869°F)
BORE TEMP	95°C (203°F)	237°C (459°F)	297°C (568°F)	368°C (696°F)	382°C (720°F)
RIM TEMP	118°C (245°F)	309°C (589°F)	416°C (781°F)	491°C (916°F)	555°C (1032°F)

Figure 29   Rotor Temperature and Stress Summary for the Integrated Core/Low Spool High-Pressure Compressor

46

3.1.2.2.2 Drum Rim Spacer Welds

The welded drum has an electron beam weld between each disk. These welds are located between the knife edges and are clear of the disk bores or any protruding wings except for spacer 8/9 where the combined effect of the axial broach clearance and protruding bore basket support requires a double weld.

The bore of the 13th disk and the solid body bleed-tube inner support on the rear of the 12th disk require the spacer weld to be located near the region of maximum axial bending stress. Due to this high stress location, this weld has a low cycle fatigue life of 5300 cycles, which is adequate for rig and integrated core/low spool testing. An increase in thickness to reduce the bending stress combined with spacer thickness tapering to distribute the stress will increase this weld life to the flight propulsion system goal of 20,000 cycles. This change has not been made in the integrated core/low spool rotor to permit the use of existing weld shrinkage parameters and eliminate an electron beam weld development program. Spacer stress and life characteristics are summarized in Table VIII and Figure 28.

3.1.2.2.3 Blade Tangential Slots

Blade tangential attachment slot bending stress finite element analysis indicated that while the concentrated stresses were within limits for the rig and integrated core/low spool running, the local stresses must be reduced to meet the flight propulsion system criteria. This can be accomplished through added thickness or increased fillet radii in the blade root slots. Attachment geometry and representative stresses for selected stages are shown in Figure 30. Stresses for all stages are summarized in Table XI for the maximum flight propulsion system high-pressure compressor rotor speed of 14,270 rpm and the maximum integrated core/low spool high-pressure compressor rotor speed of 13,936 rpm, both at sea level takeoff power conditions.

Because of the size and tip speed of the first stage high-pressure compressor blade, combined P/A and untwist stresses were checked to ensure adequate airfoil low cycle fatigue life. Combined stresses are satisfactory for low cycle fatigue life of titanium blades.

R-6, R-7 AND R-8
- EXHIBITING P&W AXIAL BROACH TOOLING
- MEET ALL ATTACHMENT DESIGN CRITERIA
  FOR THE PLANNED TEST PROGRAM
- BROACHES CAN BE OPTIMIZED FOR IMPROVED
  LCF LIFE AND TO REDUCE 8-STAGE BEARING
  STRESS

R-9 THROUGH R-15
- USE EXISTING ATTACHMENT PROFILE TOOLING
- ATTACHMENTS MEET ALL DESIGN CRITERIA FOR
  THE PLANNED TEST PROGRAM
- BEARING STRESSES ON STAGES 9, 10 AND 13
  DO NOT MEET FPS CRITERIA, BUT CAN BE
  REDUCED BY SLOT OPTIMIZATION
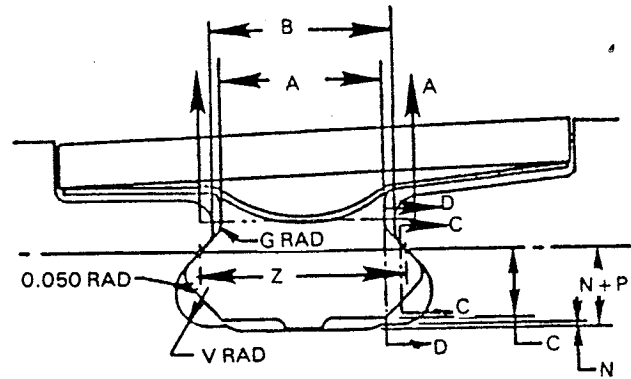
BLADE ATTACHMENT GEOMETRY
CM (IN)

STAGE	A	B	C	G	N + P	V	Z
9	1.066 (0.420)	1.143 (0.450)	0.355 (0.140)	0.180 (0.071)	0.403 (0.159)	0.139 (0.055)	1.397 (0.550)
13	0.838 (0.330)	0.914 (0.360)	0.284 (0.112)	0.127 (0.050)	0.332 (0.131)	0.127 (0.050)	1.056 (0.416)
15	0.660 (0.260)	0.736 (0.290)	0.309 (0.122)	0.127 (0.050)	0.370 (0.146)	0.127 (0.050)	0.878 (0.346)

ATTACHMENT STRESSES AT N = 14,270 RPM
MPa (PSI)

SECTION STAGE	A-A TENSION	C-C SHEAR	D-D BENDING	BEARING	COMBINED
9	172.37 (25,000)	178.57 (25,900)	343.01 (49,750)	458.92 (66,560)	515.38 (74,750)
13	110.32 (16,000)	117.21 (17,000)	196.50 (28,500)	434.37 (63,000)	307.51 (44,600)
15	108.94 (15,800)	91.70 (13,300)	153.06 (22,200)	337.84 (49,000)	262.00 (38,000)

Figure 30 High-Pressure Compressor Blade Attachment Summary

TABLE XI

ATTACHMENT STRESSES

Stage	Stress Type	Stress Level, MPa (psi)			
		at N = 14,270 rpm (Flight Propulsion System)		at N = 13,936 rpm (Integrated Core/ Low Spool)	
6	Combined	312.608	(45,340)		
	Tensile	149.616	(21,700)	142.032	(20,600)
	Shear	112.729	(16,350)	106.869	(15,500)
	Bending	162.992	(23,640)	155.132	(22,500)
	Bearing	281.237	(40,790)		
7	Combined	383.349	(55,600)		
	Tensile	99.285	(14,400)	94.458	(13,700)
	Shear	82.737	(12,000)	79.290	(11,500)
	Bending	210.980	(30,600)	201.327	(29,200)
	Bearing	284.064	(41,200)		
8	Combined	439.886	(63,800)		
	Tensile	140.653	(20,400)	134.448	(19,500)
	Shear	119.279	(17,300)	113.764	(16,500)
	Bending	299.233	(43,400)	285.443	(41,400)
	Bearing	402.654	(58,400)		
9	Combined	515.383	(74,750)		
	Tensile	172.369	(25,000)	164.095	(23,800)
	Shear	178.574	(25,900)	170.301	(24,700)
	Bending	343.014	(49,750)	327.501	(47,500)
	Bearing	458.915	(66,560)		
10	Combined	410.928	(59,600)		
	Tensile	148.927	(21,600)	142.032	(20,600)
	Shear	136.516	(19,800)	130.311	(18,900)
	Bending	262.001	(38,000)	250.280	(36,300)
	Bearing	365.422	(53,000)		
11	Combined	365.422	(53,000)		
	Tensile	133.069	(19,300)	126.864	(18,400)
	Shear	121.348	(17,600)	115.832	(16,800)
	Bending	233.043	(33,800)	222.701	(32,300)
	Bearing	296.475	(43,000)		
12	Combined	290.959	(42,200)		
	Tensile	122.037	(17,700)	116.521	(16,900)
	Shear	99.285	(14,400)	95.148	(13,800)
	Bending	168.922	(24,500)	161.337	(23,400)
	Bearing	243.385	(35,300)		
13	Combined	307.506	(44,600)		
	Tensile	110.316	(16,000)	105.490	(15,300)
	Shear	117.211	(17,000)	111.695	(16,200)
	Bending	196.501	(28,500)	187.537	(27,200)
	Bearing	434.370	(63,000)		
14	Combined	284.064	(41,200)		
	Tensile	118.590	(17,200)	113.074	(16,400)
	Shear	99.974	(14,500)	95.148	(13,800)
	Bending	165.474	(24,000)	157.890	(22,900)
	Bearing	367.491	(53,300)		
15	Combined	262.001	(38,000)		
	Tensile	108.937	(15,800)	104.111	(15,100)
	Shear	91.700	(13,300)	87.563	(12,700)
	Bending	153.064	(22,200)	146.169	(21,200)
	Bearing	337.843	(49,000)		

3.1.2.2.4 Oil Weep and Bore Cooling Air Holes

Two small holes (Figure 28) have been provided in front of the seventh and eighth stage disks to drain accumulated liquid. The stages inside the bore basket do not have drain holes since the center tube seals the area sufficiently to prevent oil from entering. Also, the bleed tubes will act as a centrifugal separator in the event that oil might inadvertently become entrapped in the drum bleed air.

The low cycle fatigue life (Table VIII) is adequate for rig and integrated core/low spool testing but does not meet the flight propulsion system design criteria. This life can be increased to meet that criteria by improving the hole surface finish.

The sixth stage hub bore cooling air holes are located in a low stress area and meet the low cycle fatigue requirements. The holes are located close enough to the disk bore to prevent a significant accumulation of oil. The front seal support flange was designed to meet the blade retention criteria. The flange is scalloped to shield the bolt holes and to drain any oil through holes in the continuous seal flange.

3.1.2.2.5 Solid Body Bleed Tube

The high-pressure compressor bleed shown in Figure 31 is located behind the 12th-stage blade. Radial tubes are provided to force solid body radial motion of the bleed air. There are 22 bleed tubes providing 20 cm^2 (3.1 in^2) of total flow area. The tubes are carried on the drum rim and are supported by a flange off the bore of the 12th-stage disk.

The entrance through the drum is race-track shaped to reduce the stress concentration to acceptable levels for integrated core/low spool operation. The 15,000 cycle life can be increased to the required 20,000 cycle flight propulsion system life by increasing the drum rim edge distance (Figure 31) to reduce the concentration. This space will be available, without increasing the rotor length, when adjustable stators in the rig are eliminated.

The bleed tubes are 0.051 cm (0.020 in) thick titanium sheet, with a machined support flange welded to the outer end. The outer end is flared into a conical recess in the drum rim to retain the tubes. The inner support has keyhole slots to facilitate assembly. When installed, the tubes have a 3-degree axial slope to clear the 12th disk bore. This slope causes a 4.45 kN (1,000 lb) total axial load and a resultant moment, both of which were included in the analysis of the disk and tube.
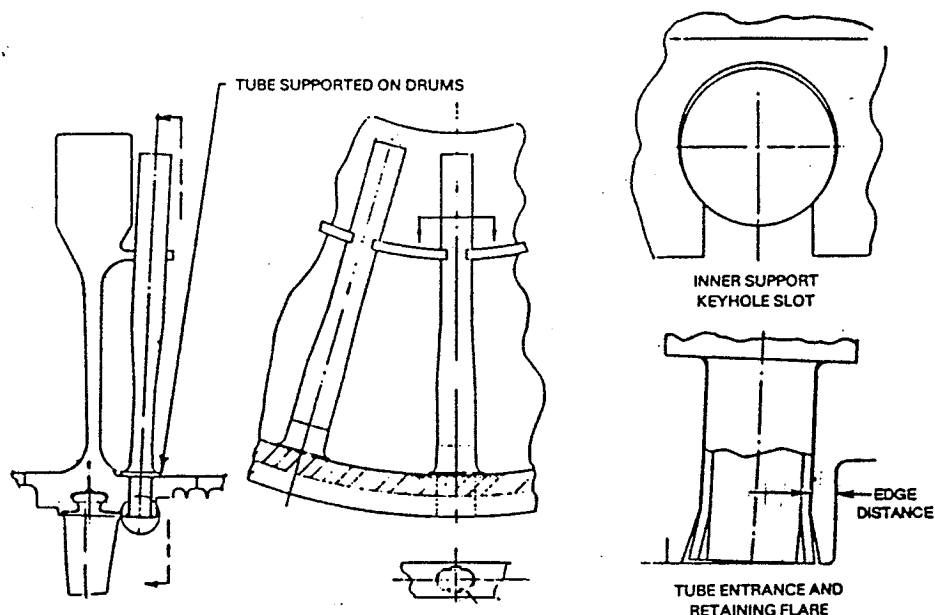
Figure 31   High-Pressure Compressor Solid Body Bleed Tube

3.1.2.2.6 Center Tube

The center tube, or bore basket, is used to seal the drum from the eighth stage rearward to the high-pressure compressor/high-pressure turbine flange, to ensure that proper turbine cooling and rotor thrust balance can be accomplished. A piston ring is employed on the front to provide a positive air seal with the support flange off the bore of the eighth stage disk. The support is isolated from the bore stresses by a thin conical section. The rear of the tube is supported by a flange off the high-pressure turbine spacer.

A lightweight thin tube with "I" section stiffeners has been designed for the flight propulsion system while the integrated core/low spool employs a heavier, less expensive, thick tube with no stiffeners. Figure 32 shows the center tube design for the flight propulsion system.

3.1.2.2.7 Knife-Edge Seals

The rotor features 0.254 cm (0.100 in) flow guides on both sides of the ninth through fourteenth inner diameter cavities. Figure 33 shows a typical inner cavity. The integral knife-edge seals are shown. A silicon carbide coating will be used in the flight propulsion system to improve seal wear characteristics. It is not required for the experimental test programs. The clearances shown are goal values; actual clearances vary slightly stage-to-stage as shown in Table XII.

A four knife-edge front seal is attached to the front of the sixth-stage disk by 18 bolts and self-locking nuts (Figure 34); bolt diameter: 0.635 cm (0.250 in). The seal mounting flange is deeply scalloped to allow oil draining and provides a mount position for balance weights, as required.

PISTON RING SEAL   CENTER TUBE

WELD
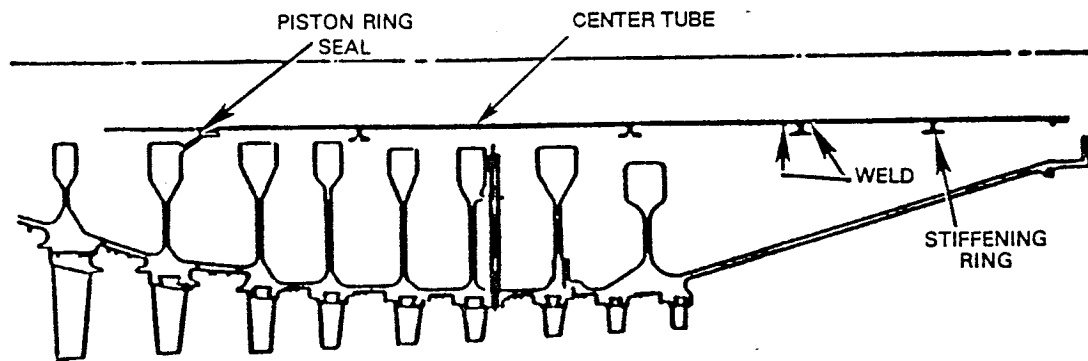
STIFFENING RING

FLIGHT PROPULSION SYSTEM
• ELEVEN PIECE — LIGHT WEIGHT TUBE CONSTRUCTION
• FOUR STIFFENING RINGS TO CONTROL RESONANCE
• PISTON RING SEAL ON FRONT SUPPORT

INTEGRATED CORE/LOW SPOOL
• THREE PIECE — LOW COST TUBE CONSTRUCTION
• TUBE THICKNESS SET TO CONTROL RESONANCE (NO STIFFENING RINGS)
• PISTON RING SEAL ON FRONT SUPPORT

Figure 32   High-Pressure Compressor Center Tube Design

SMOOTH ABRASIVE
(FLIGHT PROPULSION ONLY)

0.254 CM
(0.100 IN)

0.038 CM
(0.015 IN)

0.254 CM
(0.100 IN)

ABRADABLE

R-11   S-11   R-12
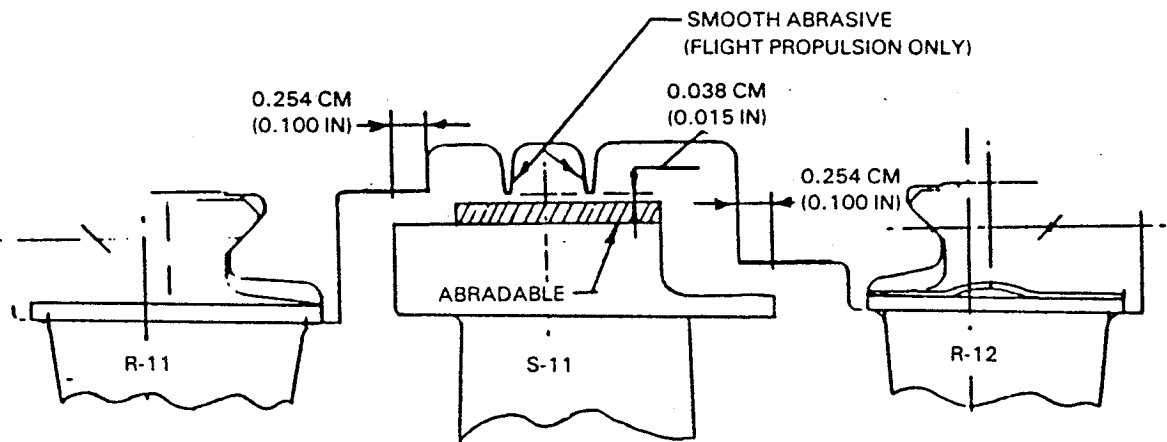
HOT POSITION — SHOWING POSITIVE RADIAL OVERLAPS
FLOWGUIDE ON STATOR TRAILING EDGE

S6-S8 = RUBBER
S9-S14 = ABRADABLE

Figure 33   High-Pressure Compressor Inner Cavity Seals

52

TABLE XII

KNIFE-EDGE SEAL GAPS
INTEGRATED CORE/LOW SPOOL

Stator	Sea Level Takeoff Gap, cm (in)		Cold Gap, cm (in)	
Inlet Guide Vane	0.038	(0.015)	0.064	(0.025)
6	0.038	(0.015)	0.064	(0.025)
7	0.038	(0.015)	0.066	(0.026)
8	0.038	(0.015)	0.071	(0.028)
9	0.038	(0.015)	0.081	(0.035)
10	0.028	(0.011)	0.081	(0.035)
11	0.030	(0.012)	0.097	(0.038)
12	0.064	(0.025)	0.130	(0.051)
13	0.043	(0.017)	0.140	(0.055)
14	0.038	(0.015)	0.094	(0.037)
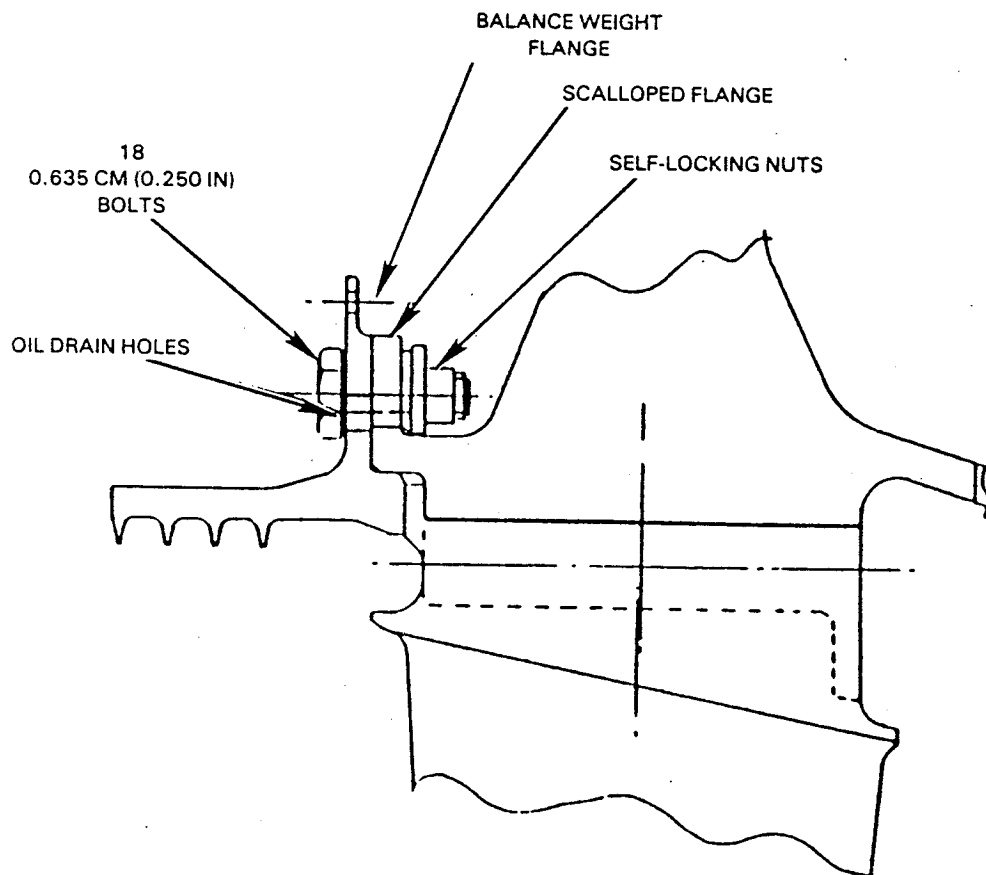
Figure 34   High-Pressure Compressor Front Seal Design

3.1.2.2.8 Rotor Tie-Bolts

Thirty-six Inconel 718 bolts, 0.794 cm (0.3125 in.) in diameter (Figure 35) are used at the drum-to-tandem disk joint for the integrated core/low spool. Torque is specified to set bolt preload rather than angle of turn because of the difficulty in measuring angle inside the rotor.

To establish the torque/tension relationship with the self locking nut, a preliminary dummy stack bolting procedure is specified for use during assembly. This dummy stack will establish the torque to be used during final assembly.

Assembly load per bolt is 26.689 kN (6000 lb), which results in a bolt tensile stress of 772.240 MPa (112,000 psi). Table XIII summarizes the bolt design information.
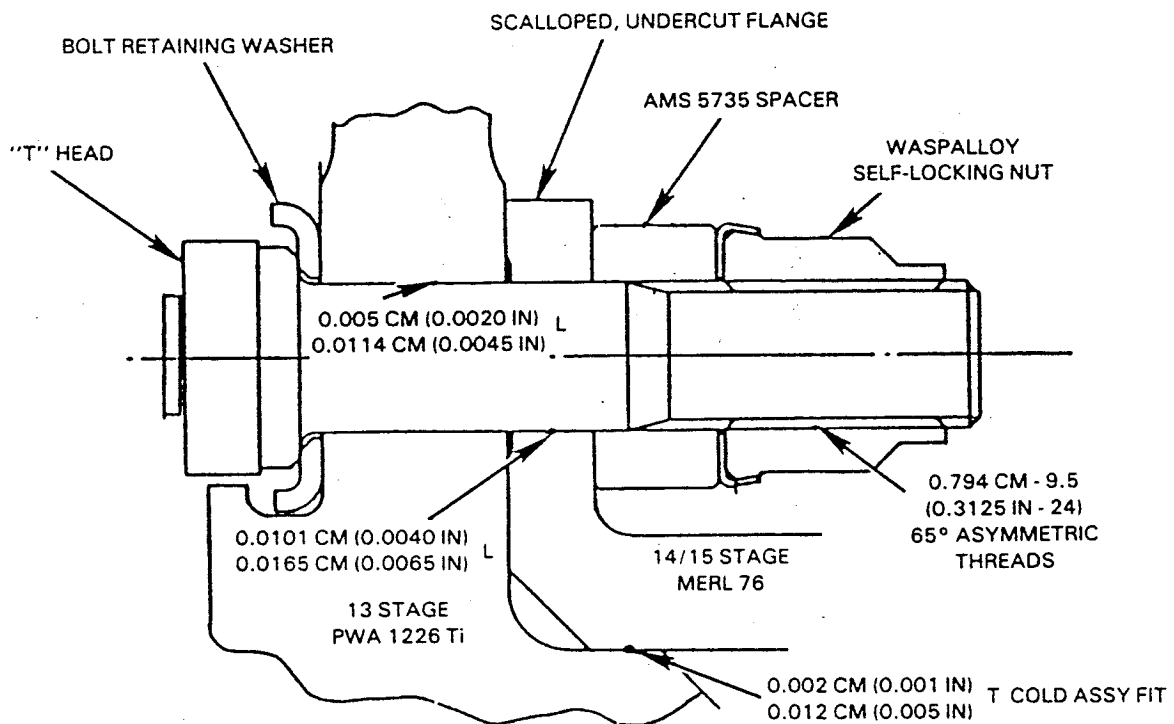
Figure 35   Mid-Compressor Tie-Bolt Configuration

54

TABLE XIII

ROTOR TIE-BOLT DESIGN INFORMATION

36 Bolts; 0.794 cm (0.3125 in. diameter); 24 UNIF Thread
(Except Asymmetric Flight Propulsion System Only)

	Integrated Core/Low Spool	Flight Propulsion System
Material	PWA 96 (INCO 718)	MP 159 (cobalt alloy)
Loads:		
Cold Preload, kN (lb)	26.689 (6000)	41.813 (9400)
Bolt at Joint Separation, kN (lb)	19.483 (4380)	37.427 (8414)
Clamping Ratio	1.36	1.67
Stresses, MPa (psi):		
Assembly Tensile	772.240 (112,000)	1227.267 (178,000)
Assembly Principal Shear at Coeff. of Friction = 0.05	503.317 (73,000)	813.581 (118,000)
Assembly Thread Shear (Nut)	217.874 (31,600)	341.980 (49,600)
Separation Tensile	571.575 (82,900)	1165.214 (169,000)
Separation Principal Shear	300.611 (43,600)	586.054 (85,000)
Separation Thread Shear (Nut)	158.579 (23,000)	322.675 (46,800)
Rotor Seizure Bolt Shear	74.463 (10,800)	74.463 (10,800)
Low Cycle Fatigue Life (cycles)	10,000	30,000
Blade Loss Parameters	1.47	1.47
Creep Life (hours)	10,000	10,000

3.1.2.3 Blades

3.1.2.3.1 General Description

Multiple circular arc airfoils are used in rotors 6 and 7 and controlled diffusion airfoils are used in rotors 8 through 15. Axial attachments are used on rotors 6 through 8 and tangential broaches are used on the remainder of the blades. The blade attachments are similar to earlier designs to maximize use of existing tooling.

Blade tilts were computed to give low airfoil leading and trailing edge buckling stresses at takeoff. Blade radial lengths were set 0.127 cm (0.050 in) over the cold span to permit grinding in assembly to obtain accurate cold gaps. Foil untwist was calculated at the aerodynamic design point.

Axial-attachment blades are retained by a trapped tang on the sixth stage behind the knife-edge seal and by shear pin locks on the seventh and eighth stages. The tangential-attachment blades use turreted "in groove" locks. These locks are loaded through slots in the rotor disk rim, slid into position one blade pitch either way, and are elevated into the disk rim lock slots with trapped, internally wrenched jack screws.

Airfoils are glass bead peened for fatigue strength improvement and subsequently burnished to obtain a 20AA smoothness on aerodynamic surfaces. A general description of all blades is presented in Table XIV.

3.1.2.3.2 Blade Attachments

For the axial attachments used in the sixth, seventh, and eighth stage blades, standard broach chart tools were selected for tool availability and most favorable bearing stress factors. Broach angles were set at 15 degrees to obtain reasonable airfoil overhang limits while meeting stress ratio requirements.

For the tangential attachments used in the ninth through fifteenth stages, experience in rig and engine running suggested the use of the existing tooth profiles with new neck widths tailored to the Energy Efficient Engine requirements. Nickel alloy blades are utilized in the eighth stage for fire avoidance. Use of this material did not compromise limits on the titanium disk rim loads or bearing stresses.

3.1.2.3.3 Platforms

Platforms were designed to avoid resonant vibration. Curling and buckling loads were checked and found to be within experience ranges. Airfoil overhangs on the rearmost stages are large, but low airfoil loadings compensate for the large overhang.

Platform widths are sized for zero gap at assembly. This is accomplished by using oversize blade platforms as needed to share dimension adjustments. The ladder-seal clearance hole is sized to accommodate these adjustments. It also acts to damp free vibration, but no credit for this damping was taken in the platform frequency calculations.

The fillet radius at the airfoil/platform interface is 0.368 cm (0.145 in) for stage six, 0.198 cm (0.078 in) for stage seven, and 0.127 cm (0.050 in) for all other stages.

56

TABLE XIV

HIGH-PRESSURE COMPRESSOR GENERAL BLADE DESCRIPTION

	R6	R7	R8	R9	R10	R11	R12	R13	R14	R15
Materials: Test Rig	PWA 1202	PWA 1202	PWA 1003	PWA 1003	PWA 1003	PWA 1003	PWA 1003	PWA 1003	PWA 1003	PWA 1003
Flt. Proplsn. System	PWA 1202	PWA 1202	PWA 1010	PWA 1010	PWA 1010	PWA 1010	PWA 1010	PWA 1010	PWA 1010	PWA 1010
Integ. Core/Low Spool	AMS 4928	AMS 4928	PWA 1010	PWA 1010	PWA 1010	PWA 1010	PWA 1010	PWA 1010	PWA 1010	PWA 1010
Airfoil Series *	MCA	MCA	CDA	CDA	CDA	CDA	CDA	CDA	CDA	CDA
No. of Blades	26	50	60	66	62	56	64	70	76	78
Root radius (hot), cm	17.399	20.173	21.887	22.987	23.584	24.016	24.237	24.282	24.282	24.282
(in.)	(6.850)	(7.942)	(8.617)	(9.050)	(9.285)	(9.455)	(9.542)	(9.560)	(9.560)	(9.560)
Tip radius (hot), cm	29.680	29.093	28.811	28.382	28.064	27.719	27.422	27.069	26.800	26.543
(in.)	(11.685)	(11.454)	(11.343)	(11.174)	(11.049)	(10.913)	(10.796)	(10.657)	(10.551)	(10.450)
Root chord, cm	7.087	3.823	3.440	3.0096	2.6220	2.9246	2.5695	2.31120	2.13093	2.07513
(in.)	(2.790)	(1.505)	(1.354)	(1.1849)	(1.0323)	(1.1514)	(1.0116)	(0.90992)	(0.83895)	(0.81698)
Tip chord, cm	9.063	4.100	3.025	2.7242	2.6271	2.9256	2.56642	2.30883	2.12903	2.07147
(in.)	(3.568)	(1.614)	(1.191)	(1.0725)	(1.0343)	(1.1518)	(1.0104)	(0.90899)	(0.83820)	(0.81554)
Max thickness/chord, root	0.097	0.08154	0.0906	0.0974	0.1006	0.1115	0.101	0.101	0.1011	0.1007
Max thickness/chord, tip	0.0237	0.0467	0.0454	0.0454	0.0456	0.0406	0.0457	0.0458	0.0461	0.0457
Camber, root, deg	69.4	50.1	44.5	45.0	48.2	49.4	51.2	47.2	47.1	38.5
Camber, tip, deg	16.9	20.6	25.0	28.5	33.6	33.0	30.0	31.1	30.2	28.9
Chord angle, root, deg	72.3	70.7	70.2	65.9	60.8	57.2	58.9	55.2	52.0	45.6
Chord angle, tip, deg	33.7	37.4	36.1	37.6	37.3	37.4	38.1	37.4	36.9	36.1
Aspect ratio, average	1.733	2.332	2.000	1.786	1.697	1.258	1.235	1.206	1.181	1.089
Hub/tip ratio, average	0.586	0.694	0.761	0.811	0.841	0.867	0.884	0.897	0.906	0.915
Tip Speed, m/sec	443	435	430	424	419	413	410	404	401	297
(ft/sec)	(1455)	(1426)	(1412)	(1391)	(1376)	(1356)	(1344)	(1327)	(1314)	(1301)
Broach type	Axial	Axial	Axial	Tangential	Tangential	Tangential	Tangential	Tangential	Tangential	Tangential

* See List of Symbols

57

3.1.2.3.4 Sealing

Sixth and seventh stage axial-attachment blades incorporate silicone rubber lip seals along one platform edge. Disk flange "dams" will be fitted under the aft ends of these conical platforms to inhibit gas recirculation. The axial-attachment blades in the eighth stage incorporate polyimide tip seals along one platform edge and flange drums similar to the sixth and seventh stages.

All tangential stages are fitted with light sheet-metal ladder seals (Figure 36) except at the locking and loading slots. These seals incorporate a precurved "rung" section which, under centrifugal forces, expands the seal rails axially against the disk rim lips to provide further sealing around platform edges.
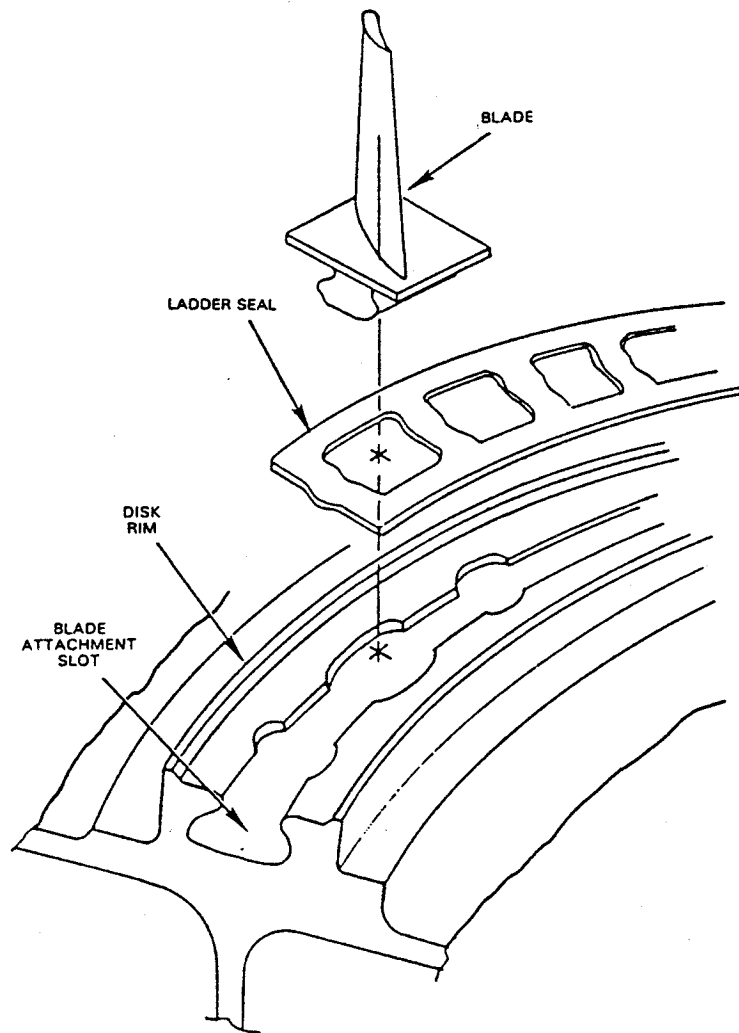
Figure 36   Sheet-Metal Ladder Seal

3.1.2.3.5 Locks

Axial-attachment blades are retained by shear pins for the seventh and eighth stages and by a tang on the sixth stage. Tangential-attachment blades use turret "in groove" locks. These locks are loaded through slots, slid into position one pitch either way, and elevated into disk rim lock slots with trapped, internally wrenched jack screws. Titanium locks are used for ninth through thirteenth stages and nickel alloy locks in the fourteenth and fifteenth stages. Screws are held in position by self locking helicoil inserts.

3.1.2.3.6 Surface Finish

Airfoils are glass bead peened for fatigue strength improvement and subsequently burnished in a cutting medium to obtain 20AA smoothness on aerodynamic surfaces. Performance goals requiring this level of airfoil smoothness will require blade coating against erosion to preserve the surface finish. Blade attachments are shot peened for improved fatigue strength and treated with antigalling materials.

3.1.2.3.7 Blade Vibration Analysis

All rotors have been tuned to avoid low order and other critical resonances between minimum cruise and red-line rotor speed. Frequency margins were determined as required by commercial engine design practice using a coupled bending-torsion beam analysis. Particular attention was paid to stages 6 and 7, which were tuned to avoid a 10E (intermediate case strut order) resonance in the engine operating range. Sufficient chord was included in both of these stages to avoid a 2E first mode resonance. Stages 8 and 9 were stiffened in the root area of the blade to provide margin on 3E first mode and 4E first mode resonances, respectively. The ninth stage was considered particularly critical, because of the bleed extraction immediately forward of this stage. The eleventh stage gap-to-chord ratio (τ/b) distribution was revised to provide frequency margin on an 8E first mode resonance at red-line speed. This change was made to avoid a stator order of 8 in the immediate area. The remaining stages did not require further resonance tuning. Resonance diagrams are shown in Figures 37 through 46. Note that rotor 15 was tuned to avoid possible excitation from downstream diffuser case struts.

All rotor blades are within the bending and torsion flutter limits as defined by flutter experience curves (Figures 47 and 48).

All blade platforms have been sized to provide acceptable frequency margin on adjacent vane passing orders. Axial and tangential attachments have been designed to provide adequate low cycle fatigue life under normal vibratory loading.
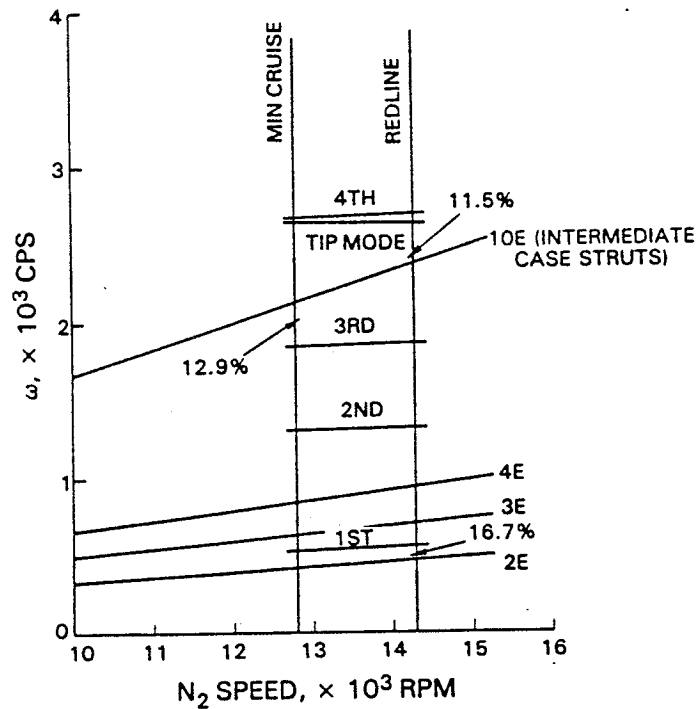
Figure 37   Resonance Diagram for Energy Efficient Engine, High-Pressure
             Compressor, Rotor 6
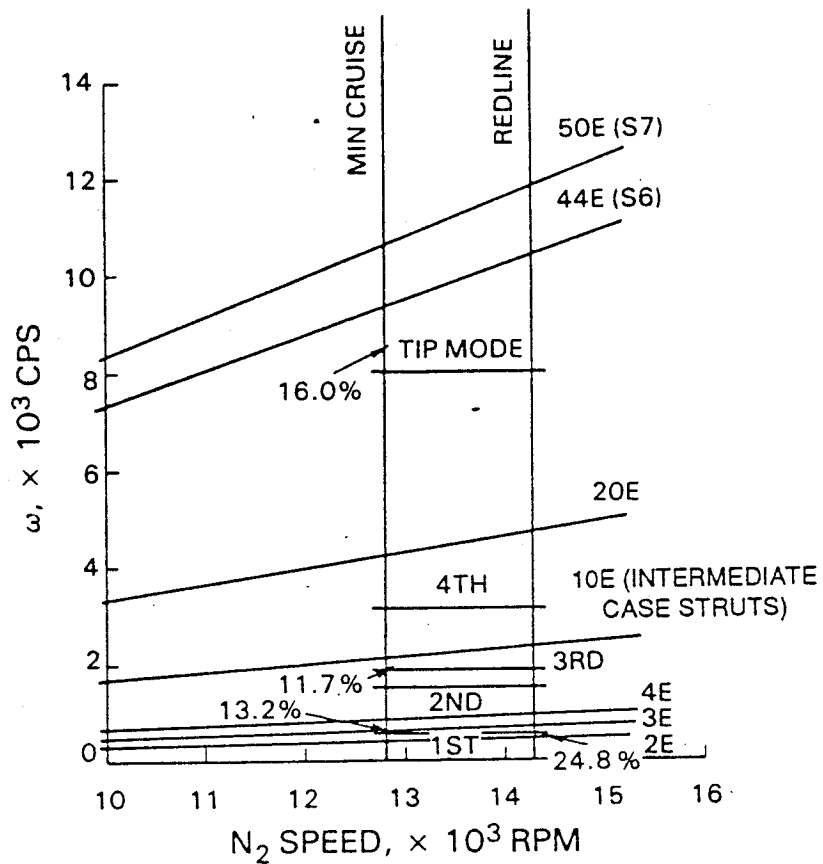
Figure 38   Resonance Diagram for Energy Efficient Engine, High-Pressure
             Compressor, Rotor 7

60
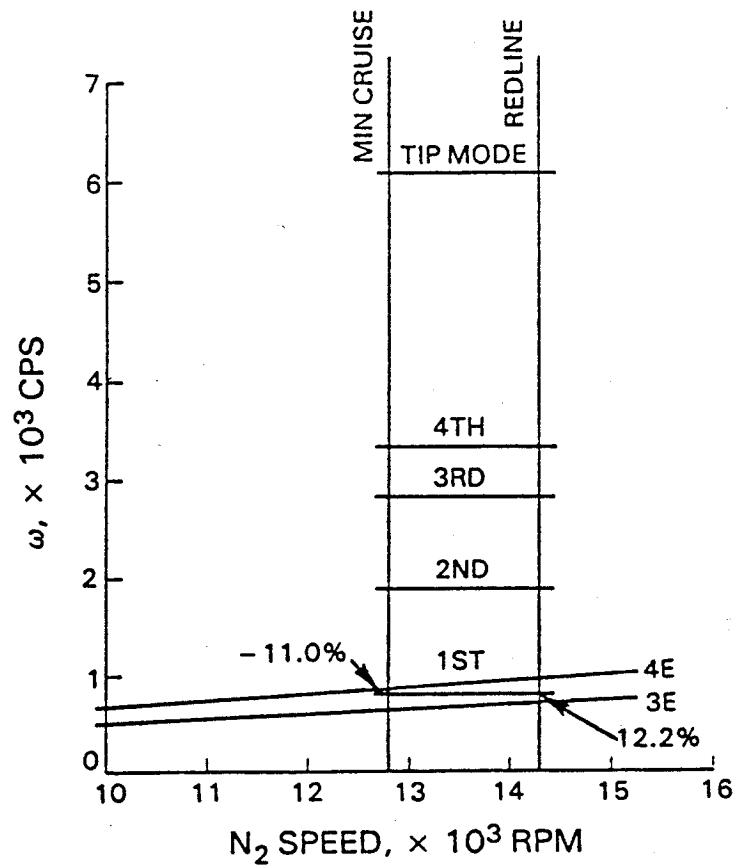
Figure 39   Resonance Diagram for Energy Efficient Engine; High-Pressure Compressor, Rotor 8
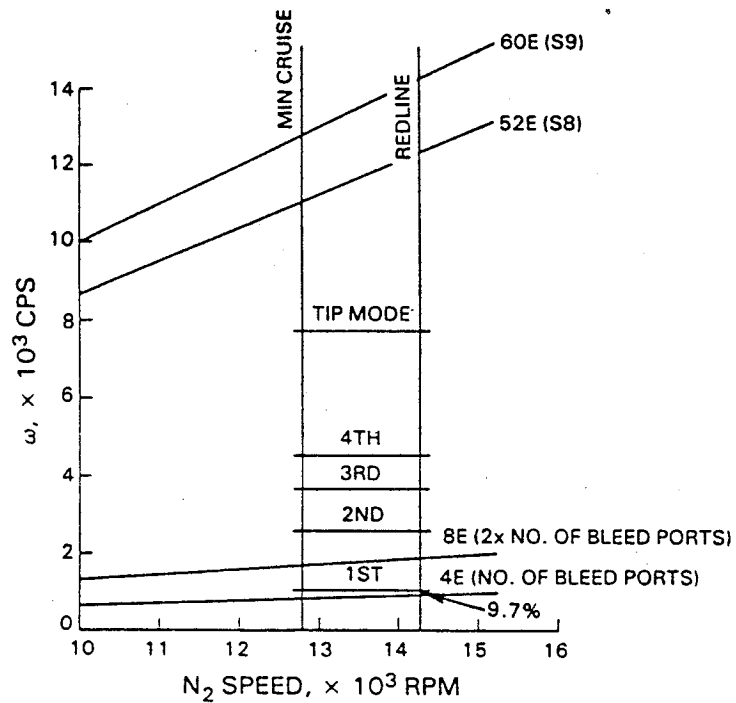
Figure 40   Resonance Diagram for Energy Efficient Engine, High-Pressure Compressor, Rotor 9
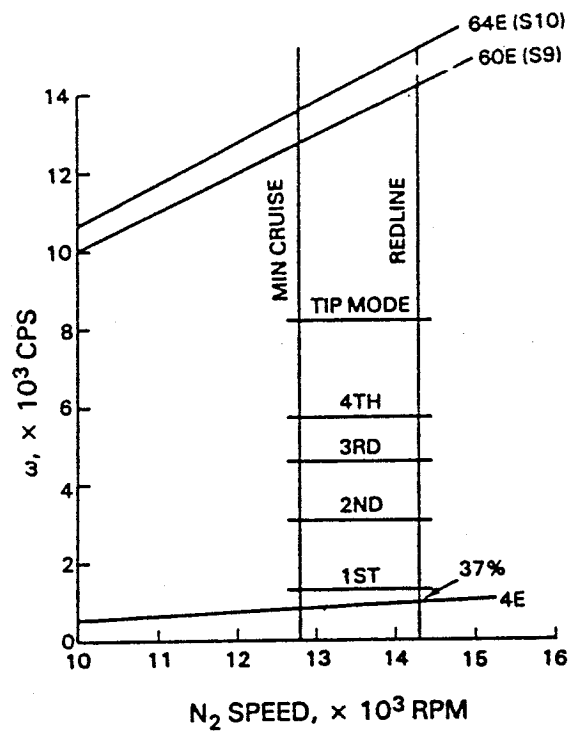
Figure 41   Resonance Diagram for Energy Efficient Engine, High-Pressure
             Compressor, Rotor 10
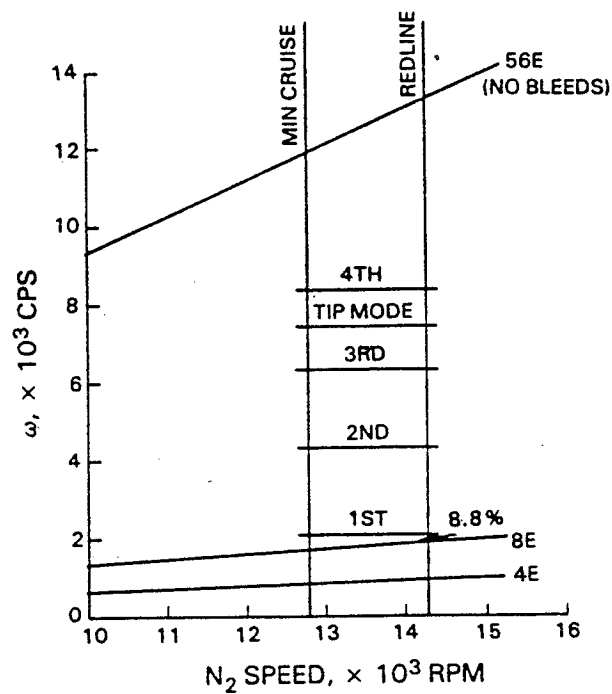
Figure 42   Resonance Diagram for Energy Efficient Engine, High-Pressure
             Compressor, Rotor 11
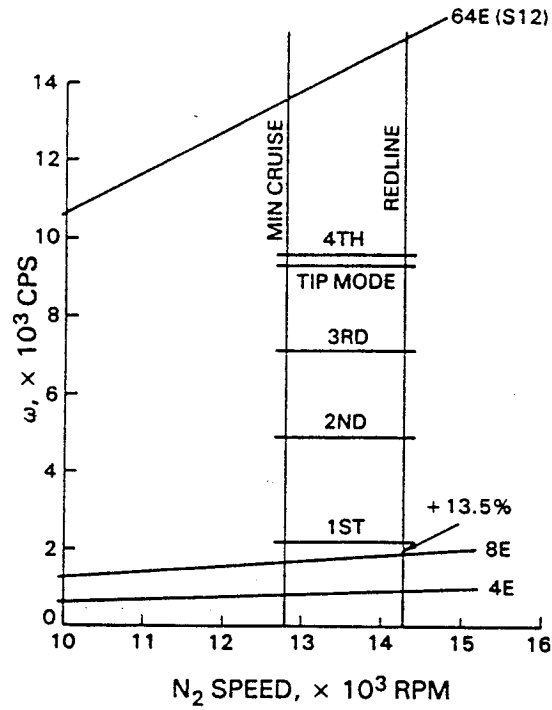
Figure 43   Resonance Diagram for Energy Efficient Engine, High-Pressure
             Compressor, Rotor 12
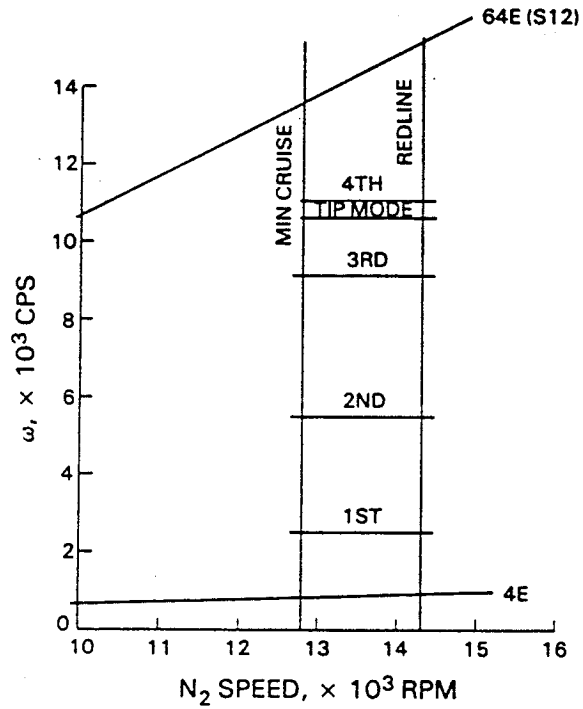
Figure 44   Resonance Diagram for Energy Efficient Engine, High-Pressure
             Compressor, Rotor 13
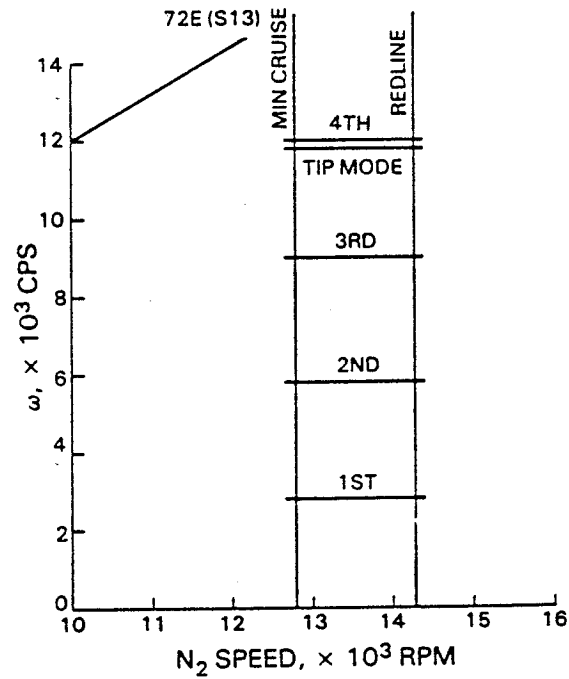
Figure 45   Resonance Diagram for Energy Efficient Engine, High-Pressure
             Compressor, Rotor 14
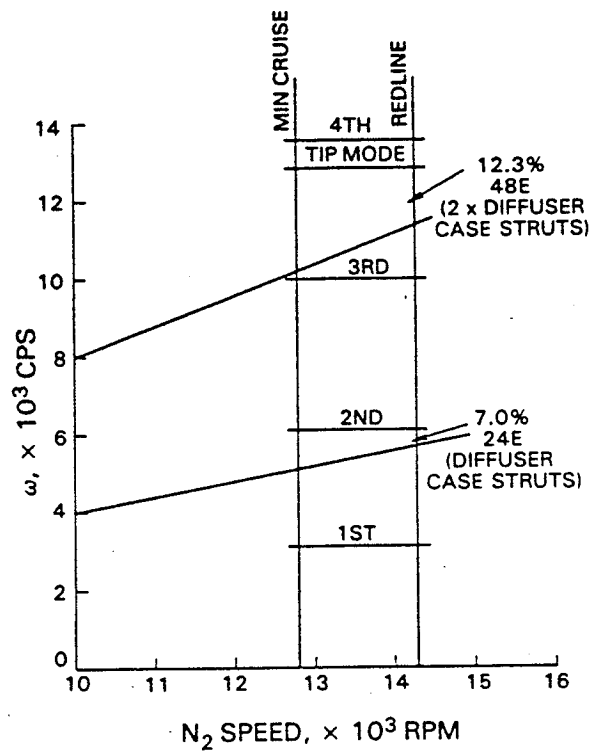
Figure 46   Resonance Diagram for Energy Efficient Engine, High-Pressure
             Compressor, Rotor 15
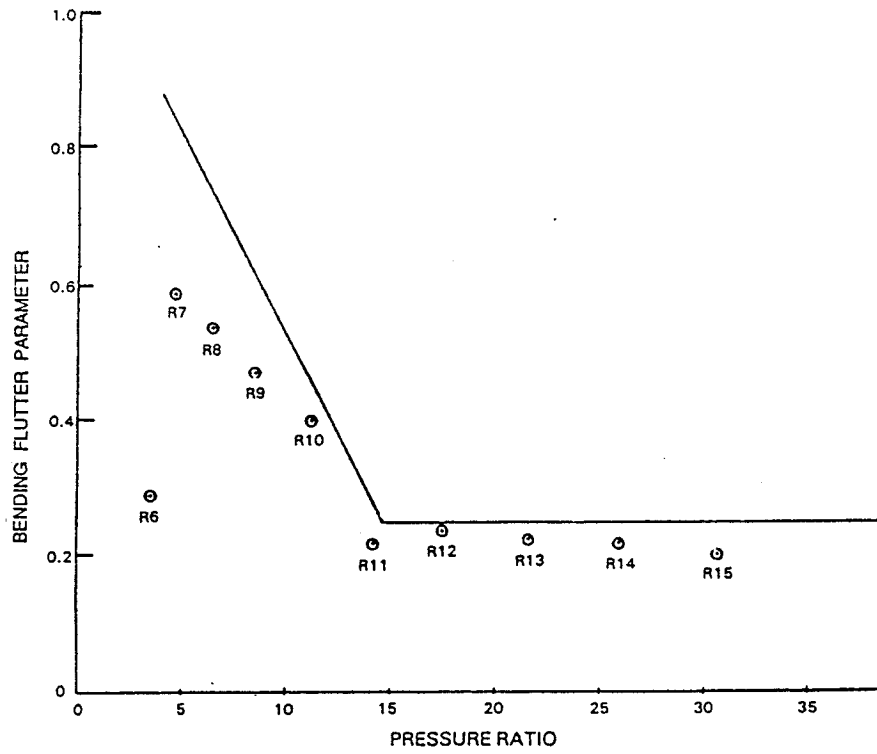
Figure 47   Energy Efficient Engine High-Pressure Compressor Rotor Bending
Flutter
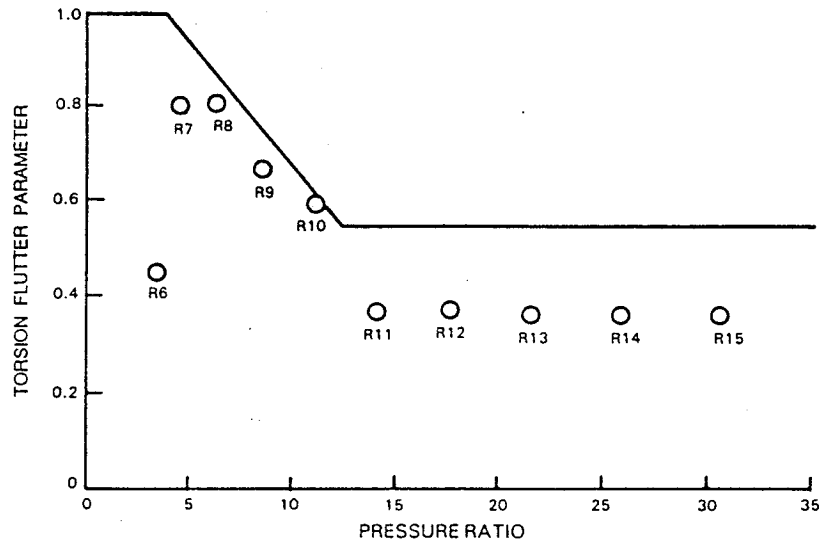
Figure 48   Energy Efficient Engine High-Pressure Compressor Rotor Torsional
Flutter

3.1.2.4 Rotor Assembly and Balance Procedure

For the flight propulsion system, the titanium drum and tandem disk units are individually bladed and balanced as subassemblies. They are bolted together with flange face runouts opposed to minimize rotor bow. Final rotor balance is then done in the two end planes, with allowance made for the addition of weights at the rotor joint, if necessary, to provide for balance adjustments. Standard saddle counter weights are used at the front and rear balance planes and dovetail groove counter weights are used at R-13 and R-14 of the subassemblies.

Integrated core/low spool and component test rig balance procedures differ from the flight propulsion system in that the subassembly balance is done without blades. The different approach is due to the difficulty of removing instrumented blades, once installed, in order to add dovetail balance weights. Dovetail counter weight locations and amounts are determined for the unbladed rotor and then the weights are installed when the rotor is bladed. Since the major portion of the subassembly imbalance will result from the drum weldment rather than the blades, this procedure is satisfactory. Final assembly balance is accomplished at the front and rear balance flanges, as in the flight propulsion system.

3.1.2.5 Blade Length Determination

To ensure attainment of optimum blade tip to case clearances, the blade tips will be ground to final dimension at assembly. The final dimension is calculated by subtracting the cold build clearance for the particular stage from the actual as-machined case rub-strip diameter. Blade tip to case clearances for the integrated core/low spool, cold and at sea level takeoff, are shown in Table XV.

3.1.2.6 Rotor Materials

A summary of materials to be used in the rotors of the test rig, integrated core/low spool, and flight propulsion system is shown in Figure 49.

66

TABLE XV

ROTOR BLADE TIP CLEARANCE
INTEGRATED CORE/LOW SPOOL

Rotor	Sea Level Takeoff Clearance, cm (in)		Cold Clearance, cm (in)	
6	0.041	(0.016)	0.079	(0.031)
7	0.038	(0.015)	0.086	(0.034)
8	0.036	(0.014)	0.109	(0.043)
9	0.030	(0.012)	0.079	(0.031)
10	0.025	(0.010)	0.084	(0.033)
11	0.025	(0.010)	0.091	(0.036)
12	0.030	(0.012)	0.097	(0.038)
13	0.041	(0.016)	0.099	(0.039)
14	0.036	(0.014)	0.119	(0.047)
15	0.033	(0.013)	0.090	(0.035)
Average	0.0335	(0.0132)	0.0932	(0.0367)
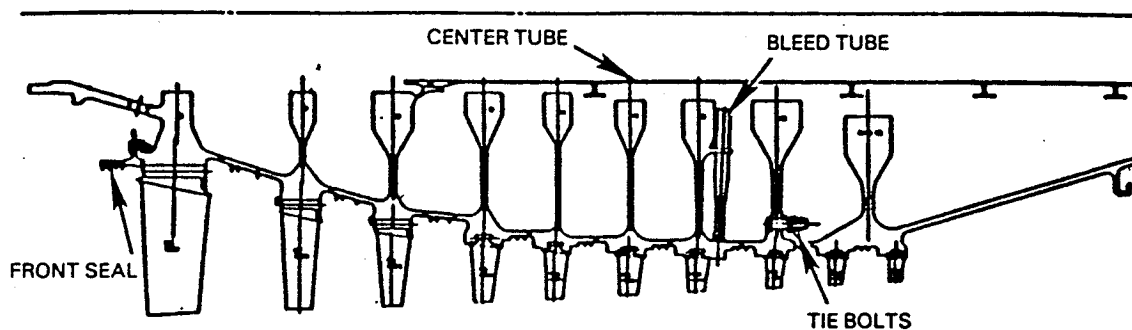
ITEM	STAGE	RIG	INTEGRATED CORE/LOW SPOOL	FLIGHT PROPULSION SYSTEM
DISKS	R6-7	AMS 4928 (6-4 TI)	AMS 4928 TI	4928 TI
	R 8-11	PWA 1209 (6-2-4-2)	PWA 1224 (6-2-4-2 TI)	PWA 1224 TI
	R 12-13	PWA 1226 (6-2-4-2 TI)	PWA 1226 TI	PWA 1226 TI
	R 14/15	PWA 1099 N1	PWA 1099 NI	MERL 80 TI
BLADES	R 6-7	PWA 1202 (8-1-1 TI)	AMS 4928 TI	PWA 1202 TI
	R 8-15	PWA 1003 NI	PWA 1010 NI	PWA 1010 NI
FRONT SEAL	6	AMS 4928 TI	AMS 4928 TI	AMS 4928 T
CENTER TUBE		AMS 5613 ST	AMS 5613 ST	AMS 5613 ST
BLEED TUBE	12	AMS 4911 (6-4 TI)	AMS 4911 TI	AMS 4911 TI
TIE BOLTS	13	PWA 92 (WASPALLOY)	PWA 96 NI	MP 159 NI

Figure 49   High-Pressure Compressor Rotor Materials Summary

3.1.3 Front Case and Stator Assembly

3.1.3.1 General Description

The compressor front case provides the base for four variable vane rows (inlet guide vane through the eighth stage stator). The titanium case is split into equal, 180-degree segments with bolt flanges located at the horizontal center line. Steel inserts are used under the blade tip abradable to prevent blade tip contact with the titanium case and provide fire avoidance in the event of severe blade rub or blade loss. Pressed-in bushings are used in the case to support the variable vanes.

The inner shroud design consists of a two-piece half ring construction, pinned and bolted together. Incorporated in the shroud is a bushing to support the inner diameter vane trunnion.

Vane actuation levers and unison rings with slide type mountings are used to operate the variable geometry vanes. A general description of the front case and stator assembly is shown in Figure 50.

3.1.3.2 Materials

The case and axial flanges are AMS 4928 titanium. An AMS 5504 steel insert is used in the flight propulsion system under rubber on the blade rub strips. Vanes and inner shrouds are fabricated from AMS 5613 steel. A summary of the case and stator assembly materials is shown in Figure 51.

3.1.3.3 Case Design and Analysis

The case was designed to meet the requirements of the flight propulsion system. It meets these requirements with minimum machining. With considerable skip turning between the surface required for the unison ring bearing pads, additional weight could be saved without compromising case integrity. The case is modified at two locations for use in the integrated core/low spool to allow incorporation of blade tip clearance probes. Borescope bosses are provided at suitable locations to allow direct viewing of the flowpath hardware.

Structural analysis of the front and rear compressor cases employed the same analytical procedures that were utilized in the rotor design. A finite element analysis of the temperature distributions within the case structure was used to provide input data for the structural (shell) analysis routine. Figure 52 shows the thermal analysis model, and Table XVI indicates some typical temperature distributions at two of the engine operating conditions. Figure 53 shows the complementary structural analysis model for the front case.

Thermal buckling and ovalization analyses were performed to ensure that case deflections and stresses were within allowable limits. The case was designed to meet Pratt & Whitney commercial engine allowable stresses, and case thickness was sized to withstand fan blade loss as well as to contain a compressor blade loss. A front case stress summary is shown in Figure 54.

RUBBER TIP AND
INNER AIR SEALS

TYPICAL VARIABLE
GEOMETRY VANE WITH
LEADING EDGES ON
BUTTONS

180° INNER
SHROUD SEGMENTS

IGV

S6

S7

S8

SLIDER TYPE
MOUNTING SYSTEM

SPLIT FRONT CASE
2 AXIAL FLANGES

POLYIMIDE AND GRAPHITE
BEARINGS

STEEL INSERTS TO
PREVENT TITANIUM RUBS
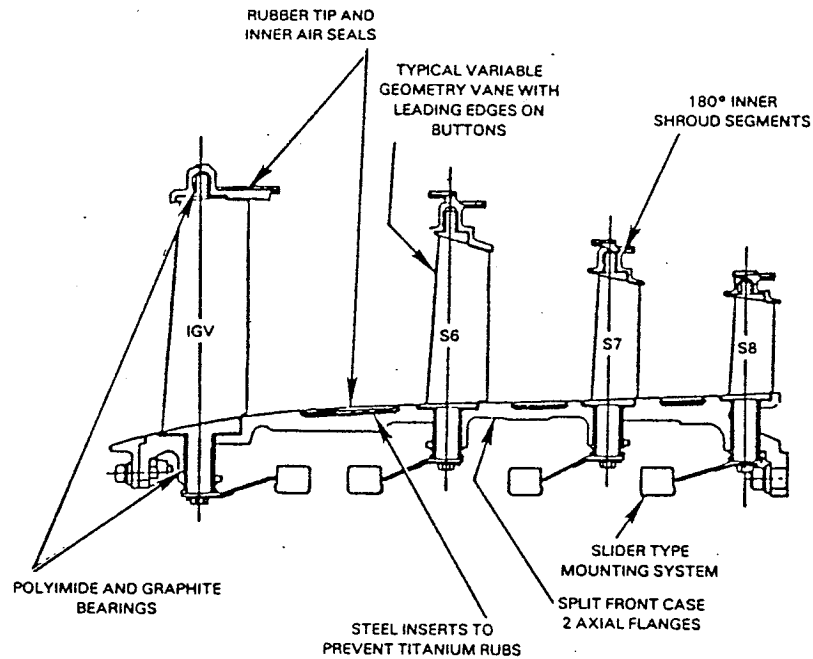
Figure 50   High-Pressure Compressor Front Case and Stator Assembly

INNER AIR SEALS
(RUBBER)

BUSHINGS
VESPEL-21

VANES
AMS5613

INNER SHROUDS
AMS 5613

TIP SEALS
(RUBBER)

IGV

S6

S7

S8

STEEL
INSERT
AMS 5504

CASE
AMS 4928

ACTUATOR LEVER
ARMS AMS 5504

BUSHINGS
FABROID-X

UNISON RING
AMS 4132
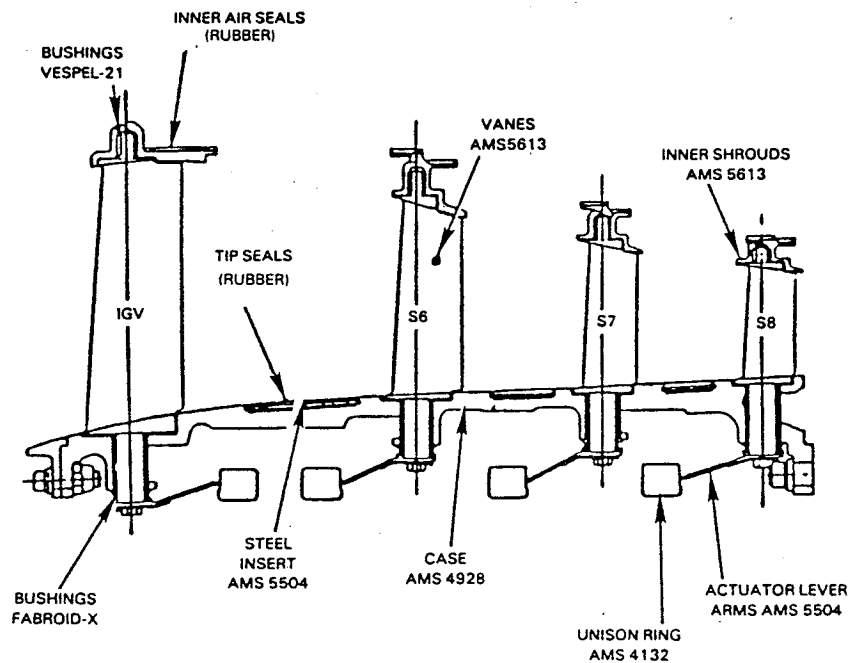
Figure 51   High-Pressure Compressor Front Case and Stator Assembly Materials

TABLE XVI

CASE THERMALS

MINIMUM TEMPERATURE REGIONS:

NODE NUMBER	FIG. 52 REF.	TEMP. AT ADP °F (°C)	TEMP. AT TAKEOFF °F (°C)
10		157 (69)	257 (125)
11		154 (67)	253 (122)
12	A	141 (60)	234 (112)
13		134 (56)	225 (107)
14		125 (51)	212 (100)
19		157 (69)	258 (125)
20	B	158 (70)	258 (125)
21		158 (70)	258 (125)
22		158 (70)	258 (125)
85		412 (211)	553 (289)
86	C	405 (207)	523 (272)
87		395 (201)	509 (265)
89		246 (118)	304 (151)
90	D	262 (127)	324 (162)
91		293 (145)	365 (185)
99		327 (164)	411 (210)

MAXIMUM TEMPERATURE REGIONS:

NODE NUMBER	FIG. 52 REF.	TEMP. AT ADP °F (°C)	TEMP. AT TAKEOFF °F (°C)
366		880 (471)	1038 (558)
367		882 (472)	1040 (560)
368		883 (472)	1041 (560)
374	E	882 (472)	1039 (559)
373		879 (470)	1035 (557)
369		871 (466)	1025 (551)
370		861 (460)	1013 (545)
371		850 (454)	1000 (537)
396		759 (403)	865 (462)
397		779 (415)	891 (477)
398		885 (473)	1033 (556)
406		924 (495)	1084 (584)
407		931 (499)	1092 (588)
408		936 (502)	1098 (592)
418	F	939 (503)	1103 (595)
419		943 (506)	1106 (596)
420		943 (506)	1107 (596)
421		943 (506)	1107 (596)
422		943 (506)	1107 (596)

E³HIGH COMPRESSOR FRONT AND REAR CASE A
THERMAL ANALYSIS MODEL
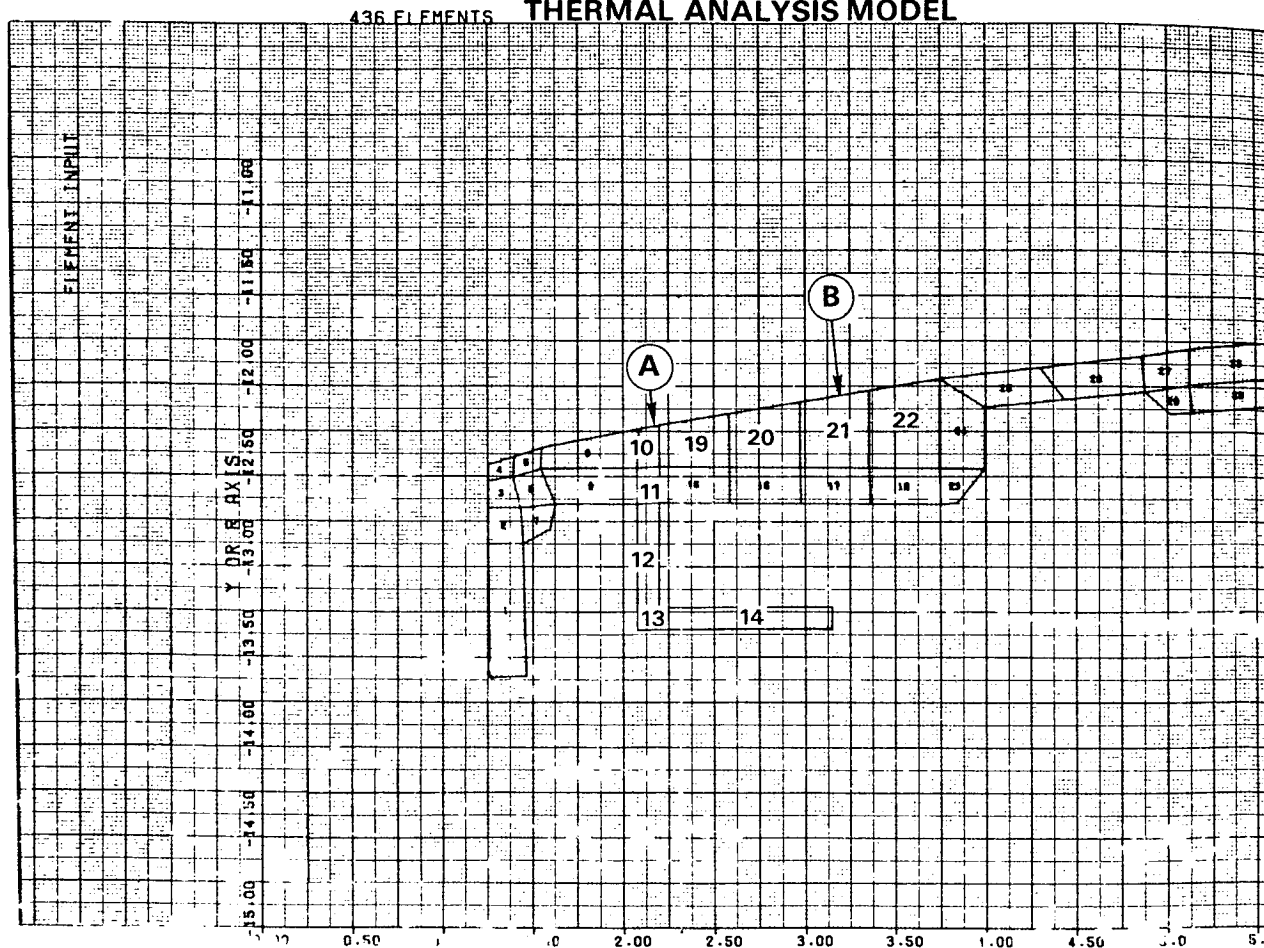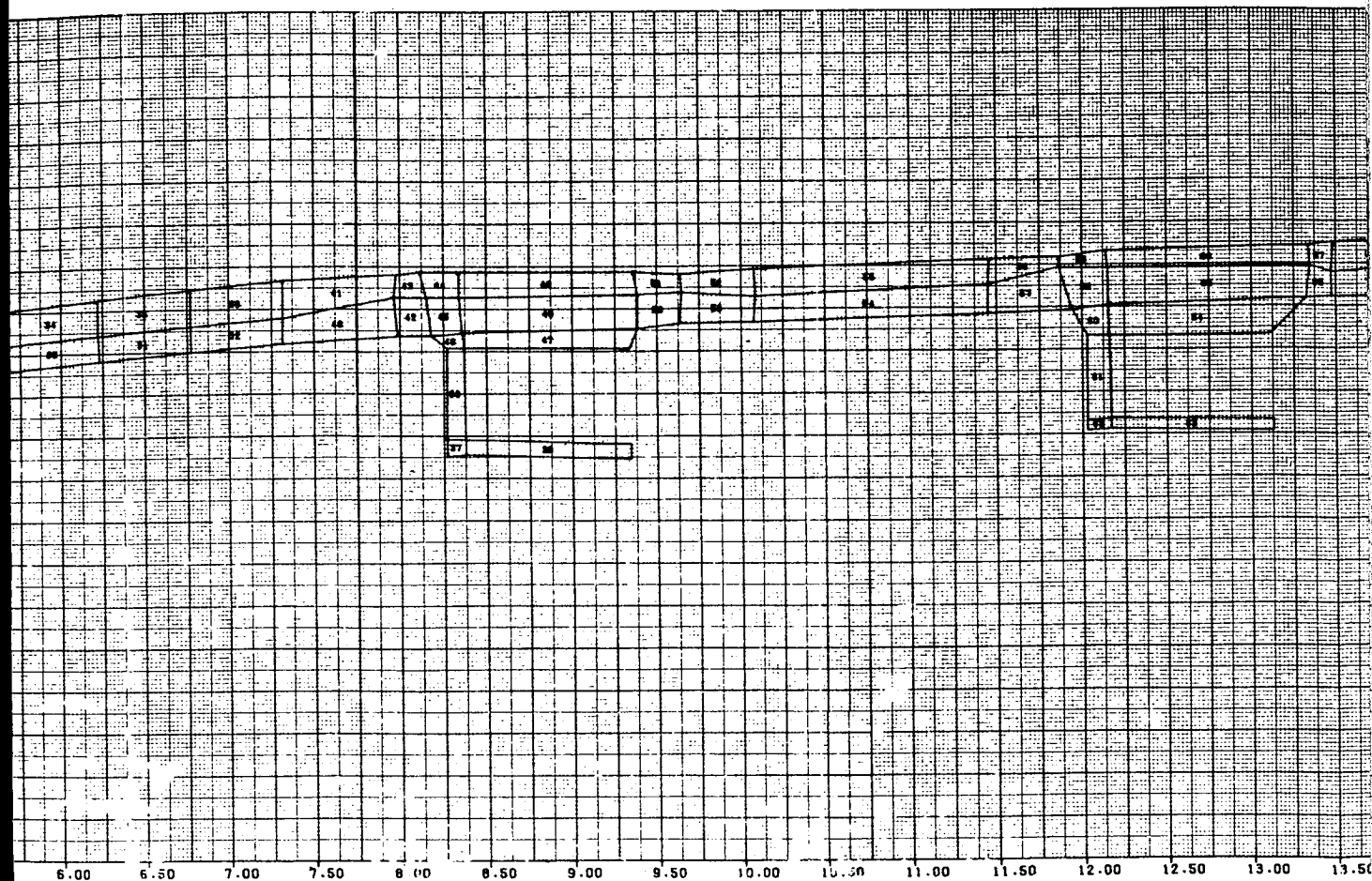
FOLDOUT FRAME

X AXIS

14.00　14.50　15.00　15.50　16.00　16.50　17.00　17.50　18.00　18.50　19.00　19.50　20.00　20.50　21.00

21.50 22.00 22.50 23.00 23.50 24.00 24.50 25.00 25.50 26.00 26.50 27.00 27.50 28.00 28.50
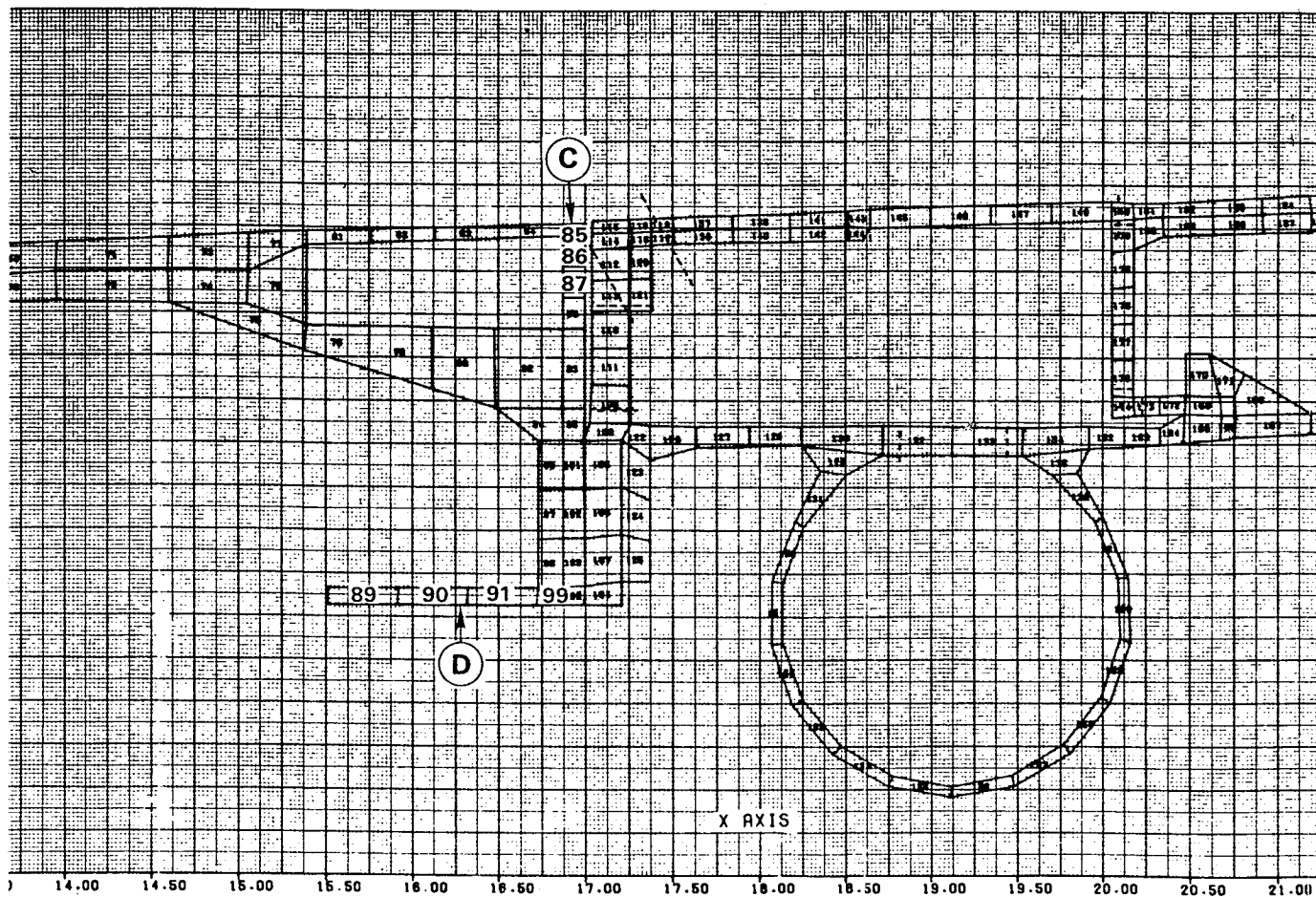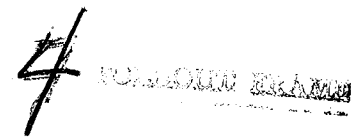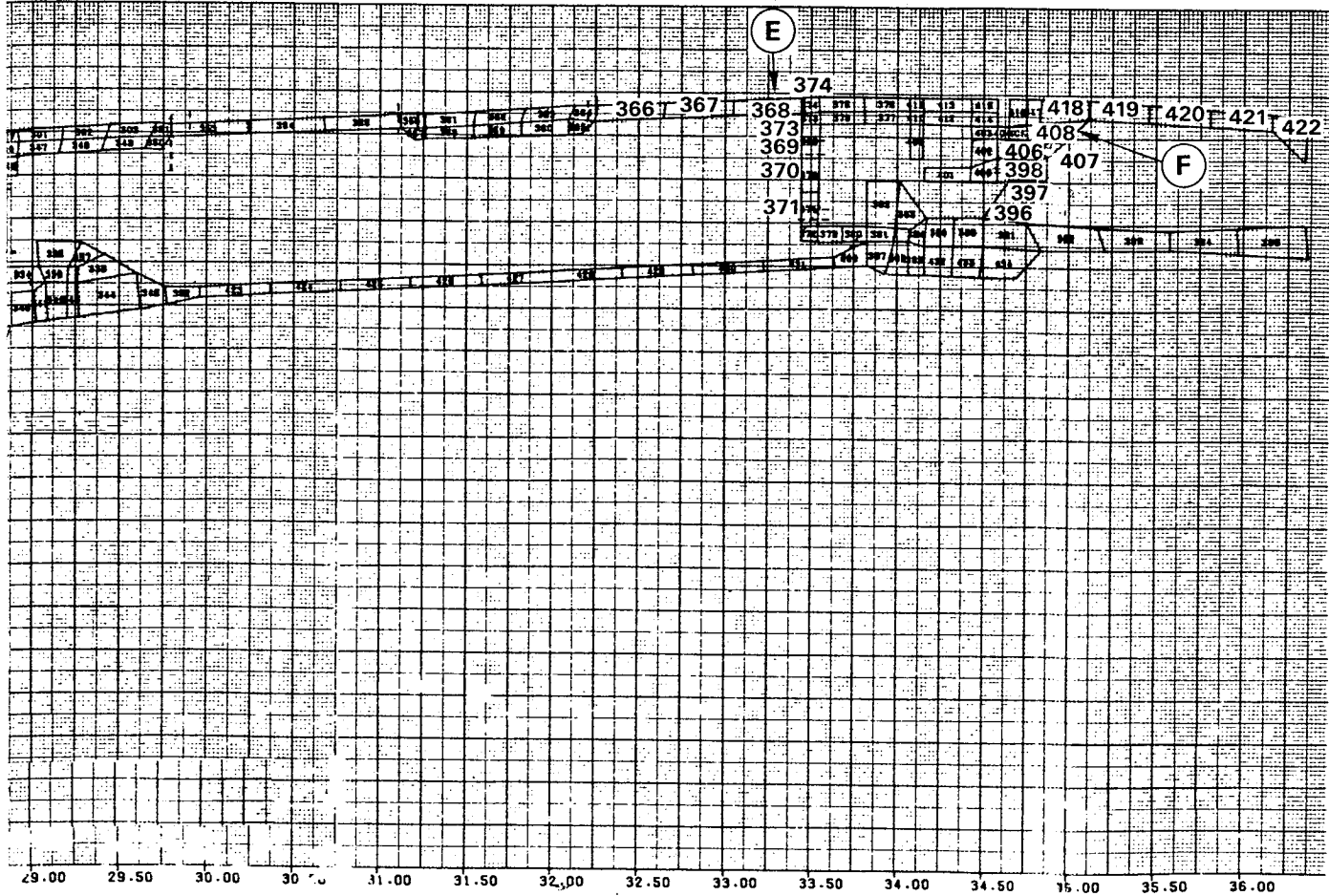
Figure 52   Energy Efficient Engine Compressor Front and Rear Case
Assemblies Thermal Analysis Model

E³ HIGH COMPRESSOR FRONT SPLIT CASE
SHELL ANALYSIS MODEL
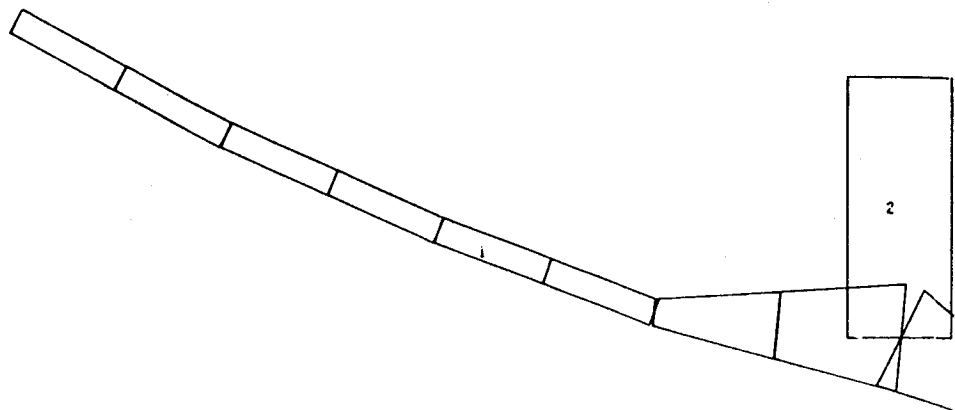
SCALE FACTOR = 2.0959

2 BUILDING BRANCH

1

15
14
13
22
23
10
11
12
16
17
19
20
21
25
26

4 FORMIN ...
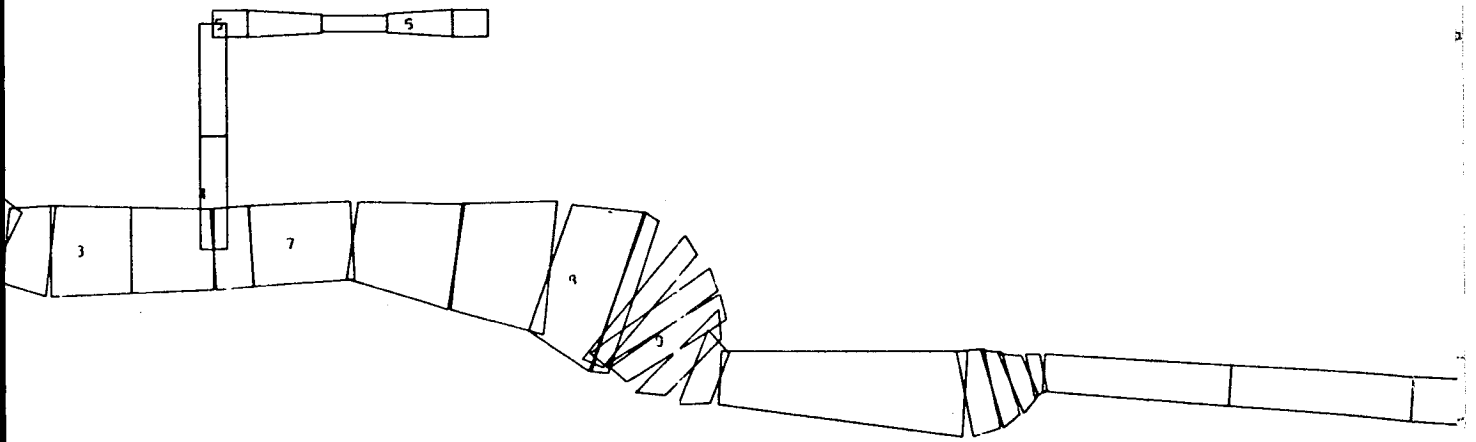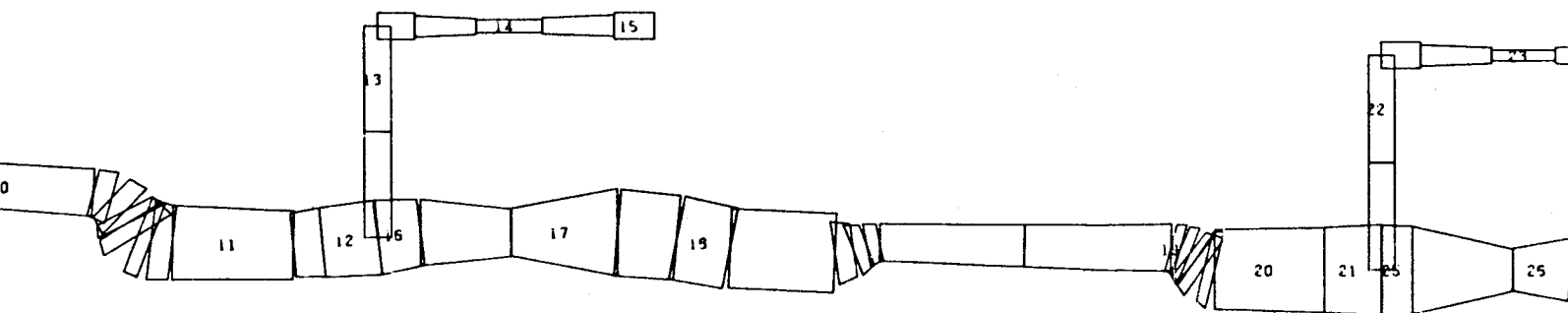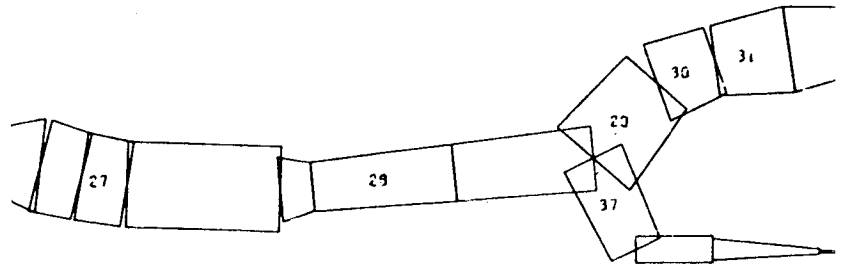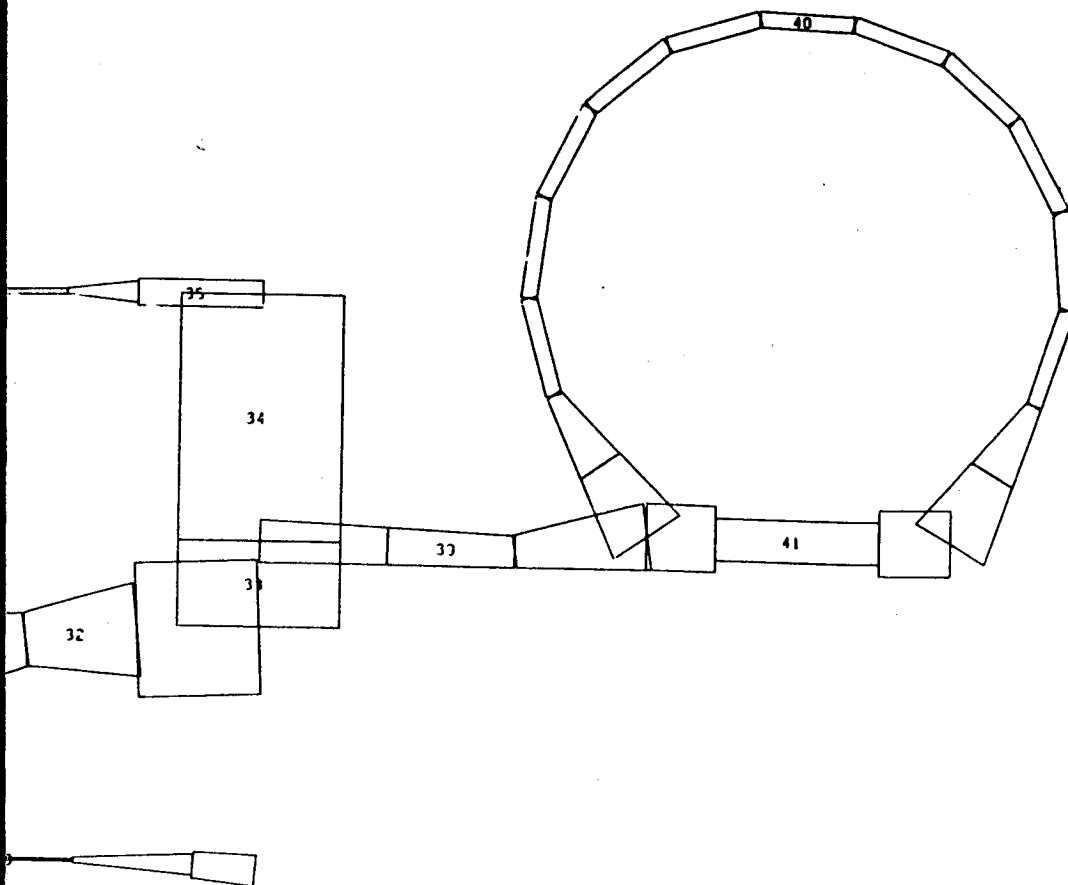
Figure 53   Energy Efficient Engine Compressor Front Split Case Shell
Analysis Model

73

STRESSES EVALUATED AT MAX BURNER PRESSURE

TYPICAL CONCENTRATED STRESS
AROUND STATOR HOLES
HOOP STRESS: 172.37 MPa (25,000 PSI)
MEMBRANE STRESS: 310.26 MPa (45,000 PSI)
BENDING STRESS: 144.79 MPa (21,000 PSI)

AIRFOIL GAS LOAD BENDING
STRESSES RANGE FROM
75.84 TO 282.69 MPa (11,000 TO 41,000 PSI)

0.863 CM (0.340 IN)
THICKNESS LIMITED BY
FAN BLADE LOSS MOMENT

0.309 CM
(0.122 IN)

0.297 CM
(0.117 IN)

0.302 CM
(0.119 IN)

IGV

0.299 CM
(0.118 IN)

S6

S7

S8

ALL STRESSES ARE
WITHIN P&W COMMERCIAL
ENGINE ALLOWABLE LIMITS

TYPICAL CONCENTRATED STRESS
AROUND STATOR HOLES
HOOP STRESS: 551.58 MPa (80,000 PSI)
BENDING STRESS: 89.63 MPa (13,000 PSI)

Figure 54   High-Pressure Compressor Front Case and Stator Assembly Stress
Summary

PRECEDING PAGE BLANK NOT FILMED

The vane actuation system is similar to a successful production engine system. The inlet guide vane, and the sixth, seventh, and eighth stage vanes are fully variable throughout the engine operating regime.

Aluminum unison rings are incorporated. Each ring is supported in at least eight places on the case by plastic Vespel® sliders. A finite element analysis of ring distortion was done to ensure that the system deflection under maximum load conditions is within tolerable limits.

Maximum anticipated ring actuation loads were calculated for distortion and other stress factors and to assure that the actuators have adequate capacity. This calculation considered the aerodynamic vane load, friction of the vane pins in their bushings, and twisting of the lever arms by the unison ring pins. The calculated loads and the maximum tangential ring deflection are shown in Table XVII.

TABLE XVII

CALCULATED LOADS AND MAXIMUM TANGENTIAL RING DEFLECTION

| Stage | Unison Ring Actuating Loads, N (lb) | | Maximum Tangential Deflection, cm (in) |
	at Max N_2	at Idle	
Inlet Guide Vane	1659 (373)	182 (41)	0.018 (0.007)
6	1054 (237)	116 (26)	0.008 (0.003)
7	1108 (249)	125 (28)	0.010 (0.004)
8	1237 (278)	138 (31)	0.015 (0.006)

3.1.4 Rear Case and Stator Assembly

3.1.4.1 General Description

The high-pressure compressor rear case for the flight propulsion system is a one-piece (not split), PWA 1214 titanium case. Compressor cases for similar applications are normally split axially for assembly considerations. A major effort was undertaken to avoid the axial flange to preclude case ovalization caused by the presence of a flange. The case is made from titanium to match the thermal growth characteristics of the titanium drum rotor in stages 9 through 12. An extension of the Inconel 718 diffuser case provides material compatibility over the PWA 1099 nickel rear drum rotor on stages 14 and 15.

The bleed case retains the shroud assemblies for stages 9 through 14. Each shroud assembly includes two rows of vanes, resulting in the need for only three shroud assemblies. The forged vanes are brazed with airfoil-shaped lugs at the outer diameter and "stab-lugs" at the inner diameter which are inserted into openings in the inner shroud.

C-2

The outer shrouds are cut into quarter circle segments and are connected by hooks to the outer case. The inner shrouds are cut into three or four vane clusters to reduce stress and increase active clearance control response. Feather seals are used to seal the gap between outer diameter quarter segments; "W-seals" are used to seal the case-to-shroud hook joints.

Bleed manifolds for eighth-stage customer air bleed, tenth-stage starting air, and turbine active clearance control bleed air are an integral part of the case design. Heat shields are incorporated in all bleed holes to minimize the possibility of titanium fires. Borescope inspection ports have been provided at each stator, except the eleventh which is located over a hook, making case penetration impossible. Three bosses have been provided in the plane of the bore bleed tubes for rotor fixturing support during turbine assembly.

Figure 55 defines the case configuration, and Figure 56 defines case material. Figures 57 and 58 illustrate the shroud assembly.

A separate rear case and stator assembly was designed for the component test rig. This was necessary to accommodate adjustable vane settings, for test purposes, in the rear stages. This assembly is described in Section 4.1.3.2 of this report.

3.1.4.2 Case and Stator Design and Analysis

The design of the rear case required a sequential analysis process similar to that used for the front case to identify and quantify the following structural characteristics: 1) radial growths for use in calculating blade tip clearance, 2) axial growths for use in calculating vane hook engagements and "W-seal" travel, 3) bending stresses in the vane hooks, and 4) thermal stresses in the flanges and integral bleed manifolds. Figure 59 shows the structural analysis model used in these analyses.

In addition, a buckling analysis was conducted to determine wall thickness requirements and an analysis of the vane shrouds was accomplished to investigate asymmetric properties and determine circumferential variations in radial deflection. A containment analysis was performed to establish the thicknesses required to contain a blade failure at each stage and to determine fan blade loss effects on case design. Static load and blow-off load considerations were included throughout the analysis.

As a result of these analyses, case wall thickness was set by buckling under limit loads. The size of the flanges and bolts was set by the fan blade loss load. The resultant design produced a case in which all stresses are within Pratt & Whitney commercial engine allowable limits. A rear case stress summary at maximum engine burner pressure rating is shown in Figure 60. A case thickness summary, with respective controlling parameters, is shown in Figure 61.
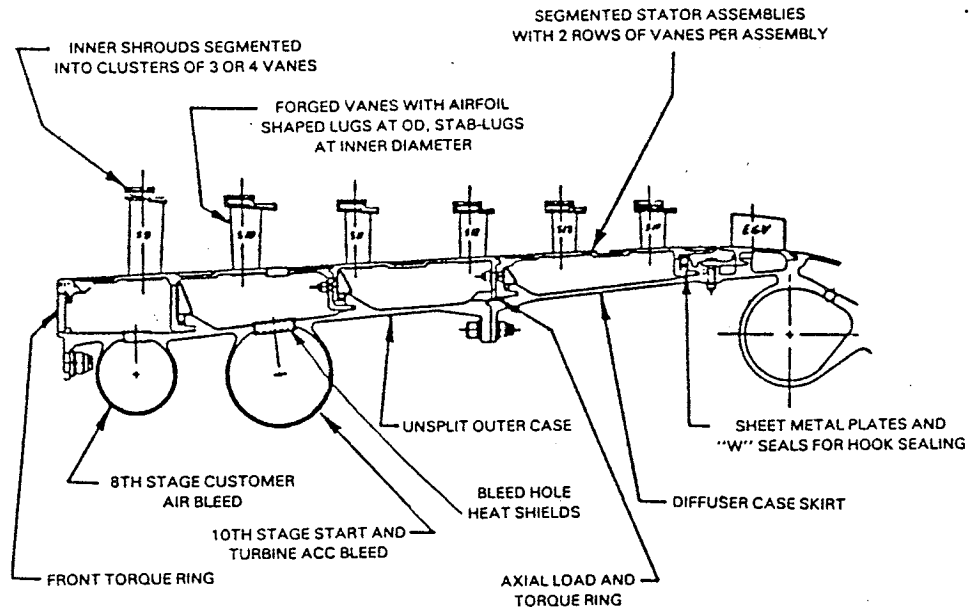
Figure 55   High-Pressure Compressor Rear Case Configuration
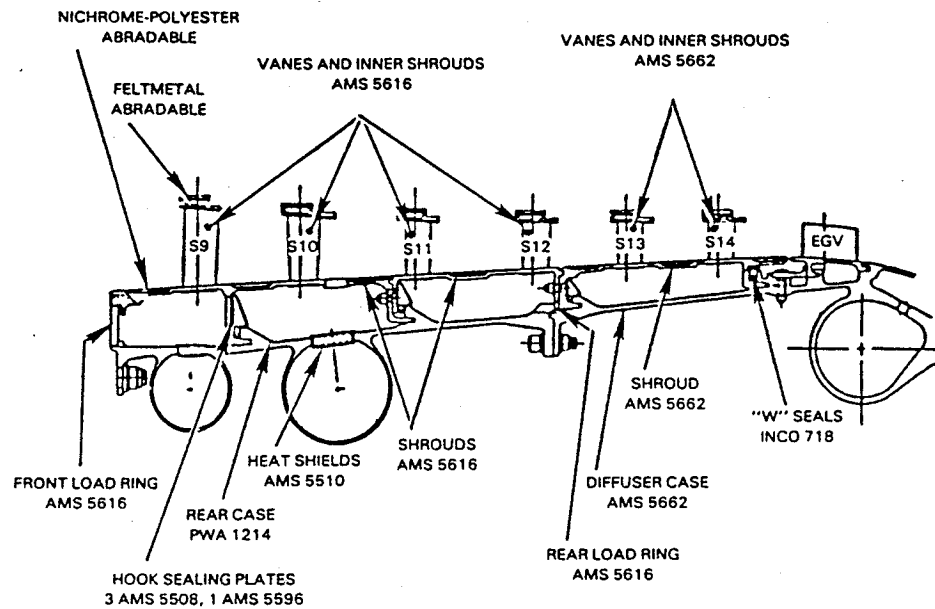
Figure 56   High-Pressure Compressor Rear Case Materials

FEATHER SEAL
4 PLACES

VIEW A

A
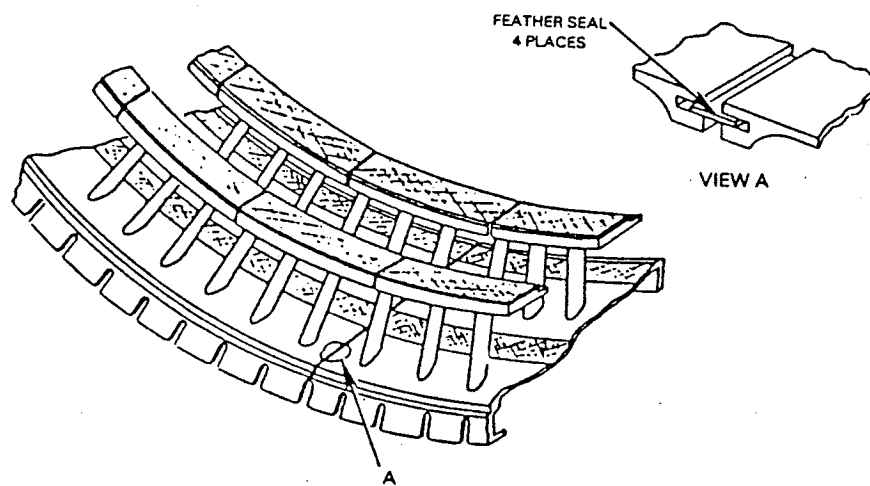
Figure 57   High-Pressure Compressor Rear Stator and Shroud Assembly

ELECTRON BEAM
WELDED JOINTS

FELTMETAL™

DOUBLE WALL BRAZED
CONSTRUCTION
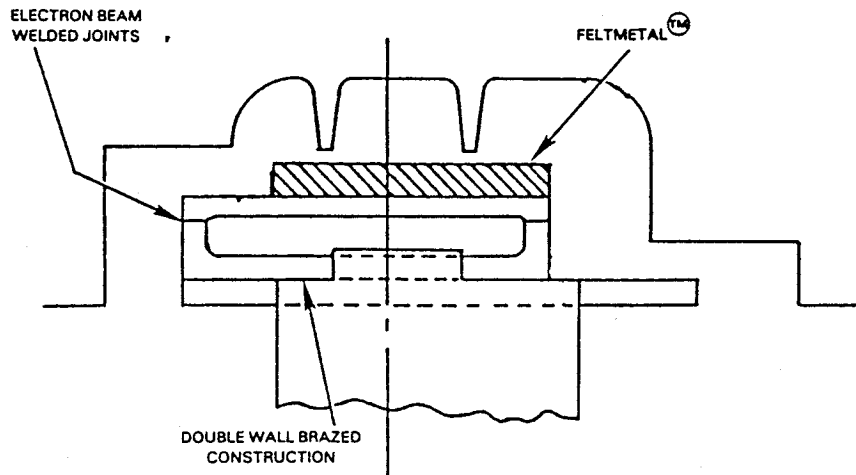
Figure 58   High-Pressure Compressor Inner Shroud Configuration
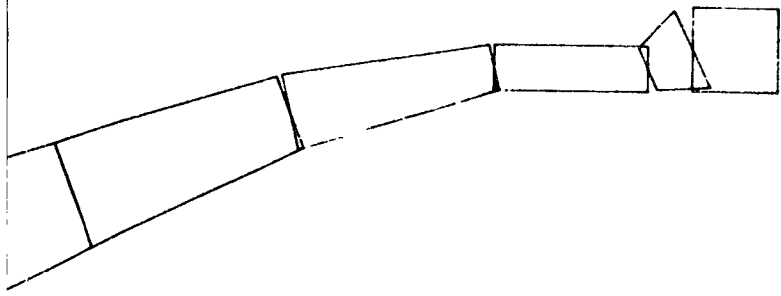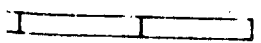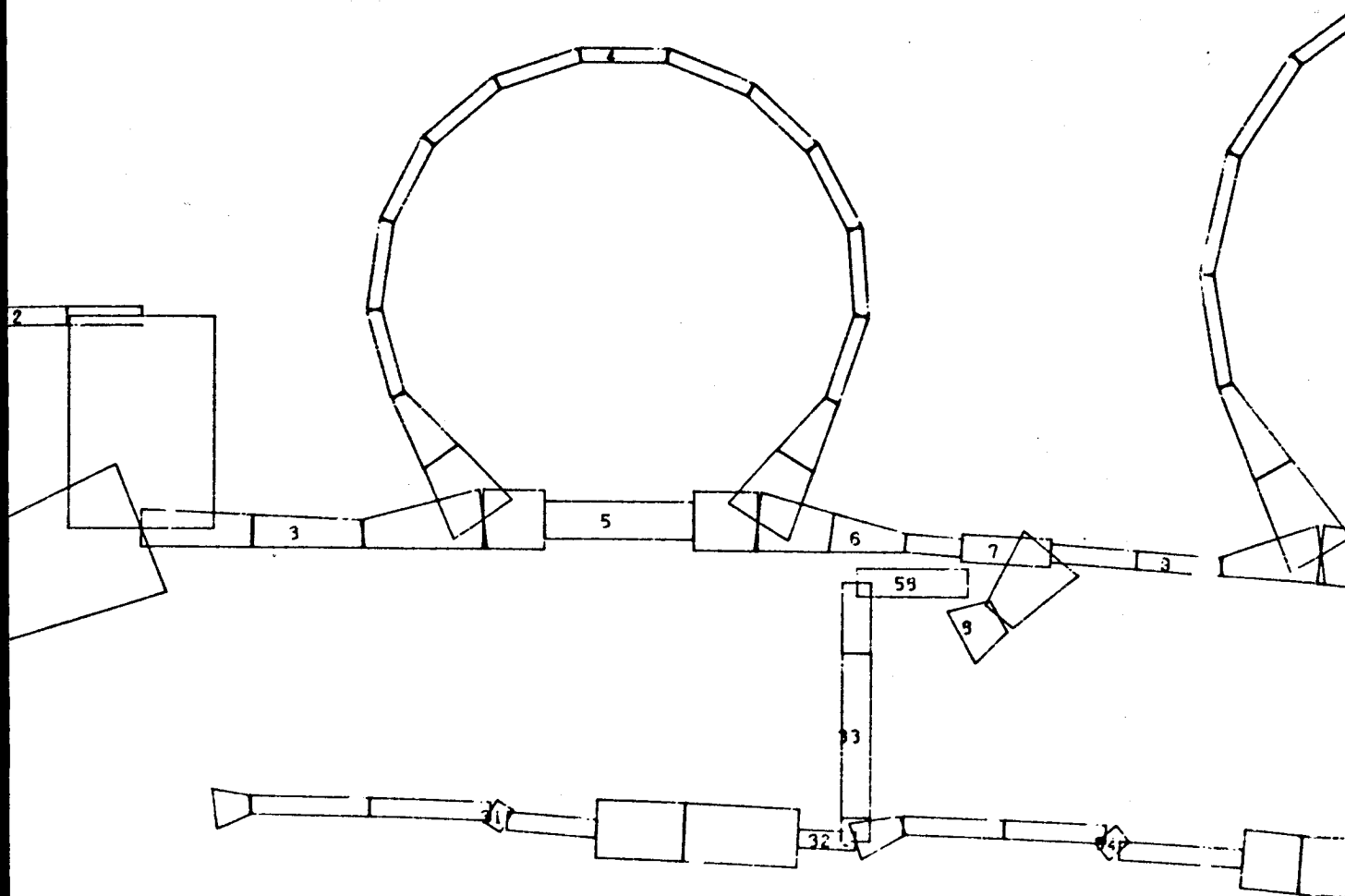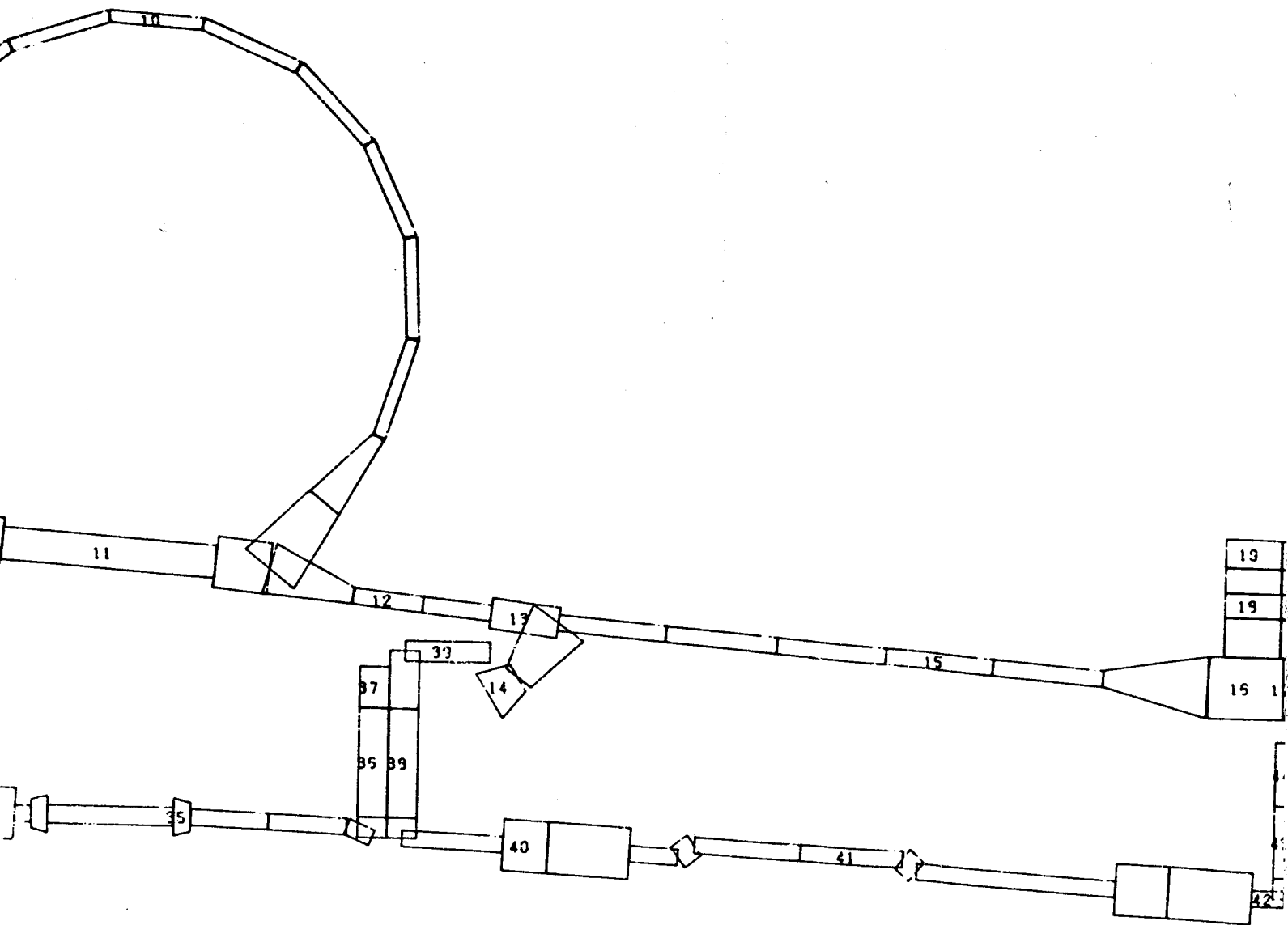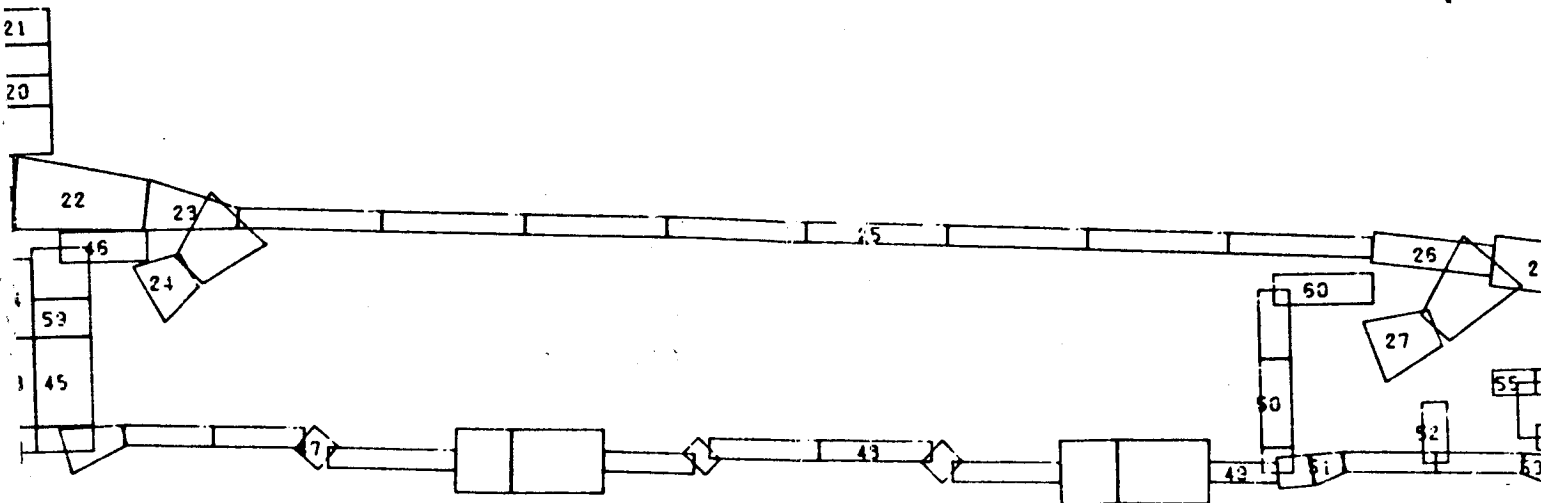
Figure 59   Energy Efficient Engine Comp
             Analysis Model

30

57
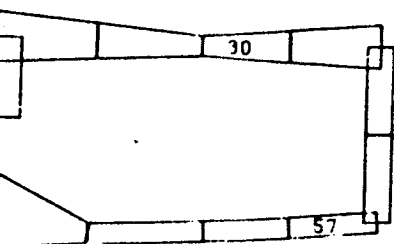
r Rear Case Assembly Shell

81

LOADS AT MAX·BURNER PRESSURE

TORQUE FEATURE
SHEAR 27.58 MPa (4000 PSI)
BEARING 96.53 MPa (14,000 PSI)

AIRFOIL GAS LOAD BENDING
STRESSES RANGE FROM
241.32 TO 386.11 MPa (35,000 TO 56,000 PSI)

TORQUE FEATURE
SHEAR 137.9 MPa (20,000 PSI)
BEARING 399.9 MPa (58,000 PSI)

LOADED HOOK BENDING
STRESS 275.8 MPa (40,000 PSI)

UNLOADED HOOK
BENDING STRESS
13.79 MPa (2000 PSI)

CASE HOOP STRESS
324.07 MPa (47,000 PSI)

TORQUE FEATURE
SHEAR 46.19 MPa (6700 PSI)
BEARING 310.26 MPa (45,000 PSI)

MANIFOLD BENDING
STRESS 220.63 MPa (32,000 PSI)

FLANGE BENDING
STRESS 144.79
MPa (21,000 PSI)

FLANGE HOOP STRESS
193.05 MPa (28,000 PSI)

TORQUE FEATURE
SHEAR 9.65 MPa (1400 PSI)
BEARING 18.62 MPa (2700 PSI)

AXIAL LOAD FEATURE
SHEAR 62.05 MPa (9000 PSI)
BEARING 172.37 MPa (25,000 PSI)
BENDING 275.79 MPa (40,000 PSI)

Figure 60   High-Pressure Compressor Rear Case Stress Summary

0.309 (0.122)*
0.033 (0.013)O
0.203 (0.080)□

0.266 (0.105)*
0.073 (0.029)O
0.137 (0.054)□
0.180 (0.071)△

0.104 (0.041)O
0.121 (0.048)□
0.101 (0.040)*

0.15 (0.06)*
0.076 (0.03)O
0.068 (0.027)□
0.055 (0.022)⊗

0.165 (0.065)*
0.172 (0.068)△

0.205 (0.081)*
0.101 (0.040)O
0.213 (0.084)△

0.175 (0.069)*
0.091 (0.036)O
0.081 (0.032)□

0.226 (0.089)*
0.076 (0.030)O
0.101 (0.040)⊗

0.139 (0.055)□
0.104 (0.041)⊗

NOTE: MACHINING LIMIT IS 0.139 (0.055) MIN.

NOTE: DIMENSIONS ARE IN CM (IN)

* = CONTAINMENT
O = PRESSURE
□ = FAN BLADE LOSS
△ = BUCKLING
⊗ = LIMIT LOADS

0.779 (0.307)□
0.231 (0.091)□
0.492 (0.194)□
3.91 (1.54)□

0.711 (0.280)□
0.762 (0.300)□
0.660 (0.260)□
0.457 (0.180)□
3.556 (1.400)□
3.302 (1.300)□

Figure 61   High-Pressure Compressor Rear Case Thickness Summary

84

3.1.5 Vanes

3.1.5.1 General Description

Series 400 airfoils are used in the inlet guide vane, and controlled diffusion airfoils are used for stators 6 through 14 and the exit guide vane. As noted earlier, the inlet guide vane and stators 6, 7, and 8 are adjustable, whereas stators 9 through 14 are fixed position (in the flight propulsion system). The mechanical design of the exit guide vane was included in the design of the combustor component and is described in Reference 3. Airfoils are burnished to obtain a 20AA smoothness on the aerodynamic surfaces. A general description of all stator vanes is presented in Table XVIII.

3.1.5.2 Structural Analysis

Structural analysis of the vane clusters indicated that steady stresses were all well below allowables, and that clustering of vanes was a significant factor in reducing steady stresses. Table XIX presents the stress summary. All stators were analyzed for bending and torsional flutter stability and were found to be satisfactory as shown in Figures 62 and 63.

In addition, the exit guide vane was tuned to avoid a possible tip mode resonance with the 15th-stage blades at minimum cruise speed. The resulting resonance diagram is shown in Figure 64, which indicates adequate margin.

TABLE XVIII

HIGH-PRESSURE COMPRESSOR GENERAL STATOR VANE DESCRIPTION

	IGV	S6	S7	S8	S9	S10	S11	S12	S13	S14	EGV
Materials: Test Rig	AMS 5613	AMS 5613	AMS 5613	AMS 5613	AMS 5616	AMS 5616	AMS 5616	AMS 5616	AMS 5663	AMS 5663	INCO 718
Flt. Proplsn. System	Aluminum	AMS 5613	AMS 5613	AMS 5613	AMS 5508	AMS 5508	AMS 5508	AMS 5508	AMS 5596	AMS 5596	
Integ. Core/Low Spool	AMS 5613	AMS 5613	AMS 5613	AMS 5613	AMS 5616	AMS 5616	AMS 5616	AMS 5616	AMS 5662	AMS 5662	
Airfoil Series *	400	CDA	CDA	CDA	CDA	CDA	CDA	CDA	CDA	CDA	CDA
No. of Vanes	32	44	50	52	60	64	72	64	72	80	100
Root radius (hot), cm	16.459	18.969	21.204	22.504	23.327	23.820	24.158	24.282	24.282	24.282	24.524
(in.)	(6.48)	(7.468)	(8.348)	(8.86)	(9.184)	(9.378)	(9.511)	(9.56)	(9.56)	(9.56)	(9.655)
Tip radius (hot), cm	30.709	29.268	28.946	28.588	28.202	27.855	27.559	27.219	26.939	26.673	26.627
(in.)	(12.09)	(11.523)	(11.396)	(11.255)	(11.103)	(10.984)	(10.85)	(10.716)	(10.606)	(10.501)	(10.483)
Root chord, cm	4.201	3.851	3.244	3.175	2.799	2.540	2.263	2.530	2.291	2.258	3.985
(in.)	(1.654)	(1.516)	(1.277)	(1.250)	(1.102)	(1.000)	(0.891)	(0.996)	(0.902)	(0.889)	(1.569)
Tip chord, cm	5.459	4.923	4.097	3.983	2.804	2.540	2.263	2.530	2.291	2.258	4.021
(in.)	(2.149)	(1.938)	(1.613)	(1.568)	(1.104)	(1.000)	(0.891)	(0.996)	(0.902)	(0.889)	(1.583)
Max thickness/chord, root	0.090	0.052	0.051	0.051	0.073	0.070	0.084	0.082	0.073	0.071	0.080
Max thickness/chord, tip	0.090	0.090	0.090	0.090	0.073	0.071	0.084	0.082	0.073	0.071	0.081
Chord angle, root, deg	99.1	61.0	56.6	55.0	54.5	52.6	50.6	47.7	47.1	49.1	67.0
Chord angle, tip, deg	104.5	51.6	47.4	45.5	44.0	42.6	42.5	41.6	41.6	43.8	71.7
Aspect ratio	2.61	2.09	1.89	1.53	1.74	1.61	1.50	1.16	1.16	1.06	0.52
Hub/tip ratio, average	0.536	0.648	0.733	0.787	0.827	0.854	0.877	0.892	0.901	0.910	0.921

* See List of Symbols

TABLE XIX

STATOR VANE STRESS SUMMARY

Stator	Steady Stress, MPa (psi)
Inlet Guide Vane	73.78 (10,700)
6	185.47 (26,900)
7	284.75 (41,300)
8	273.72 (39,700)
9	354.39 (51,400)
10	381.97 (55,400)
11	349.56 (50,700)
12	252.35 (36,600)
13	328.88 (47,700)
14	300.61 (43,600)
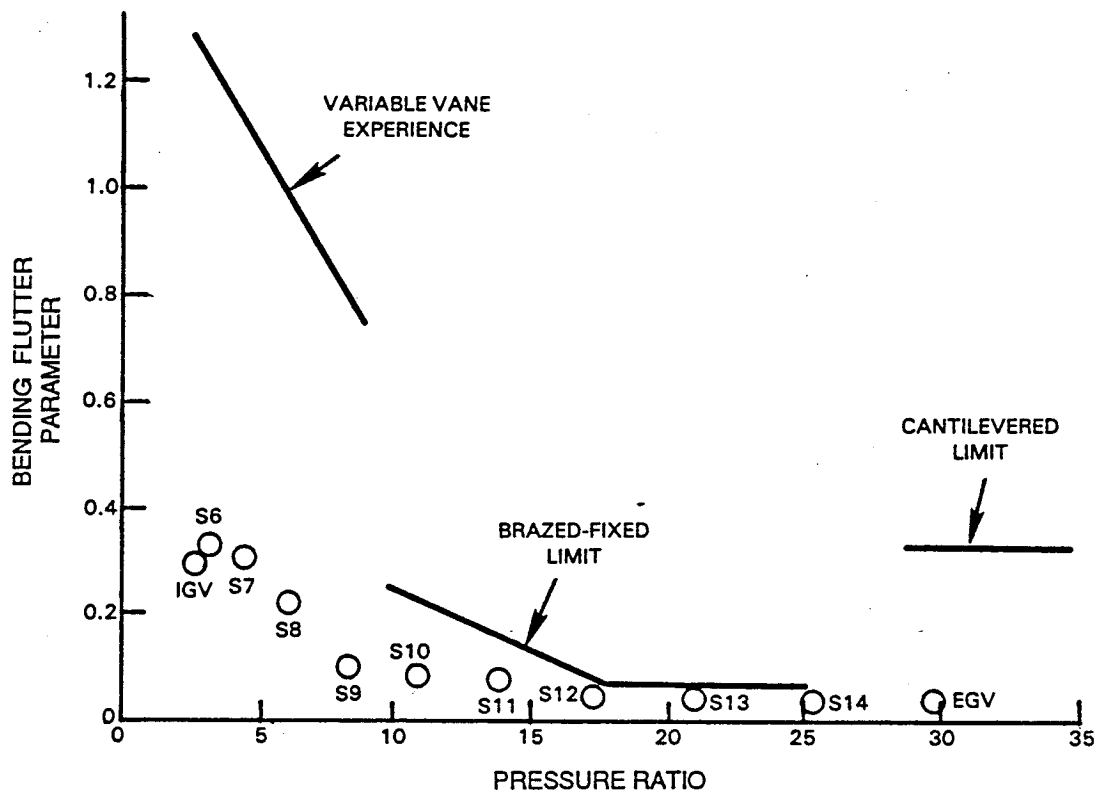
Figure 62   Energy Efficient Engine High-Pressure Compressor Vane Bending Flutter
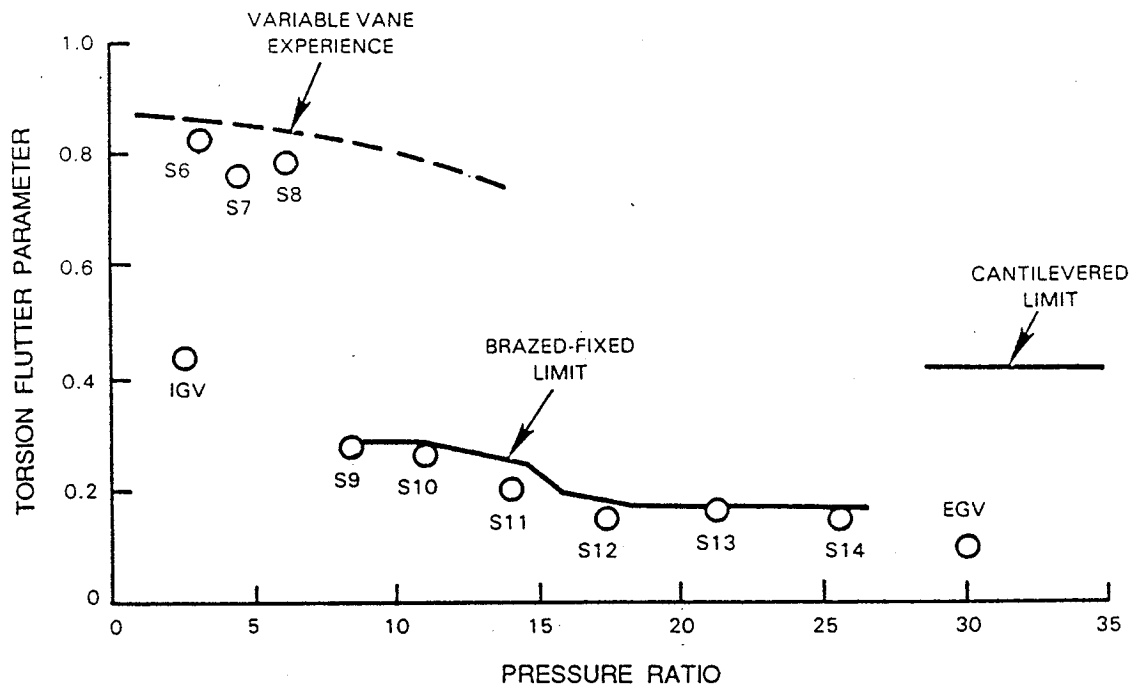
Figure 63   Energy Efficient Engine High-Pressure Compressor Vane Torsional
             Flutter
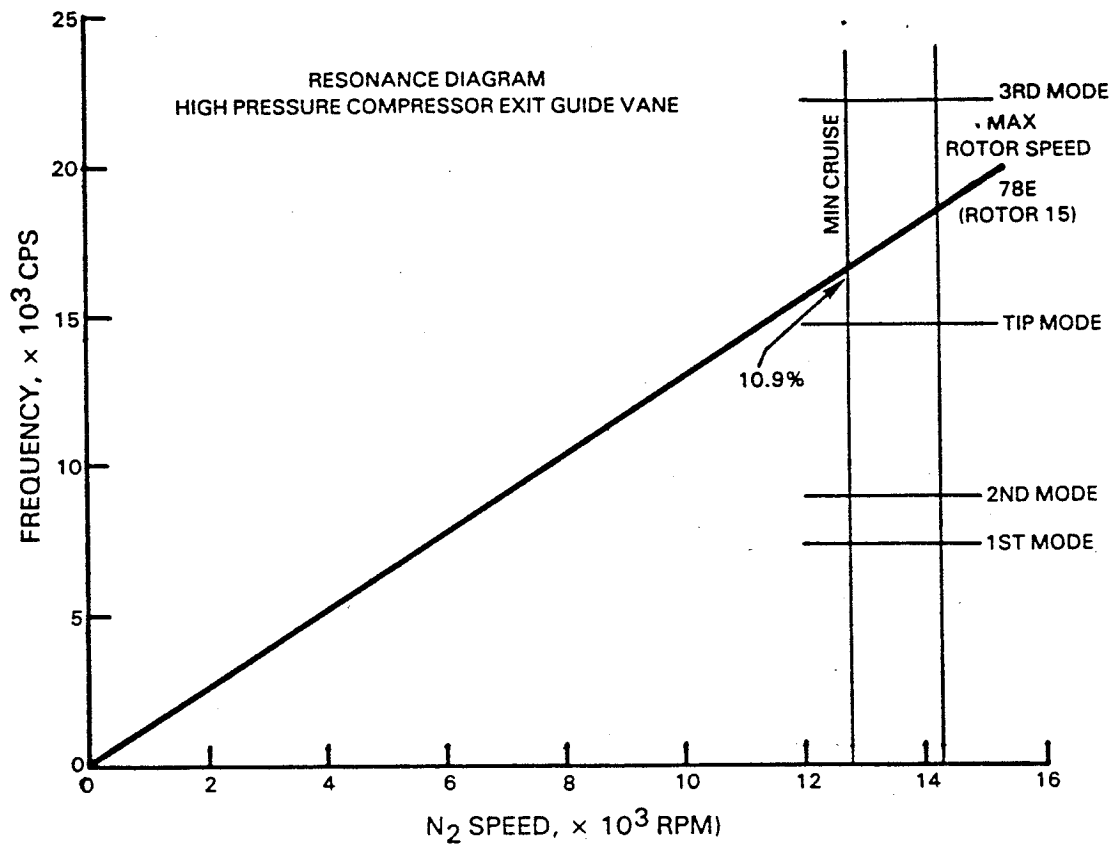
Figure 64   Resonance Diagram for the High-Pressure Compressor Exit Guide Vane

88

3.2 INTERMEDIATE CASE

As noted in Part I, Section 2.0 of this report, the high-pressure compressor intermediate case was an integral part of the component design procedure. The configuration resulting from analysis and design efforts is illustrated in Figure 65. The subelements of this assembly are described in detail in the following sections of this report.
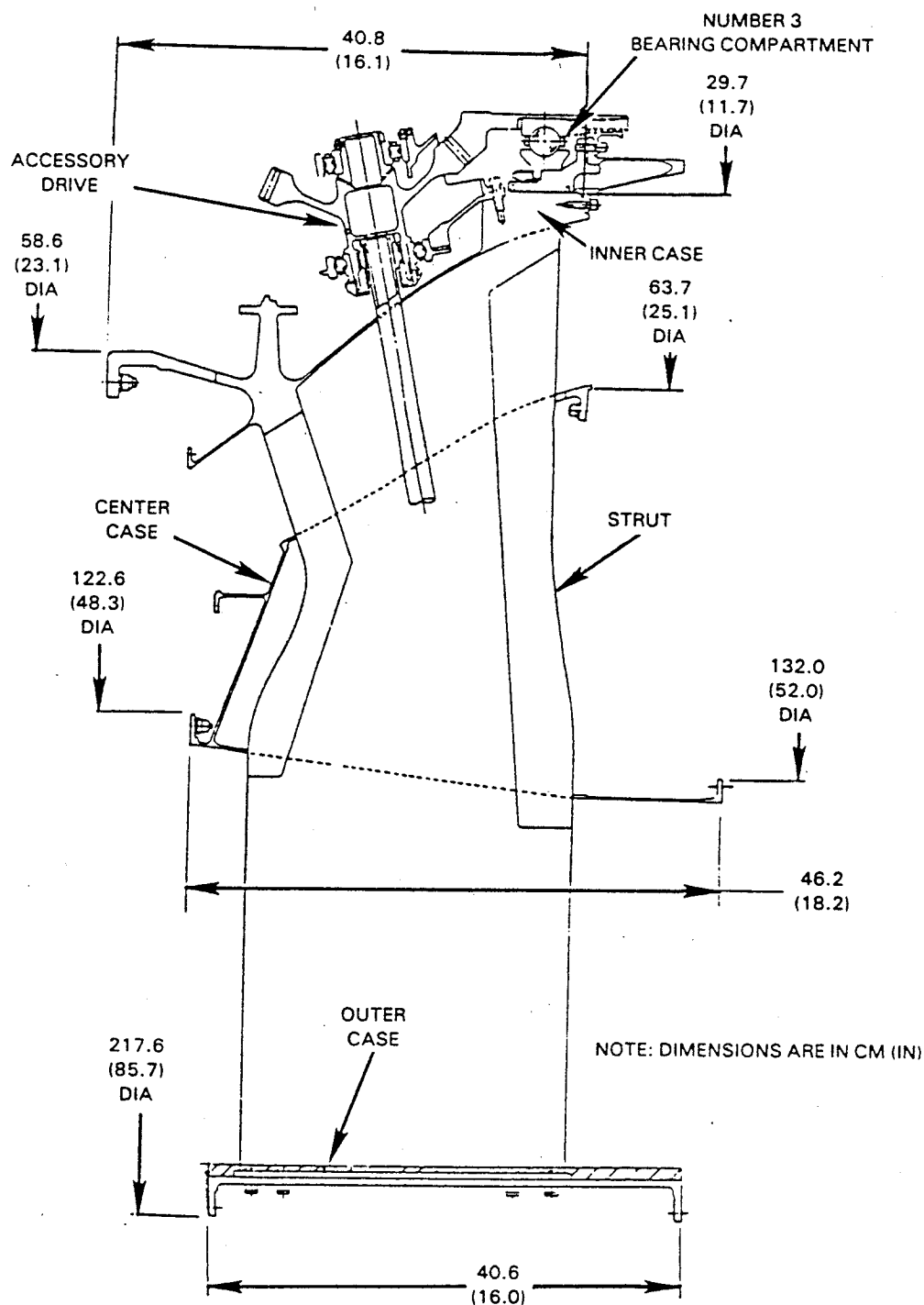
Figure 65   High-Pressure Compressor Intermediate Case Assembly

3.2.1 No. 3 Bearing Compartment

3.2.1.1 General Description

The No. 3 bearing compartment comprises the No. 3 ball bearing, bearing damper, damper spring, No. 3 rear labyrinth seal, and the bearing support. These features are illustrated in Figure 66. The function of the No. 3 bearing is to provide support for the front of the high-pressure spool, react the spool thrust and position the shaft axially and radially. Consideration of rotor dynamic vibrational modes resulted in the incorporation of a spring and damper. The high-pressure rotor pitch and bounce modes were driven below idle speed by incorporating the soft effective bearing support. Whirl during hot (bowed) rotor starting and turbine blade loss conditions is minimized by the high efficiency viscous damper on the bearing support structure. The No. 3 six-lip knife-edge labyrinth seal isolates the rear of the forward compartment from the compartment buffer environment.
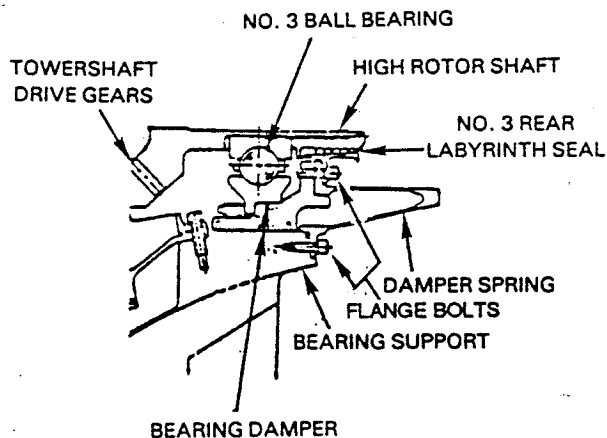
Figure 66   No. 3 Bearing Compartment

Existing bearing and seal hardware are used to minimize program cost for the integrated core/low spool. The larger diameter (165 mm x 255 mm) bearing relative to the flight propulsion system (160 mm x 250 mm) bearing results in larger shaft diameters under the bearing races. Also, an additional bolted joint was required at the inner diameter of the bearing support to facilitate assembly of the existing bearing.

The No. 3 bearing material is M50 steel alloy. AMS 4928, a 6Al-4V titanium alloy, is used for the bearing outer-diameter support, support for the static portion of the rear labyrinth seal, and the damper spring. An iron base alloy, AMS 5616, is used for the damper. The rotating portion of the labyrinth seal and its knife edges are AMS 5613 iron base alloy.

3.2.1.2 Spring and Damper Design

Various combinations of spring and damper configurations were considered and analyzed with emphasis placed on minimizing rotor and seal clearance. The selected spring design is a mechanical concept shown in Figure 67. It features a wind-back shell structure to control stiffness. The bearing outer ring serves as the inner member of the damper. Damper operation is achieved by controlling an oil film between this inner member and the outer damper body. This "squeeze film" damping approach uses engine lubrication system oil as the damping fluid. The final estimated spring rate for the bearing support assembly was 0.613 to 0.876 x 10^6 N/cm (0.35 to 0.50 x 10^6 lb/in).
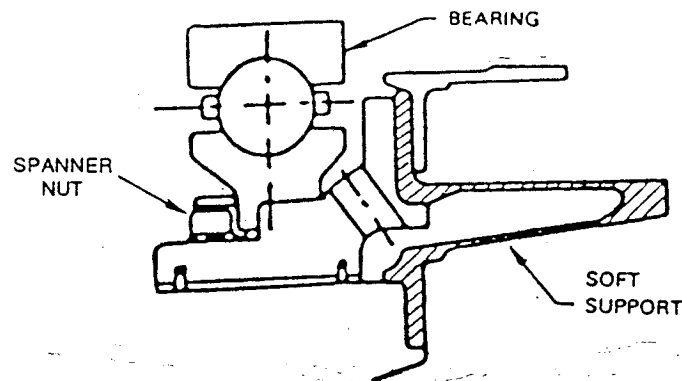
Figure 67   Selected Damper Spring Design for No. 3 Bearing

The soft outer-diameter support is designed to accommodate a 133.447 kN (30,000 lb) thrust load. Since the loading is rearward, the flange bolts are in tension. Analysis indicated that use of 24 0.635-cm (0.25 in) diameter bolts resulted in a structurally adequate design. In addition, the flange is spot-faced to assure continuous contact at the bearing support mating surface. For purposes of assembling the existing bearing into the space imposed by the flight propulsion system flowpath, a bolted joint was similarly designed at the inner diameter of the soft support.

3.2.1.3 Bearing Design

The No. 3 bearing is an existing item. The only change made to the configuration was one necessitated by space limitations of the flowpath. This compromise removes 0.635 cm (0.25 in) of bolting flange radial height to obtain the necessary space. The bolting feature is replaced by clamping the, remaining portion of the flange with a spanner nut shown in Figure 67. The bearing outer diameter fit is sized to prevent outer race spinning.

Projected maximum nominal high-pressure rotor thrust at takeoff is 22.241 kN (5000 lb) rearward. However, to ensure successful operation during integrated core/low spool testing, the bearing stack is designed to maintain a 44.482 kN (10,000 lb) load at worst conditions, and is preloaded to accommodate a ± 88.964 kN ($\pm 20,000$ lb) variation. A resulting stack spring rate of 8.76×10^6 N/cm (5×10^6 lb/in) was calculated. Stack preload is provided by a second spanner nut grounded at the towershaft drive gear front face. Analysis indicated low nut stress levels for these design conditions.

A B_1 life of 3200 hours is predicted, which is adequate for this bearing under integrated core/low spool test conditions. Support flexibility effects are included in this estimate.

A summary of the No. 3 bearing design is given in Table XX.

TABLE XX

INTEGRATED CORE/LOW SPOOL NO. 3 BEARING DESIGN SUMMARY

Diameter:

Inner	165 mm
Outer	255 mm
Ball	2.54 cm (1.0 in)
DN	2.3×10^6 mm x rpm
Thrust (Nominal Takeoff)	22.241 kN (5,000 lb)
(Maximum)	44.482 kN (10,000 lb)
Maximum N_2 Speed	13,936 rpm
B_1 Duty Cycle Life	3,200 hours

3.2.1.4 Oiling System

The No. 3 bearing inner race is under-the-race cooled and lubricated by oil supplied to an axial scoop. Based on test data, 9.072 kg/min (20 lb/min) of oil flow will be required to lubricate and cool the bearing. In addition, 2.268 kg/min (5 lb/min) are required for the damper. Total heat generation at the takeoff rating is estimated to be 800 Btu/min.

3.2.2 Accessory Drive System

3.2.2.1 General Description

The integrated core/low spool accessory drive system consists of engine accessories, mounted on the top of the outer fan case, which are driven by a shaft geared to the high-pressure spool rotor. Figure 68 shows the arrangement which was used to facilitate integrated core/low spool testing. Accessory power is taken off the front of the high-pressure rotor shaft by an integral bull gear, a spiral bevel pinion shaft gear, and a towershaft. The towershaft, shown in Figure 69, consists of inner, middle, and outer shaft portions. Bevel gear shaft support is provided by a roller bearing at the inboard portion and a ball bearing at the outer portion. An internal spline drives the inner shaft, which, in turn, is internally splined to the center shaft. The center shaft is positioned by two ball bearings which are preloaded by a spring (Figure 68). This assembly is mounted in the center case. An external spline on the outer end of the center shaft drives the outer shaft. The outer shaft is positioned at its outer end by a roller bearing and shaft gear mounted in the external right angle gearbox. The integrated core/low spool gearbox is mounted on top of the case. It consists of an existing right angle gearbox, that is driven via the towershaft, and line shaft driving an adapter mounted on an existing accessory gearbox. All towershaft bearings are existing parts. Flight propulsion system accessories are core mounted at the bottom of the engine and are described in Reference 1.

Towershaft gears are made of AMS 6265 wrought steel alloy. Wrought alloy steels, AMS 6263 and 6260, are used for the inner shaft, and the center and outer shafts, respectively. Bearings are constructed of M50 steel alloy.
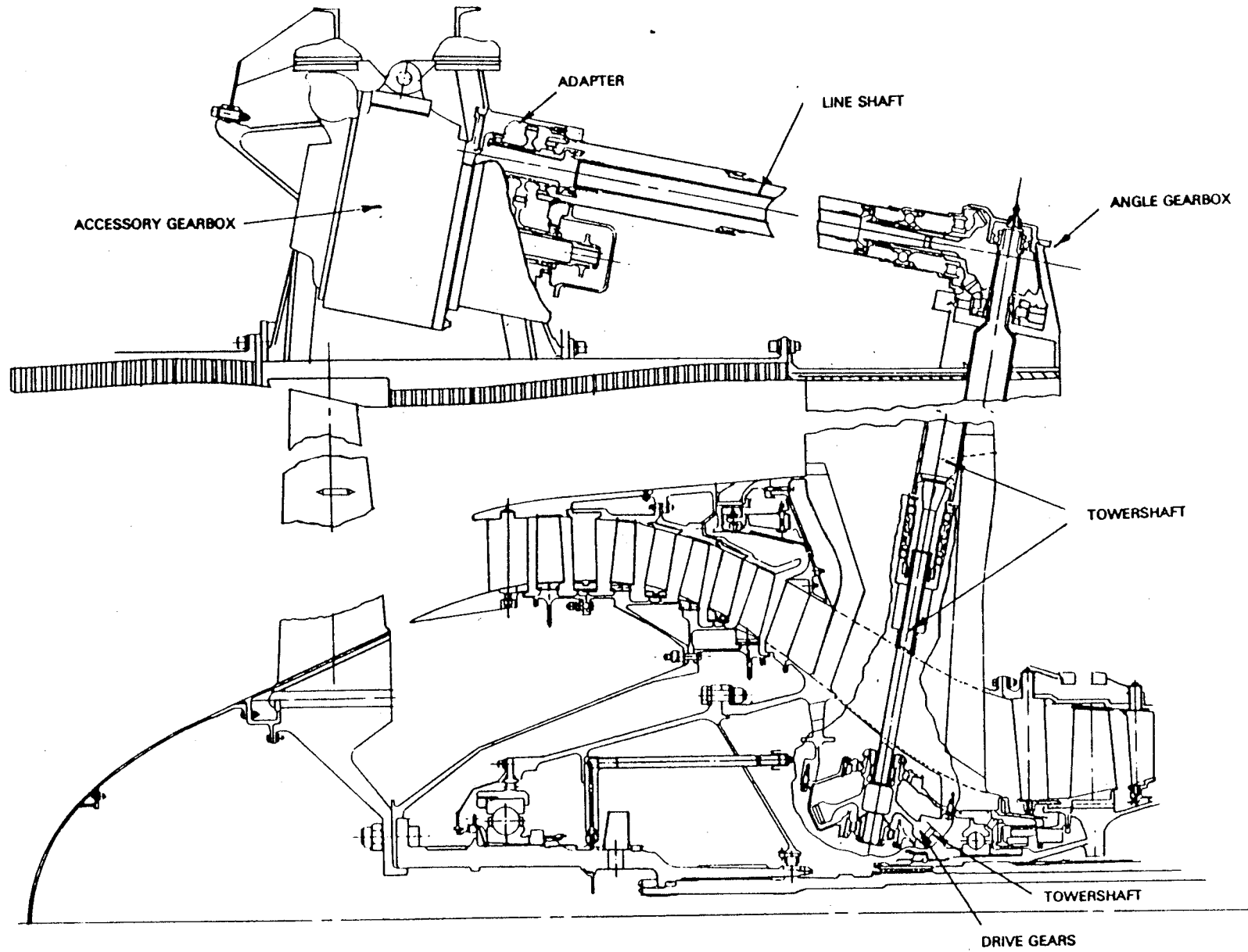
Figure 68   Integrated Core/Low Spool Towershaft/Gear System

NO. 6 BEARING

HIGH ROTOR SHAFT

BULL GEAR

SPIRAL
BEVEL GEAR

INNER TOWERSHAFT

MID TOWERSHAFT

OUTER TOWERSHAFT

EXTERNAL RIGHT ANGLE
GEARBOX SHAFT GEAR
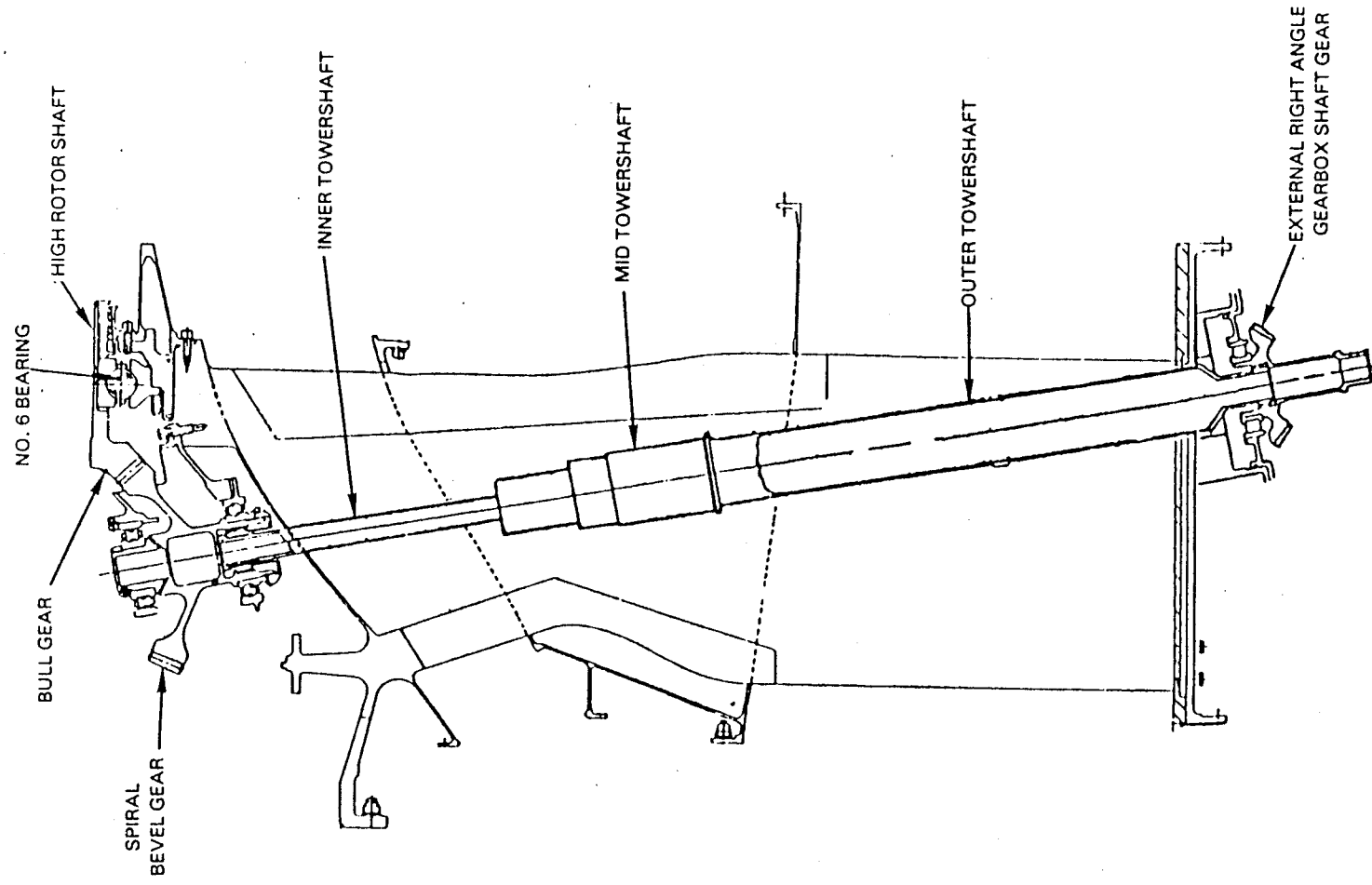
Figure 69   Towershaft/Gear System

3.2.2.2 Gear Design

Standard design procedures were used to define the towershaft bull and bevel gears. Loads imposed on the drive gears during integrated core/low spool testing result from a 677.91 N-m (500 lb-ft) starter torque input and a 37.285 kW (50 horsepower) fuel pump. Bull and bevel gear pitch-line velocities are, 10972.8 m/min (36000 ft/min).

Special features have been incorporated in the gear design to assure successful operation at this pitch line velocity. Gear lubrication and cooling are provided by a surrounding oil mist environment and an oil jet directed at the ingoing side of the gear mesh. The jet is oriented to minimize churning and maximize heat dissipation. Gear assembly tolerance controls will assure proper gear alignment. In addition, the shaft gear is dynamically balanced. A gear spiral angle of 0.611 radian (35 degrees) was selected to increase contact ratio and, subsequently, gear tooth load-carrying capability.

In terms of towershaft rotational speed and running condition torque combinations, the gear design is within Pratt & Whitney operating experience. Pitch line velocity to be demonstrated by the integrated core/low spool encompasses that projected for the flight propulsion system. Commercially viable durability for the more highly loaded flight propulsion system gears would be achieved during the engine development program.

A summary of gear design parameters is given in Table XXI.

TABLE XXI

INTEGRATED CORE/LOW SPOOL
TOWERSHAFT GEAR DESIGN SUMMARY

Operating Torque Capacity, N-m (lb-in)	742.88 (6575)
Static Torque Capacity, N-m (lb-in)	3224.02 (28535)
Contact Ratio	2.79
Number Pinion Teeth	59
Number Gear Teeth	81
Diametral Pitch, cm^{-1} (in^{-1})	3.26 (8.28)
Pitch Line Velocity, m/min (ft/min)	10972.8 (36000)
Pressure Angle, rad (deg)	0.349 (20.0)
Spiral Angle, rad (deg)	0.611 (35.0)
Shaft Angle, rad (deg)	1.375 (78.7)
Face Width, cm (in)	3.048 (1.2)

3.2.2.3 Shaft Design

Standard design procedures were used to configure the towershaft. Shaft diameters were defined by starting-torque requirements, constraints imposed by the use of existing bearings, and rotor dynamics considerations. Spline teeth, were designed based on load-carrying requirements and misalignments imposed by fan outer case deflections.

Intermediate case structural analyses indicated a net outer case rotation of 0.508 cm (0.200 in) between the starting and maximum thrust conditions (Section 3.2.5.2). This deflection was compensated for by offsetting the angle gearbox top mount 0.254 cm (0.100 in) tangentially in the direction opposite to case rotation to achieve the proper balance between inner and outer towershaft spline misalignments as a function of operating condition. Spline misalignment distributions that resulted with thrust level are summarized in Table XXII.

TABLE XXII

TOWERSHAFT SPLINE MISALIGNMENT DESIGN SUMMARY

	Inner Shaft *		Outer Shaft *	
	Inner End	Outer End	Inner End	Outer End
Starting	0.0000 (0.0000)	0.0000 (0.0000)	0.013 (0.0050)	0.008 (0.0030)
50% Maximum Thrust	0.004 (0.0015)	0.004 (0.0015)	0.009 (0.0035)	0.005 (0.0020)
Maximum Thrust	0.008 (0.0030)	0.010 (0.0040)	0.0000 (0.0000)	0.004 (0.0015)

* All dimensions are in cm/cm (in/in)

Based on these spline misalignment analyses, standard spline configurations were defined for all towershaft couplings. This choice was made since the maximum running misalignment of 0.010 cm/cm (0.004 in/in), while transmitting 18.304 N-m (162 lb-in) of torque at 19,146 rpm is within experience for standard splines. With consideration for misalignment, spline stresses were estimated to be only 4 percent of those of current Pratt & Whitney engines with outer-diameter fan case-mounted accessories. A spline misalignment of 0.013 cm/cm (0.005 in/in) does occur during starting, but is not considered to be a problem.

Stiff-bearing critical speed analysis results showed the inner portion of the towershaft to have a 68 percent frequency margin; the outer shaft was estimated to have a 71 percent margin. Both of these margins meet the established design practice. The flexible-bearing critical speed analysis resulted in mode shapes for the first two flexible-bearing critical speeds as shown in Figure 70. From these data, the minimum critical speed margin is 38 percent. Again, this satisfies commercial engine design practice, and the towershaft is predicted to have no critical speed problems.
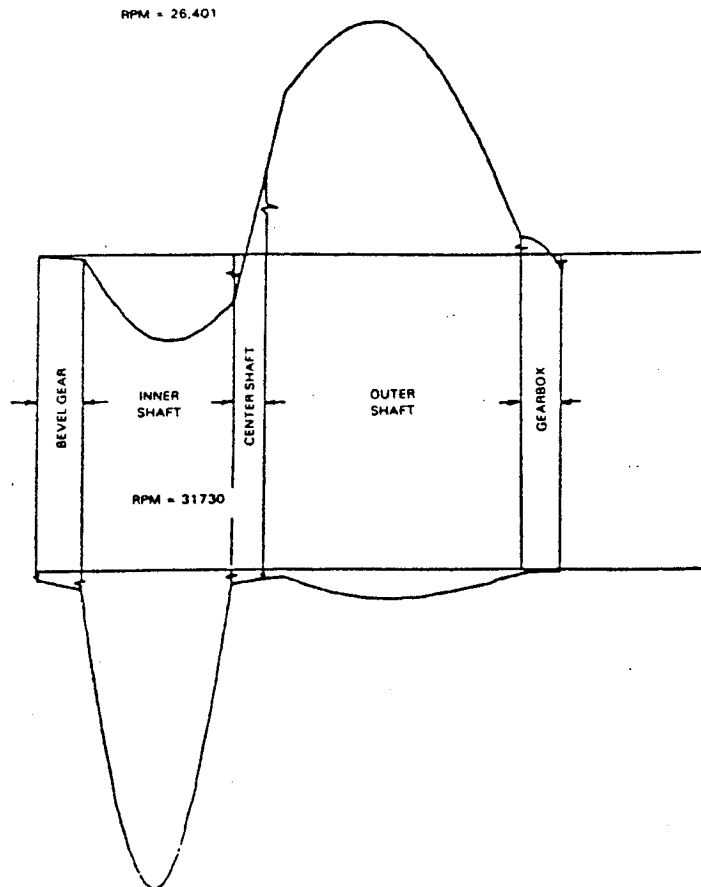
Figure 70 Towershaft Critical Speed Mode Shapes from Flexible-Bearing Analysis

3.2.2.4 Bearing Design

The towershaft bearings are all proven, existing designs. Analyses showed that all towershaft thrust and radial loads are well within the capacity of the bearings. As a result, all bearings were estimated to have B10 duty cycle lives in excess of 10,000 hours. Bearing design parameters are presented in Table XXIII.

98

TABLE XXIII

INTEGRATED CORE/LOW SPOOL TOWERSHAFT BEARING SUMMARY

Location*	1	2	3 & 4	5
Type	Roller	Ball	Ball	Roller
Size (mm)	35x80x21	50x90x29	40x68x15	50x90x20
Features	Straight-through Outer Race	Flanged Outer Race, Split Inner Race	Deep Groove, Preloaded through Wave Washer	Straight-through, Flanged Outer Race
Material	M-50	52100	M-50	M-50
Cage Riding Land	Inner	Inner	Inner	Inner
Loads, N (lb):				
Starting	5636 (1267) Radial	863 (194) Thrust	222 (50) Thrust (preload)	--
Max. Running	334 (75) Radial	205 (46) Thrust	258 (58) Thrust (preload)	151 (34) Radial

*See Figure 71

3.2.2.5 Oiling System

Figure 71 is a schematic of the accessory drive system lubrication system. Oil is directed to the towershaft gear, bearings, and splines, as described in the following paragraphs. In all cases, oil draining is by gravity.

The towershaft drive gear operates in an oil mist environment within the gear housing. In addition, a 0.91 kg/min (2 lb/min) oil jet is aimed directly at the ingoing gear mesh. Analysis indicated the maximum oil temperature increase caused by heat generation to be 8.3°C (15°F) for the jet flow, which is satisfactory for integrated core/low spool testing. Since the flight propulsion system will have full duty loads, more oil flow may be required to reject its heat generation.

The No. 1 towershaft bearing is lubricated by an oil jet aimed at the inner diameter of the inner end of the inner shaft. Oil is then directed through holes in the shaft wall and at the bearing by a slinger. Lubrication for the Nos. 2, 3, and 4 bearings is accomplished by external jets directed between the cage and the outer race. The No. 5 bearing is lubricated externally from the accessory gearbox. Design oil flow rates are presented in Table XXIV.
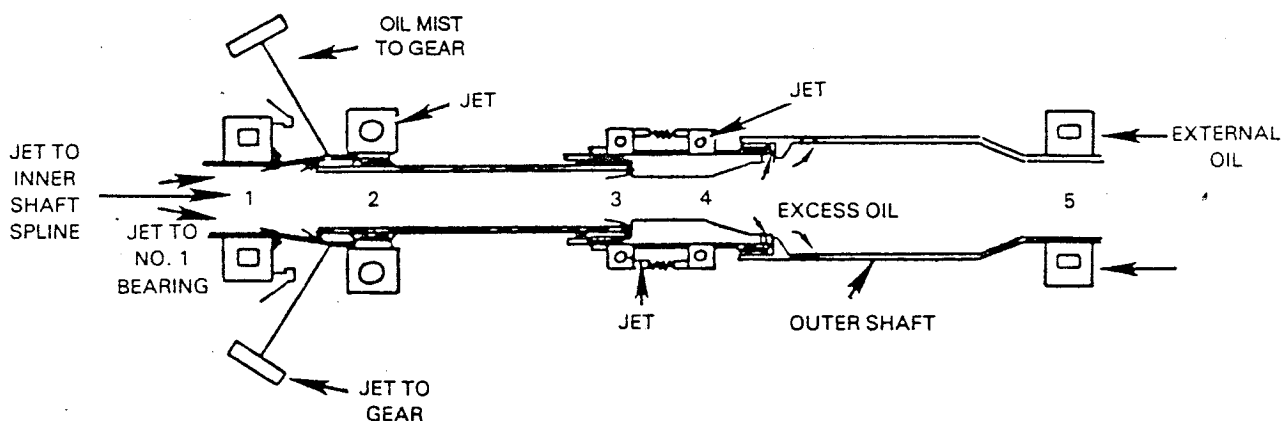
Figure 71   Schematic of Lubrication Scheme for the Accessory Drive System

TABLE XXIV

INTEGRATED CORE/LOW SPOOL TOWERSHAFT BEARING LUBRICATION SUMMARY

Bearing Number	Oil Flow Rate, kg/min (lb/min)
1	0.91 (2.0)
2	0.68 (1.5)
3 } 4 }	0.68 (1.5) [Combined]
5	1.36 (3.0)

The towershaft spline lubrication source is a 0.91 kg/min (2 lb/min) oil jet that is located at the inner end of the inner shaft and is directed toward the inner spline. Outward movement of the lubricating oil is assisted by centrifugal pumping effects. All of the splines are oil mist lubricated except for the one at the outer end of the inner shaft. This spline is flooded with oil, because of a seal incorporated in its assembly. Excess oil is extracted through drain holes located in the outer towershaft wall, just outboard of the inner-end spline coupling.

3.2.3 Structural Struts

3.2.3.1 General Description

The intermediate case structural struts join the core cases directly to the fan cases. The ten struts are equally spaced circumferentially, with one each located at the top and bottom center, as shown by Figure 72. Core gaspath portion cross sections are axial, symmetrical, uncambered airfoils. The fan gaspath portions of the structural struts are turning, fan exit guide vanes. A transitional section within the center casing connects the core and fan portions. The struts are hollow to reduce weight and to provide passages for the accessory drive towershaft and lubrication system piping. The thicker top strut forms the forward portion of the pylon. The rest of the structural/ nonstructural strut array consists of adjacent airfoil sections that are aerodynamically matched to the pylon airflow blockage. This configuration results in both a nominal and a 15-degree uncambered structural strut configuration in the fan stream. Pads in the transitional section of the struts receive mount ring bolts to transfer engine loads to the mount system.

Titanium is used to construct the structural struts. Specifically, AMS 4911 and AMS 4928, 6Al-4V alloys, are used for the regular and pylon struts, respectively. The pylon strut for the flight propulsion system is PWA 1262 material, a cast 6Al-4V alloy, for reduced cost.

FRONT VIEW
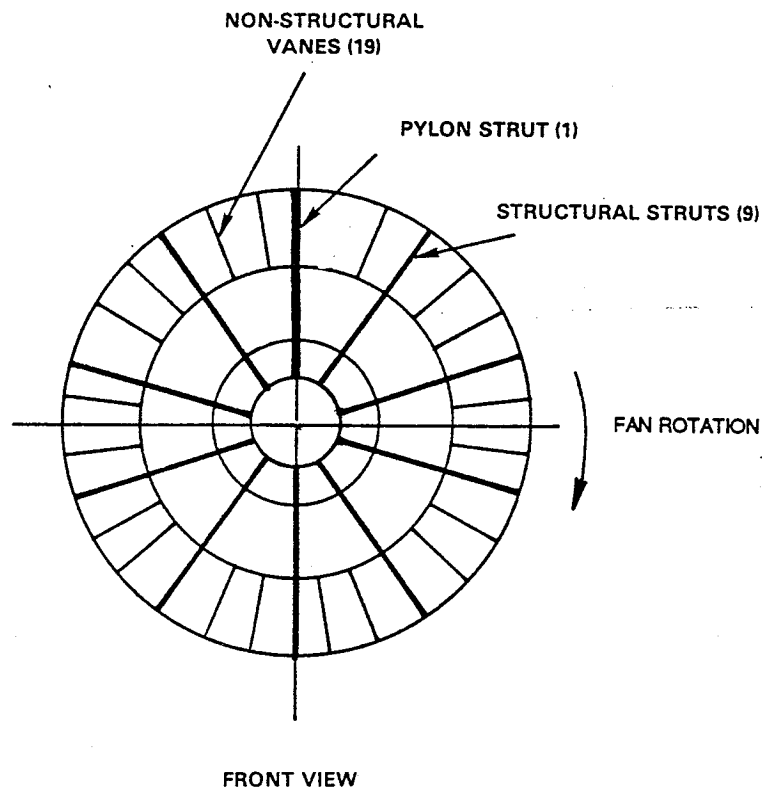
Figure 72   Intermediate Case Strut Assembly

The structural struts, except for the pylon, are fabricated using diffusion bonding and superplastic forming of titanium sheets to shape. Leading and trailing edge inserts in the core and transitional portions of the struts are premachined and welded into the strut sheets to reduce program costs and risks. In the flight propulsion system, these inserts are full span and diffusion bonded to the sheet. Collars, which are diffusion bonded to the strut to minimize stress concentration in the regions of strut-case interface welds, are deleted also to reduce cost.

The pylon strut is a fabricated titanium assembly. The inner portion is a solid piece, machined to accept the accessory drive towershaft. A stand-up is machined at the inner end to form an attachment with the inner case. A solid leading edge piece is welded between the outer end of the inner portion and a solid tip cap. Sheet titanium 0.4763 cm (0.1875 in) thick welded to the inner portion of the solid leading edge and the tip cap completes the fan stream portion fabrication. This fabrication approach was selected to eliminate high costs associated with pursuing the cast fabrication approach for the flight propulsion system for only one demonstrator part.

3.2.3.2 Strut Design

The design configuration for the nine regular structural struts is shown in Figure 73. These struts were sized and shaped based on aerodynamic considerations. Wall thicknesses were set at 0.254 cm (0.10 in) to ensure that the intermediate case is structurally deflection limited and that stresses in the struts themselves are low. Internal ribbing was added in the regions of camber and twist to provide shear ties between the outer sheets. Solid leading and trailing edge inserts were incorporated in the transitional and core portions of the strut as rigid load paths for thrust loads.

The final design configuration for the single pylon strut is shown in Figure 74. This strut was sized to contain the towershaft and to aerodynamically fair the leading edge into the pylon. The outer portion of this strut is hollow, whereas the inner portion is a solid body.

The structural struts are designed to carry flight propulsion system loads. These include aerodynamic gust loads and moments imposed on the inlet and outer fan case which are carried through the struts, thrust loads, aerodynamic loads on the struts themselves, and fan blade loss loads. The general design approach suggests that case deflections are the primary concern, because of tip clearance effects; therefore, stresses in the stiff structural struts themselves are low. Analyses indicated that maximum stress is under 206.8 MPa (30,000 lb/in^2), occurring locally at the rear of the struts as a result of high-pressure compressor case axial loads. More detailed structural analyses, in terms of case deflections caused by the imposed loadings, are presented in Section 3.1.5.2.

102

LEADING EDGE
INSERT

ENGINE AIR

TRAILING EDGE
INSERT

FAN AIR

SECT A-A

SECT B-2

SECT C-C
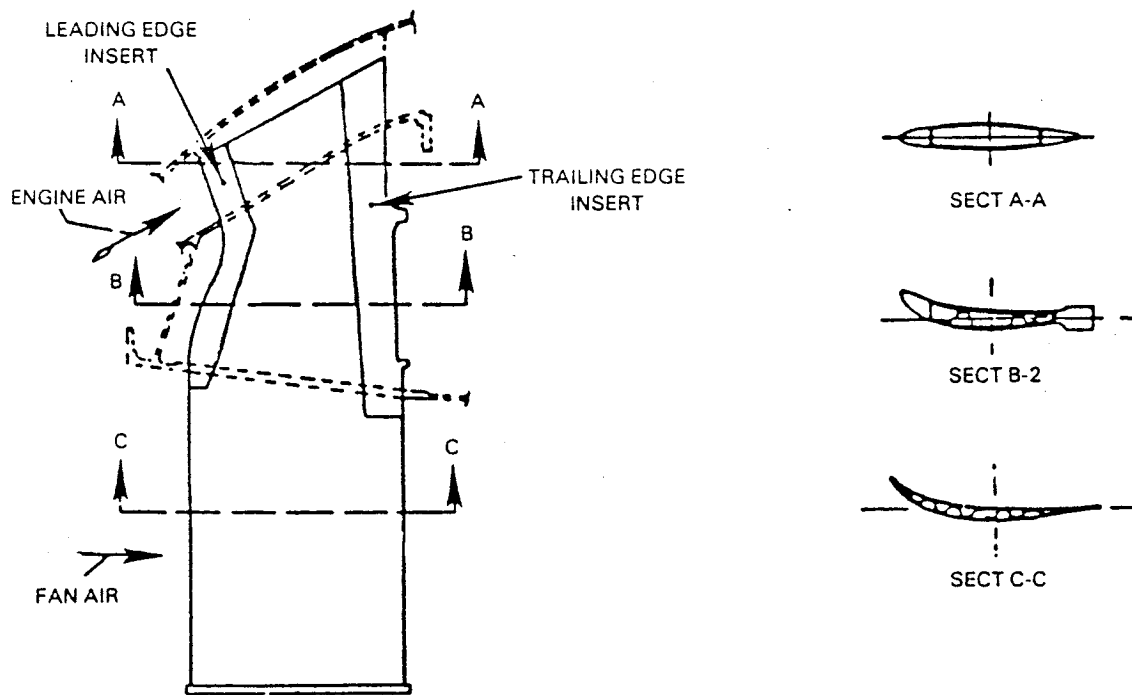
Figure 73   Regular Structural Strut Design

SECTION A-A

STAND-UP

BODY

SHEET

CAP

L.E.
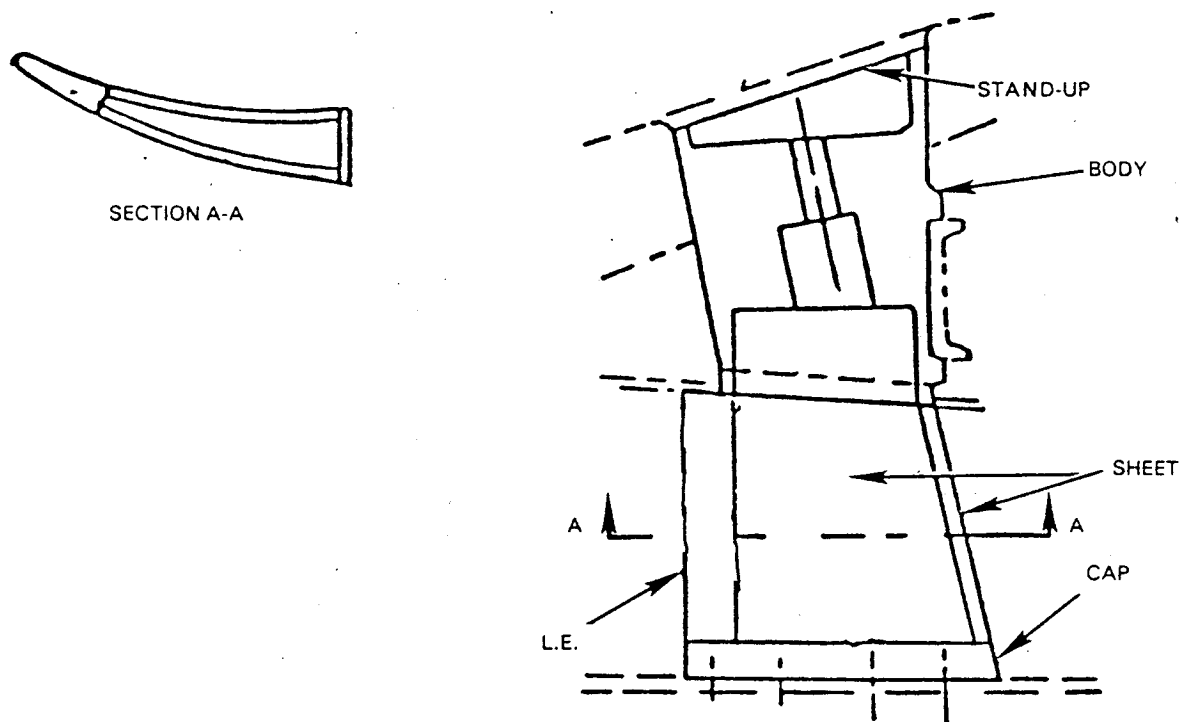
Figure 74   Integrated Core/Low Spool Pylon Strut Design

103

3.2.4 Nonstructural Struts

3.2.4.1 General Description

The intermediate case nonstructural struts or vanes are mounted in the fan stream between the center and outer cases as shown in Figure 72. They are generally located in groups of two between the ten structural struts. However, as shown, the vane immediately adjacent to the pylon on the convex side was eliminated during pylon matching in order to reduce flow area blockage. Pylon matching results in a nominal nonstructural strut and six variations: 5-, 10-, and 15-degrees over camber and uncamber.

The nonstructural struts are made from wrought aluminum base alloy, AMS 4115, to minimize experimental costs associated with the seven aerodynamically-different parts required. Flight propulsion system vanes are hollow, AMS 4911, 6Al-4V titanium alloy construction for light weight.

The nonstructural struts are machined from solid aluminum blocks to minimize program fabrication costs associated with the six types of camber variation. In the flight propulsion system, the vanes are fabricated in a manner similar to that of the structural struts, using diffusion bonding and superplastic forming of titanium sheets to the required shapes.

3.2.4.2 Strut Design

Design of the nonstructural struts is shown in Figure 75. These vanes were shaped by aerodynamic requirements. The vane mounting was designed to ensure that the vanes do not carry external loads. Soft mounting was accomplished by positioning the vanes over "tongue" stand-up supports that are fastened to the center and outer case walls. The clearance between the "tongue" and vane is filled with rubber to provide damping and flexibility in the joint. The object of this design approach is to ensure that the nonstructural struts carry only their own tangential aerodynamic loads. Resulting vane stresses were predicted to be insignificant.
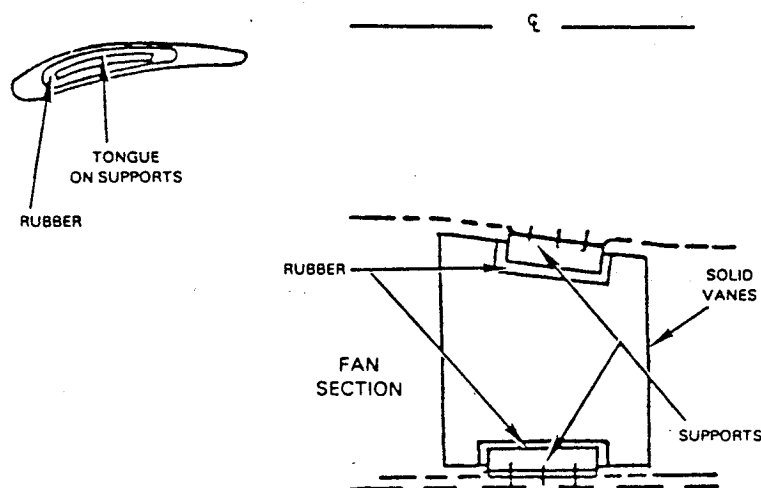
Figure 75   Nonstructural Strut Design

Nonstructural strut flutter stability was assessed. Calculations included nominal vane bending and torsion frequencies. Flutter analysis concluded that the vane design is substantially more conservative from a flutter standpoint than other Pratt & Whitney designs. This result is caused by the low (1.2) aspect ratio of the Energy Efficient Engine vane.

3.2.5 Cases

3.2.5.1 General Description

The intermediate case assembly includes three major casing rings, as shown by Figure 76. The inner casing forms the outer wall of the front bearing compartment and the inner wall of the flowpath transition between the low-pressure and high-pressure compressors. All support for the No. 1, No. 2, and No. 3 main shaft bearings and the inner support for the accessory drive towershaft is provided by the inner casing. Stand-ups are provided on the outer portion of the inner ring to which the structural struts are attached by welding. A center casing, which forms the core flowpath outer wall and the fan flowpath inner wall, is welded to the structural struts. This casing carries low-pressure and high-pressure compressor case loads, casing pressure loads, fan duct loads, and engine torque loads. The inner ends of the nonstructural struts are fastened to support tongues on the outer portion of the center casing. The outer case forms the fan flowpath outer wall. It provides support for the top-mounted accessory gearbox assembly and the outer ends of the structural struts which are fastened via flanges. The outer ends of the nonstructural struts are fastened to support tongues on the outer casing. Fan duct loads and loads associated with nacelle moments are carried by the outer casing.
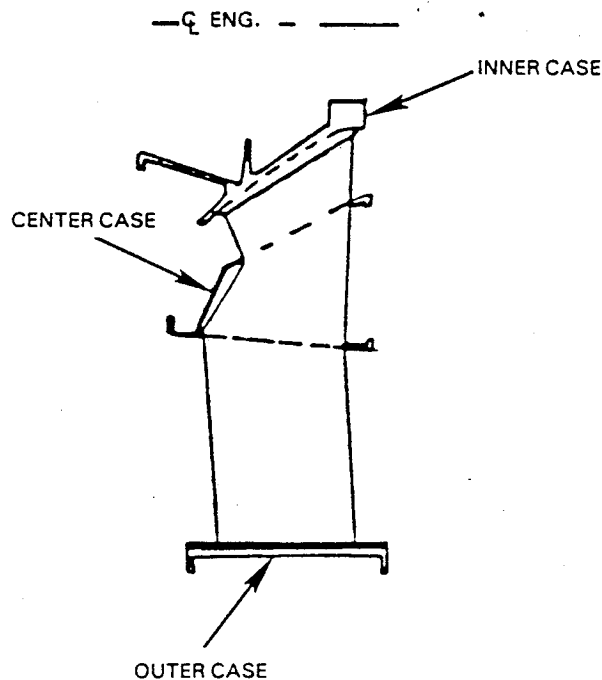
Figure 76   Casing Ring Configuration for the Intermediate Case Assembly

The inner and center casings are made of titanium, and the outer casing is aluminum. The inner ring is AMS 4928, a 6Al-4V titanium base alloy. AMS 4928 is also used in the center casing construction. A 2014 wrought aluminum base alloy, AMS 4135, is the material for the outer casing. These alloys will be used in the test demonstrator to provide the lowest costs. Variations of these materials are used in the flight propulsion system. Namely, PWA 1262, a 6Al-4V titanium base alloy, is used in the inner ring; AMS 4966, an A-110 titanium base alloy is in the center casing; and AMS 4150, a 6061 wrought aluminum alloy, is in the outer casing.

3.2.5.2 Case Design

Various loadings imposed on the casings are summarized in Figure 77. To accommodate the variety of loads, the compressor intermediate case is designed as a highly redundant structure to ensure adequate case stiffness and minimum deflections.

Nacelle gust moment and shear loadings and the thrust loadings analyzed are shown schematically in Figure 78. Analyses focused on inner casing distortion as it might impact No. 3 bearing radial positioning, high-pressure compressor case distortion in terms of airfoil tip clearance effects, fan case distortions and their impact on blade tip clearance, and identification of any areas of high stress.
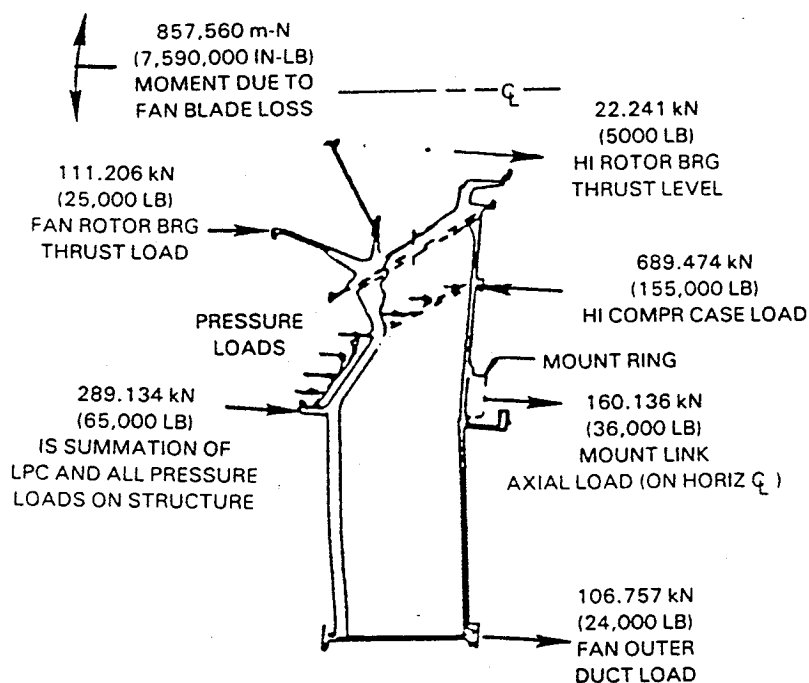
Figure 77   Intermediate Case Structural Loading at Sea Level Takeoff Thrust

106
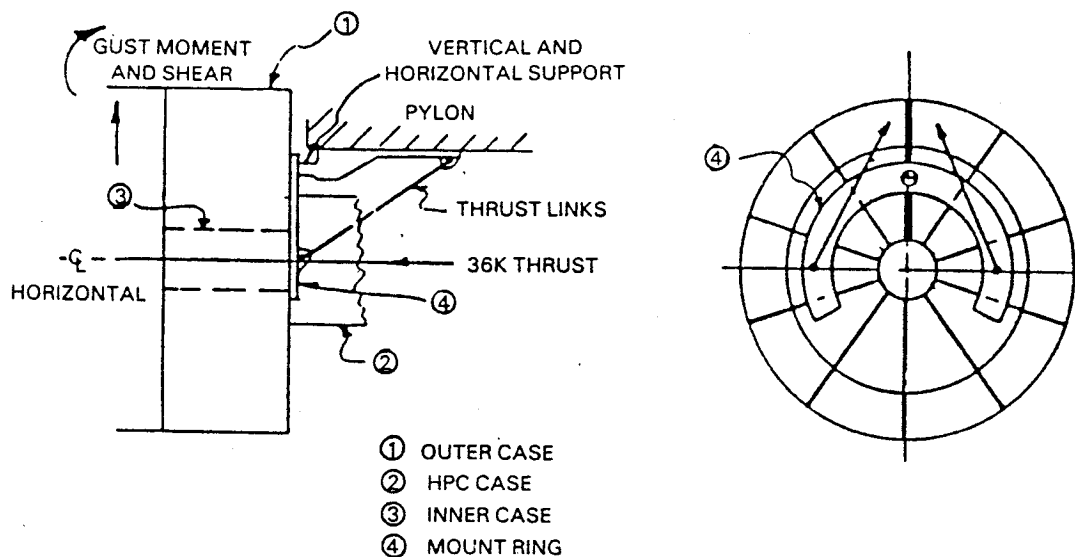
Figure 78   Schematic of Gust and Thrust Loadings

① OUTER CASE
② HPC CASE
③ INNER CASE
④ MOUNT RING

Inner casing radial stiffness is the primary factor in controlling roundness of the No. 3 bearing support ring when the system is subjected to radial loads. The integrated core/low spool uses an existing larger outer diameter No. 3 main shaft bearing which causes the inner casing, because of space limitations, to be only half as stiff as the flight propulsion system configuration. Analytical results showed that the static loads imposed on the intermediate case during maximum thrust operation will result in radial ovalization of approximately 0.01 cm (0.004 in). Further analysis indicated that the function of the No. 3 bearing support damper will not be affected by this deflection because damping occurs at low high-pressure spool speeds where case distortion is negligible. The flight propulsion system inner casing radial deflection at maximum thrust was estimated to be 0.008 cm (0.003 in). Distortion of the high-pressure compressor front case under maximum thrust conditions was determined to be 0.008 cm (0.003 in) radially, a small impact on blade tip clearances.

Nacelle gust loading effects were estimated on the basis of 50 percent load sharing between the nacelle and engine cases (no gust loads are imposed on the integrated core/low spool), with the result being 14,123 m-N (125,000 in-lb) of pitch moment and 66,723 N (15,000 lb) of shear load being carried by the intermediate case. Results showed that, because of the high case stiffness, nacelle loadings did not increase inner casing ovalization. Also, nacelle moments were estimated to produce a fan tip clearance at the aerodynamic design point of only 0.183 cm (0.072 in) relative to a goal level of 0.206 cm (0.081 in). Because nacelle gust loadings will not be imposed on the integrated core/low spool, the solid leading and trailing edge stiffener inserts are deleted in the fan stream portion of the structural strut to reduce program cost. Overall stress analysis in key areas of the intermediate case showed maximum stress to be under 205.84 MPa (30,000 lb/in^2); well within allowables.

Fan blade loss assessment resulted in the thickening of flange and wall connections, at the No. 1 to No. 2 bearing support interface and at the front high-pressure compressor to front case interface, in order to achieve acceptable stress margins.

Strut gas loadings are shown schematically in Figure 79. The primary concern associated with these loadings was case tangential deflection, which affects accessory drive towershaft misalignment. The design approach taken to accommodate towershaft misalignment is described in Section 3.2.2.3.
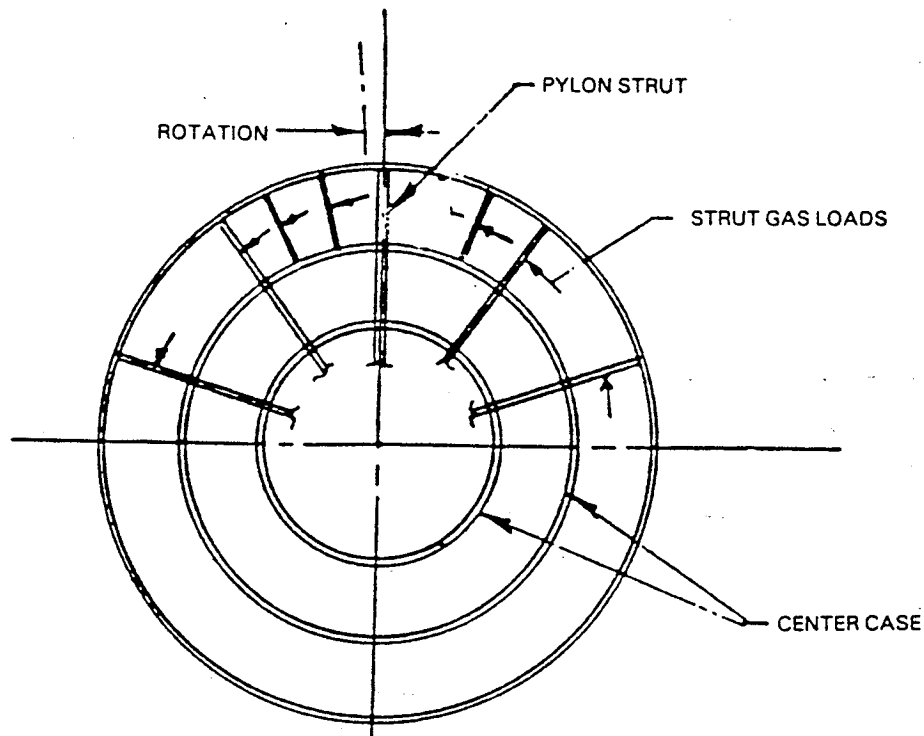
Figure 79   Schematic of Strut Gas Loading

Analysis of strut gas loadings showed center casing tangential deflection between starting and maximum thrust conditions to cause 0.33 cm (0.130 in) rotation of the outer casing. In addition, deflection of the pylon strut itself because of these loads was found to result in 0.178 cm (0.070 in) of outer case rotation. The net 0.508 cm (0.200 in) rotation of the outer case is in itself no problem for the flight propulsion system with its core mounted accessories. However, since the integrated core/low spool has its towershaft driving an accessory gearbox mounted on the outer casing, this rotation would result in excessive towershaft spline misalignment if the special design approach of mounting the gearbox pad 0.254 cm (0.100 in) tangentially in the opposite direction to case rotation had not been taken.

Twisting of the inner casing system caused by strut induced axial moments was investigated, and results showed case stiffness to be such that twisting deflections were negligible. Additionally, no local distortions were predicted.

108

SECTION 4.0

HIGH-PRESSURE COMPRESSOR COMPONENT TEST RIG

4.1 TEST RIG ASSEMBLY

4.1.1 General Description

The Energy Efficient Engine high-pressure compressor rig is the vehicle in which the component will be first tested and the aerodynamic performance fully measured.

Major features of the test rig assembly include: 1) the rig inlet section, that simulates the low-pressure compressor flowpath, with inlet distortion capability; 2) the high-pressure compressor component rotor assembly and front vane case; 3) remotely variable rear stators; 4) a simulated diffuser and burner section; and 5) a close-coupled throttling valve. Figure 80 shows a cross section of the rig.

The rig conceptual arrangement uses as much existing high-pressure compressor rig hardware as possible to reduce program cost. The distance between the No. 3 and No. 4 bearings was retained the same as in a similar Pratt & Whitney advanced high-pressure compressor rig, while the distance between the No. 4 and 4 1/2 bearings was increased by 5.45 cm (2.144 in) in order to be able to use an existing rear shaft, coupling nut, and assembly tooling.

Other features incorporated to increase the slip ring drive-bearing life when operating with a heated inlet include: 1) installation of insulation around the slip ring area, 2) slip ring inboard drive bearing heat shielding and insulation, 3) liquid cooled drive bearing housing supports, 4) grease packed bearings, and 5) increased cooling air capacity to the outboard bearing.

4.1.2 Rig Static Hardware

4.1.2.1 Inlet and Simulated Hot-Section Design

The rig design requirements to simulate engine inlet and exit conditions, as well as secondary flow systems and engine thermal response, resulted in the selection of AMS 5613 stainless steel for the inlet section and AMS 5662 to meet the high temperature strength requirements of the simulated diffuser-burner section.

All inlet cases and slip-ring supports were detailed to the basic design configuration (Figure 80). Simulation of the engine low-pressure compressor bleed (Figure 89) was accomplished by designing a manifold with eight take off ports for measuring and controlling the quantity of bleed air. To evaluate the effects of the low-pressure compressor bleed opening on compressor performance, the outer case of the manifold is split for removal and a filler ring inserted to close off the annular bleed at the flowpath.

The plumbing required for cooling the slip ring and fulfilling the requirements of the secondary flow system (described in Section 4.1.4) was incorporated into the intermediate case by passing the jumper tubes through the struts. The nozzle for lubricating the No. 3 bearing and cooling the carbon seal rings is similar to that used in a recent advanced high-pressure compressor rig. This nozzle provides for lubricating the preloaded bearing, prior to rig start, to avoid possible scuffing.

The two most important considerations in the design of the diffuser case were: 1) duplicating the engine diffuser flowpath configuration, and 2) accommodating the engine exit guide vanes. To minimize any relative axial movement between the inner and outer walls of the diffuser due to differential thermal growth, the inner case is welded to the inner end of the struts and features a slip joint sealed by a piston ring aft of the struts. The inlet to the diffuser was designed to accommodate the engine exit guide vane and inner sealing hardware.

In the design of the No. 4 bearing case, it was necessary to provide for dissipation of the thermal stresses at the junction of the cool bearing housing and the hot main case. This was done by joining the bearing housing to the main case by a long thin cylindrical member with a heat shield around the cylinder in order to insulate it from direct exposure to the surrounding hot environment.

HIGH

THRUST BEARING

INSULATED INNER
NOSE CONE

50.1" DIA

BELLMOUTH

DISTORTION SCREEN
ROTATOR
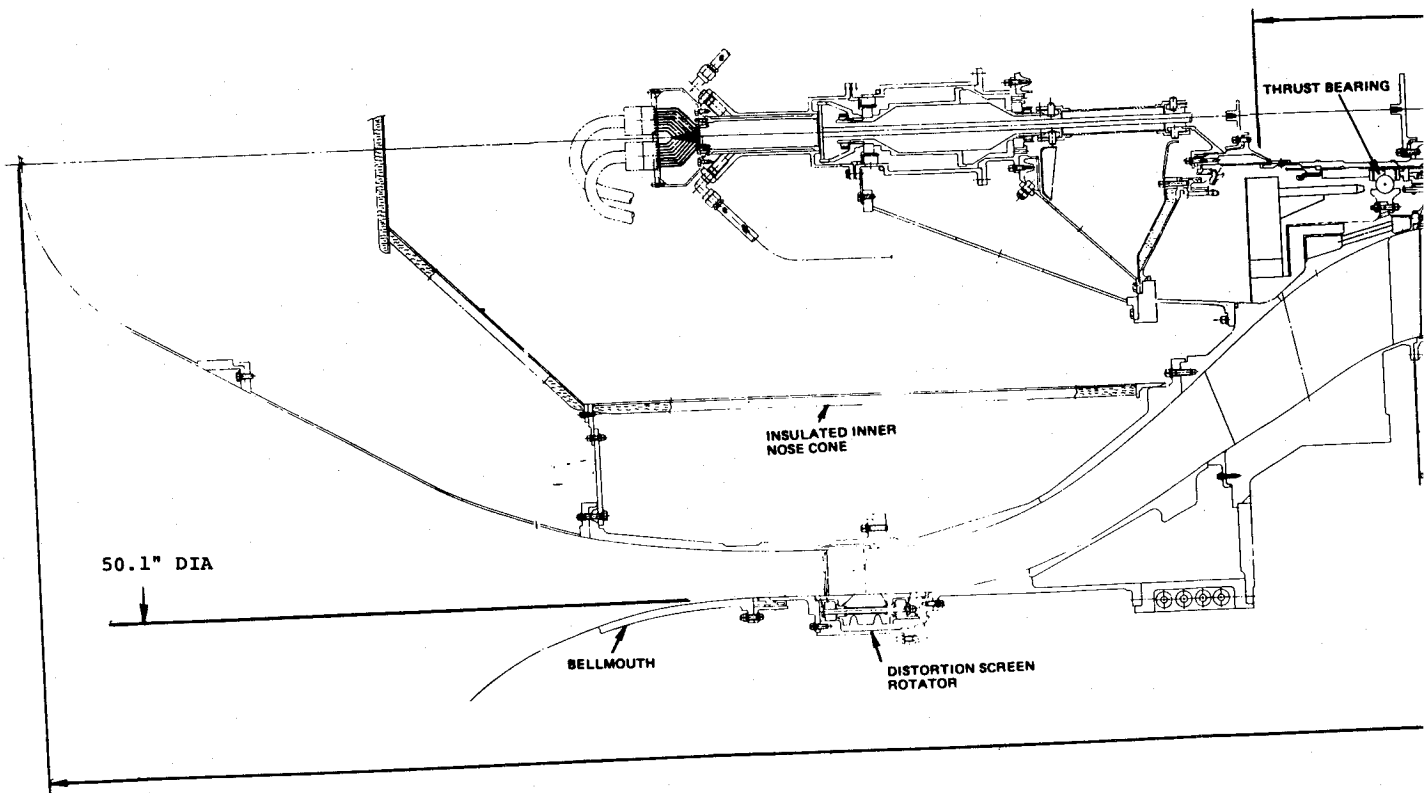
FOLDOUT FRAME

PRESSURE COMPRESSOR RIG.
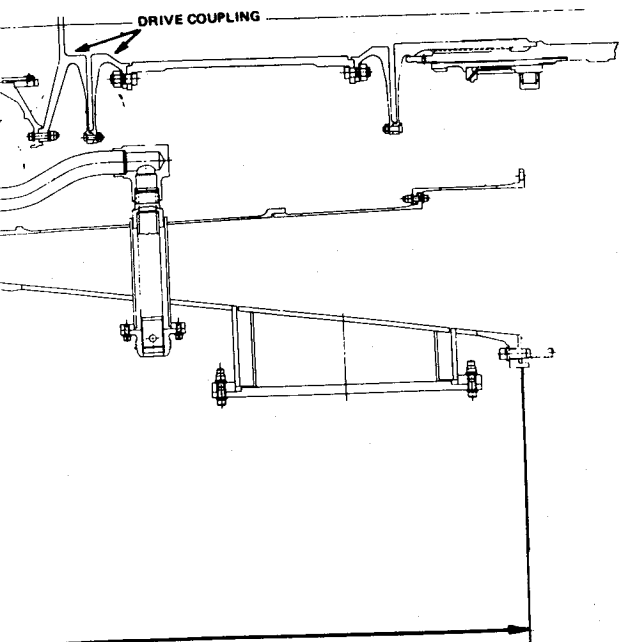
56.9"

THRUST BALANCE
PISTON SEAL

#4 1/2
BEARING

#4 BEARING

MOCK TURBINE
COUPLING SHAFT

THRUST BALANCE
PISTON SEAL

EXIT GUIDE VANE

CLOSE - COUPLED
THROTTLE VALVE

16.5"

189.4"

O/A LENGTH

Figure 8

2 FOLDOUT FRAME

DRIVE COUPLING

80   High-Pressure Compressor Rig

3 **FOLDOUT FRAME**

111

4.1.2.2 Rear Variable Vane Case and Adjustable Vanes

The rig rear case and stator assembly (stages 9 through 14) was designed consistent with recent advanced high-pressure compressor rigs, with the exception that full vane remote variability was incorporated for greater flexibility in developing the vane schedules and optimizing compressor performance. The rear case and stator assembly is built in half-segments with axial flanges bolted together with 26 Waspaloy fasteners, as shown in Figure 81.
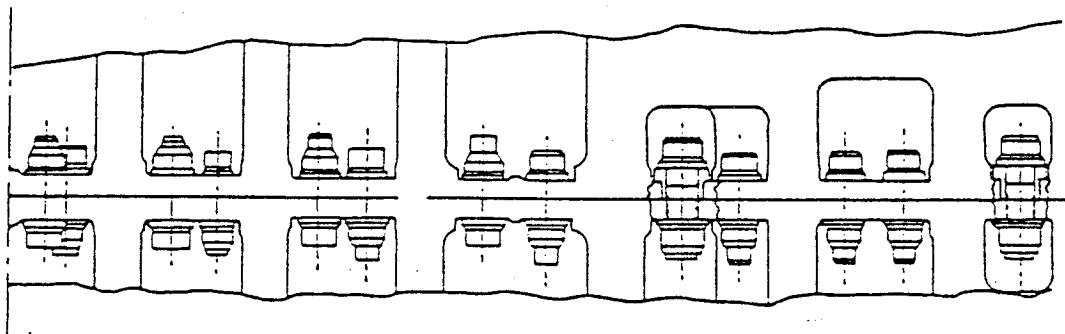
Figure 81   Bolted Axial Flange Used on Compressor Rig Rear Vane Case

This case is designed to the rig test-condition requirements and with consideration of recent advanced high-pressure compressor rig rear case experience. The rig case flowpath matches the engine flowpath at the aerodynamic design point; the machining dimensions are a function of the high expansion Inconel-718 material. Full 180-degree rings are provided at the stator trunnion locations to reduce case ovalization. The case bleed manifolds have been designed to attempt equalization of ring stiffness around the circumference. Also, the axial flange is designed to provide a maximum number of fasteners (11 doweled and 2 standard bolt fasteners per flange). Analysis of thermal stresses at the aerodynamic design point and maximum stress at maximum pressure indicated a maximum stress level of 310.26 MPa (45,000 lb/in^2) and case ovalization of less than 0.025 mm (0.001 in). As shown in Table XXV, the blade tip gap is 0.254 mm (0.010 in) average at the aerodynamic design point with the cold assembly tip gap of 0.432 mm (0.017 in) average. Corresponding knife-edge seal gaps are shown in Table XXVI. Analysis indicates the tip clearance pinch point will occur during acceleration; therefore, the rig must be accelerated slowly to the steady-state aerodynamic design point. The blade tip rub strip consists of Nichrome polyester abradable material 2.285 mm (0.090 in) deep. Because of the mass of the rear case, no problems are expected during deceleration. Standard carbon-faced journal bearings are provided at the vane trunnion locations.

The eighth- and tenth-stage bleed hole area and pattern are identical to those incorporated in the engine. A cross section of the rig rear vane case is shown in Figure 82.

The case includes provisions for borescope inspection, tip clearance probes, and wall static instrumentation and meets all rig requirements.

TABLE XXV

BLADE TIP CLEARANCE

| Rotor Number | Growth, Cold-to-Hot, mm (in) | | Clearances, mm (in) | |
	Cases	Rotors	Aerodynamic Design Point	Cold at Assembly
9	0.762 (0.030)	0.965 (0.038)	0.330 (0.013)	0.533 (0.021)
10	0.965 (0.038)	1.270 (0.050)	0.279 (0.011)	0.584 (0.023)
11	1.143 (0.045)	1.346 (0.053)	0.297 (0.011)	0.483 (0.019)
12	1.372 (0.054)	1.422 (0.056)	0.254 (0.010)	0.305 (0.012)
13	1.549 (0.061)	1.499 (0.059)	0.254 (0.010)	0.203 (0.008)
14	1.651 (0.065)	1.905 (0.075)	0.254 (0.010)	0.508 (0.020)
15	1.753 (0.069)	2.032 (0.080)	0.229 (0.009)	0.508 (0.020)
	Average Clearance =		0.254 (0.010)	0.432 (0.017)

TABLE XXVI

KNIFE-EDGE SEAL CLEARANCE

| Rotor Number | Growth, Cold-to-Hot, mm (in) | | Clearances, mm (in) | |
	Cases	Rotors	Aerodynamic Design Point	Cold at Assembly
9	0.762 (0.030)	0.813 (0.032)	0.381 (0.015)	0.432 (0.017)
10	0.914 (0.036)	1.041 (0.041)	0.381 (0.015)	0.508 (0.020)
11	1.092 (0.043)	1.168 (0.046)	0.381 (0.015)	0.457 (0.018)
12	1.295 (0.051)	1.270 (0.050)	0.381 (0.015)	0.356 (0.014)
13	1.422 (0.056)	1.372 (0.054)	0.381 (0.015)	0.330 (0.013)
14	1.473 (0.058)	1.778 (0.070)	0.381 (0.015)	0.686 (0.027)
	Average Clearance =		0.381 (0.015)	0.457 (0.018)
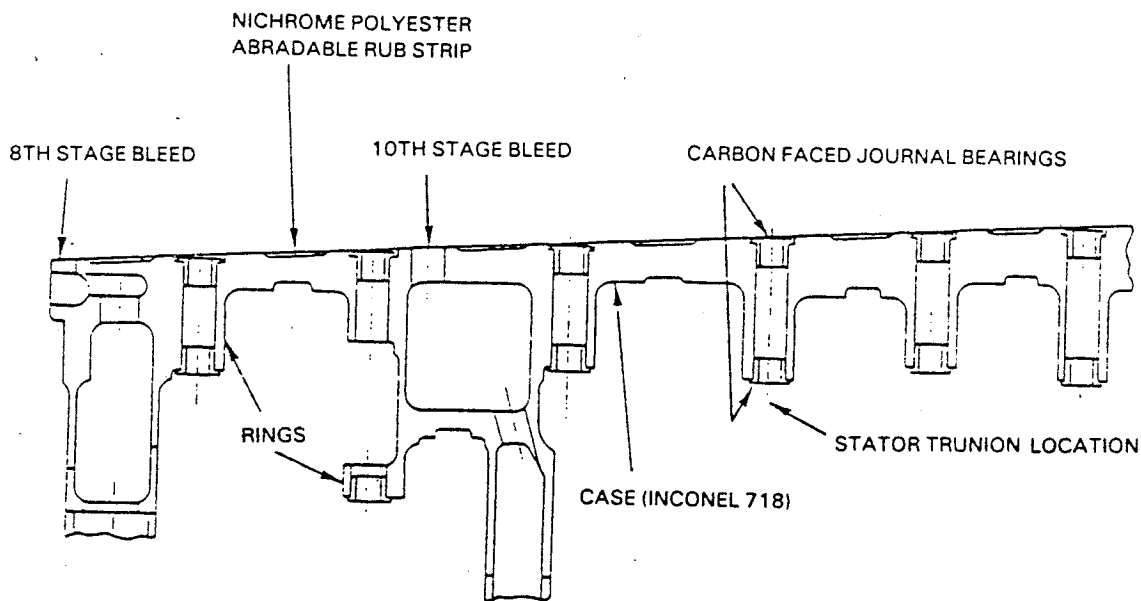
Figure 82   Cross Section of Compressor Rig Rear Vane Case

The variable vanes in stators 9 through 14 are all of a similar configuration. The design consists of an inner diameter pedestal with a lock ring groove, an inner diameter button, the airfoil, an outer diameter button, and an outer diameter trunnion. This configuration is shown in Figure 83. The button diameter is optimized to reduce high-pressure compressor length and provide approximately 60 percent airfoil coverage to reduce vane flutter. The rotation point is located at the 30 percent chord station (maximum thickness) to facilitate instrumentation installation. Stators 10 through 14 are designed with provision for ±10-degree stagger variation, while the 9th stage is provided with a stagger variation from -30 to +10 degrees.

The stator trunnions are inserted radially into the outer case. The inner diameter shrouds, which couple four stators together, are then assembled radially onto the stator inner diameter pedestals and secured with a lock ring on each vane. The inner diameter seal is circumferentially assembled on the shroud and locked with a tab lock. This configuration is shown in View B, Figure 84. The lever arms are symmetrical about their center line and may be attached to the vane trunnion either side out. Also belleville washers are provided for positive outward positioning, eliminating the necessity of classified spacers. The 6.35 mm (0.25 in) bolt fastener is designed to preclude thread engagement unless the actuation arm is properly assembled to the trunnion. A cross section of the vane inner button and inner shroud assembly and the actuation lever arm assembly is shown in Views A and B, Figure 84.

The inner diameter seal comprises a FELTMETAL™ abradable rub strip and is designed to run at 0.381 mm (0.015 in) clearance at the aerodynamic design point, with the same acceleration and deceleration ground rules as assigned to the case. This arrangement approximates the engine leakage pattern and precludes thermal binding. The shroud geometry is optimized to reduce the high-pressure compressor rig length and cavity depth.

PEDESTAL

LOCK RING

INNER DIAMETER
BUTTON

FOIL

OUTER DIAMETER
BUTTON

OUTER DIAMETER
TRUNION

STAGE	MATL
9	AMS 5616
10	AMS 5616
11	AMS 5616
12	AMS 5616
13	AMS 5663
14	AMS 5663
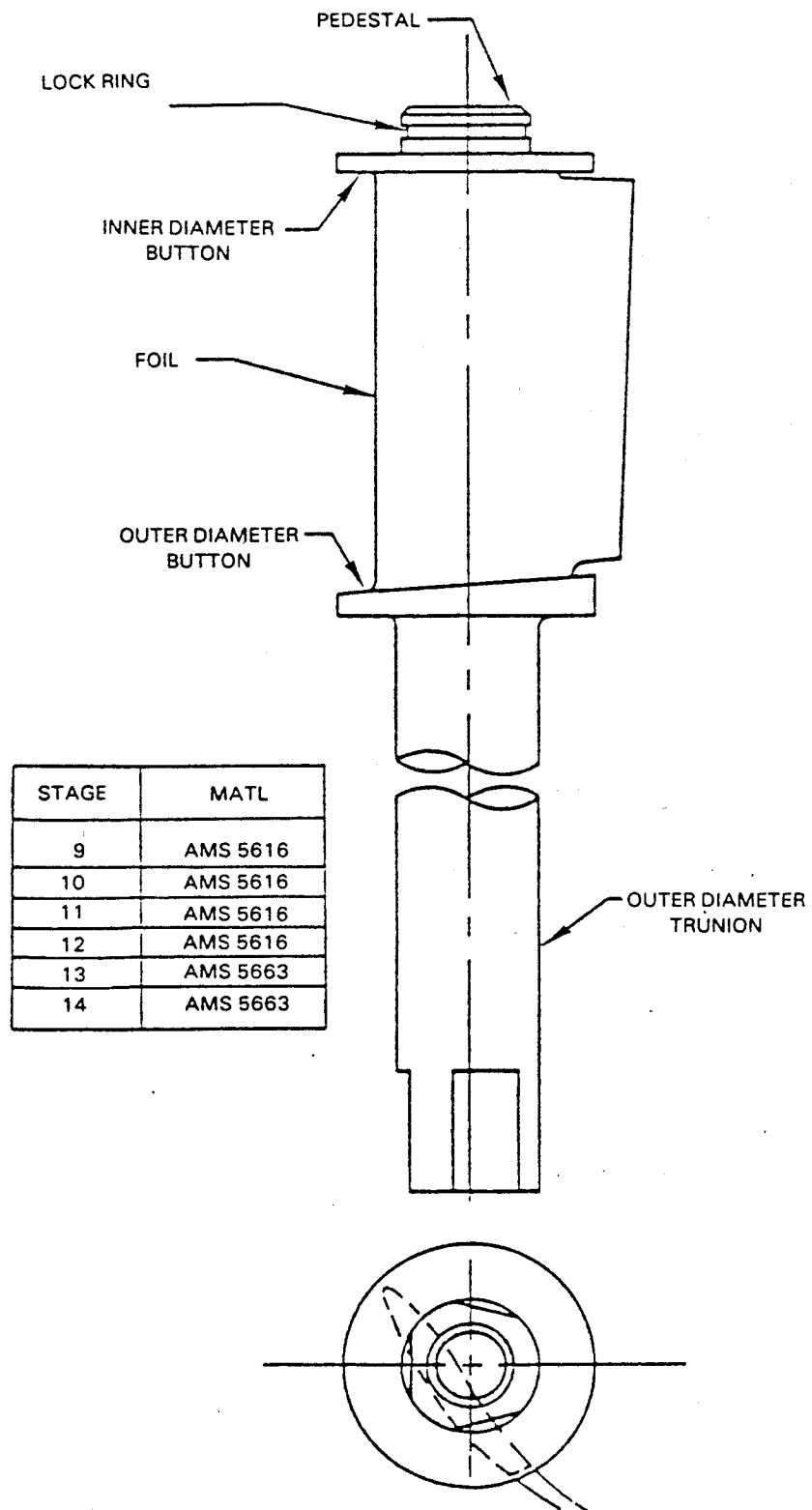
Figure 83   Typical Rig Rear Variable Stator Vane
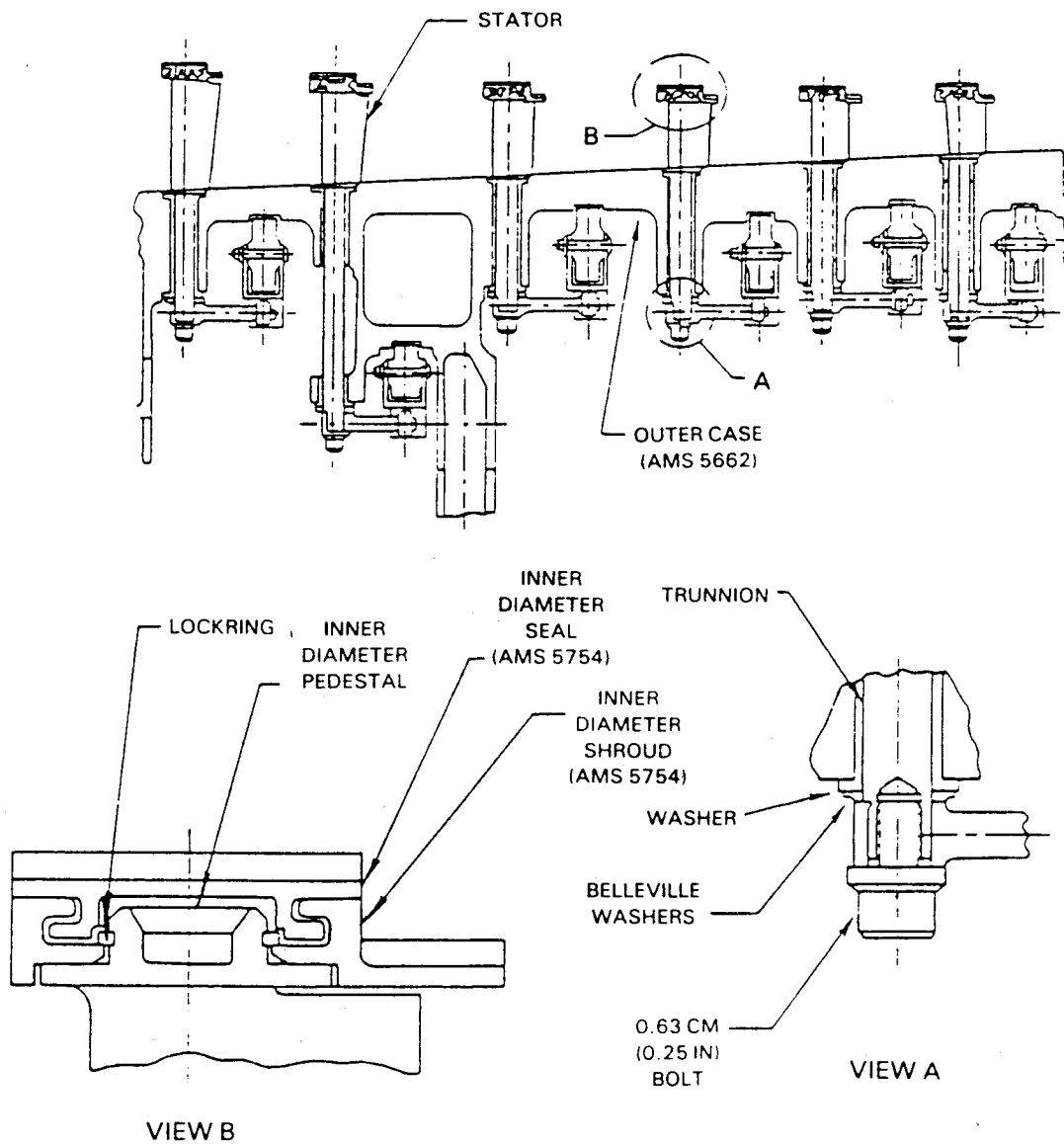
Figure 84   Stator Trunnions and Inner Shroud Configuration

4.1.2.3 Actuation System for Ten Variable Stators

An actuation system shown in Figure 85 has been designed to provide independent, remote, hydraulic control of each of the ten variable stators with dual electronic position feedback and readout, plus single visual position readout.

The close axial spacing of the rear vane unison rings dictated that the unison ring actuation cylinders be either alternately oriented in one gang or separated into two gangs to maintain unidirectional actuation. The former arrangement was chosen, because of limited compartment space and cost benefits.
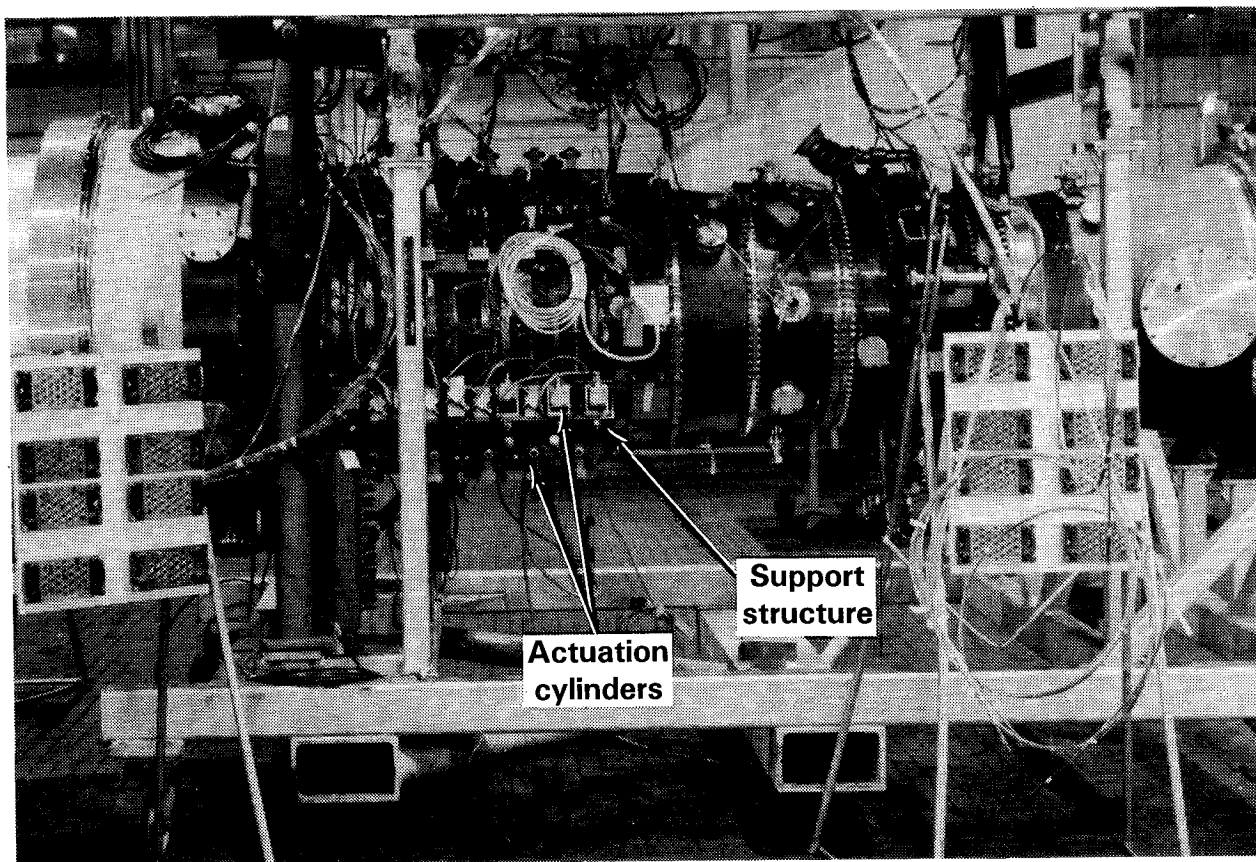
Figure 85 Variable Stator Actuation System Showing Support Structure and Orientation of Unison Ring Actuation Cylinders

To house and support the cylinders, a welded I-beam type structure was chosen. Gimballed cylinders are alternately placed within the beam, in a plane perpendicular to the beam axis. To preclude transfer of high bending moments to the case flanges, the beam is simply supported at one end, and pinned at the other. Rod ends are dressed with turnbuckles and stop nuts (common for all stages) for adjustment capability. Each rod end attaches to a unison ring by a clevis and bolt.

Hydraulic cylinder control valves are positioned between cylinders on a dual function base which serves as a fluid line distributor and beam flange stiffening gusset.

Two banks of resolvers, which are the electronic vane angle position indicators, mounted 180 degrees apart are used for comparison purposes. Dial indicators and pointers are included on one bank of resolvers for visual readout of vane angle position. Coupling the resolver shaft to the vane trunnion demanded a connector with precision angular transmission capability and unhindered lateral flexibility. This need was provided by an "off the shelf" telescoping double universal-joint coupler featuring zero backlash, 6.35 mm (0.25 in) extension capability, and sealed lubrication.

To ensure actuated-vane position stability, the hydraulic cylinder/resolver support beam was designed for stiffness. Loads used include system weight of 113.4 kg (250 lbm) under 10 g's and a resultant cylinder unison ring actuation load of 0.156 MN (3500 lbf). A compartment temperature of 149°C (300°F) was assumed.

The beam analysis revealed negligible bending stresses [under 27.6 MPa (4000 psi)] and 0.076 mm (0.003 in) maximum deflection. Deflection compares with assigned clearances of beam suspension system components. Converted to vane angle deviation, this amounts to less than 1×10^{-6} radian (0.2 second) of arc.

4.1.3 Rig Rotating Hardware

The rig rotating hardware meets or exceeds the requirements for burst margin, critical speed margin, coincidence margin, and resonant frequency margin. This rig hardware is capable of running at the planned operating conditions shown in Table XXVII.

4.1.3.1 Bearings

The rig No. 3 bearing has the same internal geometry as the integrated core/low spool No. 3 bearing, except that it uses a flanged bearing race due to the possibility of high-pressure rotor thrust reversals during rig operation. The rig high-pressure rotor is thrusted forward. The thrust load is 22,241 to 26,689 N (5,000 to 6,000 lbf) at the aerodynamic design point condition excluding coupling preload. The rotor has been positioned axially to run at the same hot running position as it would in the integrated core/low spool engine. The No. 3 bearing hub was modified to provide a support surface for the center tube and an axial extension for a slip-ring drive provision.

An existing No. 4 bearing was utilized in the rig. The bearing compartment, however, incorporates a new hub that is compatible with the front thrust balance seal and an existing rear shaft and coupling nut. A new damper was also designed to provide the desired radial damper clearances.

Rotor dynamics analysis indicated the need for a damped No. 4 1/2 bearing. A revised No. 4 1/2 bearing, incorporating the better features of previously tested No. 4 and 4 1/2 bearings, was specified. The radial damper clearances were established, and a new bearing support structure was designed to accommodate the damped bearing.

TABLE XXVII

HIGH-PRESSURE COMPRESSOR RIG TEST CONDITIONS

	I	II	III	IV	V	VI	VII	VIII	IX
	Aerodynamic Design Point	100% Ncorr, Near Surge	Maximum Mechanical Speed	Max Ncorr, High Operating Line	100% Ncorr, Wide Open Discharge	Rig Idle	Engine Starting Region	100% Ncorr, Minimum PT2.5	100% Ncorr, Maximum TT2.5
PT Inlet, kPa	100*	100	100	100	100	100	100	35	100
(psia)	14.5*	14.5	14.5	14.5	14.5	14.5	14.5	35	14.5
TT Inlet, °C	66.7	66.7	76.1	66.7	66.7	15	15	66.7	104.4*
(°F)	152	152	169	152	152	59	59	152	220*
PT Exit, kPa	1400	1751	1648	1800*	951.5	200	117	482.6	1400
(psia)	203	254	239	261*	138	29	17	70	203
TT Exit, °C	519.4	595	603.3*	602.2	471.1	112.8	39.4	519.4	582.2
(°F)	967	1103	1118*	1116	880	235	103	967	1080
W corr, kg/sec	35.2	35.2	39.0*	39.0	35.2	6.4	4.5	35.2	35.2
(lb/sec)	77.5	77.5	86.0*	86.0	77.5	14.0	10.0	77.5	77.5
W actual, kg/sec	32.1	32.1	35.1	35.6*	32.1	6.4	4.5	11.0	30.8
(lb/sec)	70.7	70.7	77.3	78.5*	70.7	14.0	10.0	24.3	68.0
Pressure Ratio	14.0	17.5	16.5	18.0	9.5	2.0	1.2	14.0	14.0
% Design N corr	100	100	105	105	100	50	25	100	100
N corr, rpm	12,136	12,136	12,743	12,743	12,136	6,068	3,034	12,136	12,136
N mech, rpm	13,168	13,168	14,025*	13,186	13,186	6,068	3,034	13,168	13,680
Power Input, kW	15,257	17,945	19,612	20,216*	13,558	627	111	5,244	16,820
(hp)	20,460	24,064	26,300	27,110*	18,181	841	149	7,032	22,556
Torque, m-N	11,063	13,013	13,353	13,962*	9,831	987	350	3,802	11,355
(ft-lb)	8,160	9,598	9,849	10,298*	7,251	728	258	2,804	8,656

* Maximum values for test program

4.1.3.2 Center Tube

A center tube was provided in the rig to simulate that in the engine and is used to facilitate strain gage and thermocouple lead wire routing through the high-pressure compressor to the slip ring. A welded construction center tube was investigated to reduce costs. A vibration analysis of the center tube demonstrated that it has adequate resonant frequency margin. The center tube hoop stress is 79.03 MN (11,463 psi) at maximum mechanical speed condition. It also has an 8180 N (1839 lbf) blow-off load acting across it at the maximum corrected speed, high operating line condition. This load is resisted by eight Hastelloy X rivets loaded in shear with an actual shear stress of 57.43 MN (8329 psi) versus an allowable stress of 127.3 MN (18,464 psi). Sufficient flow area, 45.16 cm^2 (7 in^2), is provided through the center tube to allow flow to the aft side of the rear thrust balance seal through an area of 10.13 cm^2 (1.57 in^2). The forward center tube support flange, connected to the eighth-stage rotor disk bore, is scalloped to provide a flow area from the forward drum rotor cavity greater than the 22.58 cm^2 (3.5 in^2) at the No. 3 bearing hub location.

4.1.3.3 Disks

The high-pressure compressor component disks were modified for use in the rig by incorporating instrumentation holes for buried metal thermocouples and blade strain-gage leads. Fracture mechanics analysis was used to assure adequate disk lives with the addition of these holes.

4.1.3.4 Thrust Balance Seals

The front thrust balance seal was designed to achieve acceptable resonant and coincidence margins, and adequate low cycle fatigue life and burst margin. The labyrinth seal clearances were set at the aerodynamic design point condition. PWA 1010, an alloy without cobalt, was selected as the seal material. Figure 86 summarizes the low cycle fatigue life at the principal stress locations on the front thrust balance seal disk.

The rear thrust balance seal was designed to achieve the resonant and coincidence margins, and adequate low cycle fatigue life and burst margin. The labyrinth seal clearances were set at the aerodynamic design point condition. PWA 1010 was again selected as the seal material to avoid using a material containing cobalt. Dampers were incorporated at the seal land locations to avoid coincidence. Figure 87 summarizes the low cycle fatigue life at the principal stress locations on the rear thrust balance seal disk.
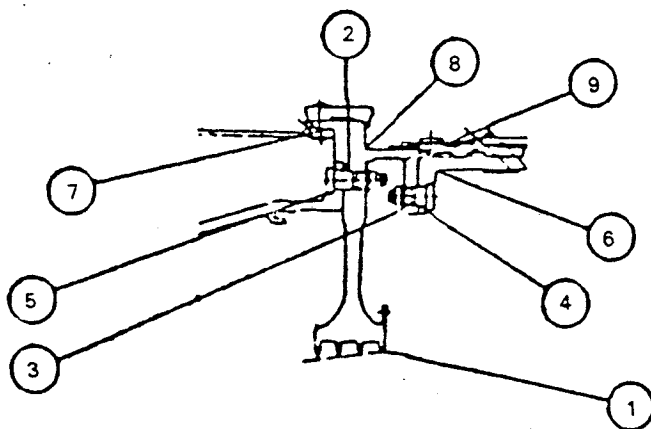
LOCATION	LOW CYCLE FATIGUE LIFE
1	$> 10^5$ CYCLES
2	30,000
3	$> 10^5$
4	$> 10^5$
5	$> 10^5$
6	$> 10^5$
7	$> 10^5$
8	$> 10^5$
9	$> 10^5$

Figure 86   Summary of Front Thrust Balance Seal Low Cycle Fatigue Life
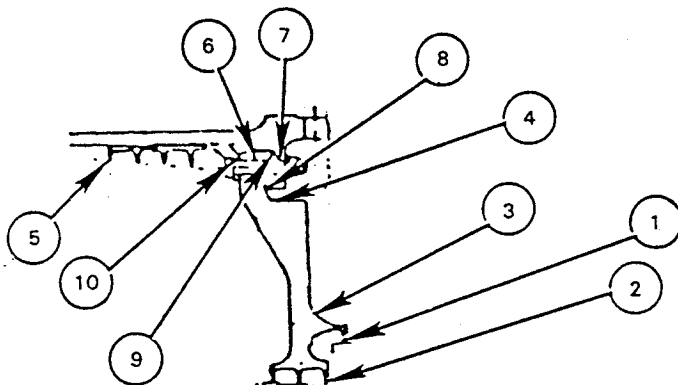
LOCATION	LOW CYCLE FATIGUE LIFE
1	12,000 CYCLES
2	100,000
3	$> 10^5$
4	$> 10^5$
5	$> 10^5$
6	5,500
7	$> 10^5$
8	$> 10^5$
9	55,000
10	$> 10^5$

Figure 87   Summary of Rear Thrust Balance Seal Low Cycle Fatigue Life

122

4.1.3.5 Rear Shaft

The rear shaft was evaluated for its torque transmission capability and its ability to transmit the rear thrust balance seal axial load. The resulting stress analysis summary for the No. 4 hub and rear shaft is shown in Figure 88. Rotor critical speed analysis indicated that the shaft has adequate margin.

LOCATION	TYPE	ACTUAL STRESS
1	NORMAL SHEAR	194.16 MPa (28,160 PSI) 97.08 MPa (14,080 PSI)
2	NORMAL SHEAR	146.08 MPa (21,187 PSI) 73.04 MPa (10,594 PSI)
3	NORMAL SHEAR	194.01 MPa (28,139 PSI) 97.01 MPa (14,070 PSI)

MATERIAL	PART
PWA 1010	No. 4 HUB
PWA 1010	NO. 4 HUB
PWA 1003	REAR SHAFT
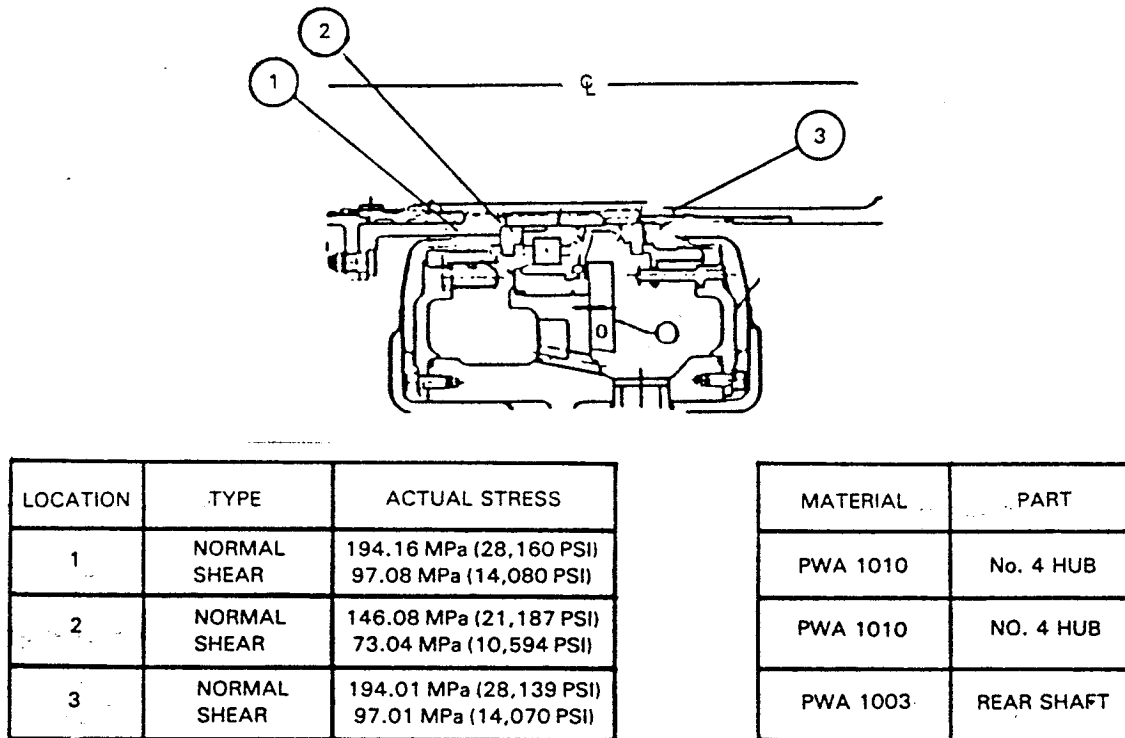
Figure 88   Summary of No. 4 Hub and Shaft Stresses

4.1.3.6 Driveshaft Couplings

The rig incorporated a Bendix flexible diaphragm coupling attached to the No. 4 1/2 hub to accommodate rig axial growth during testing. The new coupling has the same spring rate as the other three couplings in the drive system. This results in four common couplings being used. The rig axial growth was predicted for a snap deceleration from steady-state 100 percent corrected speed, near surge to rig idle and the following steady-state conditions: aerodynamic design point, maximum mechanical speed, maximum corrected speed, and 100 percent corrected speed, maximum inlet temperature. The coupling system was preloaded with consideration given to the No. 3 bearing and drive gearbox bearings loading constraints, and jackshaft axial movement constraint.

4.1.4 Rig Bleed and Secondary Flow Requirements

The rig bleed and secondary flow system facilities requirements are specified in Table XXVIII. A schematic of the rig secondary flow system is shown in Figure 89.

TABLE XXVIII

HIGH-PRESSURE COMPRESSOR RIG SECONDARY FLOW SUMMARY

Wcorr = 35.2 kg/sec (77.5 lb/sec), Wae = 32.0 kg/sec (70.5 lb/sec)

Bleed Flow	Operating Range	% Wae	Flow, kg/sec (lb/sec)	Pressure, kPa (psi)	Temperature °C (°F)	Max Pressure, kPa (psi)	Test Condition
1. Low-Pressure Compressor O D Bleed	0 to 90% Ncorr	15.00 *	2.04 (4.5)	100 (14.5)	104 (220)	100 (14.5)	90% Ncorr, Operating Line
2. Inlet Guide Vane I D Bleed	All Speeds	0.44	0.15 (0.34)	100 (14.5)	104 (220)	100 (14.5)	ADP**, nominal flow + 10%
			0.05 (0.11)	34.5 (5.0)	104 (220)		ADP, throttled
3. Rotor 6 Leading Edge I D Injection	All Speeds	0.06	0.02 (0.05)	100 (14.5)	104 (220)	100 (14.5)	ADP, nominal flow + 10%
			0.01 (0.02)	34.5 (5.0)	104 (220)		ADP, throttled
4. 8th Stage O D Bleed	Bleed Program Only	2.4%	0.84 (1.86)	234 (34)	299 (570)	276 (40)	ADP, nominal flow + 10%
5. 10th Stage OD Bleeds:							
a) Starting Bleed	70% Ncorr	15.00 *	2.04 (4.5)	138 (20)	221 (430)	138 (20)	70% Ncorr, Operating Line
b) Turbine Cooling Air Bleed	70% Ncorr	0.68	0.24 (0.52)	427 (62)	393 (740)	431 (77)	ADP, nominal flow + 10%
			0.07 (0.16)	145 (21)	393 (740)		ADP, throttled
c) Active Clearance Control Air Bleed	100% Ncorr	1.25	0.44 (0.97)	427 (62)	393 (740)	431 (77)	ADP, nominal flow + 10%
			0.14 (0.30)	145 (21)	393 (740)		ADP, throttled
6. Compressor Exit, Bleed I	All Speeds	1.52	0.54 (1.18)	1193 (173)	599 (1110)	1531 (222)	ADP, nominal flow + 10%
	All Speeds		0.17 (0.37)	414 (60)	599 (1110)		ADP, throttled
7. Compressor Exit, Bleed II	All Speeds	2.25	0.79 (1.74)	793 (115)	599 (1110)	1020 (148)	ADP, nominal flow + 10%
	All Speeds		0.25 (0.55)	269 (39)	599 (1110)		ADP, throttled
8. Tangential On-Board Injector Seal Leakage	All Speeds	0.88	0.28 (0.62)	400 (58)	599 (1110)	490 (71)	ADP
	All Speeds		0.10 (0.21)	138 (20)	599 (1110)		ADP, throttled
9. Buffer Compartment Bleed	All Speeds	2.50	0.80 (1.76)	400 (58)	599 (1110)	490 (71)	ADP
	All Speeds		0.28 (0.61)	138 (20)	599 (1110)		ADP, throttled
10. Bore Cooling Bleed	All Speeds	1.00	0.35 (0.78)	414 (60)	438 (820)	510 (74)	ADP, nominal flow + 10%
(12th Stage I D))	All Speeds		0.11 (0.24)	152 (22)	438 (820)		ADP, throttled
11. Drive Shaft Cooling Air Injection	All Speeds			345 (50)	38 (100)	(Shop Air)	

* % of engine airflow at idle.
** ADP = Aerodynamic Design Point.
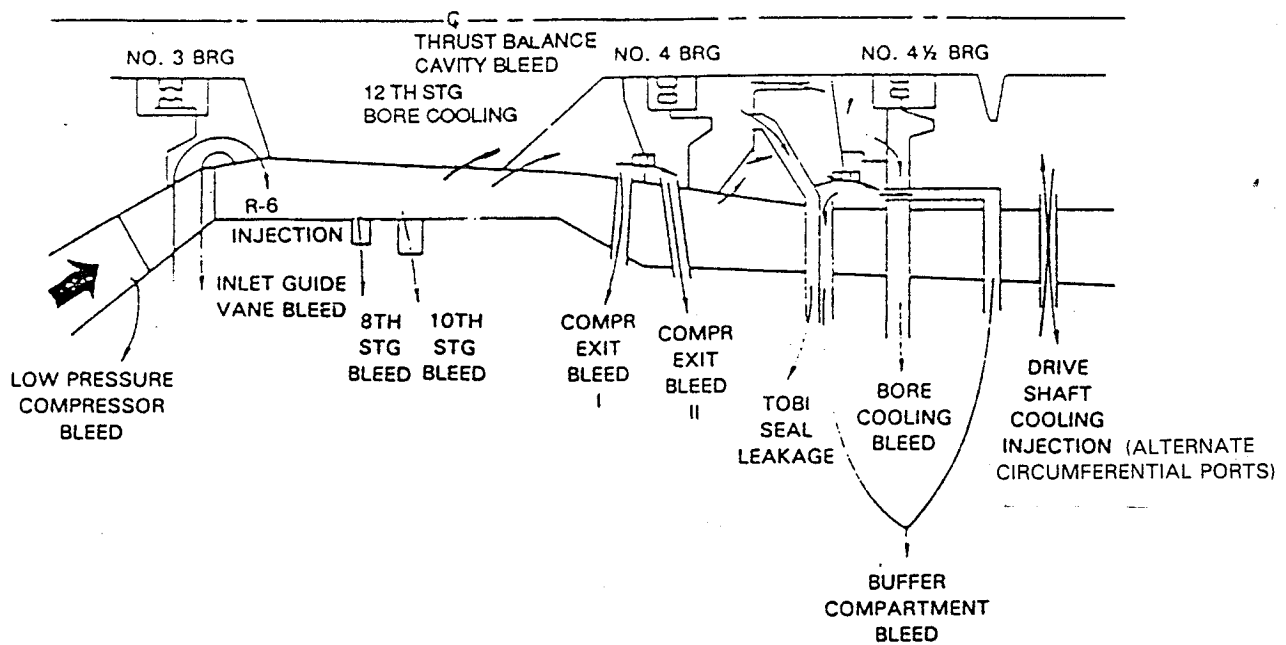
Figure 89   Secondary Flow Schematic for the Energy Efficient Engine
             High-Pressure Compressor Test Rig

4.2 INSTRUMENTATION

Instrumentation provisions have been designed for the high-pressure compressor
rig to measure overall performance, stage performance characteristics,
secondary flow and tip clearance effects, and stability/recovery
characteristics. Instrumentation is also included to monitor airfoil stresses
and rig safety parameters. This includes major station pressure and
temperature probes, interstage vane leading edge pressure and temperature
sensors, high frequency response pressure and temperature probes, metal and
air thermocouples on rotating and static structures, strain gages on all
airfoil rows, and wall static pressure taps throughout the compressor.

The major station locations are shown in Figure 90. A particle flowpath layout
showing major station and interstage instrumentation, shown in Figure 91,
provides visibility of the interstage instrumentation wakes and allows optimum
pattern selection based on aerodynamic and vibration considerations. The
interstage instrumentation is located to produce minimum excitation of known
resonances in rotors adjacent to the probes.

4.2.1 Major Station Instrumentation

The inlet major station (2.5) has four total pressure (P_T) and four total temperature (T_T) pole rake probes located between the intermediate case struts, with ten sensors centered for equal area readings. Station 2.6 has a single P_T pole rake probe with ten sensors arranged spanwise so that a higher concentration of readings is obtained near the inner diameter and outer diameter walls to better define the end-wall effects on the spanwise flow profile. All sensors are inclined to a mean pitch angle with respect to the intermediate case inner and outer diameter walls. The facility inlet and plenum are suitably instrumented to assure an accurate determination of the flow conditions entering the rig test section.

The exit major station (3.0) has six P_T pole rakes, six T_T pole rakes, two radially translating P_T wake rakes, and two radially translating T_T wake rakes. Both P_T and T_T translating wake rakes are designed to span two exit guide vane pitches and have fifteen and seven sensors, respectively. The translating actuators are mounted on the outer diffuser case with the rake guided in a bushing, and pressure sealed with a piston ring. This assembly is housed inside a bolted split bushing matching the outer wall of the diffuser. The adaptor bushing at the translating probe positions allows pole rake interchangeability at these locations. The pole rakes have five sensors centered for equal area readings. All station 3.0 instrumentation is inclined at a mean pitch angle with the inner diameter and outer diameter diffuser walls.
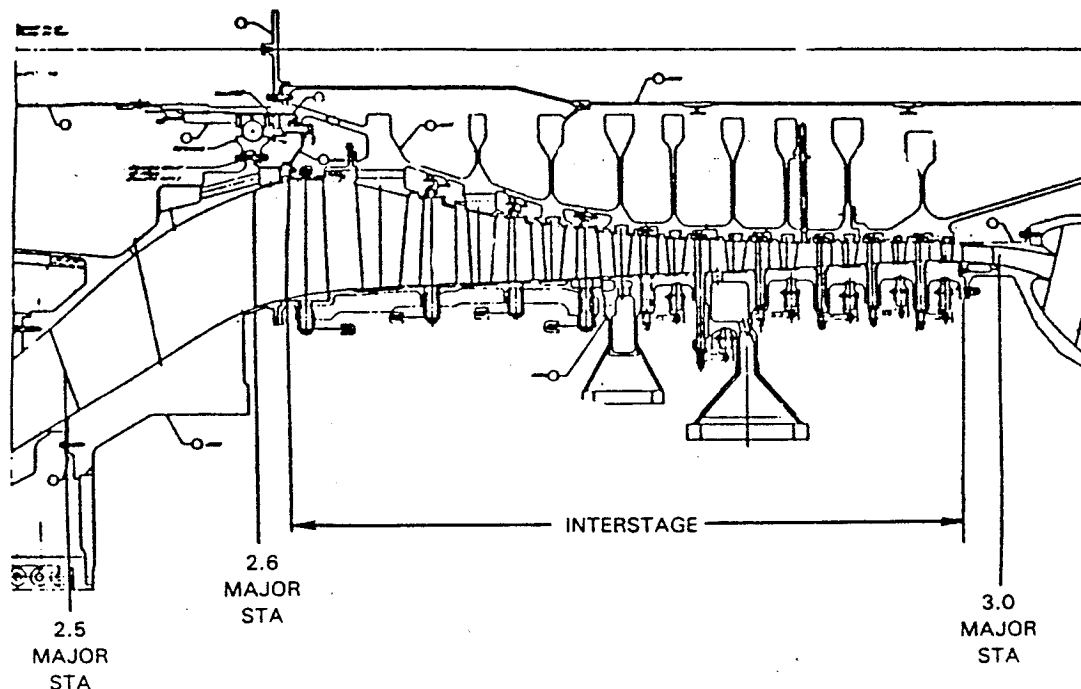
Figure 90   Major Station Locations

STA 2.6 270° 0° 90° 180°

IGV

S6
S7
S8
S9
S10
S11
S12
S13
S14
EGV

270° 0° 90° 18
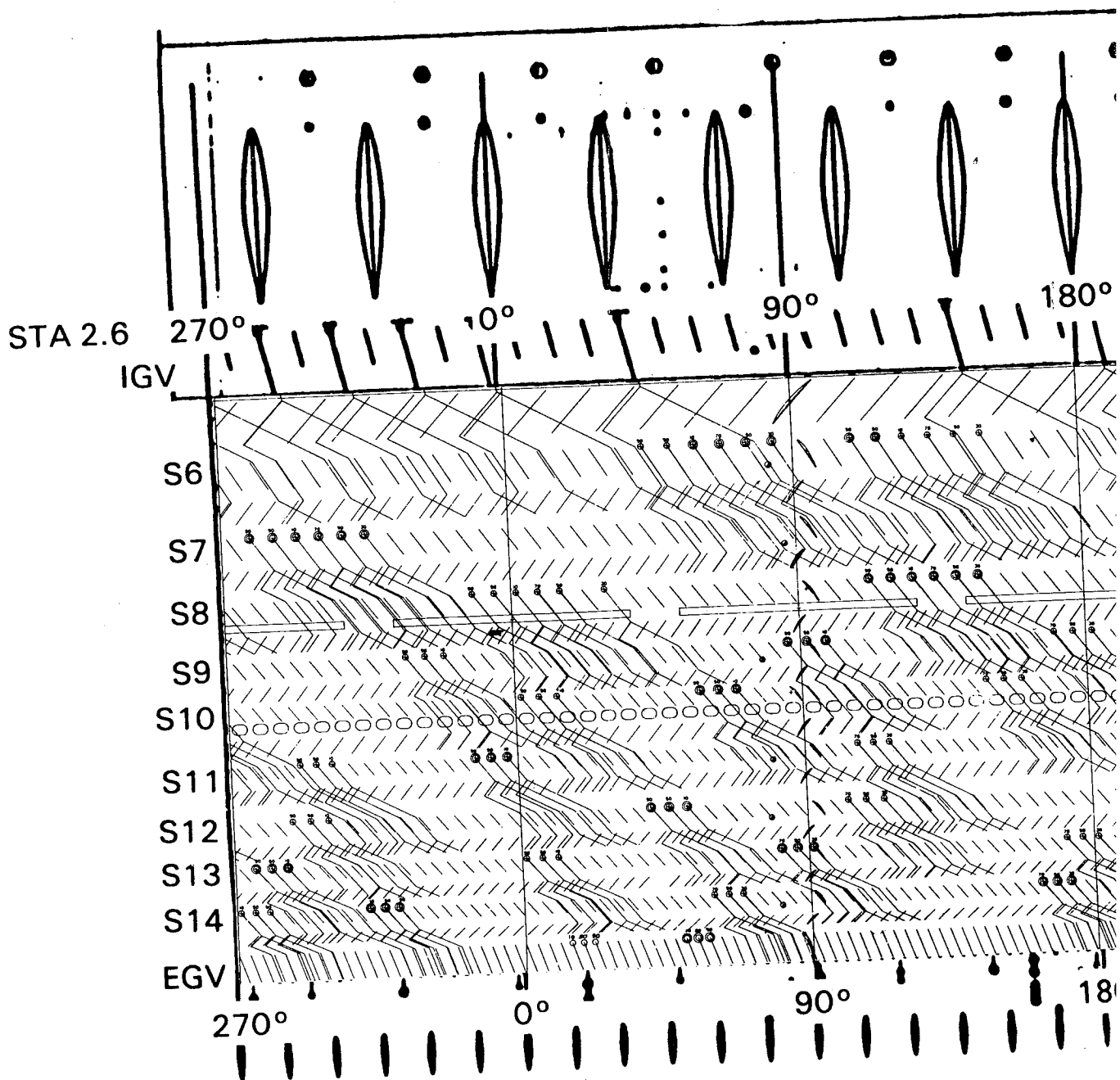
NOTE:
WALL STATICS SHOWN AT I.C. S1
ARE POSITIONED ON BOTH INNER
OUTER WALLS. ALL OTHER WALL
ARE POSITIONED ON OUTER WAL
THRU TO T.E. OR E.G.V. UNLESS
OTHERWISE STATED.

FOLDOUT FRAME

STA 2.5

270°

IGV

R6

R7

R8

R9

R10

R11

R12

R13

R14

R15

EGV

270° STA 3.0

UT

ND

TATICS

ONLY,

⊠ HIGH PRESSURE

◑ BOROSCOPE

⊗ WALL STATIC (INNER DIA. ONLY)

◉ FLUSH SURFACE TEMP. PROBE (HOT FILM

● THERMOCOUPLE-METAL

▢ STRAIN GAGE

✶ WALL STATICS

◎ PRESSURE SENSOR

▲ TEMPERATURE SENSOR

▣ PRESSURE SENSOR (TRAVERSING)

⬡ TEMPERATURE SENSOR (TRAVERSING)

△ INT. CASE STRUT GAP LOCATIONS

△ DIAL INDICATOR RESOLVER

▭ ROLLER AND SLIDER TRAVEL

▭ LASER PROBES

Figure 91   Flowpath Layout Showing Location
of Major Station and Interstage
Instrumentation

127

4.2.2 Vane Leading Edge Instrumentation

The inlet guide vane assembly is designed to incorporate multiple total pressure sensors. These sensors are located to give maximum intermediate case strut gap coverage, with sensors at 7, 14, 20, 32, 45, 57, 70, 82, 89, and 95 percent of gap. Vanes in the sixth stator through the exit guide vane assembly are instrumented with a single kielhead sensor per vane with six P_T and six T_T instrumented vanes per stage. These sensors provide spanwise coverage at 10, 30, 50, 70, and 90 percent span, with two sensors located at the 50 percent span position. Circumferential location is based on vibration analysis and particle flowpath analysis. The interstage sensors are inclined at the mean pitch angle with the inner and outer diameter, and parallel to the vane section incidence angle.

4.2.3 High Response Instrumentation

High frequency response instrumentation consists of miniature pressure transducers and quick acting thermocouples located in the vane case outer flowpath wall. The pressure sensors are located at the leading edge of the inlet guide vane, at the trailing edge of stators 7, 9, 11, and 13, and at station 3.0. There are two sensors per each axial location. The temperature sensors are located at the leading edge of stators 6, 10, and 12 and at the trailing edge of stator 8. There are two sensors per axial location.

4.2.4 Blade Tip Clearance Instrumentation

A laser probe is used to measure blade tip clearance during rig operation. This probe is of a new design which incorporates a combination rub button. The rub button, which has an abradable tip, is forced a predetermined depth into the blade tips and blocks the laser light path. The amount of material removed from the rub button is used for comparison with the actual clearance information read from the reflected laser beam. The fiber optics epoxy bond is nitrogen cooled, which permits laser operation in a high temperature environment. The nitrogen is also used to clean the optic lens and actuate the rub button both in and out. The rub button is spring loaded in the retracted position for safety purposes.

4.2.5 Strain Gage Instrumentation

Strain gages will be installed in all blade and vane airfoil rows to measure vibratory stresses during rig operation. The blade gages will be mounted on the airfoil at four basic locations: root maximum thickness, root trailing edge, root leading edge, and tip maximum thickness. Blades to be strain gaged will be selected based on first bending frequency checks made on the entire set of airfoils. The vane gages will be located at the outer diameter maximum thickness, outer diameter leading edge, outer diameter trailing edge near the overhang, and inner diameter maximum thickness. Strain gages will also be installed on the thrust balance seal disks and lands, and on the inlet station pressure and temperature pole rakes.

4.2.6 Secondary Flow System Instrumentation

Pressure and temperature measurements will be made in each of the rig internal cavities to determine the effects of the secondary flows on performance. Flow measurements will be made in the facility air supply plumbing using a standard V.D.I. (Verein Deutscher Ingenieure) orifice installation for each of the individual secondary flows and the main inlet flow.

4.2.7 Rig Safety Instrumentation

Rig safety parameters will be monitored with instrumentation installed to measure rig and slip-ring bearing temperatures, oil pressure and temperature, mechanical speed, vane angle position, rapid pressure or temperature fluctuation, ball bearing thrust load, and rig internal and external vibrations. In addition, borescope ports have been provided in the front and rear vane cases for periodic internal visual inspections. The ports are located at the trailing edge of the inlet guide vane and stators 6, 8, 9, 10, 11, 12, and 14.

SECTION 5.0

DESIGN SUBSTANTIATION

5.1   INTRODUCTION

Testing of the rig described in Section 4.0 was initiated in May, 1981 and
proceeded through two builds, necessitated by modifications to the rig during
the test program (see Part III, Section 2.0). A detailed discussion of the
test results and analysis will be provided in the forthcoming performance
report that will follow Build 3 testing.

5.2   COMPRESSOR PERFORMANCE SUMMARY

The original blading design of the high-pressure compressor achieved design
flow and pressure ratio with an efficiency within one percentage point of the
rig goal. High speed surge margin adequate to run the engine was demonstrated,
while starting region surge margin was comparable to other high-pressure
compressors. The rig achieved an efficiency of 85.1 percent and demonstrated
12.6 percent surge margin at design speed compared to the rig goals of 86.0
percent efficiency and 20 percent surge margin. The predicted compressor
performance and test results adjusted for measured deterioration and estimated
instrumentation corrections are shown in Table XXIX and Figure 92.

For the purpose of simulating engine performance, the high-pressure compressor
component is defined as extending from the intermediate-case strut leading
edge to the exit guide vane trailing edge. The design pressure ratio and
efficiency, therefore, include the intermediate-case and strut losses, and the
corrected flow is defined at the inlet to the intermediate case.

After the completion of testing, rig Build 2 was disassembled for examination
of the hardware. In general, the post-test condition of the compressor
components was excellent. However, significant wear was noted in the blade
tips, blade rub strips, and knife-edge seal lands. This wear was attributed,
in part, to tighter than anticipated running clearances as derived for Build 2
from laser closure measurements. Subsequent reassessment of case and rotor
growth calculations indicated that these clearances were smaller at the start
of test than the engine design values necessary for transients in flight
operation (Figure 93). (Rotor 12 was an exception due to an undercut during
tip grinding.) Therefore, a reduction in test efficiency was made in the
accounting shown in Table XXIX for comparison with the goal efficiency.

Crack indications were also noted on six 13th-stage blade tips. These were
attributed to tip mode stresses. These findings were incorporated into the
analyses leading to the Build 3 design update, discussed in Part III of this
report.

TABLE XXIX

ADJUSTMENTS TO MEASURED TEST RIG EFFICIENCY

Test Rig Efficiency at 100% Corrected Speed,
    Cruise Operating Line   83.6%

Adjustments to Efficiency:

Sensor Temperature Recovery Correction	+0.4%
Pole Rake Sampling	+0.1
Wake Rake Adjustment to Pole Rake	-0.3
Leading Edge Instrumentation Losses	+0.5
Measured Deterioration	+1.2
Running Clearance for Flight Propulsion System	-0.4
Total Adjustment	+1.5%

Adjusted Test Rig Efficiency   85.1%

First Aerodynamic Build Efficiency Goal   86.0%
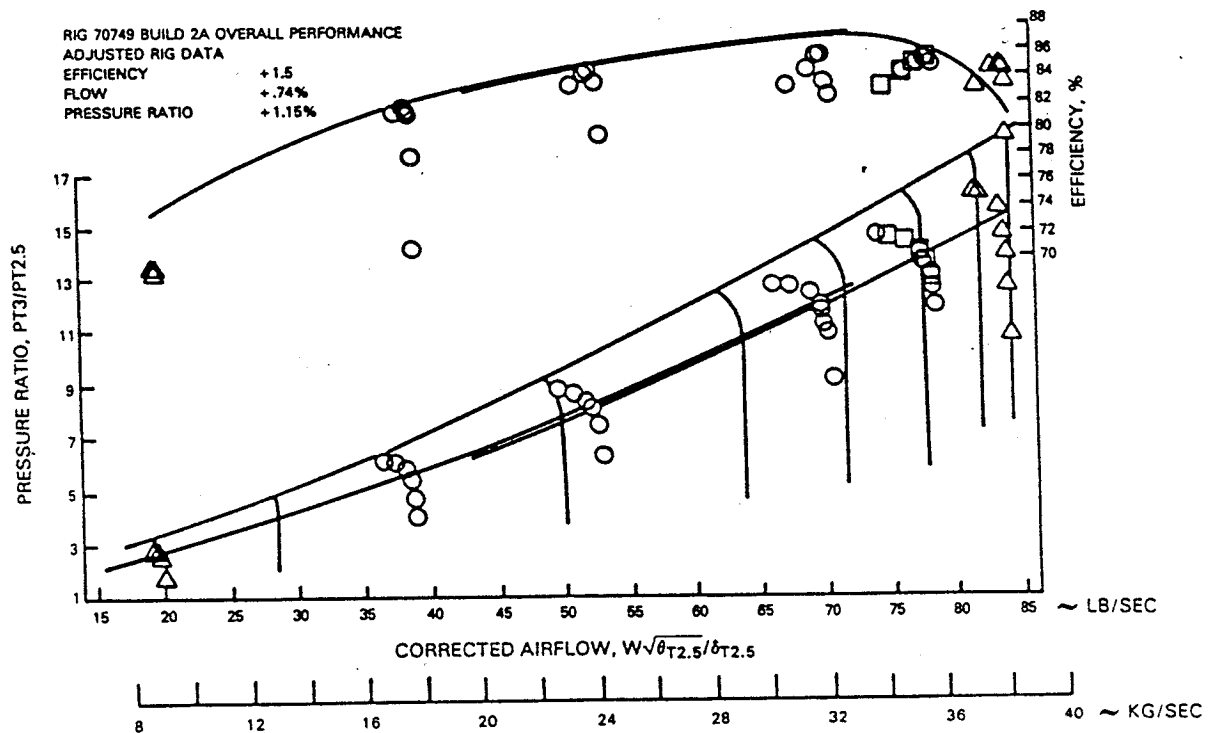
Figure 92   High-Pressure Compressor Build 2 Test Rig Performance. The compressor achieved design flow and pressure ratio with an efficiency within one percent of the goal.
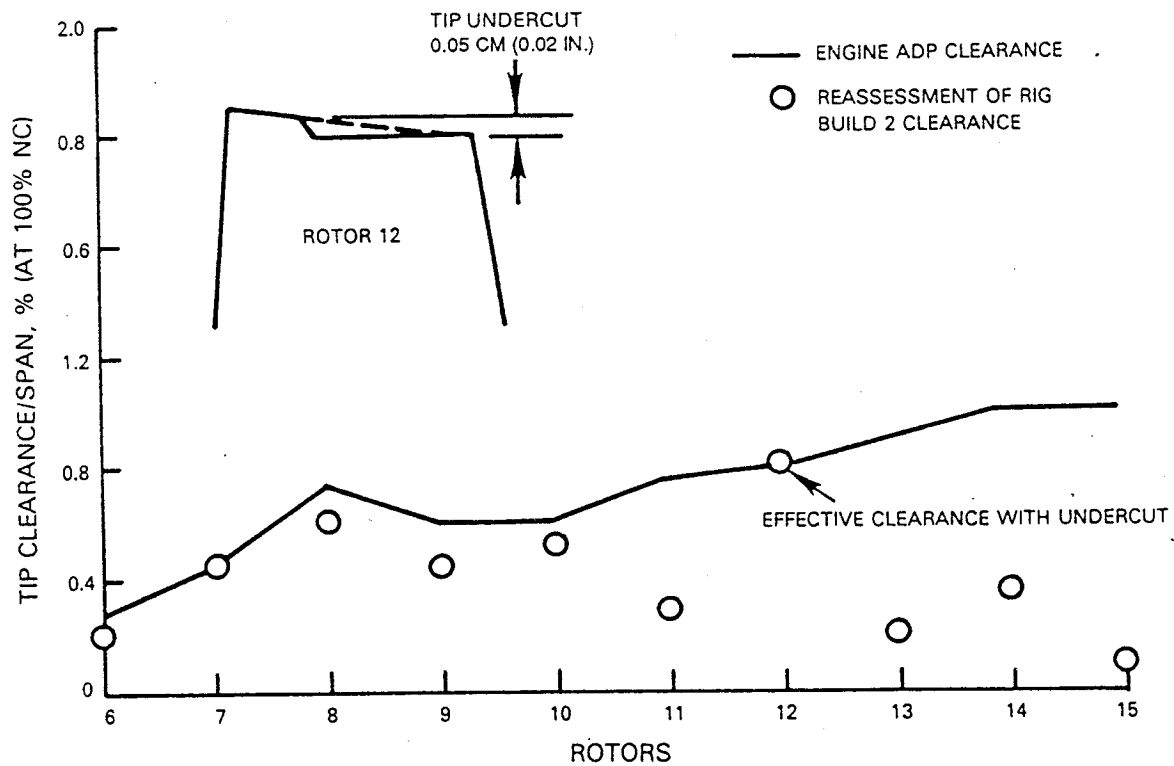
Figure 93   High-Pressure Compressor Running Clearance. Clearances at the start of test were less than design values.

PART III

HIGH-PRESSURE COMPRESSOR

COMPONENT AND TEST RIG DESIGN UPDATE

SECTION 1.0

INTRODUCTION

The objective of the redesign effort leading to Build 3 of the high-pressure compressor test rig was to expand upon the lessons learned from Build 1 and Build 2 testing in order to achieve a goal experimental efficiency of 86.5 percent. To achieve this goal, the decision was made to incorporate second-generation Controlled Diffusion Airfoils (CDA) in all blade rows and, with the exception of the inlet guide vanes and stator 6, in all vane rows. In addition, the single-row exit guide vane assembly, used in the earlier builds, was replaced with a double-row design. These design changes will provide the desired efficiency improvement, as discussed in Part III, Section 3.1.2.4 of this document.

Two additional test objectives were added to the Build 3 test program that significantly affected the mechanical design of the component test rig hardware. These objectives were: 1) feasibility demonstration of an incipient stall sensing method for surge avoidance, and 2) feasibility demonstration of the use of Laser Doppler Velocimetry (LDV) techniques to acquire data necessary for the analysis of the flow field in the front, middle, and rear stages of high-pressure compressor.

In the following, Section 2.0 describes rig mechanical modifications that were found necessary during Build 1 and Build 2 testing. The aerodynamic and mechanical design updates to the high-pressure compressor component and test rig are discussed in Section 3.0. Section 4.0 describes the test rig design updates for Build 3.

SECTION 2.0

HIGH-PRESSURE COMPRESSOR TEST RIG MECHANICAL MODIFICATIONS

Two modifications to the test rig hardware were accomplished during the early phases of the test program to correct problems that surfaced during rig operation of Builds 1 and 2. These modifications, which were retained in the Build 3 test rig configuration, are discussed in the following sections.

2.1 MODIFIED REAR THRUST BALANCE PISTON SEAL

Data review, following completion of the stress and vibration survey portion of the Build 1 performance test program, indicated unacceptably high stresses in the rear thrust balance piston seal. This high stress was attributed to seal flutter that occurred when the pressure differential across the piston was increased. In order to eliminate this flutter-induced stress condition, a replacement seal was designed which incorporated a more substantial cross section, a single knife-edge seal, and two rim ring dampers to provide improved stability. Figure 94 compares the original rig Build 1 thrust balance piston seal design with the redesigned part that was subsequently incorporated into the rig Build 2 assembly and demonstrated acceptable stresses during Build 2 testing.

BUILD 1
DESIGN

TWO RING
DAMPERS
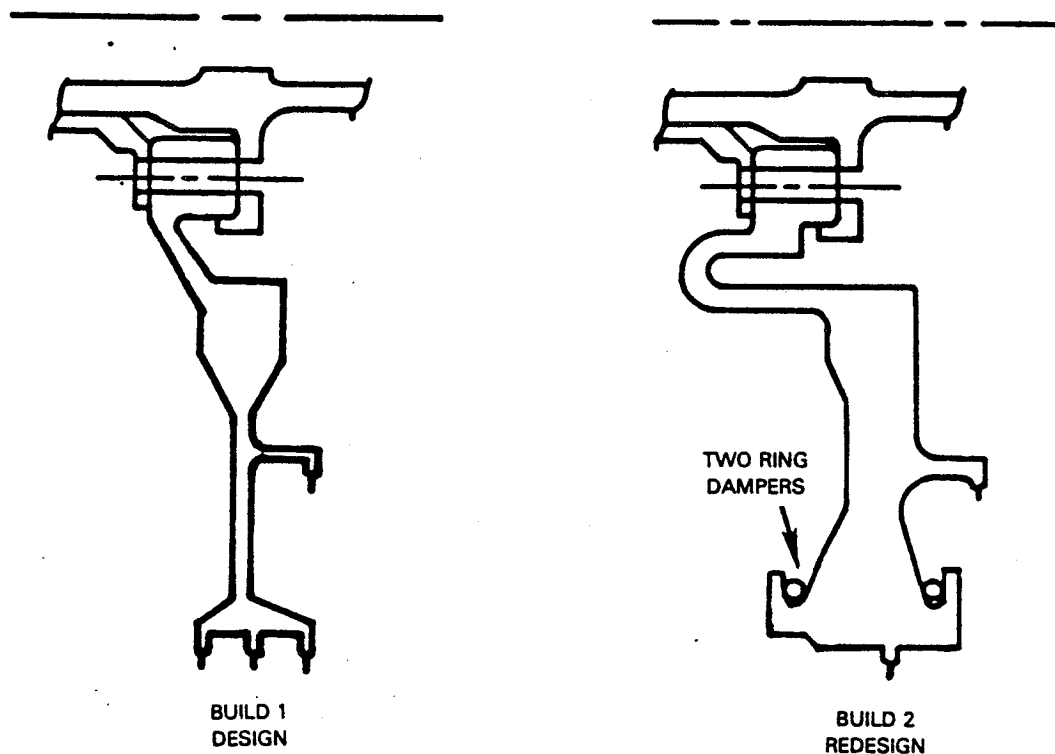
BUILD 2
REDESIGN

Figure 94   High-Pressure Compressor Rig Thrust Balance Seals, Showing the Original Build 1 Design and the Redesigned Build 2 Configuration

136

2.2 MODIFIED SLIP-RING DRIVE SHAFT

During the stress and vibration portion of the Build 2 performance test program, excessive vibration occurred in the front portion of the rig, and the rig was shut down. Investigation after shutdown revealed that the rotating strain-gage slip-ring drive shaft had separated from the front of the titanium rotor with subsequent damage to several parts. In order to preclude this problem from recurring, the slip-ring drive system was modified as shown in Figure 95. These modifications consisted of: 1) a shorter axial length to reduce the overhung moment, 2) a reduction in the axial length of the inner intermediate-case front flange, and 3) replacement of the riveted joint on the compressor front flange with a threaded joint. This modified slip-ring drive configuration was incorporated into rig Build 2 (redesignated Build 2A), and testing was completed without further incident.
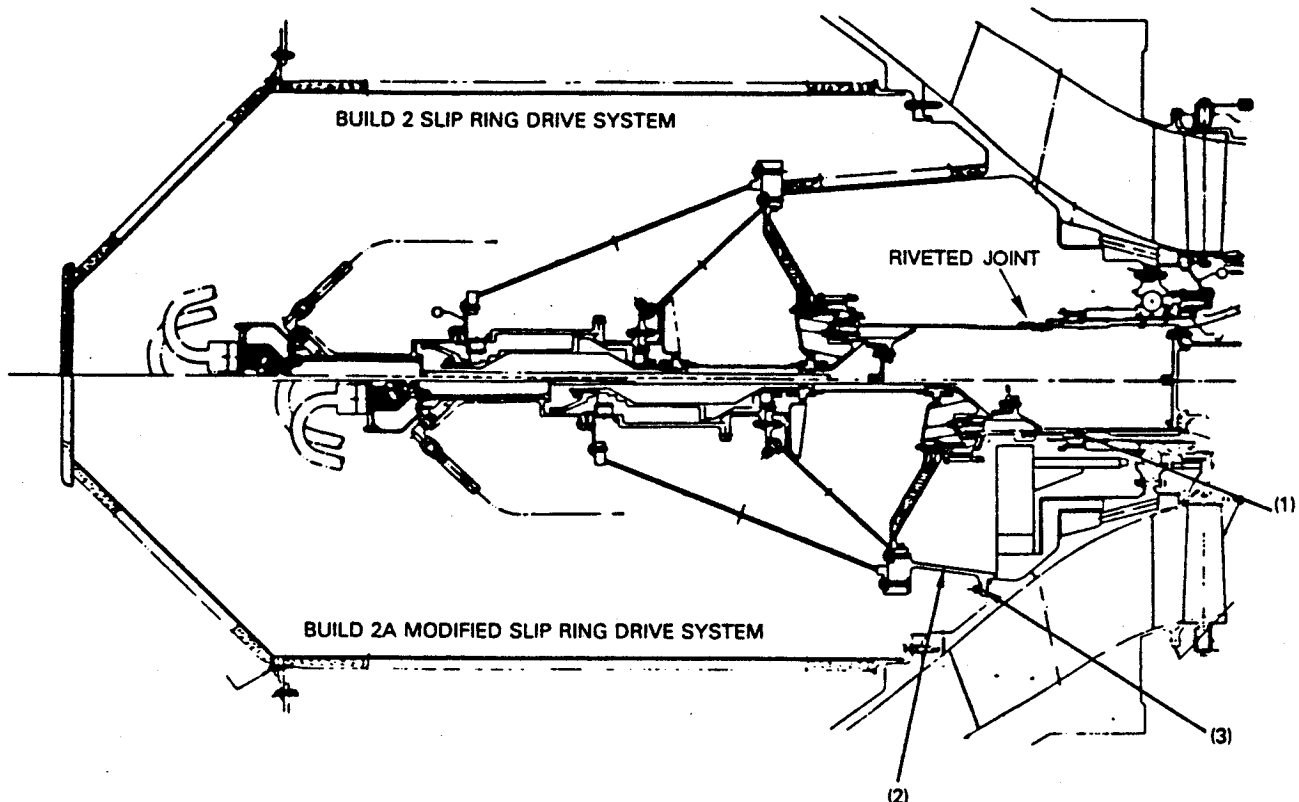
Figure 95   Original (Build 2) and Revised (Build 2A) High-Pressure Compressor Rig Slip-Ring Drive Systems

SECTION 3.0

HIGH-PRESSURE COMPRESSOR COMPONENT DESIGN UPDATE

The component design update for Build 3 included aerodynamic redesign of the airfoils and vibration analysis of the redesigned airfoils, as well as mechanical design to accommodate minor adjustments in the flowpath, axial and radial clearances, and the exit guide vane attachment. These efforts are discussed in the following sections.

3.1 AERODYNAMIC DESIGN UPDATE

3.1.1 Build 2 Test Results

Analysis of the Build 2 data indicated deficiencies that, if addressed, could lead to additional performance gains. These original deficiencies were: 1) overturning in the first rotor (rotor 6) tip, 2) underflowing in the rear stages, and 3) exit guide vane loss that was greater than the design prediction.

Overturning in rotor 6 occurred at both the design inlet guide vane setting of 0 degrees and the optimized vane setting of -3 degrees. This resulted in a spanwise total pressure skew (Figure 96) and caused incidence mismatch in the downstream rows. This effect persisted through several stages, and only in the middle of the compressor (at stator 11) did the test pressure profile again agree with the design (see Section 3.1.2.1). The abnormal tip trim cut (Figure 93) on rotor 12 skewed the pressure profile once more through stages 12 through 15. The net effect on velocity profiles was that the majority of blade and vane rows were penalized with varying degrees of incidence mismatch.

The combination of blockage, loss, and turning used in the original design resulted in underflowing in the rear stages and efficiency peaking below the operating line. During the test, the last four stators were restaggered open to bring the stages up to the desired size. Consequently, these stators were operating on the stall side of the minimum loss incidence. Efficiency improvement should be attainable by optimizing the incidence at the operating line.

Test results showed that exit guide vane loss was greater than predicted (Figure 97). It was apparent during the original design procedure that the aerodynamic loading requirements for the exit vane exceeded slightly the experience for a single-row airfoil (Figure 22). In anticipation of a potential limitation in loading, a double-row exit guide vane was designed as a backup configuration. The test analysis of the single-row vane used in Build 2 suggested that the initial reservation about the ability of a single-row airfoil to accommodate the loading level may be valid, although the unusually low aspect ratio also could be a factor. The alternate double-row vane design was evaluated in Build 3 of the test rig.

The major thrust of the aerodynamic design update was, therefore, to rectify the previously noted shortcomings. In the process, a revised compressor design system was utilized. The redesign effort is described in the following subsections.

138
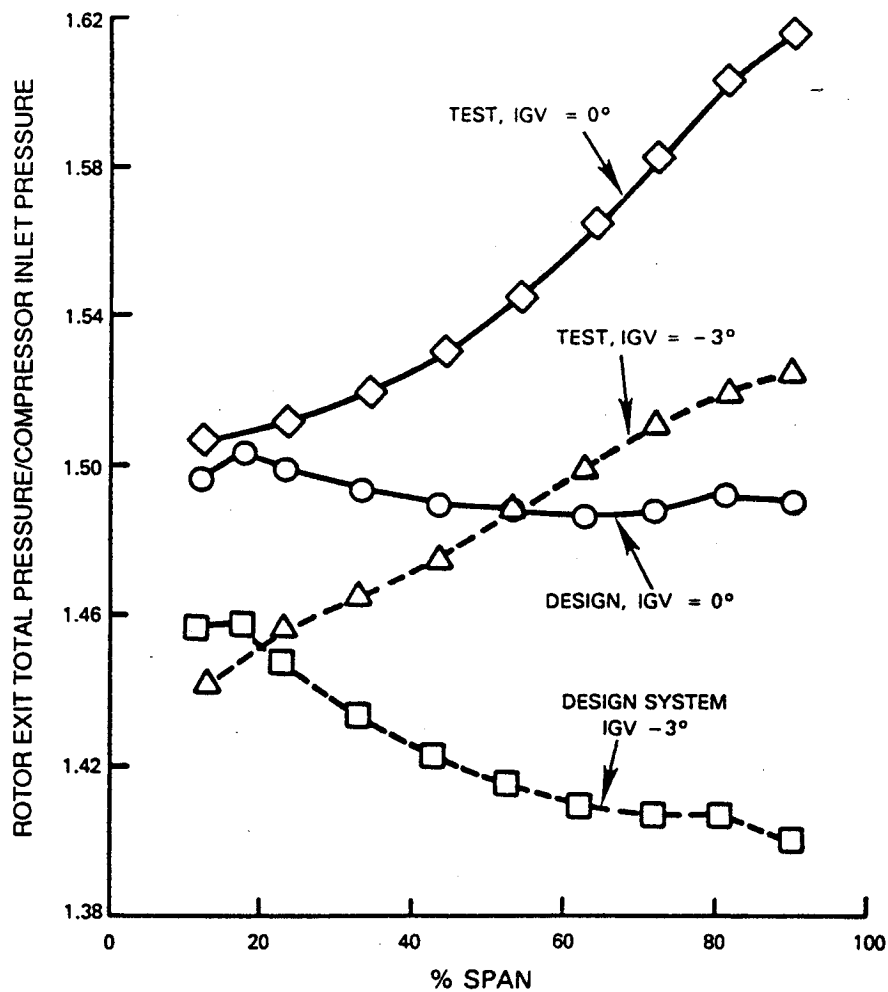
Figure 96   Rotor 6 Exit Pressure Profiles at Two Inlet Guide Vane Angle
Settings. Spanwise total pressure skew caused incidence mismatch in
downstream rows.
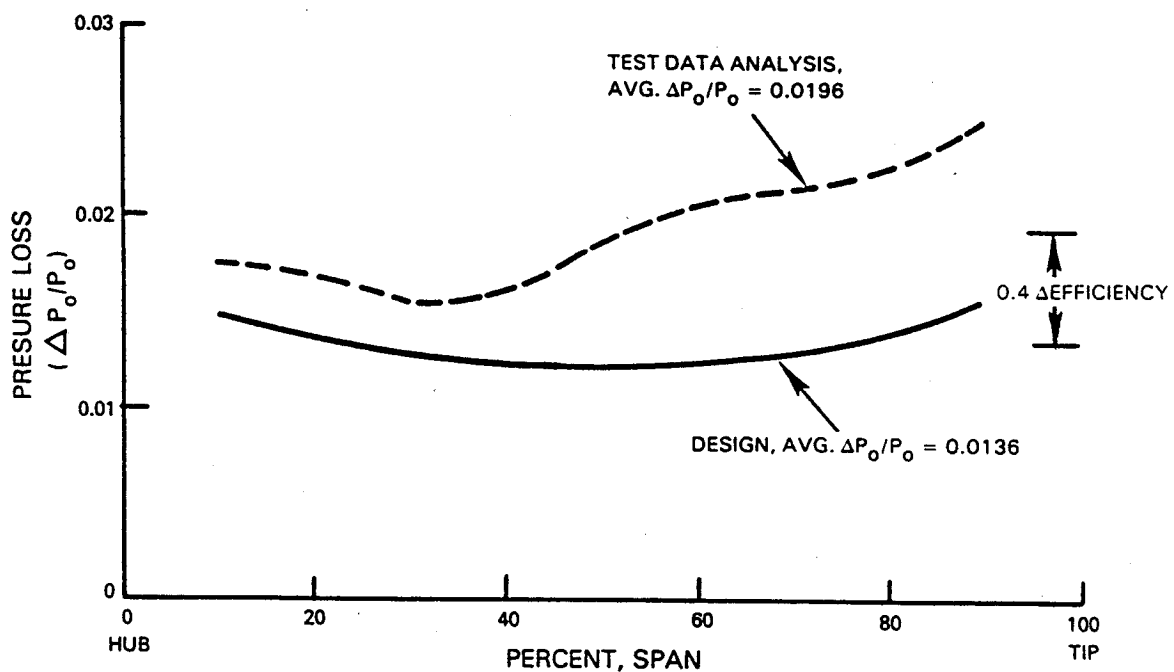
Figure 97   Single-Row Exit Guide Vane Loss at the Operating Line. Exit guide
vane loss was greater than the design prediction.

139

3.1.2 Revised Design System

A revised compressor design system has been developed, based on data evaluation of several recent compressor rigs, including contemporary Controlled Diffusion Airfoil (CDA) blading designs other than the compressor test rig, Build 2. This design system indicated 1.4 percentage points efficiency improvement potential for reblading of the compressor based on optimization of incidence at the original aerodynamic design point. The revised design system closely reproduces the flow, pressure ratio, and efficiency versus pressure ratio characteristic shape of Build 2 test data. The system under predicts the level of efficiency relative to Build 2 test data, but gives the proper ordering of stage sizes. Figure 98 shows this ability of the revised design system to reproduce the test efficiency characteristic, including the peaking of efficiency below the operating line caused by the previously mentioned incidence mismatching.

O BUILD 2 TEST DATA
☐ REVISED DESIGN SYSTEM CHECKOUT OF BUILD 2
△ BUILD 3 DESIGN
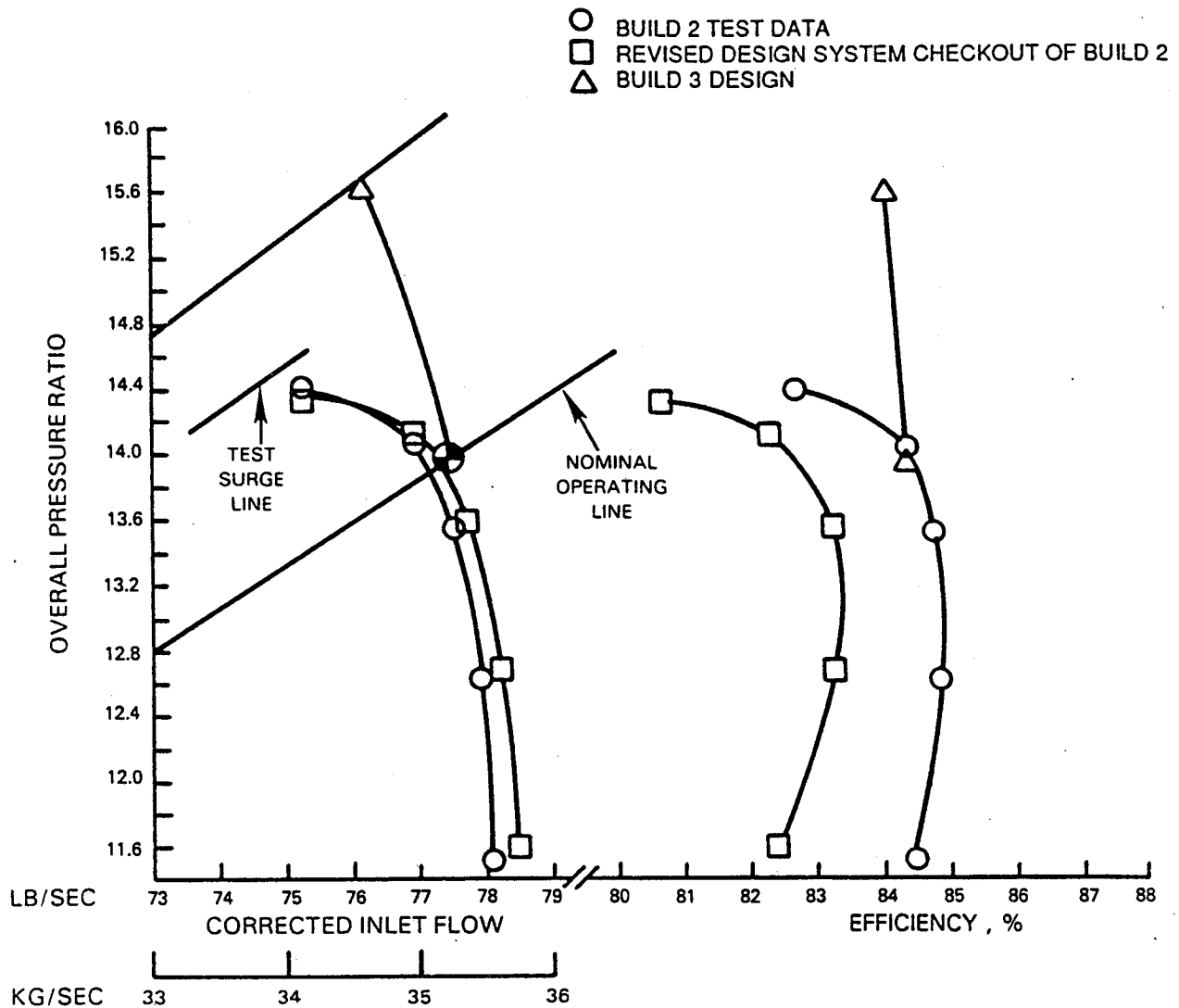
Figure 98   Compressor Performance and Predictions at Design Speed. A revised compressor design system closely reproduces the flow and efficiency versus pressure ratio characteristic shape of Build 2 test data.

3.1.2.1 Reblading Approach

The evaluation of the test data indicated that the stagewise pressure distribution of the original design would result in a desirable loading balance. Therefore, the reblading maintains the original design intent in stage size. A study of effects of design reaction versus Build 2 test reaction showed no major differences in the off-design incidence range requirements. The test reaction level of Build 2 was selected for the reblading as a logical development step which also minimizes change in rotor camber. The new reaction level, shown in Figure 99, is 0.55 for the back stages, relative to the original design value of 0.50, but still is substantially lower than for most other Pratt & Whitney high-pressure compressors. Figure 100 shows the stator exit angle distribution which fixes this reaction level.

A second major consideration in reblading for Build 3 was to correct the velocity profile skew of Build 2. At the rotor 6 exit, the first stage of the high-pressure compressor, the pressure profile was highly positive (Figure 96). Analysis of the data showed that the design assumptions of blockage level, spanwise loss distribution, and deviation relative to test results contributed to the spanwise pressure skew (Figure 101). This evaluation of rotor 6 test blockage, loss, and deviation was used in reblading the rotor to achieve the original design pressure profile. The change in trailing edge metal angle that resulted is shown in Figure 102.
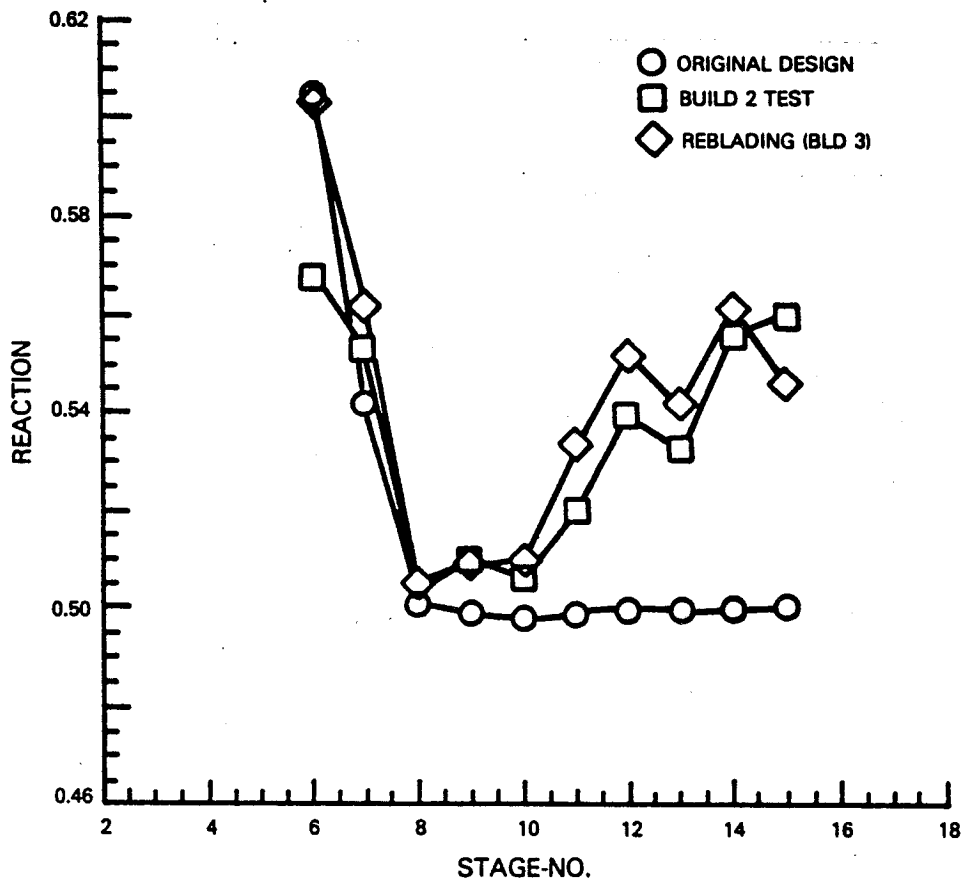
Figure 99   Comparison of Reaction Levels. Build 2 test reaction was used in reblading.
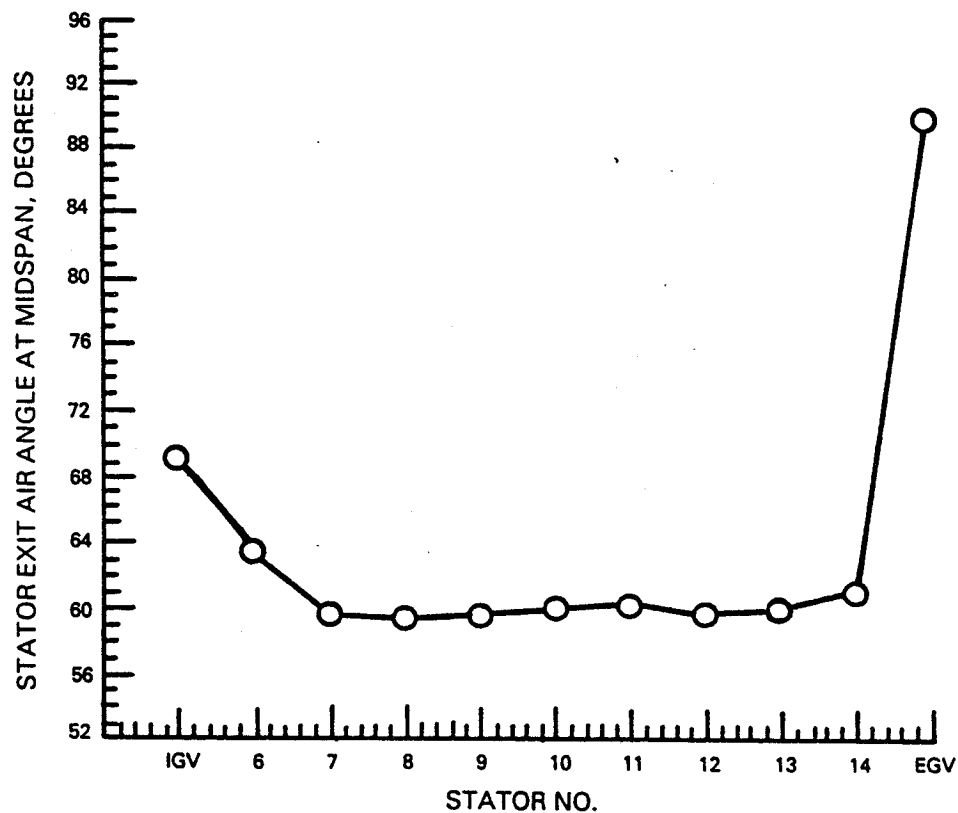
Figure 100   Stator Exit Air Angle. Reblading reaction level leads to uniform stator exit angles in the middle and rear stages.
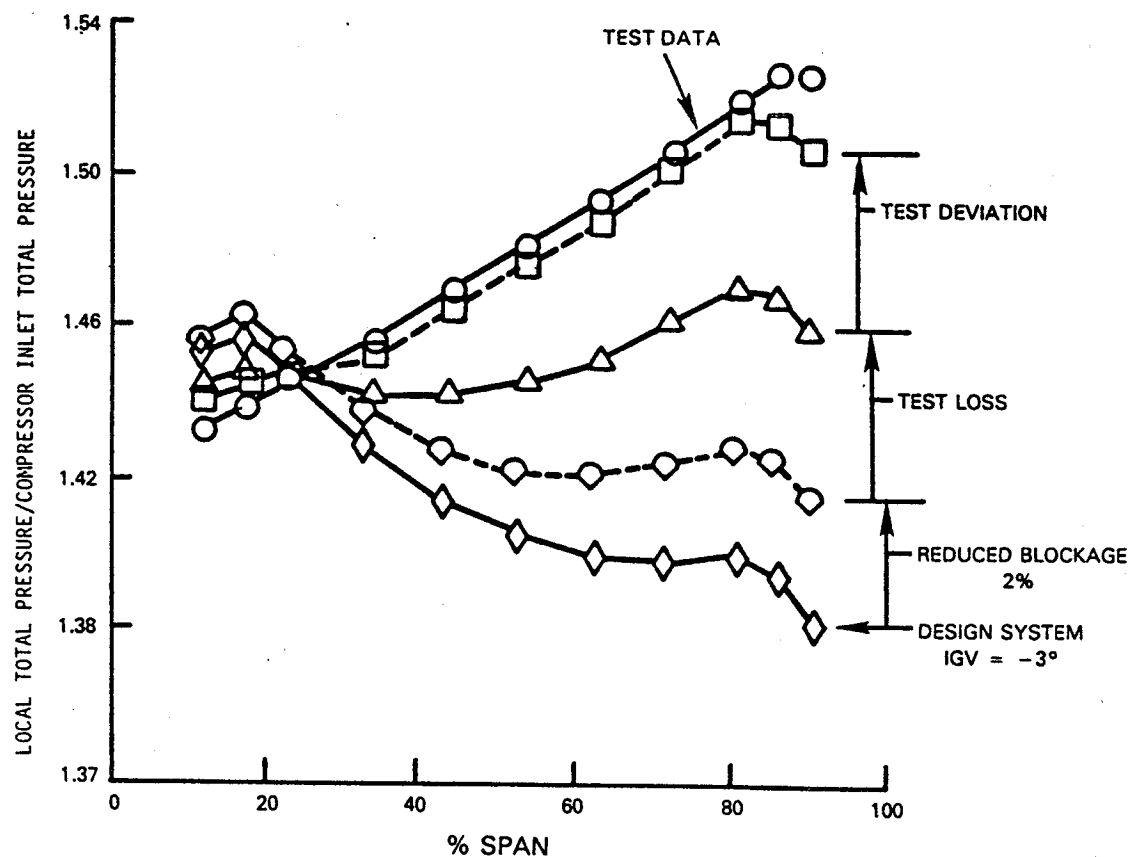
Figure 101   Rotor 6 Exit Pressure Profile Simulation. The effects of test blockage, loss, and deviation on design pressure profile are shown.
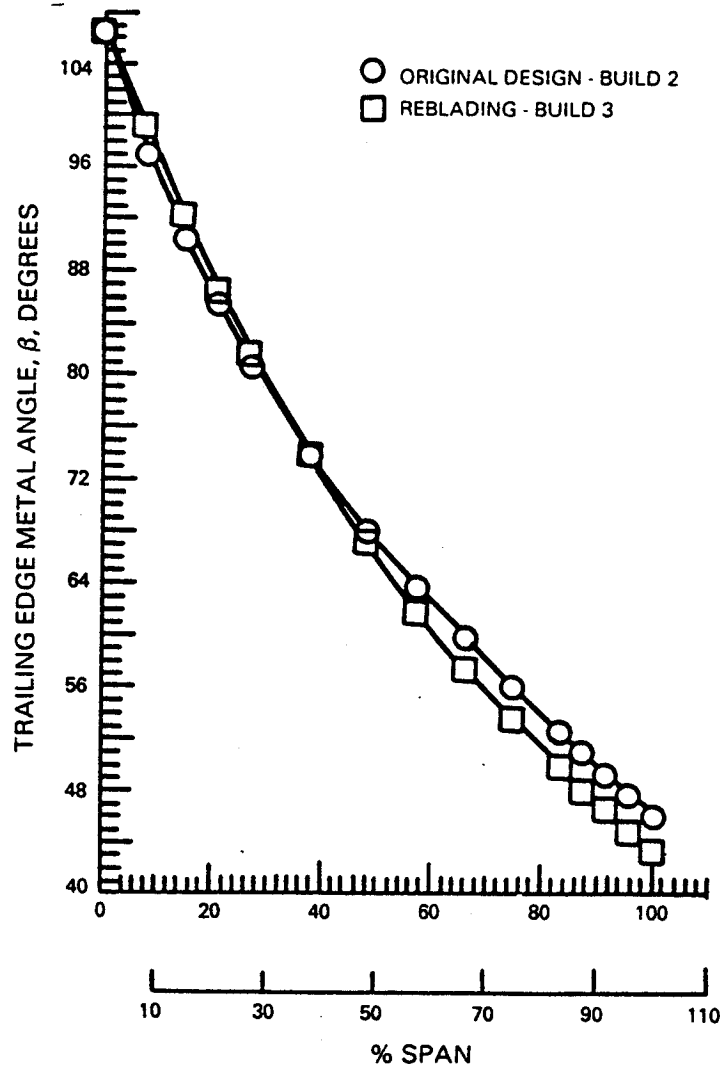
Figure 102   Trailing Edge Metal Angle. Rotor 6 trailing edge was uncambered to
eliminate pressure skew.

For the reblading, the blockage was reduced (or effective flow area increased)
throughout the compressor as shown in Figure 103. The blockage reduction was
indicated by the test data and is consistent with the revised design system
approach. The spanwise loss and deviation distributions are based on Build 2
analysis and an improved design deviation system. Figure 104 shows a typical
spanwise rotor/stator design loss, while Figure 105 shows the predicted Build
2 pressure profile at the rotor 15 (last) trailing edge resulting from this
design approach as compared with Build 2 test data.
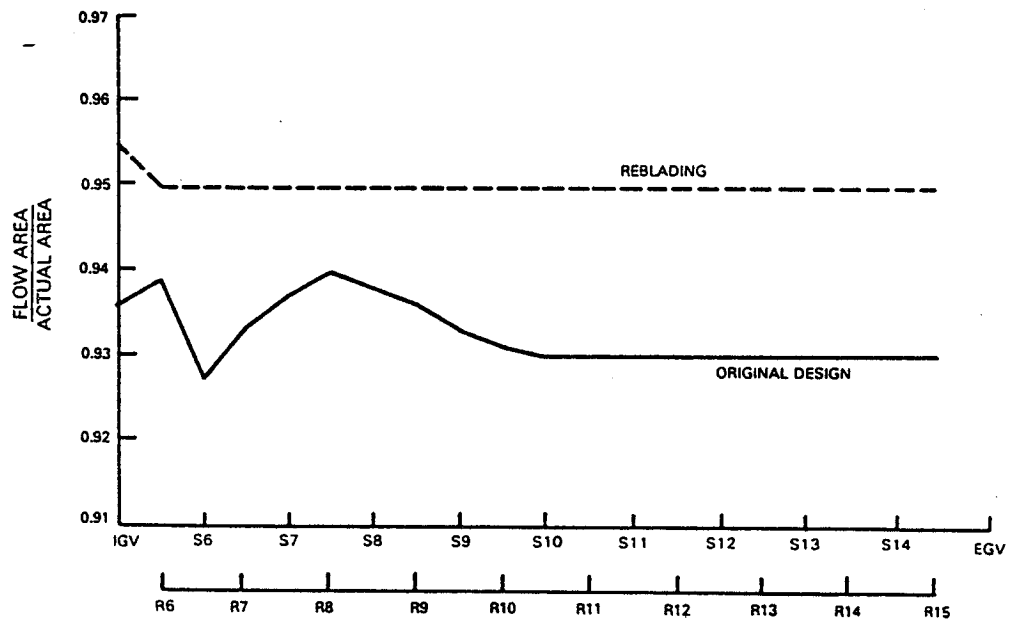
Figure 103   Aerodynamic Blockage Distribution. Blockage distribution is consistent with the revised design system approach.
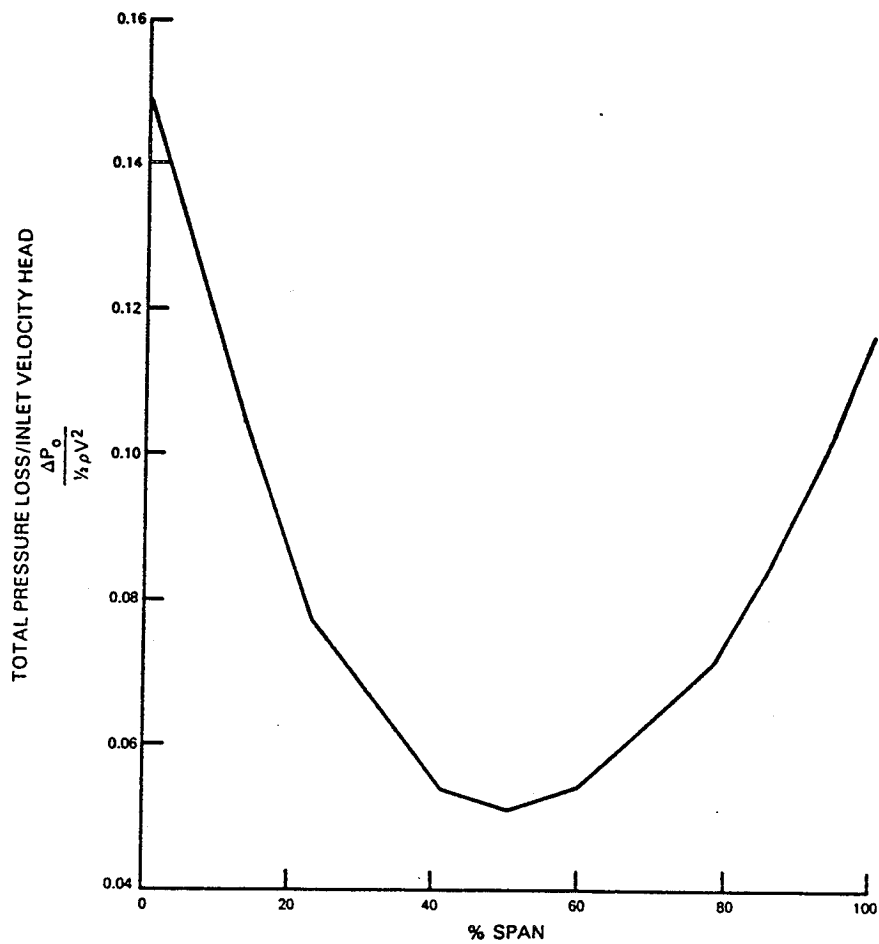
Figure 104   Typical Spanwise Loss. Design loss for reblading is based on Build 2 analysis.
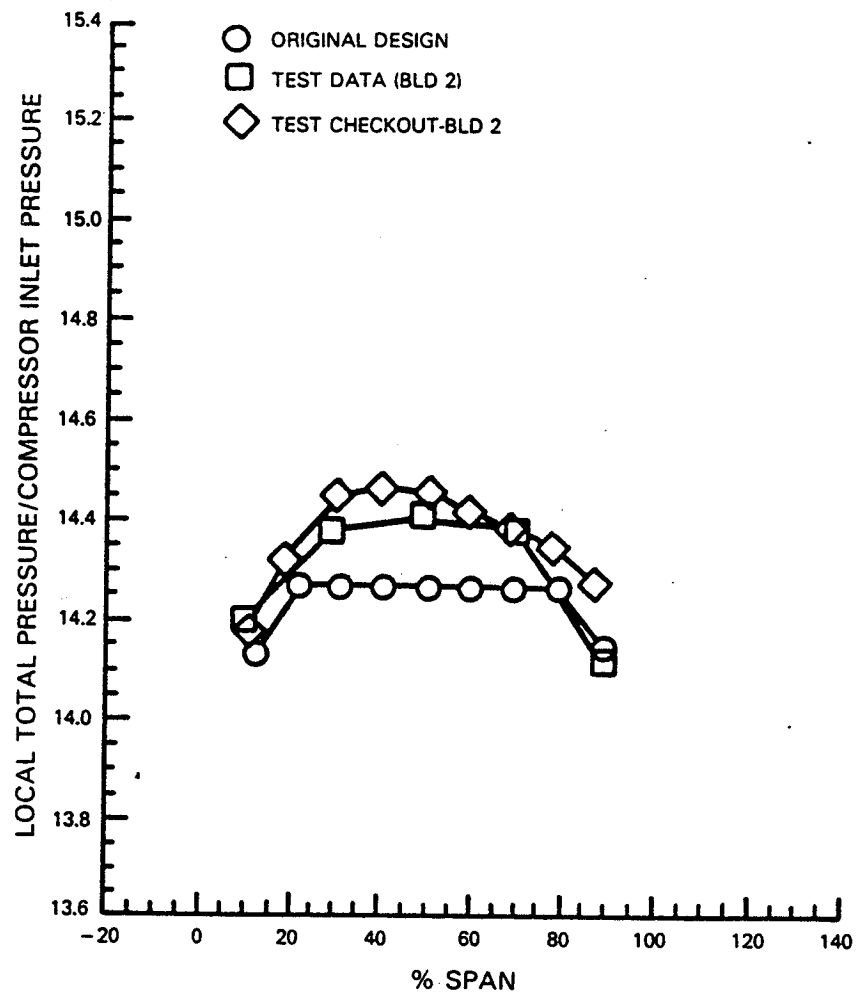
Figure 105 Pressure Profile at Rotor 15 Trailing Edge. The Build 2 test pressure profile is better predicted by the revised design system approach.

3.1.2.2 Revised Design System Predictions

The peak efficiency for Build 2 was well below the operating line. The design intent for Build 3 was to achieve peak efficiency on the altitude operating line at the original aerodynamic design point. The positive incidences caused by stator restaggers have been eliminated, and leading edges generally have been overcambered to minimize losses at the aerodynamic design point. Incorporation of the revised design system assumptions for blockage, loss, and deviation should result in the intended stage sizes and also achieve peak efficiency on the operating line. Figure 106 shows the equivalent change in incidence required to rematch peak efficiency of Build 2 blading to the operating line.

Loading levels predicted for Build 3 reblading are shown in Figure 107, blade loading, and in Figure 108, end-wall loading, at the aerodynamic design point on the nominal operating line and at 15 percent surge margin above the operating line. Also shown are the loading levels achieved in Build 2 and the loading potential based on Pratt & Whitney experience, indicating that the goal of maintaining an adequate surge margin with the reblading is achievable.
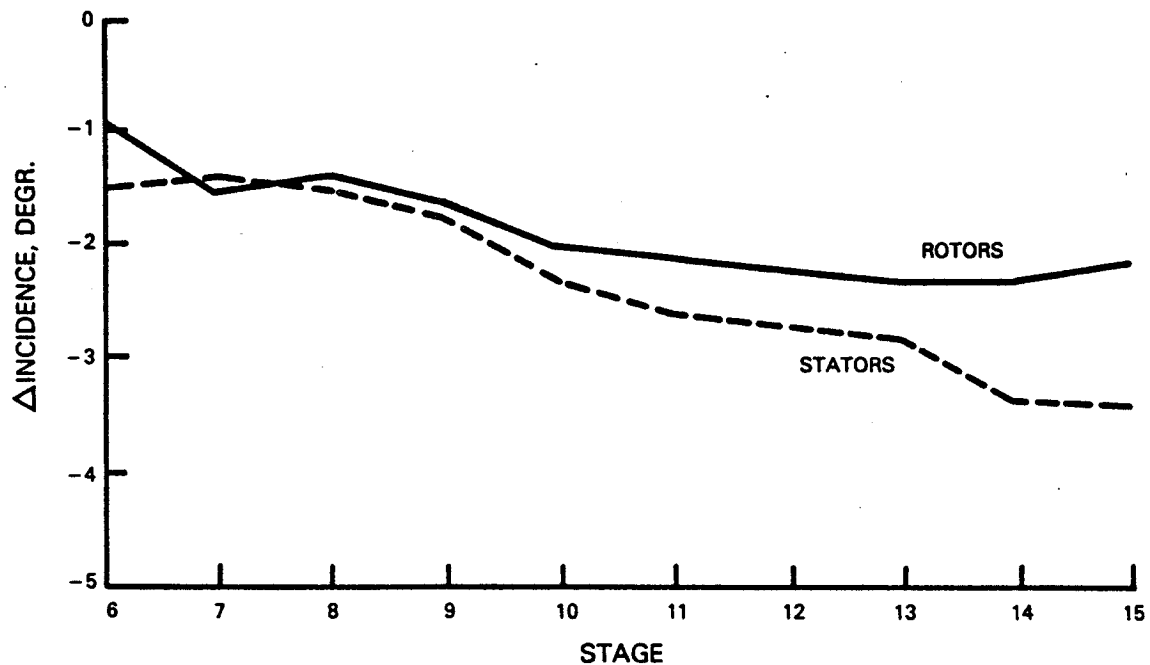
Figure 106   Incidence Change to Raise Build 2 Peak Efficiency to the Operating Line. Improved operating line efficiency should be achieved in reblading through a more favorable incidence selection.
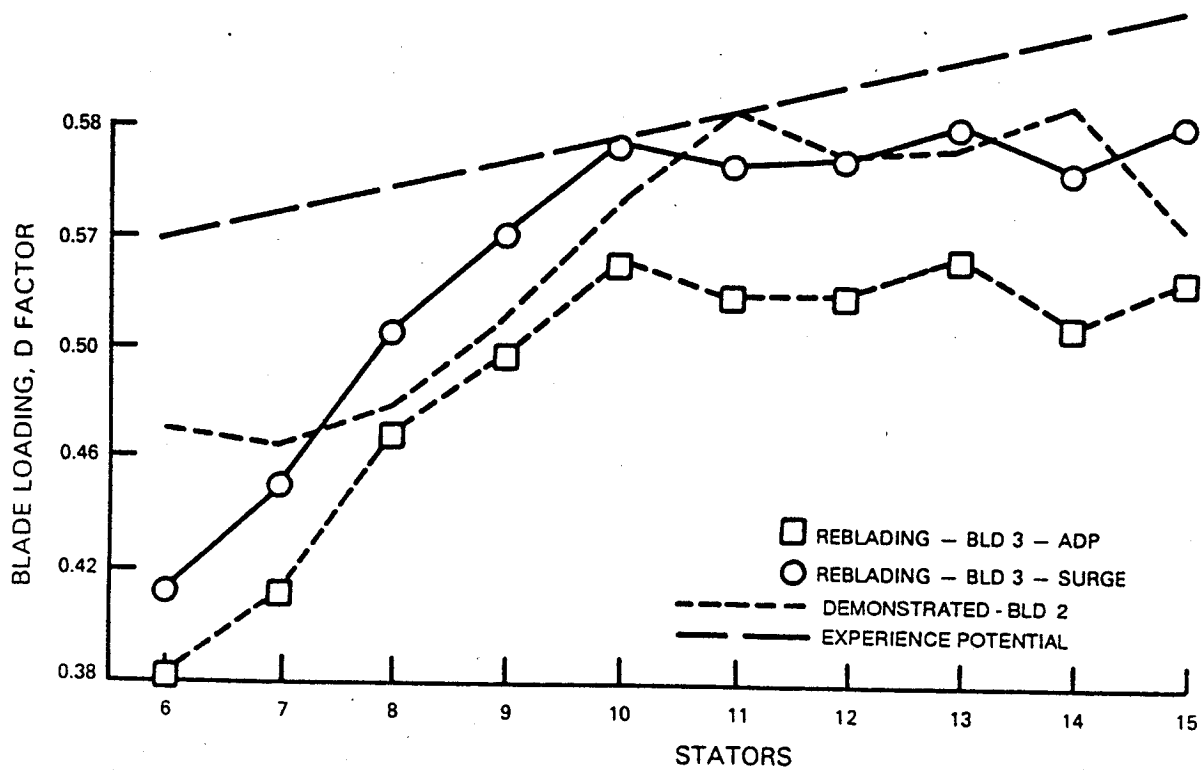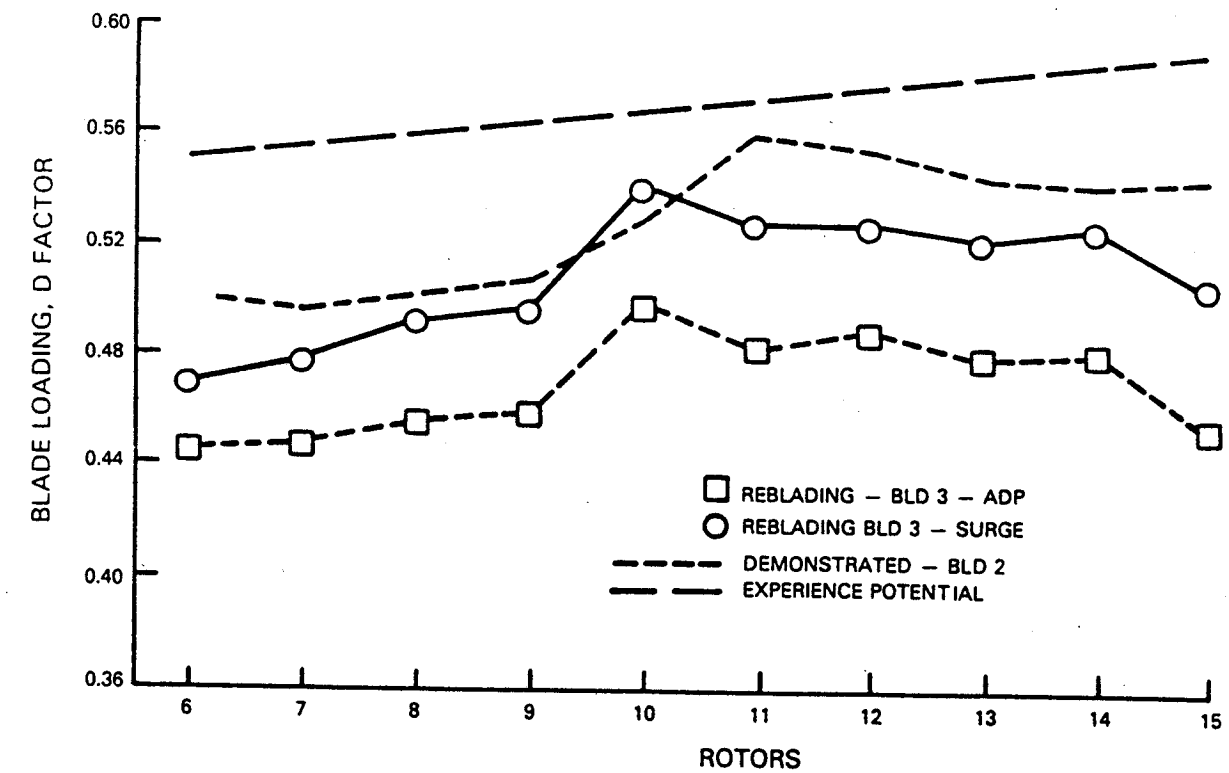
Figure 107   Blade Loading at Midspan for Rotors (above) and Stators (below). D-factors indicate adequate surge margin potential for rebladed design.
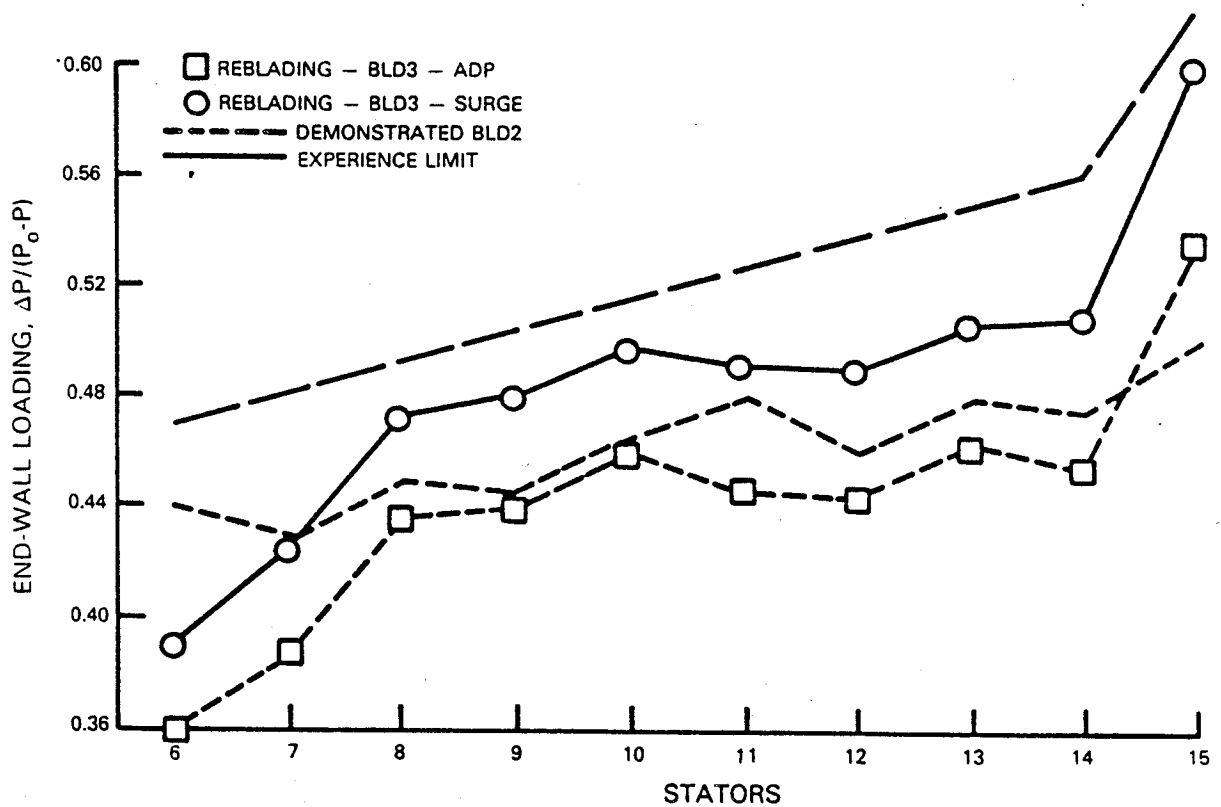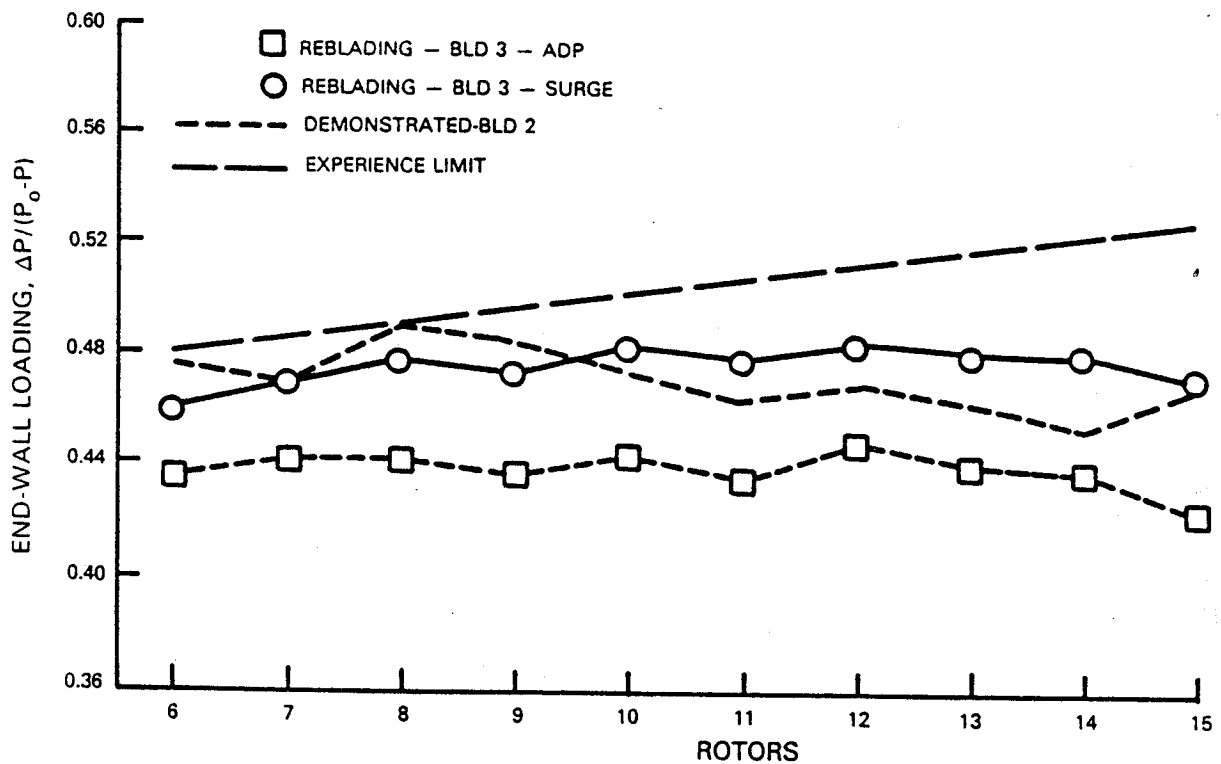
Figure 108   End-Wall Loading at Midspan for Rotors (above) and Stators
(below). Surge loading levels for the rebladed design fall within
the range of past experience.

3.1.2.3 Implementation of Reblading

In the execution of detailed blading design, the goal was to reduce the loss at the design point and still maintain 15 percent surge margin as an adequate blading design criteria. The surge margin goal for the rig remains at 20 percent, but off-design blade operation is not entirely predictable over this range. Thus, the blade design criteria were modified for the purpose of consistency in design. Design data for the redesigned airfoils are summarized in Appendix A.2.

The loss reduction has been achieved by controlling the chordwise velocity distribution (Figure 109). No changes in blade chords or numbers of blades were included in the aerodynamic design assumptions. However, the structural-vibratory requirements led in many instances to increased tip chords by as much as 10 percent in order to remove certain vibratory modes from the compressor operating range. The actual engine specification, rather than the lesser rig requirements, was used as the design criteria for vibratory analysis.
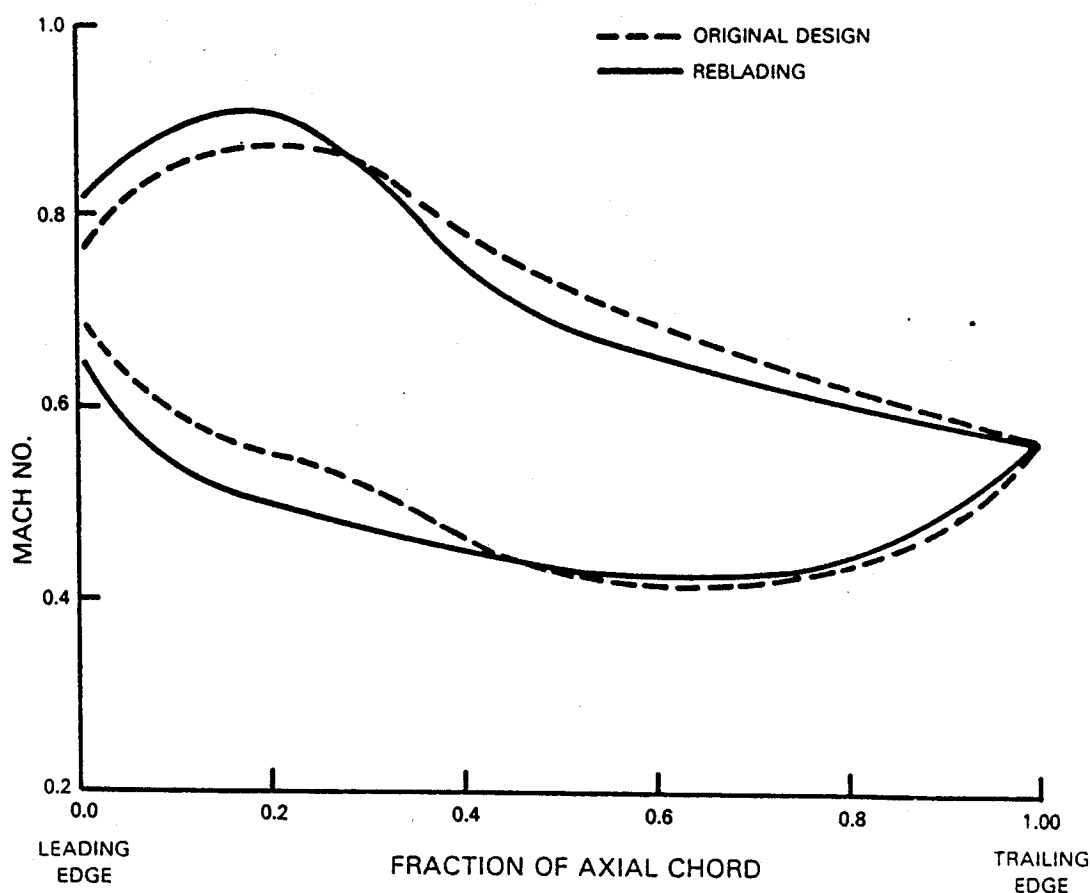
Figure 109 Typical Airfoil Surface Mach Number Distribution. Early diffusion is typical for redesigned airfoils.

3.1.2.4 Performance Potential

The maximum potential performance improvements for the reblading incorporated in Build 3 are outlined in Table XXX. The predicted adiabatic efficiency for Build 3 of 86.5 percent discounts the maximum gain in line with typical development experience. This estimate reflects the expectation that the net effect of incidence rematch and loss reductions will be less than the ideal.

TABLE XXX

PERFORMANCE POTENTIAL

	Change, %	Adiabatic Efficiency, %	Polytropic Efficiency, %
Test Rig Build 2 Adjusted Performance		85.1	89.4
Rematching Incidence in All Stages	+1.4		
Low Loss Blading Design	+0.4		
Double Row Exit Guide Vane	+0.4		
Test Rig Maximum Potential Performance	+2.2	84.3	91.0
Test Rig Build 3 Predicted Performance	+1.4	86.5	90.4

3.2 VIBRATION ANALYSIS

As noted in Part II, Section 5.0, crack indications were noted in several 13th-stage blades near the blade tips. These cracks were attributed to high first chordwise bending mode vibratory stresses. To preclude the recurrence of high tip mode stresses in Build 3, ground rules were established to: 1) reduce blade tip mode frequency to achieve 10 percent margin below idle speed where feasible, 2) tune the second tip mode above red-line speed, and 3) tune all rotor blades to avoid low order and other critical resonant frequencies between idle and red-line speeds.

The resultant airfoil characteristics are summarized in Table XXXI, and their corresponding resonance diagrams are shown in Figures 110 through 115. All rotors met the frequency margin dictated by Pratt & Whitney commercial engine criteria with the exception of rotor 11 bleed excited resonance, which was slightly below the margin. This exception was considered to be acceptable because the 56E resonance is a bleed hole order which could easily be changed for an engine design. Additionally, resonance speed occurs at idle where minimal rig running time will be needed.

TABLE XXXI

HIGH-PRESSURE COMPRESSOR TEST RIG GENERAL BLADE DESCRIPTION

	R6	R7	R8	R9	R10	R11	R12	R13	R14	R15
Blade Material	PWA 1202	PWA 1202	PWA 1003	PWA 1003	PWA 1003	PWA 1003	PWA 1003	PWA 1003	PWA 1003	PWA 1003
Airfoil Series *	MCA	MCA	CDA	CDA	CDA	CDA	CDA	CDA	CDA	CDA
No. of Blades	26	50	60	66	62	56	64	70	76	78
Root radius, cm	17.399	20.173	21.887	22.987	23.584	24.016	24.237	24.282	24.282	24.282
(in.)	(6.850)	(7.942)	(8.617)	(9.050)	(9.285)	(9.455)	(9.542)	(9.560)	(9.560)	(9.560)
Tip radius, cm	29.680	29.093	28.811	28.382	28.064	27.719	27.422	27.069	26.800	26.543
(in.)	(11.685)	(11.454)	(11.343)	(11.174)	(11.049)	(10.913)	(10.796)	(10.657)	(10.551)	(10.450)
Root chord, cm	7.127	3.828	3.454	3.010	2.614	2.977	2.568	2.311	2.129	2.075
(in.)	(2.806)	(1.507)	(1.360)	(1.185)	(1.029)	(1.172)	(1.011)	(0.910)	(0.838)	(0.817)
Tip chord, cm	9.045	4.511	3.305	2.936	2.621	2.977	2.824	2.598	2.129	2.210
(in.)	(3.561)	(1.776)	(1.301)	(1.156)	(1.032)	(1.172)	(1.112)	(1.023)	(0.838)	(0.870)
Max thickness/chord, root	0.102	0.085	0.091	0.098	0.105	0.108	0.101	0.101	0.101	0.100
Max thickness/chord, tip	0.030	0.039	0.038	0.039	0.039	0.036	0.038	0.044	0.048	0.049
Chord angle, root, deg	70.5	68.4	66.8	63.2	60.5	57.9	59.8	57.7	54.4	49.8
Chord angle, tip, deg	31.1	33.9	39.6	40.9	40.8	41.0	41.4	42.1	41.3	41.4
Aspect ratio	1.72	2.33	2.00	1.79	1.72	1.25	1.24	1.21	1.18	1.09
Tip Thickness, cm	0.272	0.175	0.124	0.114	0.102	0.107	0.107	0.114	0.102	0.109
(inch)	(0.107)	(0.069)	(0.049)	(0.045)	(0.040)	(0.042)	(0.042)	(0.045)	(0.040)	(0.043)

* See List of Symbols
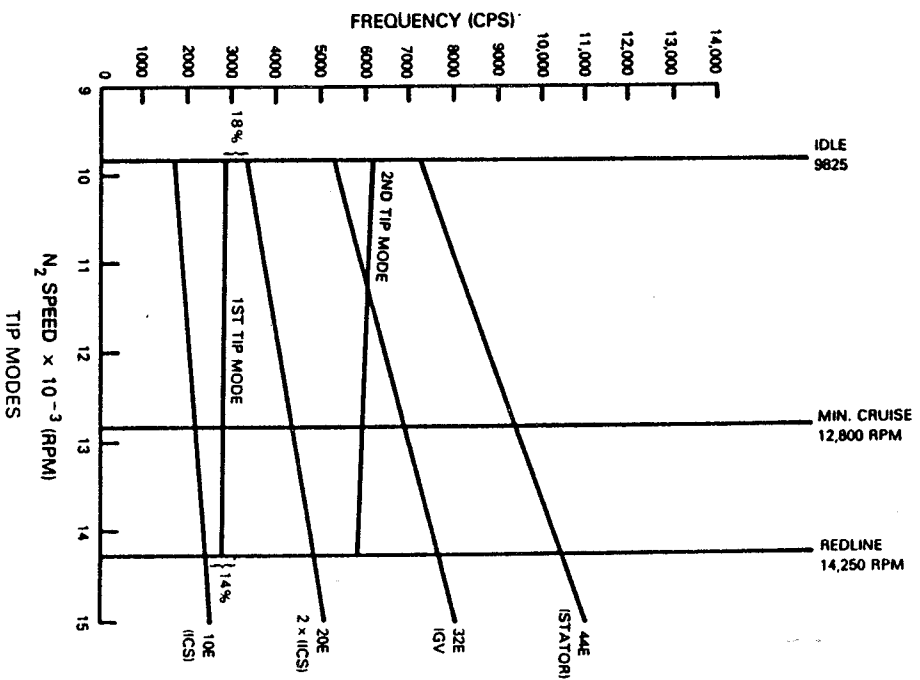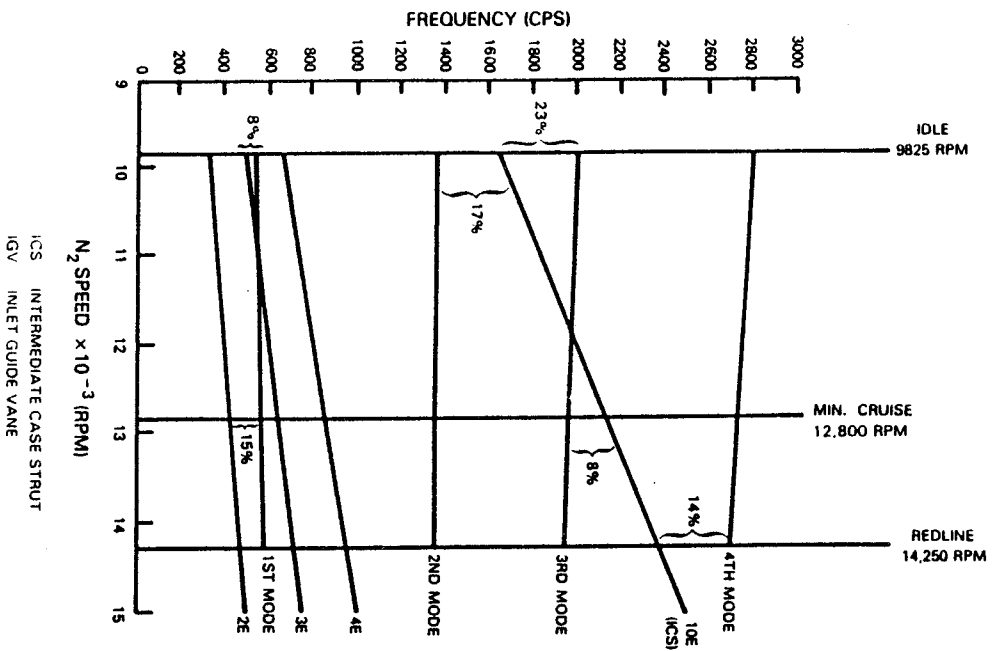
Figure 110   Resonance Diagram for Rotor 6
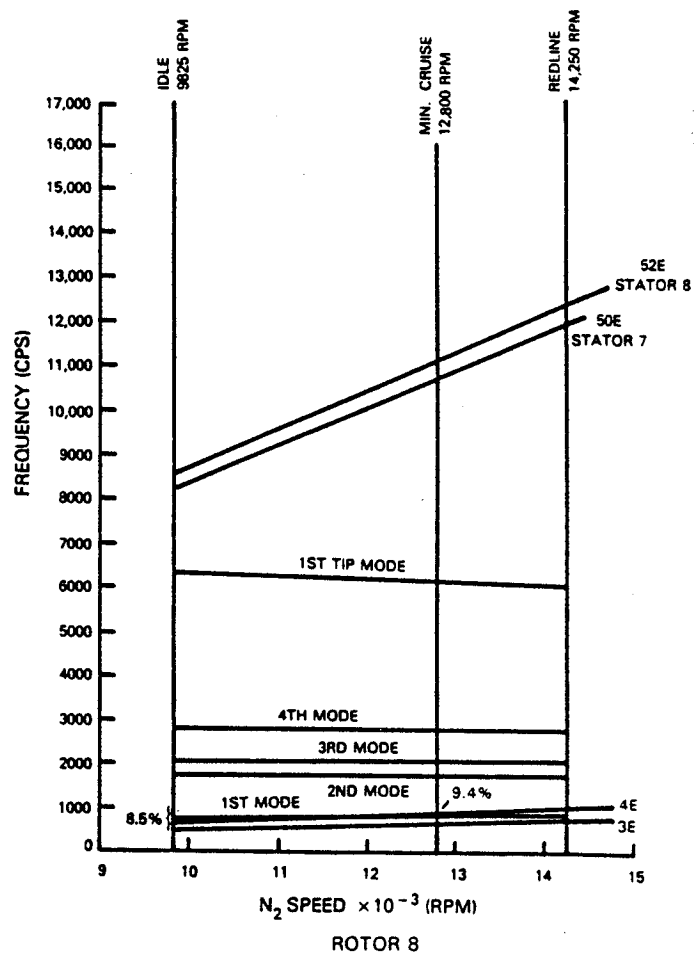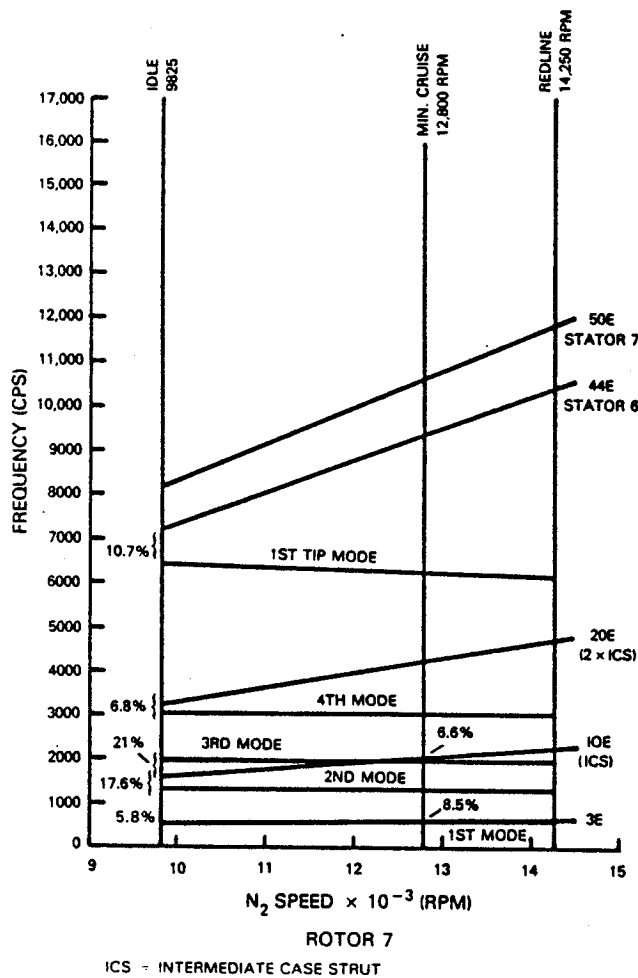
Figure 111   Resonance Diagrams for Rotors 7 and 8
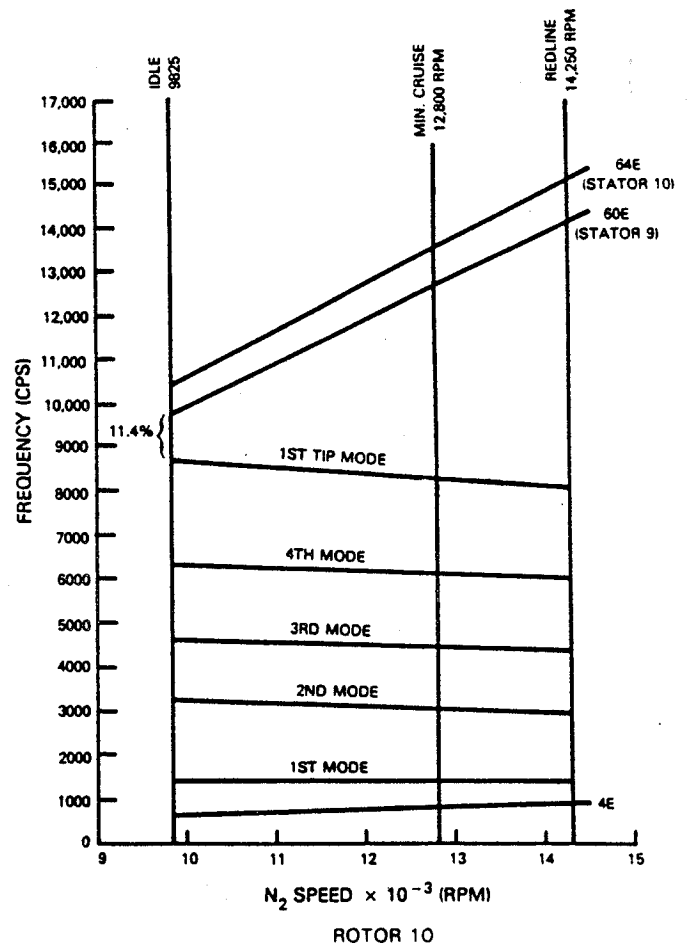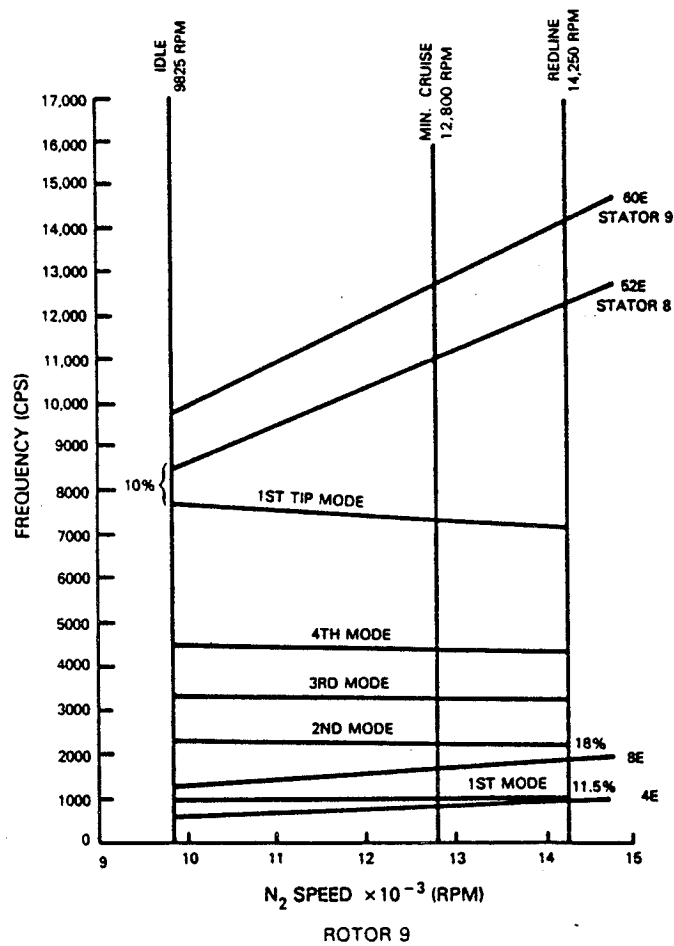
Figure 112   Resonance Diagrams for Rotors 9 and 10
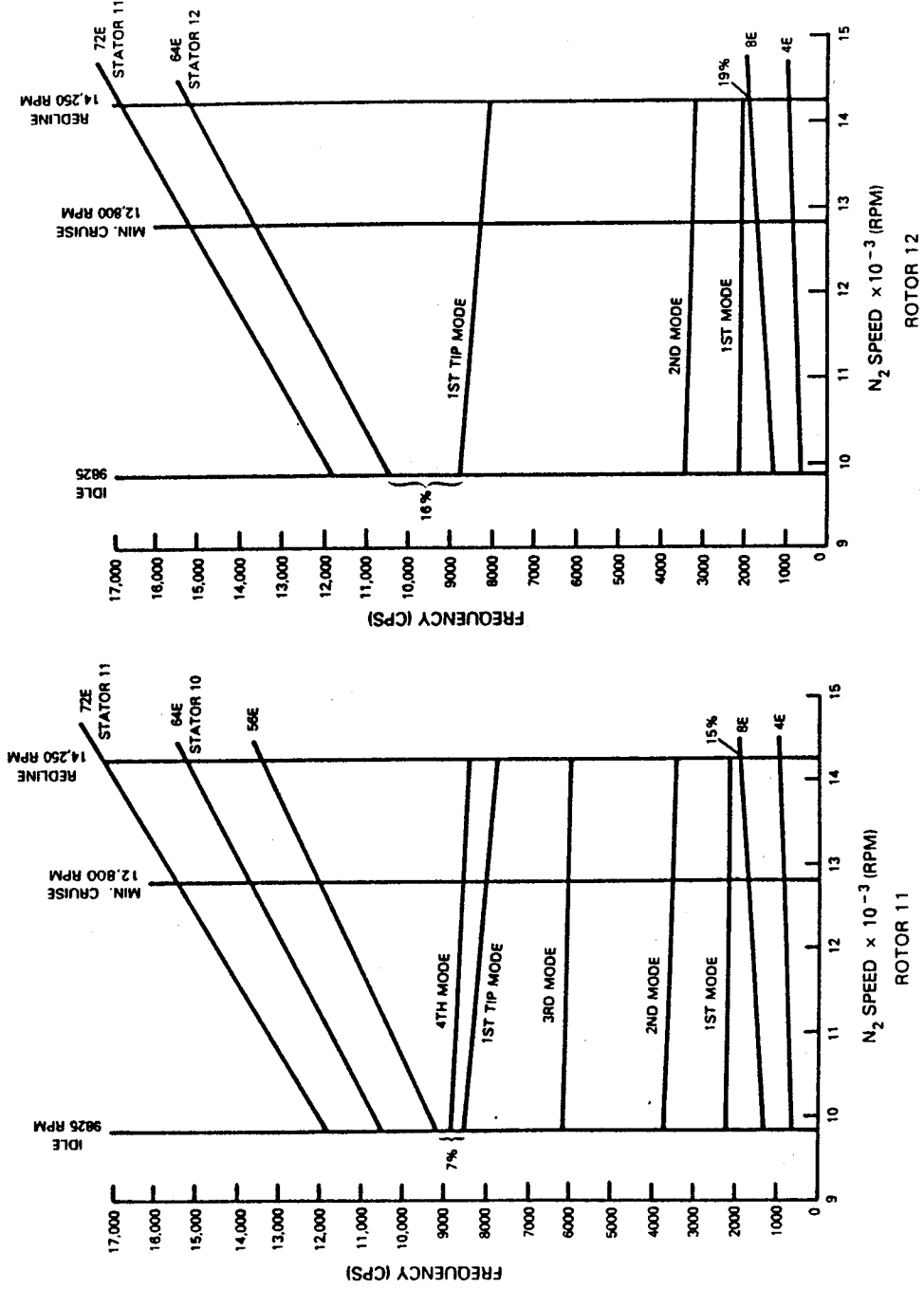
Figure 113   Resonance Diagrams for Rotors 11 and 12
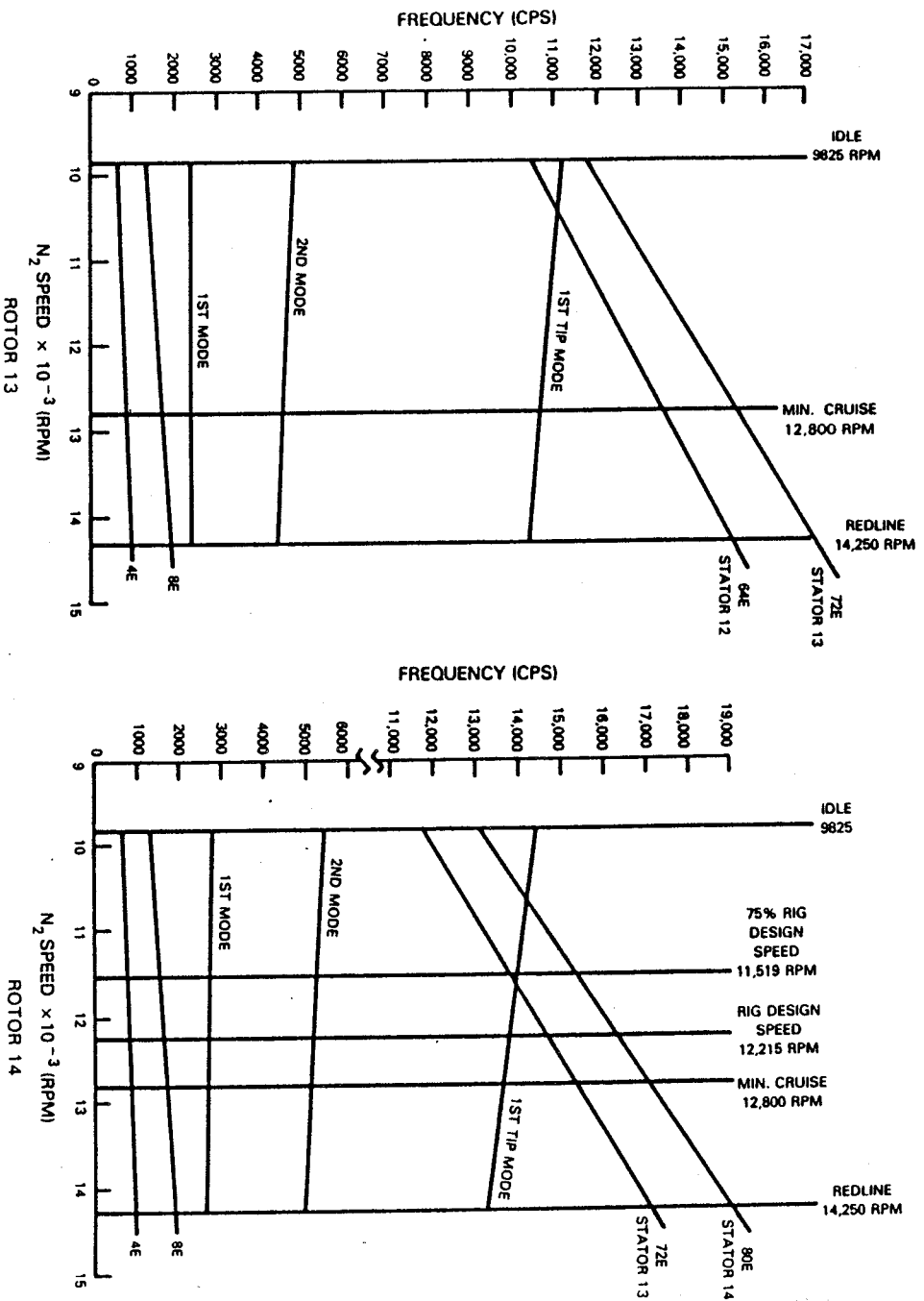
Figure 114   Resonance Diagrams for Rotors 13 and 14
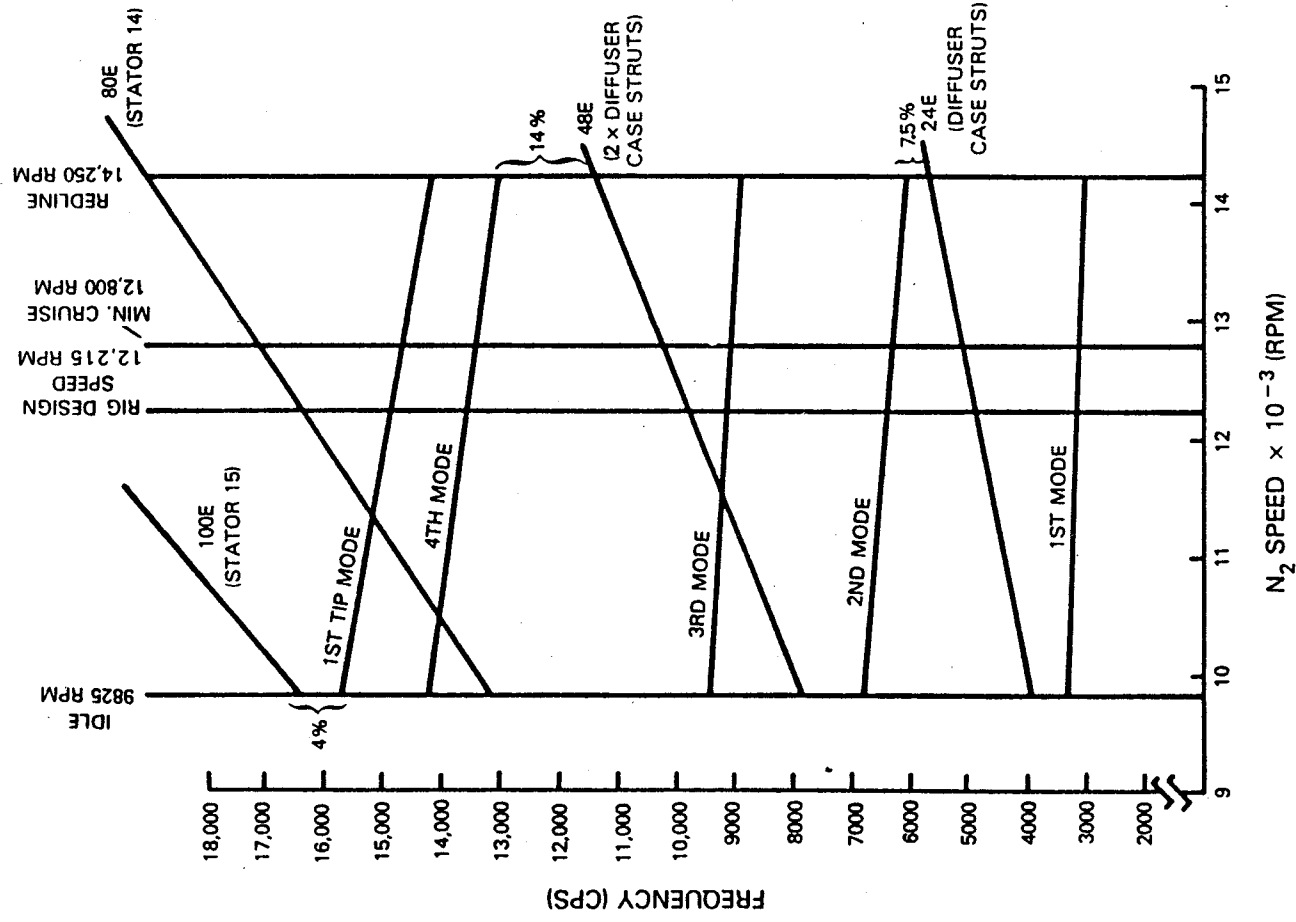
Figure 115   Resonance Diagram for Rotor 15

Blade tip mode resonant speeds are summarized in Figure 116. Most tip modes fall outside the operating speed range. The tip modes for rotors 13, 14, and 15 were permitted in the operating range, clear of the rig design speed, based on successful engine experience.

The airfoil redesign increased blade radial load on the order of 6 percent, except for rotors 13 and 15, for which radial load was increased by 10 and 17 percent, respectively. Blade root stresses and disk lug stresses were recalculated, based on these increased loads, and all stresses were found to be well below design allowable values.

Stator changes from Build 2 were very slight. Therefore, only stator flutter characteristics were checked for Build 3. All stators were predicted to have adequate bending and torsion flutter margin. The circumferential locations of all rig performance instrumentation were evaluated, and adjustments were made to ensure that instrumentation wake harmonic content would not cause high blade resonant stresses in the operating range.
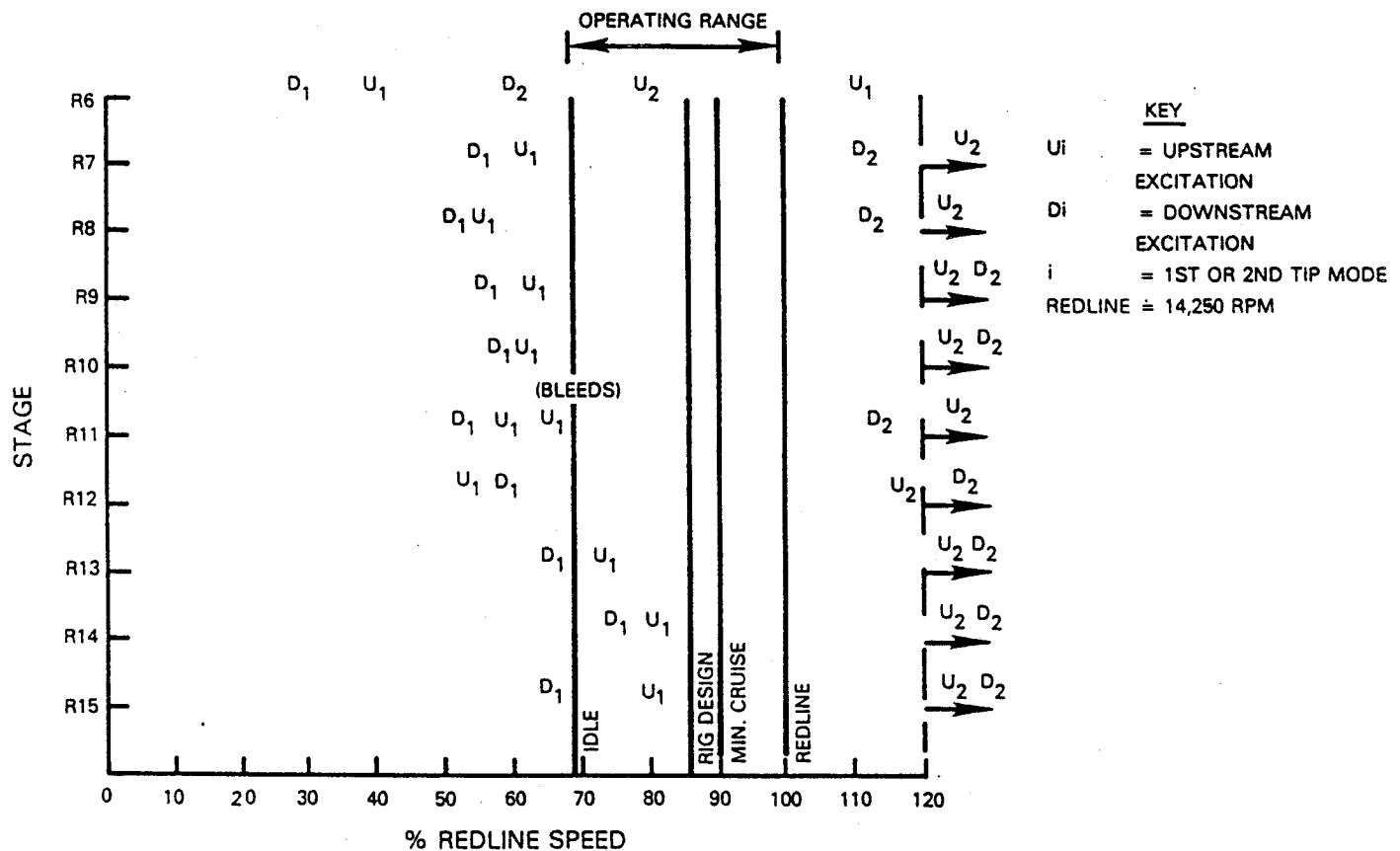
Figure 116   Summary of Build 3 Predicted Tip Mode Resonant Speeds

3.3 MECHANICAL DESIGN UPDATE

Mechanical design changes to the high-pressure compressor component configuration were minor and comprised adjustments in the flowpath to accommodate the redesigned airfoils and a change in the exit guide vane attachment. These efforts are discussed in the following subsections.

3.3.1 Flowpath Modifications

The ground rules for Build 3 flowpath modifications were to: 1) match the actual running tip clearances of Build 2 but not to run the blade tips in the trenches if at all possible, 2) adjust the trench axial position to avoid the forward or aft blade tip rubs observed in Build 2 testing, 3) maintain the waterfall/dam philosophy of Build 2 for inner diameter platform overlap (two-thirds probability of a waterfall), and 4) maintain the same distance from the leading edge of the vane "button" to the leading edge of the vane as was specified for Build 2.

For Build 3, the radial closure and axial position calculations were based on rig unheated inlet conditions rather than on engine aerodynamic design point (ADP) conditions which were used for Build 2 calculations. Running with a heated inlet was not achieved in Build 2, and it was not planned for Build 3. The depth of the trenches in Build 3 was planned to be equal to the desired running clearance for each stage; thus, the blade tips were to run "line-on-line" with the case. An exception was made in the situation where the desired clearance resulted in a trench depth less than 0.127 mm (0.005 in). In this situation, the trench depth was set at 0.127 mm (0.005 in), and the blade tip was permitted to run within the trench. Build 3 blade lengths were determined from Build 2 laser tip-clearance measurements and blade growth calculations. The final trench diameters were measured after grinding, and the blade grind diameters were adjusted to reflect any deviations from nominal. Table XXXII summarizes the variables that were calculated to obtain a cold blade grind diameter which would result in the desired flowpath conditions at the aerodynamic design point speed.

Rub strip trench widths and axial positions were also reviewed and adjusted for two reasons. First, following Build 2 testing, rubs were noted to have occurred at the aft edge of the trenches. These rubs were attributed to greater than anticipated rotor axial movement during rig running. Second, the redesigned rotor airfoils required adjustments in blade tilt to minimize bending stresses. The adjusted rotor trench dimensions and axial locations are summarized in Table XXXIII.

The new airfoil geometry required repositioning the stator vanes on the vane "buttons" to maintain the same distance from the leading edge of the vane "button" to the leading edge of the vane as was specified for Build 2. This requirement, in combination with the revised blade tilts, caused a change in the tip axial gaps between rotors and stators. This change was investigated, and the resultant gaps were found to be sufficient to preclude blade-to-vane interference. The final flowpath modification consisted of a slight change in the vane platform contours on stators 9 through 15. "Slab" cuts (Figure 117) had been incorporated in Build 2 for these stages to reduce machining costs, whereas "conical" cuts were used in stators 6 through 8 where the slope of the flowpath inner diameter was fairly steep and the inner diameter radius was sufficiently small to result in significant waterfall/dam flowpath mismatch if "slab" cuts were incorporated. The cost problem was eliminated in the Build 3 design so that conical cuts were incorporated in all vane platform contours.

TABLE XXXII

CALCULATION OF BLADE GRIND DIAMETERS
AT THE BLADE STACKING LINE

Stage Number	Cold Case Diameter, cm (in.)	Case Thermals, mm (in.)	Rotor Thermals and Growth, mm (in.)	Effect of Axial Shift of Rotor Relative to Case, mm (in.)	Trench Adjustment to Assure Minimum Trench Depth, mm (in.)	Cold Blade Grind Diameter, cm (in.)
6	59.329 (23.358)	+0.127 (+0.005)	-1.092 (-0.043)	+0.102 (+0.004)	---	59.243 (23.324)
7	58.113 (22.881)	+0.229 (+0.009)	-1.422 (-0.056)	+0.051 (+0.002)	---	58.003 (22.836)
8	57.615 (22.653)	+0.305 (+0.012)	-1.575 (-0.062)	+0.076 (+0.003)	---	57.419 (22.606)
9	56.617 (22.290)	+0.965 (+0.038)	-1.803 (-0.071)	+0.051 (+0.002)	---	56.538 (22.259)
10	55.931 (22.020)	+1.321 (+0.052)	-2.184 (-0.086)	+0.051 (+0.002)	---	55.850 (21.988)
11	55.204 (21.634)	+1.549 (+0.061)	-2.438 (-0.096)	+0.051 (+0.002)	+0.051 (+0.002)	55.126 (21.703)
12	54.559 (21.480)	+1.956 (+0.077)	-2.489 (-0.098)	+0.051 (+0.002)	+0.102 (0.004)	54.521 (21.465)
13	53.833 (21.194)	+2.210 (+0.087)	-2.616 (-0.103)	+0.051 (+0.002)	+0.152 (+0.006)	53.812 (21.186)
14	53.269 (20.972)	+2.438 (+0.096)	-3.429 (-0.135)	+0.051 (+0.002)	+0.051 (+0.002)	53.180 (20.937)
15	52.735 (20.762)	+2.591 (+0.102)	-3.454 (-0.136)	+0.051 (+0.002)	+0.203 (+0.008)	52.675 (20.738)

TABLE XXXIII

HIGH-PRESSURE COMPRESSOR TEST RIG, BUILD 3
ROTOR TRENCH DIMENSIONS

Stage Number	Dimension *			Reference Plane (*)
	X	Y	Z	
6	10.841	47.498	0.254	T
	(4.268)	(1.870)	(0.010)	T
7	24.379	26.772	0.406	T
	(9.598)	(1.054)	(0.016)	T
8	33.678	22.962	0.432	T
	(13.259)	(0.904)	(0.017)	T
9	0.958	20.803	0.254	A
	(0.377)	(0.819)	(0.010)	A
10	7.912	19.431	0.229	A
	(3.115)	(0.765)	(0.009)	A
11	15.283	21.641	0.127	A
	(6.017)	(0.852)	(0.005)	A
12	22.037	21.017	0.127	A
	(8.676)	(0.831)	(0.005)	A
13	29.812	19.990	0.127	A
	(11.737)	(0.787)	(0.005)	A
14	36.015	16.713	0.127	A
	(14.179)	(0.658)	(0.005)	A
15	41.961	16.815	0.127	A
	(16.520)	(0.662)	(0.005)	A

* NOTE: Dimension X is tabulated in units of cm (in).
Dimensions Y and Z are tabulated in units of mm (in).
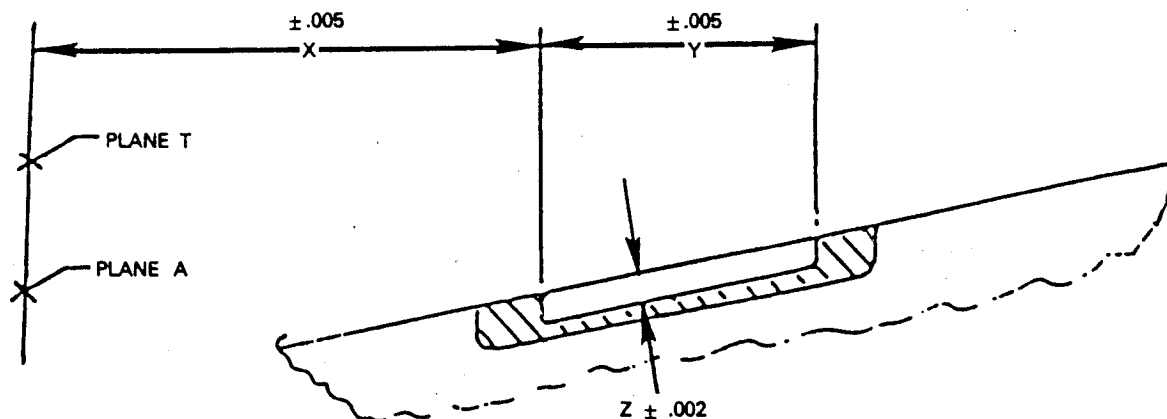
(*) Reference Planes for Establishing Dimension X

"CONICAL" CUT RESULTS
IN CYLINDRICAL SURFACE

"SLAB" CUT RESULTS
IN PLANAR SURFACE

FLOW PATH CONE ANGLE
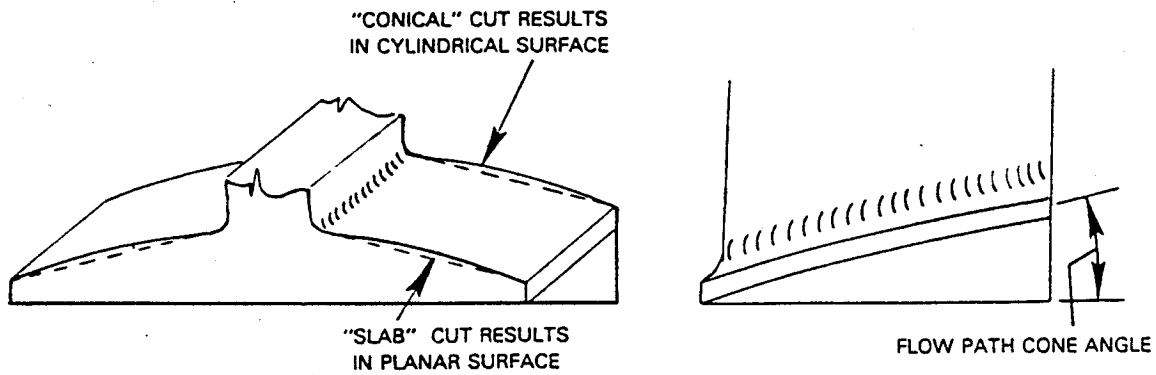
Figure 117   Comparison of "Conical" and "Slab" Machining Contours on Vane
Platforms

3.3.2   Exit Guide Vane Attachment Modification

The double row exit guide vane assembly comprises clusters of vane segments
that are welded together into a ring, the completed ring being secured at the
outer diameter by a retaining ring as shown in Figure 118. The original design
of the vane attachment "hook" at the retainer ring encompassed a generous
clearance to allow for attachment relative motion under gas load and thermal
conditions. A review of this design raised the concern that failure in the
weld joints (noted in the figure) would permit the forward section of the vane
cluster to tilt forward and engage the 15th-stage rotor blades. To preclude
this possibility, the gap on the forward hook was closed (see "Revised Design"
on Figure 118) such that the retaining ring will prevent tilting of the vane
cluster. Gap dimensions were reviewed and deemed adequate for thermal and gas
load motion.

RETAINING
RING

WELD JOINTS

REVISED
DESIGN

TWO
PIECE
EGV

ORIGINAL DESIGN
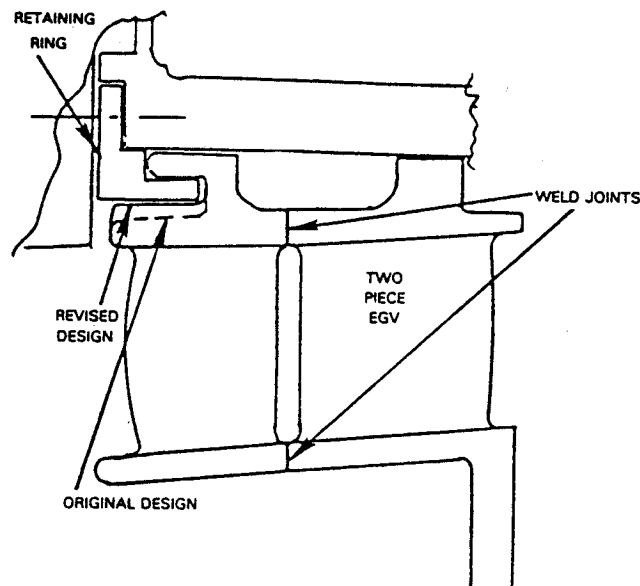
Figure 118   Exit Guide Vane Attachment Modification

SECTION 4.0

TEST RIG BUILD 3 DESIGN UPDATES

Principal contributors to the Build 3 test rig design updates comprised: 1) front and rear case modifications to accommodate installation of fused quartz windows for the laser doppler velocimetry (LDV) test program, 2) design of a rotor-speed sensing device for use in the same test program, and 3) the addition of tapped mounting holes in the cases to accommodate special high-response instrumentation for surge-sensing tests. These mechanical design modifications are described in the following subsections.

4.1 CASE MODIFICATIONS

The LDV program is intended to be a feasibility demonstration of the use of LDV systems to acquire data necessary for analysis of the flow fields in the front, middle, and rear stages of the high-pressure compressor. Three flowpath locations were chosen which include the sixth, ninth, and thirteenth stages of the compressor. These locations are identified in Figure 119. The selected locations provide the desired representative engine-core flows as well as varying degrees of risk, associated primarily with gaspath pressures and temperatures in the middle and rear stages of the compressor.
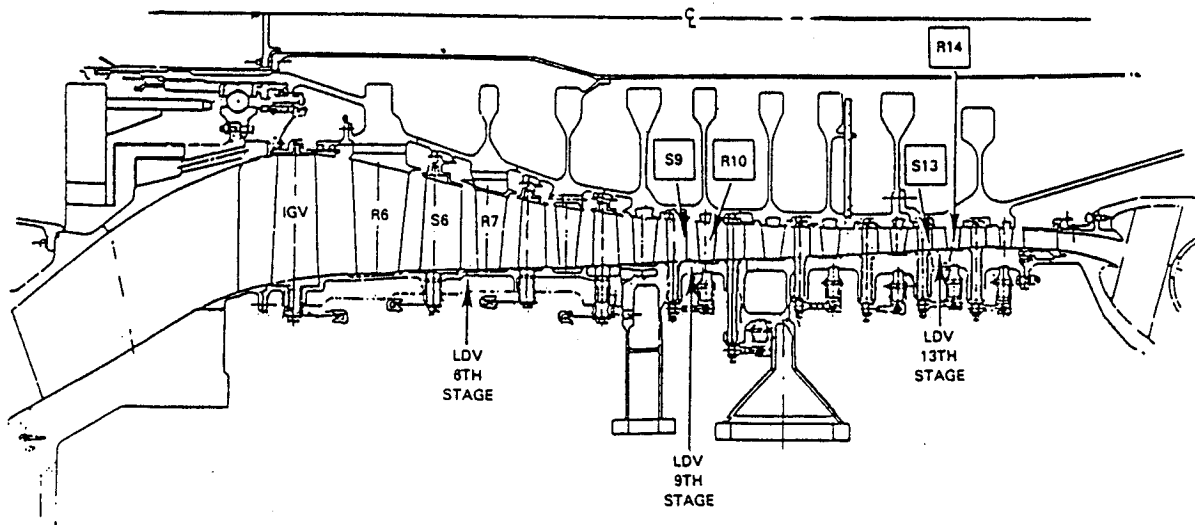
Figure 119   High-Pressure Compressor Test Rig Showing Locations of LDV Windows

4.1.1 Front Case Modifications

As shown in Figure 119, the sixth-stage LDV window is located in the front compressor case between the trailing edge of stator 6 and the leading edge of rotor 7. In fact, window axial width requirements are such that a portion of the rotor airfoil leading edge protrudes into the viewing area. Radial positioning of the window was adjusted to preclude blade tip rubs on the window surface. Circumferential window width was set by the requirement to traverse one stator wake and the full gap on either side of the stator wake. Window centerline is a nominal 17 degrees above horizontal to avoid the split-case horizontal tie-bolt flange. This angular orientation is maintained for the second and third LDV windows, as well, so that the LDV test equipment, which is mounted on a translating platform, could be relocated axially rearward without the need for repositioning the platform support structure.

A detailed view of the window assembly is shown in Figure 120, and details of the window installation are shown in Figure 121. The quartz lens is contoured to match engine flowpath curvature while maintaining the desired optical characteristics. The edges of the lens are beveled so that it can be retained in the mount frame (or carrier) as shown in Figure 121. After machining an opening of the required dimensions in the case, a boss is riveted to the case, as shown, to support the window inner and outer carriers. The carrier frames, in turn, are secured to the boss with mount screws. Provisions are made for shims to accommodate adjustments in window radial location. A tube connected to a flow passage in the window support structure supplies solvent on the upstream side of the window to clean the window surface exposed to the engine flowpath as required prior to and during testing. These installation features are retained in the middle- and rear-stage windows.

A redesign of the seventh-stage variable-stator unison ring was required as a result of the installation of the sixth-stage LDV windows. The existing unison ring blocked the line of sight required by the LDV optics. The redesign involved changing five of the vane positioning arms such that the vanes would be driven by a partial auxiliary ring located aft of the normal vane position, as shown in Figure 122. The vane arms are offset, as shown, to provide radial clearance above the eighth-stage unison ring. A rub block is provided at the partial ring position to maintain concentricity between the case and the unison ring. A resolver was added at one of the offset positioning arm locations to ensure that vane positioning in the affected sector was consistent with the rest of the vanes in the stage during testing. A capability for "fine tuning" vane position has been provided by an adjustable cam pivot on the vane arms.
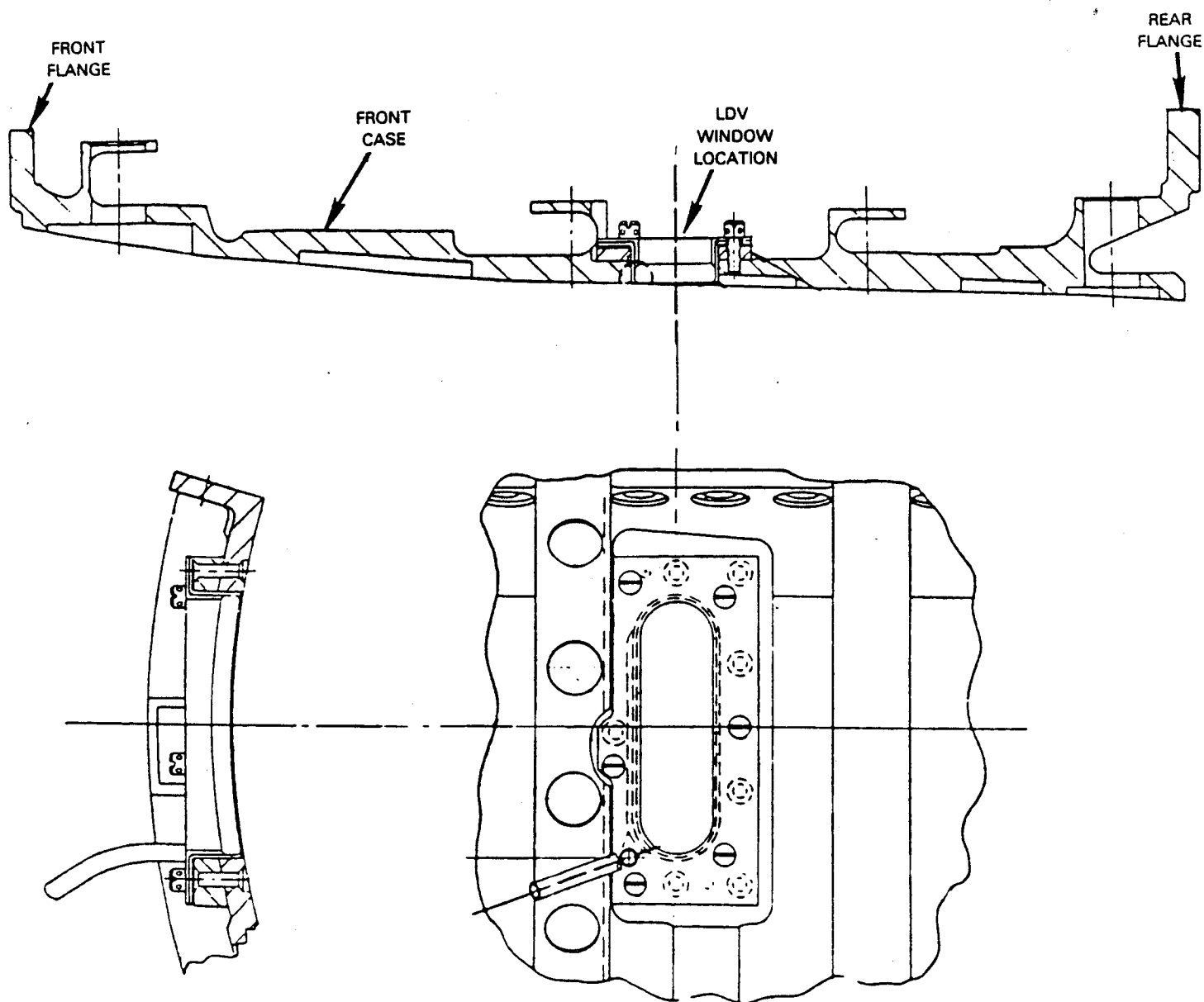
Figure 120   Sixth-Stage LDV Window Assembly
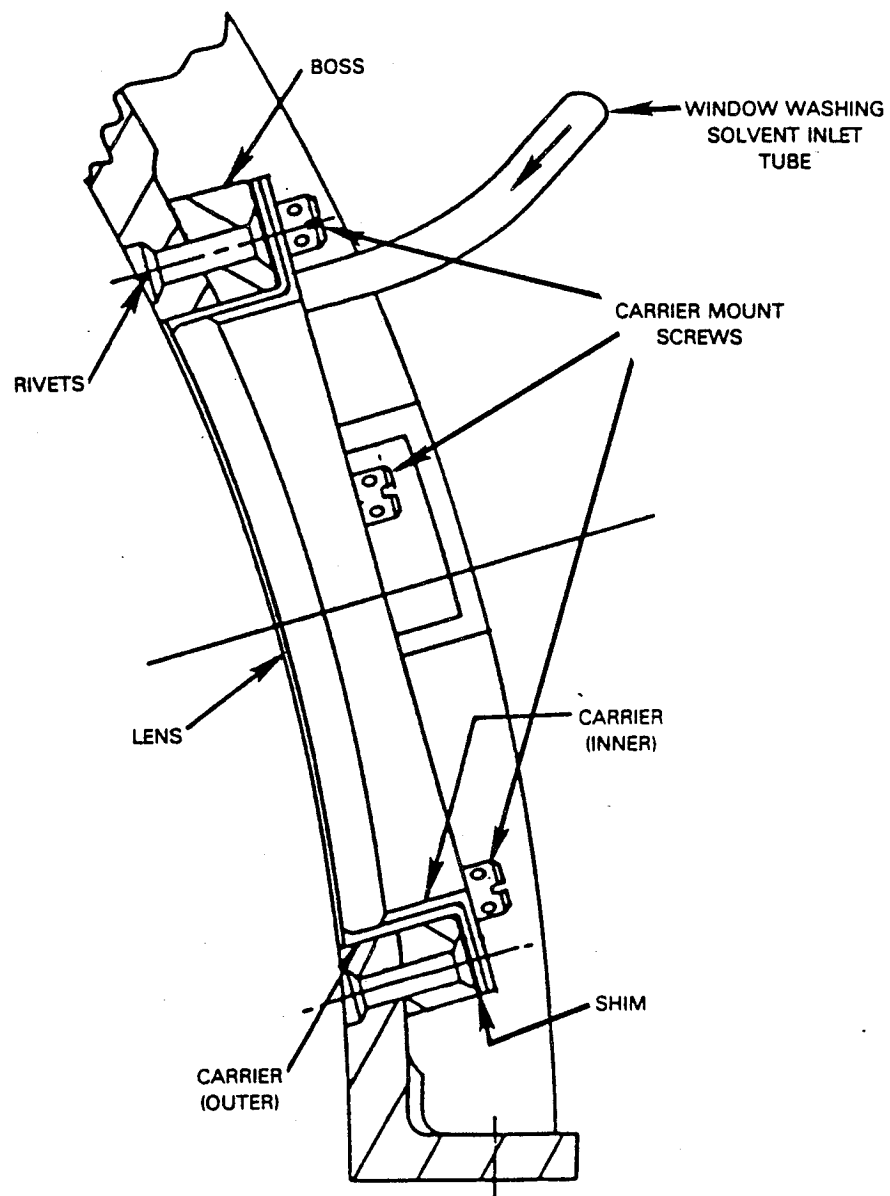
Figure 121   Details of Sixth-Stage LDV Window Installation
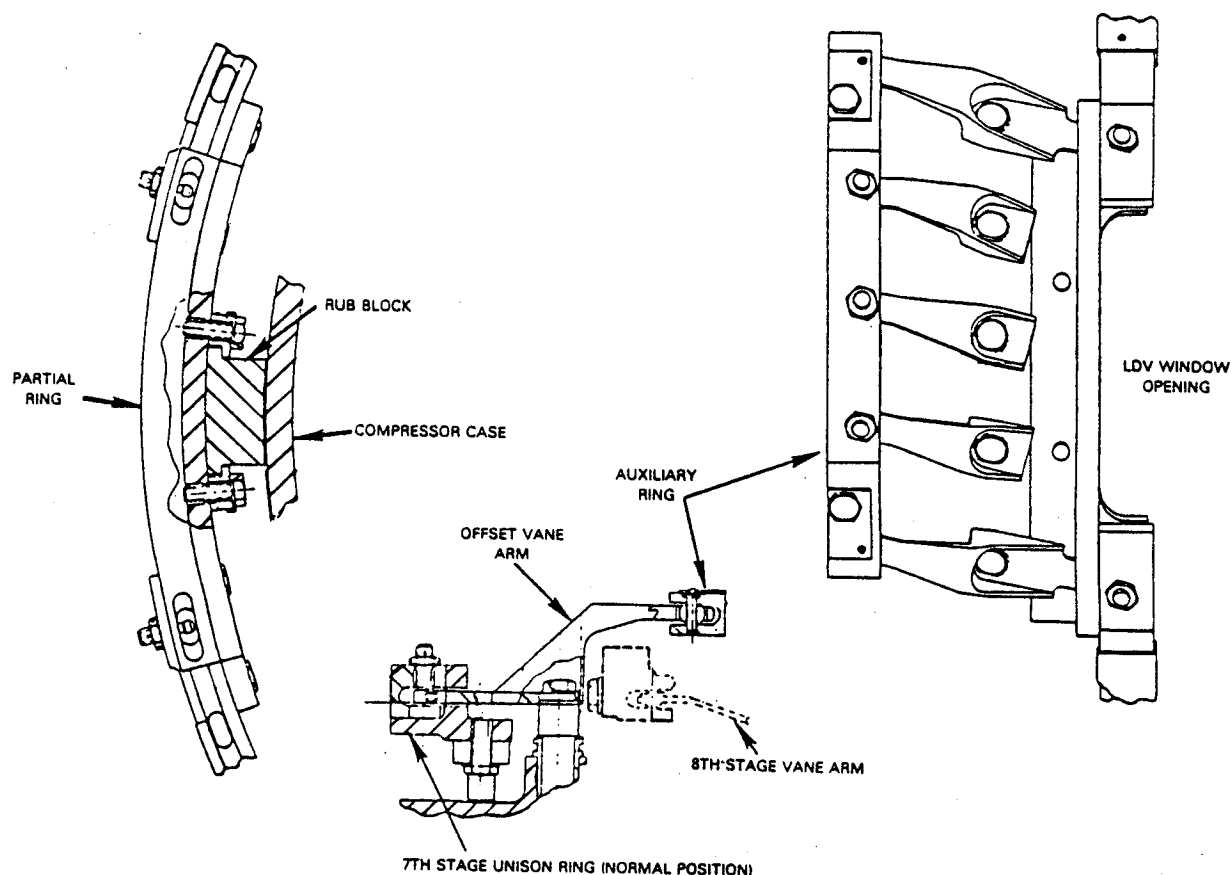
Figure 122   Modified Seventh-Stage Unison Ring

4.1.2   Rear Case Modifications

Rear case modifications comprised changes necessary to accommodate LDV testing in the ninth- and thirteenth-stage stator trailing edge locations. LDV window assemblies are similar to the front case window assembly, and unison ring modifications were required to provide a clear path for the laser beam optical probe. These modifications are discussed in the following subsections.

4.1.2.1   Ninth-Stage LDV Window

As shown in Figure 119, the ninth-stage LDV window is located between the trailing edge of stator 9 and the leading edge of rotor 10. In fact, the rotor blade tips extend nearly halfway across the window viewing area such that radial clearance must be set to preclude blade tip rubs on the window surface. Circumferential window width was again set by the requirement to traverse across one stator wake and the full gap on either side of the wake.

A detailed view of the window assembly is shown in Figure 123, and details of the window installation are shown in Figure 124. Case thickness requires that a spacer piece be matched to the case contour on one side but also provide a flat mounting surface on the opposite side, as shown in Figure 124. The spacer is attached to the case by the same mount screws which secure the lens carrier. To secure the front edge of the lens carrier, it is necessary to offset the front middle mount screw through a drilled hole in a case ring and then secure the window carrier with a mount lug. The remaining installation features are similar to the sixth-stage LDV window.

Redesign of the ninth-stage unison ring was required to avoid blockage of the LDV optics by three of the stator position control arms. Details of this redesign are illustrated in Figure 125. The redesign features a removable stator arm position control segment and an offset "bridge" structure to tie the split unison ring together and maintain ring concentricity when the segment is removed. The segment is bolted to the bridge, which, in turn, is bolted to the unison ring. Test planning is such that the optimum ninth-stage stator position will be determined when the ring segment is installed for the performance test program. Prior to LDV testing, the ring segment (noted in Figure 125) is unbolted from the bridge and removed to provide the required optical clearance. The stator control arms are then locked into the predetermined position.
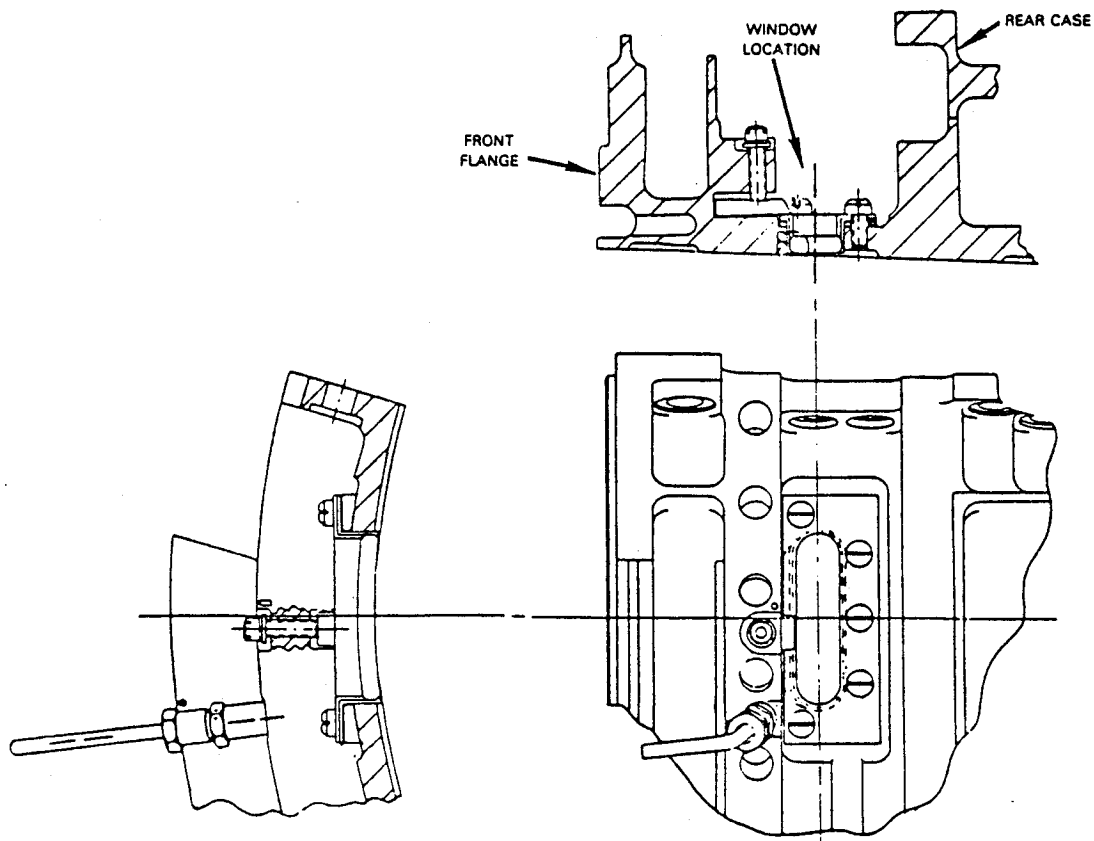
Figure 123   Ninth-Stage LDV Window Assembly

168
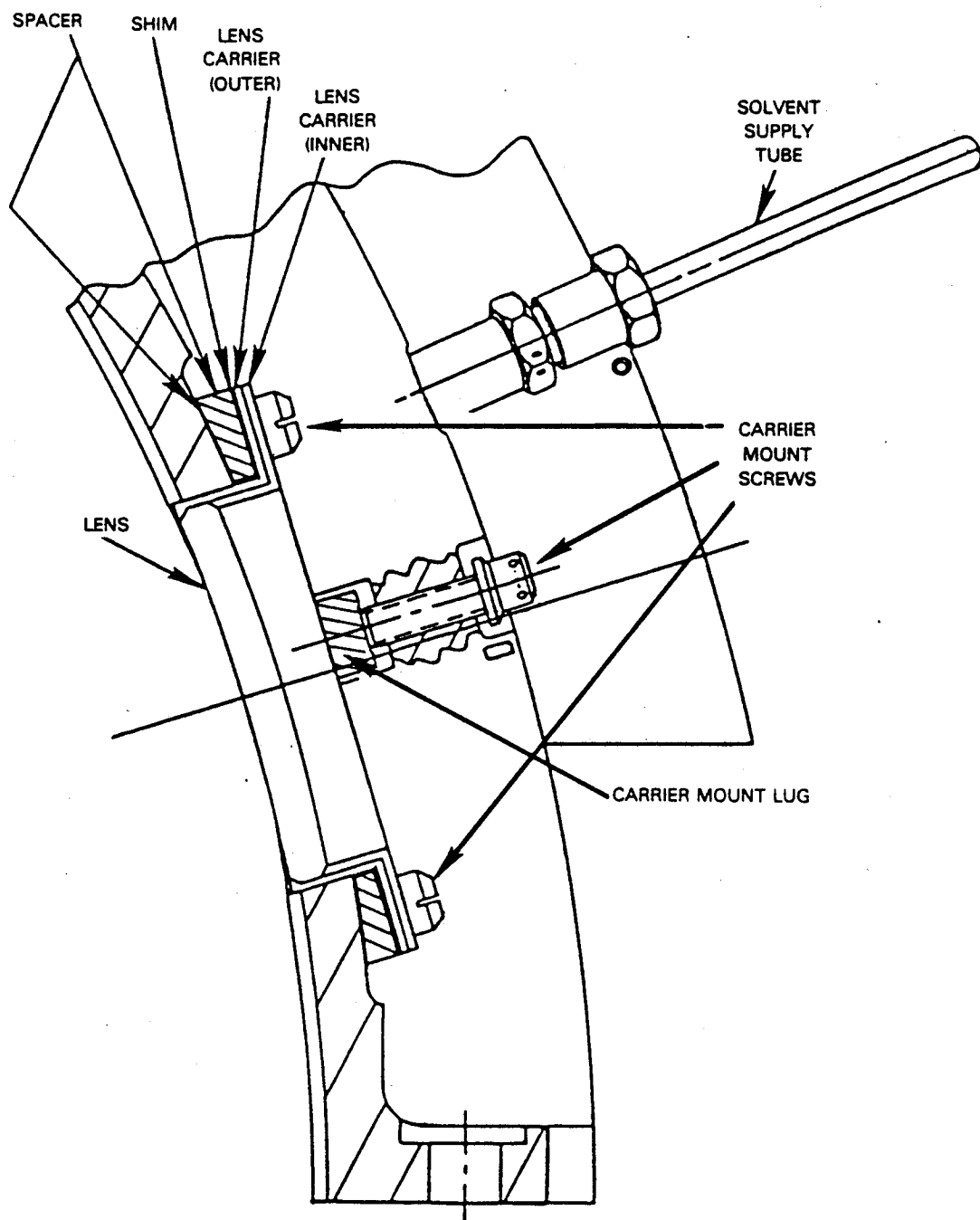
Figure 124   Details of Ninth-Stage LDV Window Installation

SPACER

LOCKING BOLT

LOCK PIN

VANE LOCKING DETAILS

CASE OPENING
FOR WINDOW

VIEW SHOWING SEGMENT
REMOVED AND VANES
LOCKED IN PLACE

REMOVABLE
RING SEGMENT
(CROSS-HATCHED)

SEGMENT-TO-BRIDGE
MOUNT BOLTS

OFFSET
BRIDGE

BRIDGE MOUNT
BOLTS
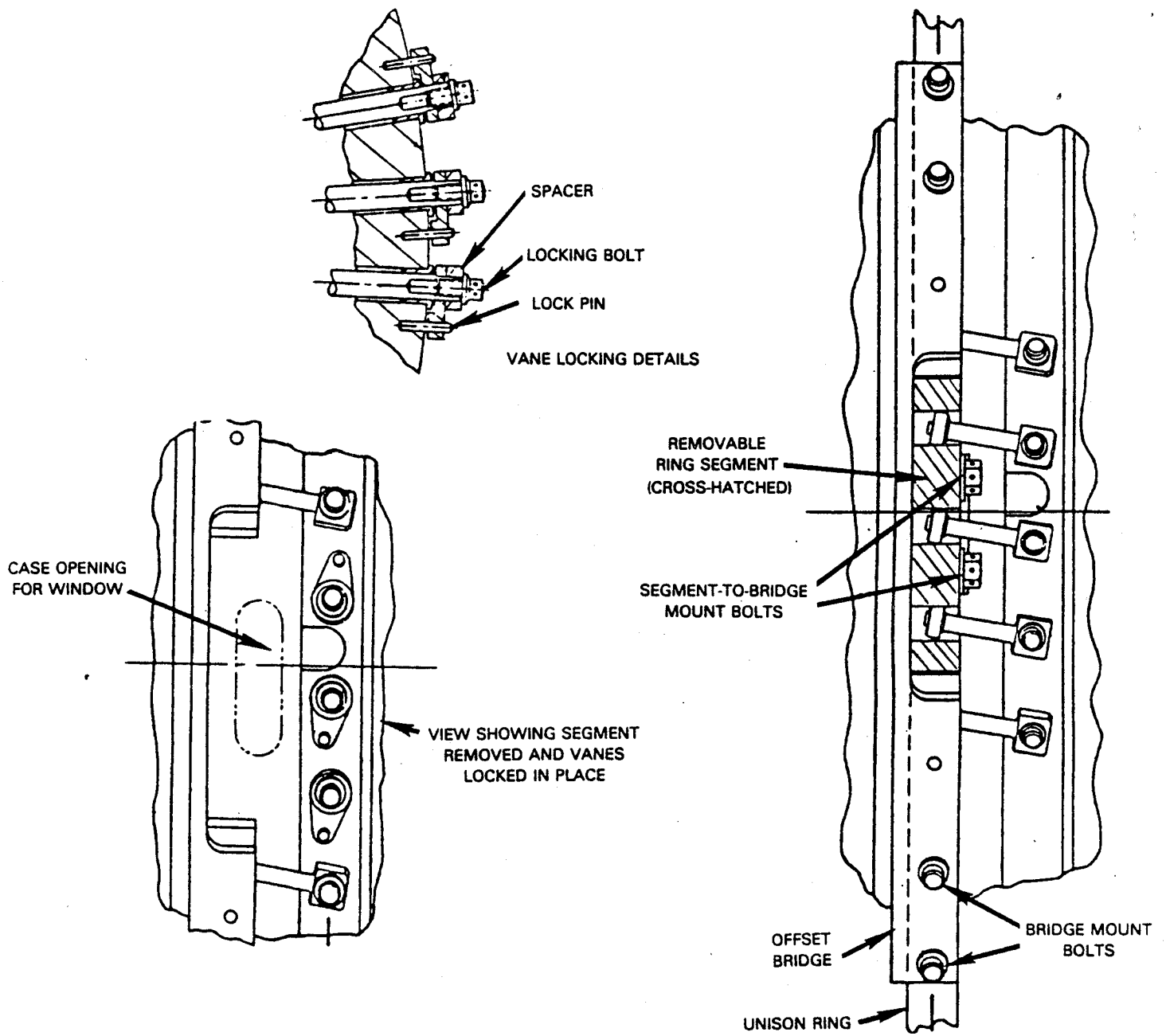
UNISON RING

Figure 125   Modified Ninth-Stage Unison Ring

170

4.1.2.2 Thirteenth-Stage LDV Window

As shown in Figure 119, the 13th-stage LDV window is located between the trailing edge of stator 13 and the leading edge of rotor 14. Here, again, the rotor blade tips extend nearly halfway across the viewing area, and circumferential window width is set by the same traverse requirements established for the sixth- and ninth-stage windows.

A detailed view of the window assembly is shown in Figure 126, and details of the window installation are shown in Figure 127. This installation is similar to that for the ninth-stage window except that the case in this location is sufficiently thick to permit machining a flat surface for the lens carrier directly on the case structure. This configuration eliminates the need for a special spacer.

Optical blockage conditions for the 13th-stage window are similar to those for the ninth-stage window. Therefore, a similar unison ring design modification has been employed and is shown in Figure 128.
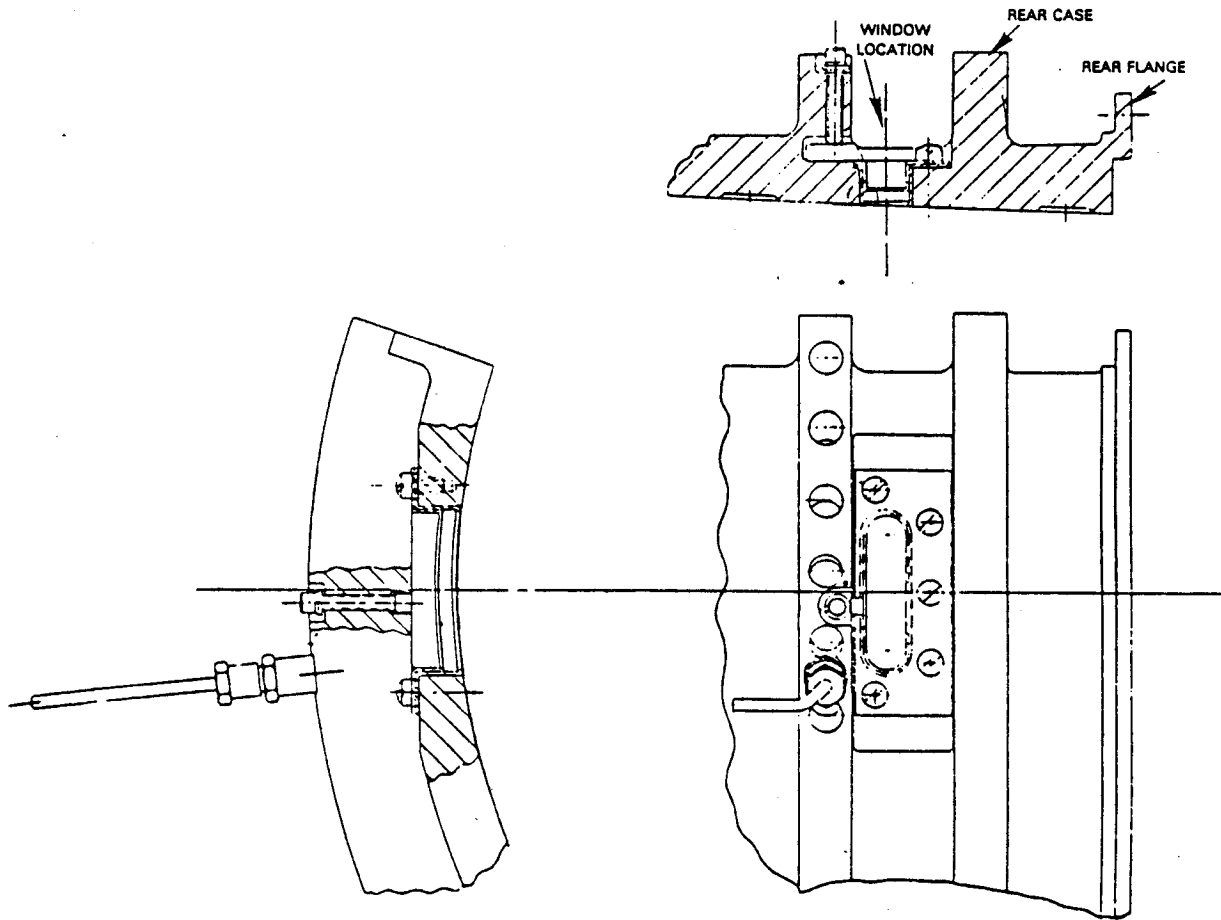
Figure 126   Thirteenth-Stage LDV Window Assembly
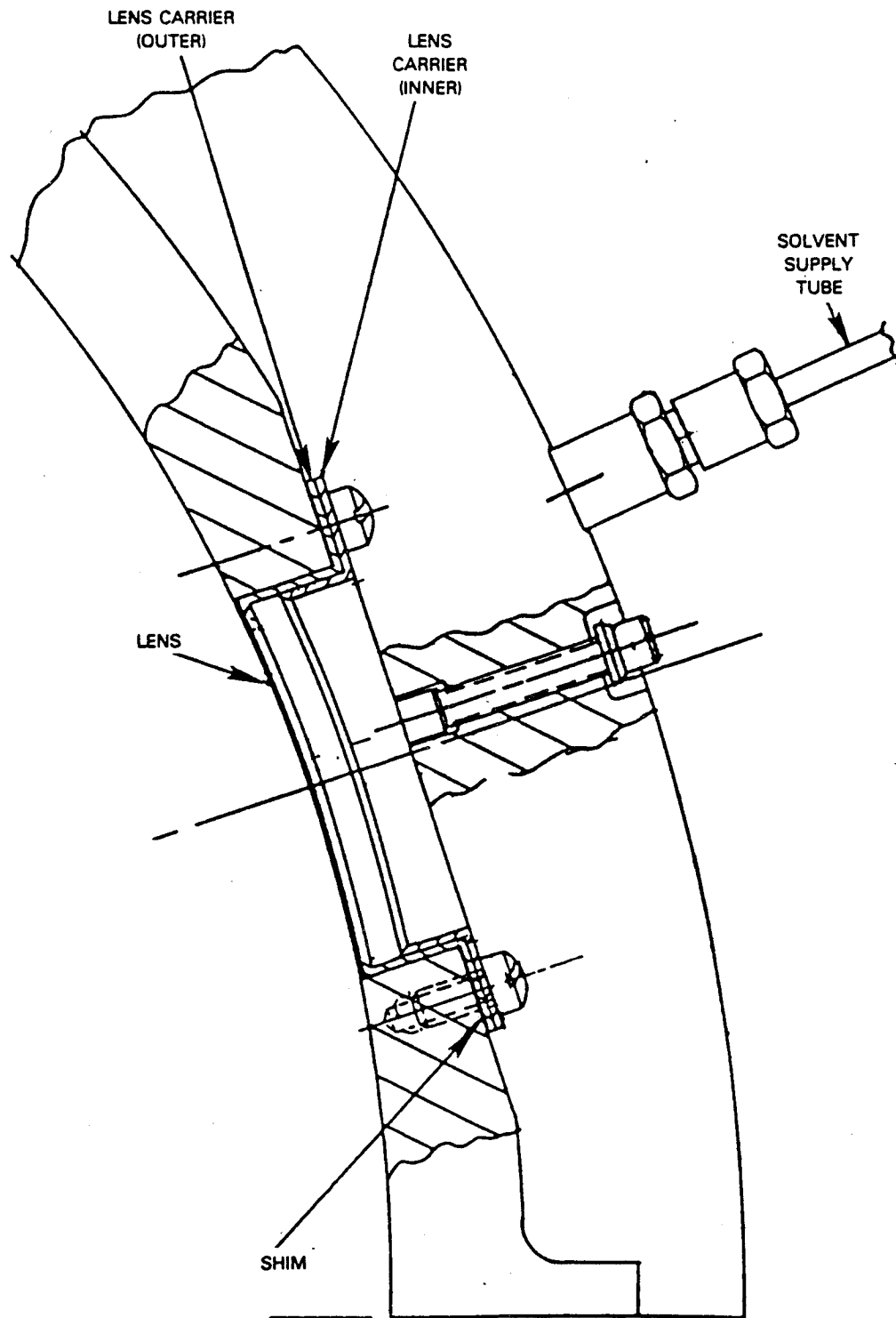
Figure 127   Details of Thirteenth-Stage LDV Window Installation

SPACER

LOCKING BOLT

LOCK PIN

REMOVABLE RING
SEGMENT
(CROSS-HATCHED)

SEGMENT-TO-BRIDGE
MOUNT BOLTS

CASE OPENING
(FOR WINDOW)

VIEW SHOWING SEGMENT
REMOVED AND VANES
LOCKED IN PLACE

OFFSET
BRIDGE
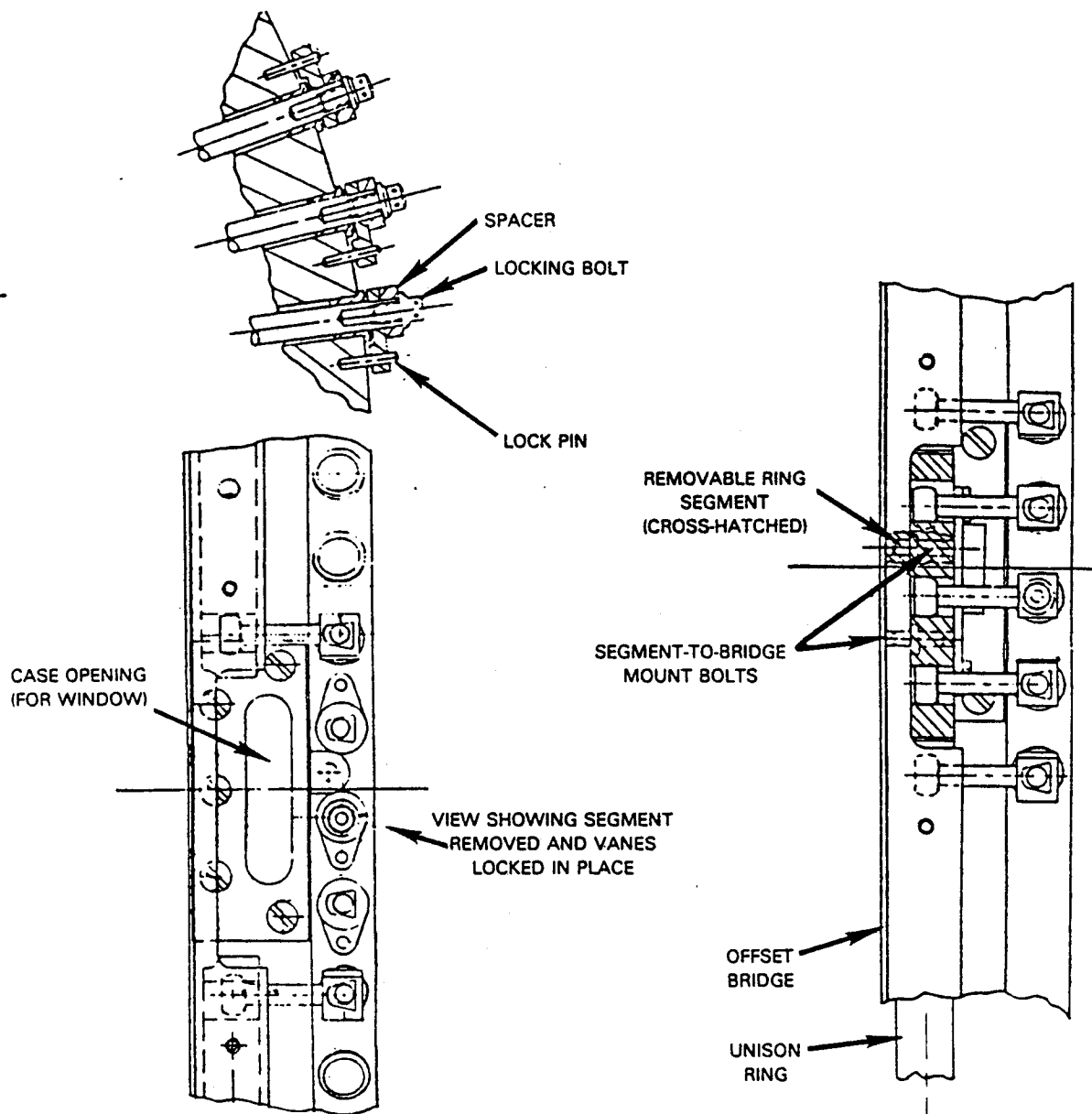
UNISON
RING

Figure 128   Modified Thirteenth-Stage Unison Ring

4.1.3 LDV Rotor Speed Sensing Device

Accurate rotor speed sensing is necessary for calibrating the LDV optical system in order to provide accurate location definition of the seeding particles in the flowpath during LDV testing. To provide this speed sensing, a pin is attached to the forward seal on the front of the sixth-stage rotor as shown in Figure 129. A magnetic speed sensor is mounted on a bracket supported from the compressor intermediate case structure at a given circumferential location. This magnetic device senses the passing frequency of the pin in the system as a function of rotor speed and provides precise rotor angular position data.

The selection of the sixth-stage rotor for this system was based, in part, on the desire to minimize rotor shaft angular distortion effects caused by torque loads. The location also provides an accessible assembly location and a cool environment necessary for the electrical wiring to the sensor unit.
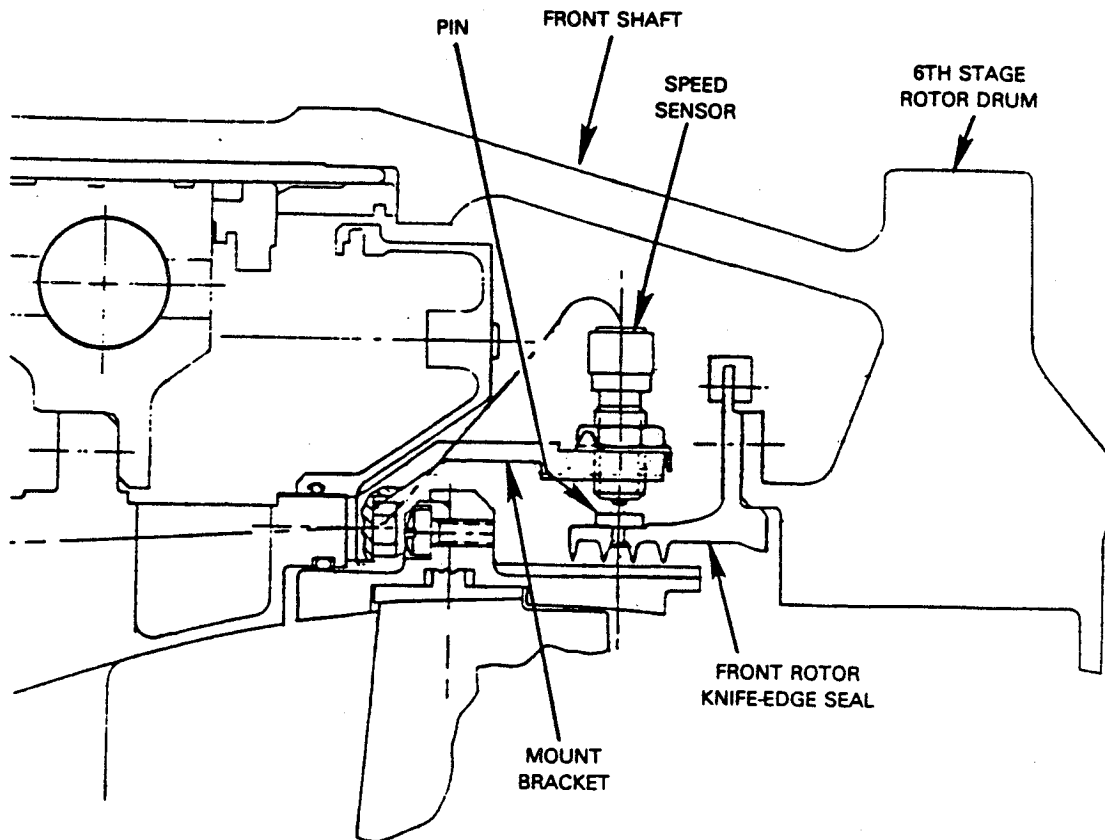
Figure 129   Rotor Speed Sensing Device for LDV Testing

4.1.4 Updated Instrumentation Requirements

To accommodate the requirements of the planned incipient stall detection test, additional high-response instrumentation was added to the test rig. This instrumentation comprises high-response static and total pressure Kulites for sensing pressure pulses and hot film elements for sensing discrete flow field velocity changes. Location of this instrumentation is based primarily on previous testing which indicated that incipient stall would most likely be initiated in the ninth stage of the compressor. Access holes were drilled in the rear case, as necessary, to accommodate this added instrumentation. Table XXXIV lists the added instrumentation, and Figure 130 shows its location in the compressor flowpath.

TABLE XXXIV

ADDED HIGH-RESPONSE INSTRUMENTATION FOR SURGE SENSING

Type	Quantity	Location
Kulite Static Pressure	4	Stator 9 Trailing Edge
Kulite Static Pressure	4	Stator 11 Trailing Edge
Kulite Static Pressure	4	Stator 13 Trailing Edge
Kulite Total Pressure	3	Stator 9 Trailing Edge, 85% Span
Hot Film	3	Stator 9 Trailing Edge, 85% Span
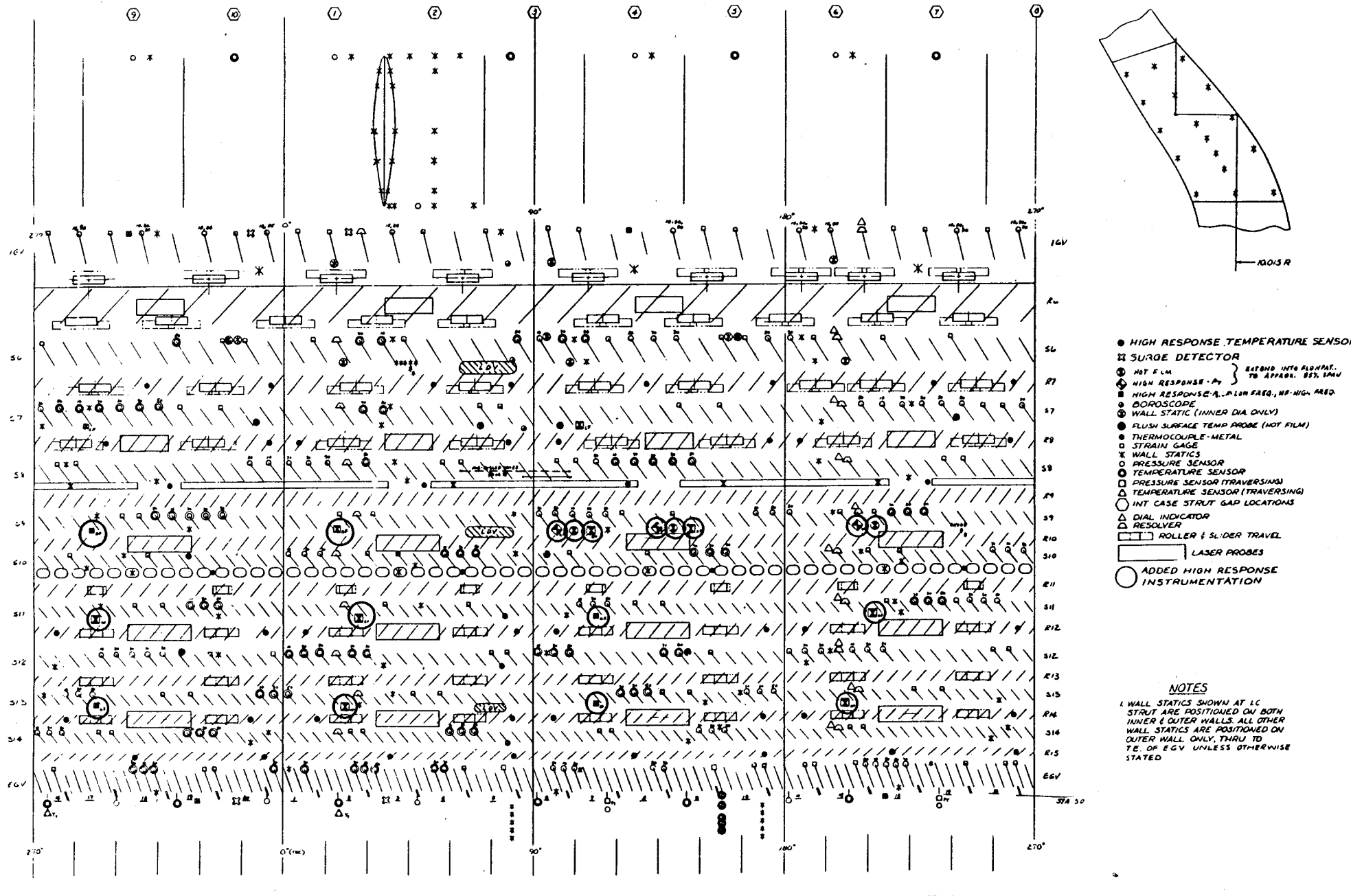
Figure 130   Road Map Identifying Location of Added High-Response Instrumentation

ACRONYMS (Organizations)

EPA	Environmental Protection Agency
FAA	Federal Aviation Administration
MERL	Materials Engineering and Research Laboratory (Pratt & Whitney)
NASA	National Aeronautics and Space Administration
P&W	Pratt & Whitney
VDI	Verein Deutscher Ingenieure (Association of [West] German Engineers)

SYMBOLS

A	Area
AA	Arithmetic average
ACC	Active clearance control
ADP	Aerodynamic design point
AMAC	Advanced Multistage Axial Compressor (program)
AR	Aspect ratio
b	Chord
Bx	Axial chord, cm (in)
CDA	Controlled diffusion airfoil
CMD	Constant mean diameter, cm (in)
Cx	Axial velocity, ft/sec (m/sec)
Cx/U	Axial velocity-to-wheel speed ratio
D	Diffusion factor for rotor:

$$= 1 - \frac{V'_2}{V'_1} + \frac{r_2 V\theta_2 - r_1 V\theta_1}{(r_1 + r_2)\, \sigma V'_1}$$

Diffusion factor for stator:

$$= 1 - \frac{V_2}{V_1} + \frac{r_1 V\theta_1 - r_2 V\partial_2}{(r_1 + r_2)\, \sigma V_1}$$

DDR	Detailed design report
D Factor	Diffusion factor
Dia	Diameter, cm (in)
DN	Bearing bore diameter x maximum rotor speed, cm-rpm (in-rpm)
DOC	Direct operating cost
EB	Electron beam
EGV	Exit guide vane

FAR	Federal Aviation Regulation
FPS	Flight propulsion system
HPC	High-pressure compressor
IC/LS	Integrated core/low spool (engine)
ID	Inside diameter, cm (in)
IGV	Inlet guide vane(s)
i_m	Incidence angle between inlet air direction and line tangent to blade mean camber line at leading edge, degrees
INCO	Inconel
LCF	Low cycle fatigue
LDV	Laser doppler velocimetry
LE	Leading edge
LPC	Low-pressure compressor
M	Mach number
MCA	Multiple circular arc (airfoil series)
Mn	Mach number
N	Rotor speed, rpm
NASTRAN	NASA STRuctural ANalysis (computer program)
Ncorr	Corrected rotational speed (= $N/\sqrt{\theta}$), rpm
OD	Outside diameter, cm (in)
P	Static pressure (absolute)
P/A	Stress; load/area, MPa (lb/in^2, psi)
PDR	Preliminary design review
Po	Total or stagnation pressure (absolute)
PR	Pressure ratio
PT, P_T	Total pressure, MPa (psi)
PWA	Prefix of P&W Specification number
ROI	Return on investment
RPM, rpm	Rotational speed
R7	Rotor seven (typical)
S7	Stator seven (typical)
T	Temperature
t/b	Maximum thickness-to-chord ratio
TE	Trailing edge
TO	Takeoff
TOBI	Tangential on-board injection
TT, T_T	Total temperature, °C (°F)

U	Rotor tangential speed
V	Air velocity
W	Weight flow
$W\sqrt{\theta}/\delta$	Corrected airflow, kg/sec (lb/sec)
400	Airfoil series designation
α_2	Inlet air angle, degrees
Δ	Change
$\Delta P/(P_o-P_s)$	Static pressure rise/compressible velocity head
δ	Pressure correction (in. Hg/29.92)
Θ	Flow turning angle, degrees
θ	Temperature correction (°R/519)
ρ	Density, g/ml (lb/ft^3)
τ/b	Gap-to-chord ratio
ω	Frequency, cycles/second
$\dot{\tau}$	Blade gap
β	Absolute air angle = COT^{-1} $(V_m/V\theta)$
β'	Relative air angle = COT^{-1} $(V_m)/(V'\theta)$
$\Delta\beta$	Turning - leading to trailing edge
β^*	Metal angle: angle between tangent to mean camber line and meridional direction
δ^o	Deviation angle - exit air angle minus metal angle at trailing edge
δ	Total pressure/standard day total pressure
ϵ	Angle between tangent to streamline projected on meridional plane and axial direction
θ	Total temperature/standard day total temperature
η	Efficiency
σ	Solidity = b/τ

$\bar{\omega}$ Loss coefficient for rotor:

$$= P'_{01} \frac{(T'_{02}/T'_{01})^{\gamma/\gamma-1} - P'_{02}}{1/2\, P_1\, V_1^2}$$

Loss coefficient for stator:

$$= \frac{P_{01} - P_{02}}{1/2\, P_1\, V_1^2}$$

γ Ratio of specific heats

SUBSCRIPTS   (For simplicity, subscripts may be written "on the line" of type, especially in text.)

ad	Adiabatic
CORR	Corrected to standard day
in	Inlet
LE	Leading edge
M,m	Meridional (velocity), Mean camber line (angle)
o	Total (pressure)
P	Profile (loss); polytropic (efficiency)
s	Static
T	Stagnation (total)
TE	Trailing edge
0	Tangential component
0	Total condition
1	Low-pressure rotor (rotor speeds)
1	Station into rotor or stator along leading edge
2	High-pressure rotor (rotor speeds)
2	Fan inlet (pressures and temperatures)
2	Station out of rotor or stator along trailing edge
2.5	High-pressure compressor inlet instrumentation station
2.6	High-pressure compressor inlet guide vanes
3	Station out of stage
3.0	High-pressure compressor discharge instrumentation station

SUPERSCRIPTS

'	Relative to rotor
*	Designates blade metal angle

APPENDIX A

AIRFOIL AERODYNAMIC DATA

APPENDIX A.1

AIRFOIL AERODYNAMIC DATA
FOR THE BASE DESIGN

AIRFOIL AERODYNAMIC SUMMARY

Corrected Speed	=	12,135 rpm
Corrected Flow	=	35.2 kg/sec (77.5 lb/sec)
Inlet Pressure	=	100.13 kN/m^2 (2091.3 lb/ft^2)
Inlet Temperature	=	66.6°C (611.6°R)

ROTOR 6

AIRFOIL AERODYNAMIC SUMMARY

SL	V-1 M/SEC	V-2 M/SEC	VM-1 M/SEC	VM-2 M/SEC	VO-1 M/SEC	VO-2 M/SEC	U-1 M/SEC	U-2 M/SEC	V'-1 M/SEC	V'-2 M/SEC	VO'-1 M/SEC	VO'-2 M/SEC	RHOVM-1 KG/M2 SEC	RHOVM-2 KG/M2 SEC	EPSI-1 RADIAN	EPSI-2 RADIAN	PO/PO INLET
1	184.3	311.1	179.1	213.9	43.5	225.9	248.8	265.3	272.4	217.5	-205.2	-39.4	153.67	205.25	0.0779	0.1659	1.4947
2	201.1	303.6	193.5	213.1	54.9	216.3	266.9	281.1	287.0	222.7	-212.0	-64.8	167.11	210.86	0.0382	0.1308	1.5016
3	210.7	295.2	201.0	207.7	63.2	209.7	285.0	296.9	299.3	225.3	-221.8	-87.1	174.08	209.65	0.0081	0.0997	1.4942
4	218.7	283.1	205.9	196.1	73.8	204.3	321.2	328.4	321.9	232.1	-247.5	-124.2	178.08	202.81	-0.0375	0.0442	1.4861
5	221.4	274.5	206.5	183.3	80.0	204.3	357.5	360.0	345.9	240.5	-277.5	-155.6	177.36	191.84	-0.0670	-0.0029	1.4846
6	220.5	271.4	204.9	176.6	81.5	206.0	375.6	375.8	358.5	244.9	-294.2	-169.7	174.79	185.08	-0.0763	-0.0238	1.4877
7	214.1	267.2	198.5	167.7	80.3	208.0	393.7	391.5	371.0	248.6	-313.4	-183.5	167.15	175.33	-0.0829	-0.0441	1.4870

SL	B-1 DEGREE	B-2 DEGREE	B'-1 DEGREE	B'-2 DEGREE	M-1	M-2	M'-1	M'-2	INCS DEGREE	INCM DEGREE	DEV DEGREE	TURN DEGREE	D FAC	OMEGA-B TOTAL	LOSS-P TOTAL	PO2/ PO1	%EFF-A TOTAL	%EFF-P TOTAL
1	13.5	46.5	48.51	10.42	0.5087	0.8385	0.7518	0.5863	0.0	0.0	0.0	38.10	0.4188	0.0689	0.0209	1.5467	94.99	95.29
2	15.7	45.3	47.26	16.86	0.5597	0.8222	0.7987	0.6031	0.0	0.0	0.0	30.41	0.4150	0.0439	0.0135	1.5147	96.22	96.45
3	17.3	45.1	47.54	22.67	0.5898	0.8006	0.8378	0.6110	0.0	0.0	0.0	24.87	0.4197	0.0400	0.0123	1.4927	96.16	96.37
4	19.7	46.1	50.15	32.27	0.6160	0.7667	0.9066	0.6284	0.0	0.0	0.0	17.88	0.4319	0.0489	0.0148	1.4780	94.61	94.91
5	21.2	48.1	53.40	40.31	0.6239	0.7380	0.9745	0.6465	0.0	0.0	0.0	13.08	0.4470	0.0766	0.0224	1.4802	90.99	91.48
6	21.7	49.4	55.21	43.87	0.6199	0.7249	1.0078	0.6543	0.0	0.0	0.0	11.34	0.4569	0.0917	0.0261	1.4934	89.16	89.76
7	22.1	51.1	57.73	47.59	0.5988	0.7076	1.0374	0.6583	0.0	0.0	0.0	10.14	0.4710	0.1043	0.0287	1.5227	87.93	88.62

SL	V-1 FT/SEC	V-2 FT/SEC	VM-1 FT/SEC	VM-2 FT/SEC	VO-1 FT/SEC	VO-2 FT/SEC	U-1 FT/SEC	U-2 FT/SEC	V'-1 FT/SEC	V'-2 FT/SEC	VO'-1 FT/SEC	VO'-2 FT/SEC	RHOVM-1 LBM/FT2SEC	RHOVM-2 LBM/FT2SEC	EPSI-1 DEGREE	EPSI-2 DEGREE	PCT TE SPAN
1	604.6	1020.8	587.5	701.9	142.8	741.2	816.2	870.6	893.7	713.7	-673.4	-129.4	31.47	42.04	4.464	9.506	0.1000
2	659.9	996.1	634.8	699.1	180.1	709.6	875.6	922.3	941.7	730.7	-695.5	-212.7	34.22	43.19	2.190	7.496	0.2000
3	691.4	968.6	659.6	681.5	207.4	688.2	935.1	974.1	982.1	739.1	-727.7	-285.9	35.65	42.94	0.462	5.712	0.3000
4	717.6	928.9	675.5	643.3	242.1	670.2	1054.0	1077.6	1056.2	761.4	-811.9	-407.4	36.47	41.54	-2.146	2.533	0.5000
5	726.5	900.8	677.4	601.6	262.5	670.4	1172.9	1181.1	1134.8	789.1	-910.4	-510.7	36.32	39.29	-3.840	-0.167	0.7000
6	723.6	890.3	672.4	579.4	267.3	676.0	1232.4	1232.9	1176.2	803.6	-965.1	-556.8	35.80	37.91	-4.369	-1.364	0.8000
7	702.6	876.8	651.3	550.3	263.6	682.6	1291.8	1284.6	1217.1	815.6	-1028.2	-602.0	34.23	35.91	-4.750	-2.526	0.9000

WC1/A1 LBM/SEC SQFT	WC1/A1 KG/SEC SQM	TO/TO INLET	PO/PO INLET	EFF-AD INLET %	EFF-P INLET %		T02/T01	P02/P01	EFF-AD ROTOR %	EFF-P ROTOR %
37.88	184.84	1.1336	1.4894	89.83	90.38		1.1332	1.5044	92.53	92.95

STATOR 6

AIRFOIL AERODYNAMIC SUMMARY

SL	V-1 M/SEC	V-2 M/SEC	VM-1 M/SEC	VM-2 M/SEC	VO-1 M/SEC	VO-2 M/SEC	RHOVM-1 KG/M2 SEC	RHOVM-2 KG/M2 SEC	PO/PO INLET	TO/TO INLET	%EFF-A TOT-INLET	%EFF-P TOT-INLET	EPSI-1 RADIAN	EPSI-2 RADIAN
1	317.0	234.3	227.0	215.2	221.3	92.7	214.87	233.08	1.4555	1.1509	74.88	76.17	0.1923	0.2017
2	311.0	237.5	226.9	219.1	212.7	91.7	220.78	242.67	1.4789	1.1344	87.70	88.37	0.1620	0.1730
3	303.4	234.1	221.8	214.3	207.1	94.3	219.79	240.16	1.4772	1.1240	94.80	95.08	0.1335	0.1444
4	291.9	228.1	209.9	205.8	202.9	98.4	213.13	233.68	1.4744	1.1169	99.97	99.97	0.0803	0.0886
5	283.8	222.7	197.2	199.1	204.0	99.8	202.56	226.21	1.4711	1.1245	93.33	93.69	0.0285	0.0350
6	281.0	221.0	190.9	196.8	206.2	100.6	196.31	222.50	1.4708	1.1346	86.29	87.03	0.0016	0.0094
7	277.6	218.0	183.1	189.9	208.7	107.0	187.68	212.28	1.4637	1.1500	76.33	77.58	-0.0263	-0.0144

SL	B-1 DEGREE	B-2 DEGREE	M-1	M-2	INCS DEGREE	INCM DEGREE	DEV DEGREE	TURN DEGREE	D-FAC	OMEGA-B TOTAL	LOSS-P TOTAL	PO2/ PO1	PO/PO STAGE	TO/TO STAGE	%EFF-A TOT-STG	%EFF-P TOT-STG
1	44.2	23.2	0.8566	0.6134	0.0	0.0	0.0	20.91	0.3951	0.0686	0.0222	0.9738	1.5067	1.1392	88.88	89.52
2	43.1	22.7	0.8450	0.6272	0.0	0.0	0.0	20.38	0.3695	0.0407	0.0135	0.9848	1.4920	1.1304	92.48	92.89
3	43.0	23.7	0.8258	0.6204	0.0	0.0	0.0	19.24	0.3599	0.0316	0.0107	0.9886	1.4759	1.1256	93.25	93.62
4	44.0	25.5	0.7935	0.6055	0.0	0.0	0.0	18.45	0.3530	0.0235	0.0081	0.9920	1.4664	1.1243	92.61	93.00
5	46.0	26.6	0.7657	0.5879	0.0	0.0	0.0	19.34	0.3611	0.0283	0.0101	0.9909	1.4665	1.1296	88.85	89.44
6	47.2	27.1	0.7536	0.5806	0.0	0.0	0.0	20.12	0.3664	0.0359	0.0131	0.9887	1.4760	1.1354	86.55	87.28
7	48.7	29.4	0.7382	0.5680	0.0	0.0	0.0	19.36	0.3680	0.0518	0.0188	0.9843	1.4984	1.1444	84.43	85.30

SL	V-1 FT/SEC	V-2 FT/SEC	VM-1 FT/SEC	VM-2 FT/SEC	VO-1 FT/SEC	VO-2 FT/SEC	RHOVM-1 LBM/FT2SEC	RHOVM-2 LBM/FT2SEC	PCT TE SPAN	TO/TO INLET	%EFF-A TOT-INLET	%EFF-P TOT-INLET	EPSI-1 DEGREE	EPSI-2 DEGREE
1	1040.0	768.8	744.7	706.2	726.0	304.0	44.01	47.74	0.1000	1.1509	74.88	76.17	11.016	11.558
2	1020.4	779.3	744.4	718.9	698.0	301.0	45.22	49.70	0.2000	1.1344	87.70	88.37	9.282	9.911
3	995.5	768.0	727.6	703.0	679.4	309.3	45.01	49.19	0.3000	1.1240	94.80	95.08	7.651	8.274
4	957.9	748.5	688.7	675.2	665.7	322.9	43.65	47.86	0.5000	1.1169	99.97	99.97	4.598	5.077
5	931.0	730.5	647.1	653.1	669.4	327.4	41.49	46.33	0.7000	1.1245	93.33	93.69	1.635	2.006
6	921.9	725.2	626.3	645.7	676.5	330.2	40.21	45.57	0.8000	1.1346	86.29	87.03	0.094	0.538
7	910.9	715.2	600.8	623.2	684.8	350.9	38.44	43.48	0.9000	1.1500	76.33	77.58	-1.506	-0.823

WCORR INLET RPM	WCORR INLET LBM/SEC	WCORR INLET KG/SEC	TO/TO INLET	PO/PO INLET	EFF-AD INLET %	EFF-P INLET %		TO/TO STAGE	PO2/PO1	PO/PO STAGE	EFF-AD STAGE %	EFF-P STAGE %
12136.50	77.52	35.16	1.1336	1.4683	86.43	87.15		1.1332	0.9858	1.4831	89.11	89.71

ROTOR 7

AIRFOIL AERODYNAMIC SUMMARY

SL	V-1 M/SEC	V-2 M/SEC	VM-1 M/SEC	VM-2 M/SEC	VO-1 M/SEC	VO-2 M/SEC	U-1 M/SEC	U-2 M/SEC	V'-1 M/SEC	V'-2 M/SEC	VO'-1 M/SEC	VO'-2 M/SEC	RHOVM-1 KG/M2 SEC	RHOVM-2 KG/M2 SEC	EPSI-1 RADIAN	EPSI-2 RADIAN	PO/PO INLET
1	244.0	323.3	226.3	212.6	91.1	243.6	285.7	295.9	298.4	219.0	-194.6	-52.3	241.16	259.64	0.1960	0.1812	2.1003
2	249.1	324.1	232.1	217.7	90.4	240.1	298.6	307.6	311.8	227.9	-208.2	-67.5	252.02	275.72	0.1658	0.1507	2.1642
3	246.9	314.5	228.6	209.7	93.2	234.4	311.5	319.3	316.1	226.2	-218.3	-84.9	250.72	271.96	0.1342	0.1202	2.1558
4	241.7	299.4	221.1	196.3	97.8	226.1	337.4	342.7	326.0	228.3	-239.6	-116.5	245.40	261.60	0.0718	0.0619	2.1371
5	235.5	290.0	213.4	187.1	99.6	221.6	363.2	366.0	339.2	236.4	-263.6	-144.5	237.59	250.92	0.0129	0.0085	2.1251
6	232.5	285.7	209.6	181.4	100.6	220.8	376.1	377.7	346.2	239.9	-275.5	-156.9	232.74	242.04	-0.0142	-0.0156	2.1134
7	227.3	271.7	200.4	156.4	107.2	222.3	389.1	389.4	345.9	228.9	-281.9	-167.1	220.83	206.13	-0.0355	-0.0319	2.0534

SL	B-1 DEGREE	B-2 DEGREE	B'-1 DEGREE	B'-2 DEGREE	M-1	M-2	M'-1	M'-2	INCS DEGREE	INCM DEGREE	DEV DEGREE	TURN DEGREE	D FAC	OMEGA-B TOTAL	LOSS-P TOTAL	PO2/ PO1	%EFF-A TOTAL	%EFF-P TOTAL
1	21.9	48.7	40.61	13.75	0.6405	0.8237	0.7836	0.5578	0.0	0.0	0.0	26.85	0.4475	0.0709	0.0237	1.4410	93.64	93.97
2	21.2	47.6	41.76	17.11	0.6602	0.8315	0.8264	0.5847	0.0	0.0	0.0	24.65	0.4436	0.0507	0.0172	1.4637	95.19	95.45
3	22.1	48.0	43.53	21.89	0.6571	0.8087	0.8414	0.5817	0.0	0.0	0.0	21.64	0.4515	0.0385	0.0131	1.4595	96.18	96.38
4	23.7	48.9	47.15	30.55	0.6445	0.7686	0.8692	0.5860	0.0	0.0	0.0	16.60	0.4571	0.0295	0.0099	1.4499	96.83	96.99
5	25.0	49.7	50.94	37.60	0.6244	0.7382	0.8993	0.6018	0.0	0.0	0.0	13.34	0.4549	0.0380	0.0125	1.4448	95.67	95.89
6	25.6	50.6	52.71	40.84	0.6129	0.7223	0.9125	0.6063	0.0	0.0	0.0	11.87	0.4550	0.0479	0.0154	1.4376	94.42	94.71
7	28.1	54.9	54.60	46.92	0.5938	0.6800	0.9037	0.5727	0.0	0.0	0.0	7.68	0.4772	0.0672	0.0201	1.4053	92.04	92.42

SL	V-1 FT/SEC	V-2 FT/SEC	VM-1 FT/SEC	VM-2 FT/SEC	VO-1 FT/SEC	VO-2 FT/SEC	U-1 FT/SEC	U-2 FT/SEC	V'-1 FT/SEC	V'-2 FT/SEC	VO'-1 FT/SEC	VO'-2 FT/SEC	RHOVM-1 LBM/FT2SEC	RHOVM-2 LBM/FT2SEC	EPSI-1 DEGREE	EPSI-2 DEGREE	PCT TE SPAN
1	800.4	1060.9	742.5	697.5	299.0	799.3	937.4	971.0	979.2	718.4	-638.4	-171.7	49.39	53.18	11.232	10.382	0.1000
2	817.2	1063.4	761.5	714.2	296.7	787.9	979.7	1009.3	1022.9	747.7	-683.0	-221.5	51.62	56.47	9.499	8.635	0.2000
3	809.9	1032.0	750.0	688.1	305.7	769.1	1022.1	1047.6	1037.2	742.3	-716.4	-278.5	51.35	55.70	7.688	6.885	0.3000
4	793.1	982.5	725.3	644.0	320.8	741.9	1106.9	1124.3	1069.6	749.0	-786.1	-382.3	50.26	53.58	4.112	3.549	0.5000
5	772.7	951.5	700.3	614.0	326.7	726.9	1191.7	1200.9	1113.0	775.7	-865.0	-474.0	48.66	51.39	0.739	0.489	0.7000
6	762.9	937.5	687.8	595.2	330.1	724.3	1234.1	1239.2	1135.9	787.0	-904.0	-514.9	47.67	49.57	-0.812	-0.892	0.8000
7	745.7	891.6	657.6	513.0	351.6	729.2	1276.5	1277.6	1134.8	750.9	-924.9	-548.3	45.23	42.22	-2.034	-1.828	0.9000

WC1/A1 LBM/SEC SQFT	WC1/A1 KG/SEC SQM	TO/TO INLET	PO/PO INLET	EFF-AD INLET %	EFF-P INLET %		T02/T01	P02/P01	EFF-AD ROTOR %	EFF-P ROTOR %
27.19	132.67	1.2636	2.1162	89.97	90.96		1.1146	1.4412	95.10	95.34

ROTOR 8

AIRFOIL AERODYNAMIC SUMMARY

SL	V-1 M/SEC	V-2 M/SEC	VM-1 M/SEC	VM-2 M/SEC	VO-1 M/SEC	VO-2 M/SEC	U-1 M/SEC	U-2 M/SEC	V'-1 M/SEC	V'-2 M/SEC	VO'-1 M/SEC	VO'-2 M/SEC	RHOVM-1 KG/M2 SEC	RHOVM-2 KG/M2 SEC	EPSI-1 RADIAN	EPSI-2 RADIAN	PO/PO INLET
1	234.4	319.6	209.0	199.6	106.1	249.6	309.2	314.9	291.4	210.0	-203.1	-65.3	292.43	313.74	0.1427	0.1114	2.8710
2	248.1	325.7	223.3	212.4	108.3	246.9	319.0	324.0	307.0	226.0	-210.7	-77.1	320.16	345.68	0.1181	0.0944	2.9793
3	244.5	317.1	218.3	204.9	110.1	242.0	328.9	333.1	309.1	224.2	-218.8	-91.1	317.53	340.82	0.0948	0.0762	2.9703
4	236.2	302.8	207.6	190.5	112.6	235.4	348.6	351.3	314.3	223.0	-236.0	-116.0	306.01	324.39	0.0496	0.0383	2.9442
5	228.8	293.6	198.8	179.2	113.3	232.6	368.3	369.5	323.4	225.5	-255.0	-136.9	292.25	305.78	0.0081	0.0010	2.9269
6	223.7	289.7	193.2	172.0	112.7	233.1	378.1	378.6	328.3	225.3	-265.4	-145.5	281.92	291.73	-0.0111	-0.0171	2.9154
7	204.9	278.2	171.6	146.7	112.0	236.4	388.0	387.7	325.0	210.8	-276.0	-151.4	246.94	245.47	-0.0291	-0.0343	2.8551

SL	B-1 DEGREE	B-2 DEGREE	B'-1 DEGREE	B'-2 DEGREE	M-1	M-2	M'-1	M'-2	INCS DEGREE	INCM DEGREE	DEV DEGREE	TURN DEGREE	D FAC	OMEGA-B TOTAL	LOSS-P TOTAL	PO2/ PO1	%EFF-A TOTAL	%EFF-P TOTAL
1	26.9	51.3	44.22	18.07	0.5791	0.7700	0.7201	0.5059	0.0	0.0	0.0	26.15	0.4549	0.0618	0.0203	1.3907	94.57	94.82
2	25.9	49.2	43.33	19.89	0.6194	0.7918	0.7663	0.5494	0.0	0.0	0.0	23.44	0.4307	0.0475	0.0162	1.3959	95.41	95.63
3	26.7	49.7	45.02	23.91	0.6132	0.7737	0.7752	0.5471	0.0	0.0	0.0	21.11	0.4388	0.0372	0.0129	1.3940	96.28	96.46
4	28.4	51.0	48.61	31.27	0.5934	0.7383	0.7898	0.5438	0.0	0.0	0.0	17.34	0.4542	0.0293	0.0103	1.3900	96.93	97.08
5	29.6	52.4	52.04	37.36	0.5711	0.7096	0.8072	0.5450	0.0	0.0	0.0	14.68	0.4693	0.0357	0.0127	1.3909	96.15	96.34
6	30.3	53.6	53.94	40.22	0.5548	0.6949	0.8141	0.5404	0.0	0.0	0.0	13.72	0.4838	0.0434	0.0154	1.3973	95.37	95.59
7	33.1	58.2	58.13	45.91	0.5033	0.6601	0.7982	0.5002	0.0	0.0	0.0	12.22	0.5327	0.0574	0.0192	1.4120	94.32	94.59

SL	V-1 FT/SEC	V-2 FT/SEC	VM-1 FT/SEC	VM-2 FT/SEC	VO-1 FT/SEC	VO-2 FT/SEC	U-1 FT/SEC	U-2 FT/SEC	V'-1 FT/SEC	V'-2 FT/SEC	VO'-1 FT/SEC	VO'-2 FT/SEC	RHOVM-1 LBM/FT2SEC	RHOVM-2 LBM/FT2SEC	EPSI-1 DEGREE	EPSI-2 DEGREE	PCT TE SPAN
1	769.0	1048.5	685.8	654.8	348.0	818.9	1014.4	1033.1	956.2	688.9	-666.4	-214.1	59.89	64.26	8.177	6.384	0.1000
2	814.1	1068.6	732.5	697.0	355.3	810.0	1046.7	1063.0	1007.2	741.5	-691.4	-252.2	65.57	70.80	6.765	5.411	0.2000
3	802.2	1040.3	716.3	672.1	361.2	794.0	1079.0	1092.9	1014.1	735.6	-717.8	-298.9	65.03	69.80	5.432	4.367	0.3000
4	774.8	993.4	681.1	625.0	369.3	772.2	1143.7	1152.6	1031.3	731.7	-774.3	-380.4	62.67	66.44	2.844	2.195	0.5000
5	750.7	963.4	652.3	587.9	371.6	763.2	1208.3	1212.4	1060.9	739.9	-836.7	-449.2	59.86	62.63	0.462	0.060	0.7000
6	734.0	950.6	633.9	564.4	369.9	764.9	1240.6	1242.3	1077.1	739.2	-870.7	-477.4	57.74	59.75	-0.635	-0.982	0.8000
7	672.4	912.8	563.1	481.4	367.5	775.5	1273.0	1272.2	1066.4	691.7	-905.5	-496.7	50.57	50.28	-1.665	-1.967	0.9000

WC1/A1 LBM/SEC SQFT	WC1/A1 KG/SEC SQM	TO/TO INLET	PO/PO INLET	EFF-AD INLET %	EFF-P INLET %		T02/T01	P02/P01	EFF-AD ROTOR %	EFF-P ROTOR %
20.15	98.34	1.3933	2.9173	90.04	91.40		1.1026	1.3948	95.61	95.82

STATOR 8

AIRFOIL AERODYNAMIC SUMMARY

SL	V-1 M/SEC	V-2 M/SEC	VM-1 M/SEC	VM-2 M/SEC	VO-1 M/SEC	VO-2 M/SEC	RHOVM-1 KG/M2 SEC	RHOVM-2 KG/M2 SEC	PO/PO INLET	TO/TO INLET	%EFF-A TOT-INLET	%EFF-P TOT-INLET	EPSI-1 RADIAN	EPSI-2 RADIAN
1	322.3	209.9	206.2	181.4	247.7	105.7	322.20	327.44	2.8039	1.4169	81.28	83.72	0.1105	0.1068
2	330.2	233.5	220.9	206.4	245.3	109.2	356.15	382.96	2.9336	1.4006	88.93	90.44	0.0957	0.0898
3	322.9	230.8	215.0	202.6	240.8	110.7	353.72	381.81	2.9386	1.3831	88.93	90.44	0.0957	0.0898
3	322.9	230.8	215.0	202.6	240.8	110.7	353.72	381.81	2.9386	1.3831	93.20	94.14	0.0957	0.0898
4	309.4	222.0	201.7	191.5	234.7	112.3	339.47	365.63	2.9189	1.3696	95.90	96.47	0.0468	0.0400
5	300.3	215.4	190.2	183.8	232.4	112.3	321.04	348.57	2.8993	1.3825	91.98	93.07	0.0142	0.0084
6	296.4	212.4	183.2	180.3	233.1	112.3	307.45	338.44	2.8875	1.3985	87.87	89.51	-0.0023	-0.0072
7	285.2	198.9	159.4	163.6	236.5	113.2	264.28	301.51	2.8281	1.4180	81.86	84.25	-0.0208	-0.0240

SL	B-1 DEGREE	B-2 DEGREE	M-1	M-2	INCS DEGREE	INCM DEGREE	DEV DEGREE	TURN DEGREE	D-FAC	OMEGA-B TOTAL	LOSS-P TOTAL	PO2/ PO1	PO/PO STAGE	TO/TO STAGE	%EFF-A TOT-STG	%EFF-P TOT-STG
1	50.3	30.3	0.7773	0.4901	0.0	0.0	0.0	20.00	0.5304	0.0501	0.0185	0.9838	1.3672	1.1025	89.60	90.05
2	48.0	27.9	0.8038	0.5514	0.0	0.0	0.0	20.14	0.4666	0.0397	0.0150	0.9863	1.3760	1.1031	91.13	91.52
3	48.3	28.7	0.7893	0.5482	0.0	0.0	0.0	19.61	0.4572	0.0340	0.0128	0.9885	1.3785	1.1020	92.68	93.01
4	49.3	30.4	0.7564	0.5287	0.0	0.0	0.0	18.93	0.4527	0.0289	0.0107	0.9909	1.3775	1.1003	94.10	94.37
5	50.7	31.4	0.7276	0.5097	0.0	0.0	0.0	19.26	0.4556	0.0327	0.0121	0.9903	1.3768	1.1010	93.30	93.60
6	51.8	31.9	0.7128	0.4995	0.0	0.0	0.0	19.93	0.4604	0.0381	0.0140	0.9890	1.3800	1.1029	92.18	92.53
7	56.0	34.7	0.6784	0.4631	0.0	0.0	0.0	21.34	0.4922	0.0478	0.0171	0.9873	1.3929	1.1074	90.83	91.24

SL	V-1 FT/SEC	V-2 FT/SEC	VM-1 FT/SEC	VM-2 FT/SEC	VO-1 FT/SEC	VO-2 FT/SEC	RHOVM-1 LBM/FT2SEC	RHOVM-2 LBM/FT2SEC	PCT TE SPAN	TO/TO INLET	%EFF-A TOT-INLET	%EFF-P TOT-INLET	EPSI-1 DEGREE	EPSI-2 DEGREE
1	1057.5	688.8	676.7	595.1	812.7	346.8	65.99	67.06	0.1000	1.4169	81.28	83.72	6.333	6.117
2	1083.2	766.2	724.9	677.3	805.0	358.2	72.94	78.43	0.2000	1.4006	88.93	90.44	5.486	5.144
3	1059.3	757.3	705.4	664.6	790.2	363.1	72.44	78.20	0.3000	1.3831	93.20	94.14	4.561	4.171
4	1015.3	728.3	661.8	628.2	769.9	368.5	69.53	74.88	0.5000	1.3696	95.90	96.47	2.684	2.291
5	985.3	706.6	624.2	602.9	762.4	368.5	65.75	71.39	0.7000	1.3825	91.98	93.07	0.814	0.482
6	972.6	697.0	601.0	591.7	764.7	368.4	62.97	69.32	0.8000	1.3985	87.87	89.51	-0.129	-0.410
7	935.8	652.6	523.1	536.8	776.0	371.2	54.13	61.75	0.9000	1.4180	81.86	84.25	-1.192	-1.374

NCORR INLET RPM	WCORR INLET LBM/SEC	WCORR INLET KG/SEC	TO/TO INLET	PO/PO INLET	EFF-AD INLET %	EFF-P INLET %	TO/TO STAGE	PO2/PO1	PO/PO STAGE	EFF-AD STAGE %	EFF-P STAGE %
12136.50	.77.52	35.16	1.3933	2.8823	88.87	90.37	1.1026	0.9880	1.3781	91.99	92.35

ROTOR 9

AIRFOIL AERODYNAMIC SUMMARY

SL	V-1 M/SEC	V-2 M/SEC	VM-1 M/SEC	VM-2 M/SEC	VO-1 M/SEC	VO-2 M/SEC	U-1 M/SEC	U-2 M/SEC	V'-1 M/SEC	V'-2 M/SEC	VO'-1 M/SEC	VO'-2 M/SEC	RHOVM-1 KG/M2 SEC	RHOVM-2 KG/M2 SEC	EPSI-1 RADIAN	EPSI-2 RADIAN	PO/PO INLET
1	222.4	310.9	196.0	186.1	105.0	249.1	323.4	326.4	293.4	201.5	-218.4	-77.3	349.45	370.92	0.0876	0.0737	3.8378
2	244.0	321.7	218.5	208.0	108.6	245.4	331.0	333.6	311.8	225.9	-222.5	-88.1	399.98	428.31	0.0705	0.0597	3.9928
3	241.3	315.1	214.7	202.9	110.2	241.0	338.7	340.7	313.6	226.1	-228.5	-99.7	399.18	426.39	0.0540	0.0453	3.9887
4	232.7	302.8	204.0	190.5	112.0	235.4	354.0	355.1	316.5	225.0	-242.0	-119.7	384.18	408.04	0.0202	0.0148	3.9551
5	225.7	295.5	195.7	181.1	112.3	233.5	369.3	369.5	323.0	226.5	-257.0	-136.0	366.58	386.55	-0.0135	-0.0163	3.9306
6	222.2	292.3	191.7	175.0	112.4	234.1	376.9	376.7	326.7	225.8	-264.6	-142.6	355.54	370.09	-0.0298	-0.0315	3.9119
7	203.5	281.0	175.0	152.5	113.4	236.1	384.6	383.9	322.8	212.4	-271.2	-147.8	319.34	317.16	-0.0440	-0.0444	3.8293

SL	B-1 DEGREE	B-2 DEGREE	B'-1 DEGREE	B'-2 DEGREE	M-1	M-2	M'-1	M'-2	INCS DEGREE	INCM DEGREE	DEV DEGREE	TURN DEGREE	D FAC	OMEGA-B TOTAL	LOSS-P TOTAL	PO2/PO1	%EFF-A TOTAL	%EFF-P TOTAL
1	28.2	53.2	48.11	22.54	0.5206	0.7109	0.6870	0.4607	0.0	0.0	0.0	25.56	0.5195	0.0663	0.0252	1.3626	94.29	94.54
2	26.4	49.7	45.51	22.94	0.5777	0.7435	0.7383	0.5221	0.0	0.0	0.0	22.57	0.4617	0.0477	0.0185	1.3593	95.29	95.48
3	27.1	49.9	46.77	26.14	0.5748	0.7320	0.7468	0.5253	0.0	0.0	0.0	20.63	0.4593	0.0388	0.0150	1.3579	96.06	96.22
4	28.8	51.0	49.85	32.13	0.5558	0.7043	0.7557	0.5234	0.0	0.0	0.0	17.72	0.4645	0.0315	0.0120	1.3556	96.69	96.83
5	29.8	52.2	52.71	36.90	0.5353	0.6816	0.7664	0.5223	0.0	0.0	0.0	15.81	0.4747	0.0381	0.0142	1.3563	95.94	96.11
6	30.4	53.2	54.09	39.18	0.5236	0.6690	0.7698	0.5168	0.0	0.0	0.0	14.91	0.4854	0.0456	0.0169	1.3567	95.14	95.35
7	32.9	57.2	57.18	44.12	0.4865	0.6363	0.7531	0.4809	0.0	0.0	0.0	13.06	0.5240	0.0570	0.0199	1.3582	94.23	94.48

SL	V-1 FT/SEC	V-2 FT/SEC	VM-1 FT/SEC	VM-2 FT/SEC	VO-1 FT/SEC	VO-2 FT/SEC	U-1 FT/SEC	U-2 FT/SEC	V'-1 FT/SEC	V'-2 FT/SEC	VO'-1 FT/SEC	VO'-2 FT/SEC	RHOVM-1 LBM/FT2SEC	RHOVM-2 LBM/FT2SEC	EPSI-1 DEGREE	EPSI-2 DEGREE	PCT TE SPAN
1	729.6	1020.1	643.0	610.5	344.6	817.3	1061.1	1070.8	962.7	661.1	-716.4	-253.6	71.57	75.97	5.019	4.224	0.1000
2	800.5	1055.6	716.9	682.6	356.2	805.2	1086.2	1094.4	1023.1	741.3	-729.9	-289.2	81.92	87.72	4.039	3.418	0.2000
3	791.9	1033.8	704.6	665.9	361.4	790.8	1111.2	1118.0	1028.9	741.9	-749.8	-327.1	81.76	87.33	3.094	2.594	0.3000
4	763.6	993.5	669.3	625.1	367.6	772.2	1161.4	1165.1	1038.3	738.3	-793.9	-392.9	78.68	83.57	1.159	0.846	0.5000
5	740.4	969.6	642.2	594.2	368.5	766.2	1211.6	1212.3	1059.9	743.0	-843.2	-446.1	75.08	79.17	-0.776	-0.937	0.7000
6	728.9	958.9	628.8	574.3	368.7	768.0	1236.7	1235.8	1071.8	740.7	-868.0	-467.9	72.82	75.80	-1.709	-1.806	0.8000
7	684.2	922.1	574.3	500.3	371.9	774.5	1261.8	1259.4	1059.1	696.8	-889.9	-484.9	65.40	64.96	-2.519	-2.542	0.9000

WC1/A1 LBM/SEC SQFT	WC1/A1 KG/SEC SQM	TO/TO INLET	PO/PO INLET	EFF-AD INLET %	EFF-P INLET %
15.35	74.93	1.5235	3.9162	89.79	91.50

T02/T01	P02/P01	EFF-AD ROTOR %	EFF-P ROTOR %
1.0935	1.3587	95.45	95.64

189

STATOR 9

AIRFOIL AERODYNAMIC SUMMARY

SL	V-1 M/SEC	V-2 M/SEC	VM-1 M/SEC	VM-2 M/SEC	VO-1 M/SEC	VO-2 M/SEC	RHOVM-1 KG/M2 SEC	RHOVM-2 KG/M2 SEC	PO/PO INLET	TO/TO INLET	%EFF-A TOT-INLET	%EFF-P TOT-INLET	EPSI-1 RADIAN	EPSI-2 RADIAN
1	314.0	202.9	192.2	173.6	248.3	105.0	380.98	389.76	3.7565	1.5523	81.95	84.88	0.0784	0.0733
2	325.7	231.1	214.9	203.5	244.8	109.6	439.10	470.36	3.9370	1.5316	88.82	90.70	0.0654	0.0606
3	320.1	228.9	211.1	200.1	240.6	111.1	439.62	470.30	3.9456	1.5108	88.82	90.70	0.0521	0.0476
4	308.5	220.1	199.7	189.3	235.2	112.3	423.72	450.60	3.9197	1.4951	95.08	95.91	0.0252	0.0216
5	301.2	213.8	190.2	182.2	233.6	112.0	402.52	429.51	3.8928	1.5115	91.45	92.88	-0.0014	-0.0041
6	297.9	210.2	184.1	178.1	234.2	111.7	386.29	414.72	3.8716	1.5301	87.76	89.80	-0.0149	-0.0167
7	286.8	194.5	162.4	158.8	236.4	112.2	335.47	362.54	3.7860	1.5530	82.43	85.30	-0.0293	-0.0299

SL	B-1 DEGREE	B-2 DEGREE	M-1	M-2	INCS DEGREE	INCM DEGREE	DEV DEGREE	TURN DEGREE	D-FAC	OMEGA-B TOTAL	LOSS-P TOTAL	PO2/ PO1	PO/PO STAGE	TO/TO STAGE	%EFF-A TOT-STG	%EFF-P TOT-STG
1	52.2	31.2	0.7185	0.4516	0.0	0.0	0.0	21.08	0.5534	0.0605	0.0230	0.9827	1.3393	1.0956	88.65	89.11
2	48.7	28.3	0.7535	0.5209	0.0	0.0	0.0	20.41	0.4766	0.0416	0.0166	0.9870	1.3417	1.0938	91.00	91.36
3	48.7	29.0	0.7445	0.5192	0.0	0.0	0.0	19.71	0.4711	0.0362	0.0146	0.9889	1.3429	1.0928	92.35	92.66
4	49.7	30.7	0.7188	0.5010	0.0	0.0	0.0	18.99	0.4774	0.0317	0.0131	0.9908	1.3431	1.0917	93.63	93.89
5	50.8	31.6	0.6960	0.4834	0.0	0.0	0.0	19.25	0.4914	0.0357	0.0152	0.9902	1.3429	1.0924	92.75	93.04
6	51.8	32.1	0.6833	0.4719	0.0	0.0	0.0	19.74	0.5038	0.0411	0.0177	0.9890	1.3418	1.0932	91.60	91.95
7	55.5	35.2	0.6507	0.4321	0.0	0.0	0.0	20.26	0.5470	0.0515	0.0218	0.9873	1.3408	1.0943	90.17	90.57

SL	V-1 FT/SEC	V-2 FT/SEC	VM-1 FT/SEC	VM-2 FT/SEC	VO-1 FT/SEC	VO-2 FT/SEC	RHOVM-1 LBM/FT2SEC	RHOVM-2 LBM/FT2SEC	PCT TE SPAN	TO/TO INLET	%EFF-A TOT-INLET	%EFF-P TOT-INLET	EPSI-1 DEGREE	EPSI-2 DEGREE
1	1030.2	665.6	630.8	569.5	814.5	344.5	78.03	79.83	0.1000	1.5523	81.95	84.88	4.493	4.201
2	1068.7	758.4	705.1	667.7	803.0	359.7	89.93	96.33	0.2000	1.5316	88.82	90.70	3.749	3.470
3	1050.2	750.9	692.6	656.5	789.4	364.5	90.04	96.32	0.3000	1.5108	92.67	93.91	2.985	2.730
4	1012.1	722.1	655.1	621.1	771.5	368.4	86.78	92.29	0.5000	1.4951	95.08	95.91	1.444	1.236
5	988.2	701.6	624.0	597.7	766.3	367.5	82.44	87.97	0.7000	1.5115	91.45	92.88	-0.082	-0.233
6	977.5	689.7	604.0	584.3	768.5	366.4	79.11	84.94	0.8000	1.5301	87.76	89.80	-0.852	-0.957
7	941.1	638.0	532.9	521.1	775.7	368.2	68.71	74.25	0.9000	1.5530	82.43	85.30	-1.679	-1.715

NCORR INLET RPM	WCORR INLET LBM/SEC	WCORR INLET KG/SEC	TO/TO INLET	PO/PO INLET	EFF-AD INLET %	EFF-P INLET %	TO/TO STAGE	PO2/PO1	PO/PO STAGE	EFF-AD STAGE %	EFF-P STAGE %
12136.50	77.52	35.16	1.5235	3.8696	88.84	90.70	1.0935	0.9881	1.3425	91.57	91.91

STATOR 10

AIRFOIL AERODYNAMIC SUMMARY

SL	V-1 M/SEC	V-2 M/SEC	VM-1 M/SEC	VM-2 M/SEC	VO-1 M/SEC	VO-2 M/SEC	RHOVM-1 KG/M2 SEC	RHOVM-2 KG/M2 SEC	PO/PO INLET	TO/TO INLET	%EFF-A TOT-INLET	%EFF-P TOT-INLET	EPSI-1 RADIAN	EPSI-2 RADIAN
1	305.8	189.1	179.8	159.0	247.3	102.5	442.10	436.27	4.8953	1.6891	81.68	85.17	0.0549	0.0502
2	318.8	222.7	206.9	194.2	242.6	108.8	524.90	549.96	5.1306	1.6616	88.26	90.57	0.0460	0.0429
3	314.2	222.1	203.9	192.7	239.0	110.5	527.45	555.01	5.1508	1.6378	91.92	93.52	0.0460	0.0429
4	304.0	214.7	193.6	183.3	234.4	111.9	509.25	534.84	5.1258	1.6193	94.34	95.46	0.0366	0.0345
5	298.4	209.9	185.5	177.5	233.8	112.1	484.71	512.09	5.0968	1.6383	91.09	92.84	0.0171	0.0181
6	296.0	207.2	179.7	174.2	235.2	112.1	464.59	495.66	5.0729	1.6602	87.69	90.10	-0.0033	0.0020
7	285.5	192.2	156.8	155.6	238.6	112.8	397.86	433.16	4.9709	1.6878	82.81	86.12	-0.0271	-0.0159

SL	B-1 DEGREE	B-2 DEGREE	M-1	M-2	INCS DEGREE	INCM DEGREE	DEV DEGREE	TURN DEGREE	D-FAC	OMEGA-B TOTAL	LOSS-P TOTAL	PO2/PO1	PO/PO STAGE	TO/TO STAGE	%EFF-A TOT-STG	%EFF-P TOT-STG
1	54.0	32.8	0.6677	0.4028	0.0	0.0	0.0	21.18	0.6014	0.0727	0.0286	0.9818	1.3064	1.0877	87.45	87.91
2	49.6	29.3	0.7047	0.4807	0.0	0.0	0.0	20.29	0.5002	0.0450	0.0187	0.9874	1.3040	1.0843	90.42	90.77
3	49.5	29.8	0.6987	0.4830	0.0	0.0	0.0	19.69	0.4909	0.0397	0.0167	0.9890	1.3053	1.0835	91.71	92.01
4	50.5	31.4	0.6780	0.4689	0.0	0.0	0.0	19.05	0.4953	0.0354	0.0151	0.9907	1.3076	1.0830	92.99	93.25
5	51.6	32.3	0.6602	0.4554	0.0	0.0	0.0	19.31	0.5069	0.0394	0.0172	0.9901	1.3092	1.0840	92.24	92.53
6	52.6	32.8	0.6497	0.4462	0.0	0.0	0.0	19.85	0.5180	0.0447	0.0197	0.9890	1.3102	1.0851	91.20	91.53
7	56.7	35.9	0.6197	0.4095	0.0	0.0	0.0	20.77	0.5626	0.0555	0.0239	0.9874	1.3128	1.0868	89.91	90.29

SL	V-1 FT/SEC	V-2 FT/SEC	VM-1 FT/SEC	VM-2 FT/SEC	VO-1 FT/SEC	VO-2 FT/SEC	RHOVM-1 LBM/FT2SEC	RHOVM-2 LBM/FT2SEC	PCT TE SPAN	TO/TO INLET	%EFF-A TOT-INLET	%EFF-P TOT-INLET	EPSI-1 DEGREE	EPSI-2 DEGREE
1	1003.2	620.6	590.0	521.6	811.4	336.2	90.55	89.35	0.1000	1.6891	81.68	85.17	3.144	2.879
2	1046.0	730.5	678.7	637.3	796.0	357.0	107.50	112.64	0.2000	1.6616	88.26	90.57	2.638	2.456
3	1030.7	728.7	669.1	632.1	784.0	362.6	108.03	113.67	0.3000	1.6378	91.92	93.52	2.100	1.977
4	997.5	704.5	635.2	601.3	769.2	367.0	104.30	109.54	0.5000	1.6193	94.34	95.46	0.979	1.038
5	979.2	688.7	608.5	582.3	767.2	367.8	99.27	104.88	0.7000	1.6383	91.09	92.84	-0.191	0.113
6	971.1	679.7	589.7	571.6	771.6	367.8	95.15	101.52	0.8000	1.6602	87.69	90.10	-0.817	-0.370
7	936.7	630.5	514.4	510.5	782.8	370.0	81.49	88.72	0.9000	1.6878	82.81	86.12	-1.552	-0.911

NCORR INLET RPM	HCORR INLET LBM/SEC	HCORR INLET KG/SEC	TO/TO INLET	PO/PO INLET	EFF-AD INLET %	EFF-P INLET %	TO/TO STAGE	PO2/PO1	PO/PO STAGE	EFF-AD STAGE %	EFF-P STAGE %
12136.50	77.52	35.16	1.6529	5.0635	88.57	90.80	1.0849	0.9882	1.3085	90.99	91.32

ROTOR 11

AIRFOIL AERODYNAMIC SUMMARY

SL	V-1 M/SEC	V-2 M/SEC	VM-1 M/SEC	VM-2 M/SEC	VO-1 M/SEC	VO-2 M/SEC	U-1 M/SEC	U-2 M/SEC	V'-1 M/SEC	V'-2 M/SEC	VO'-1 M/SEC	VO'-2 M/SEC	RHOVM-1 KG/M2 SEC	RHOVM-2 KG/M2 SEC	EPSI-1 RADIAN	EPSI-2 RADIAN	PO/PO INLET
1	196.2	299.8	167.5	168.5	102.2	248.0	336.1	337.3	287.7	190.7	-233.9	-89.3	456.93	504.32	0.0344	0.0268	6.4374
2	228.5	310.6	201.1	195.3	108.5	241.6	341.3	342.3	307.6	219.7	-232.8	-100.7	565.61	604.50	0.0254	0.0182	6.6405
3	228.3	305.8	200.0	192.6	110.2	237.5	346.5	347.2	309.5	221.7	-236.3	-109.7	572.04	608.04	0.0172	0.0102	6.6449
4	220.8	295.5	190.5	182.2	111.7	232.7	356.9	357.1	310.5	220.6	-245.2	-124.5	552.44	584.72	0.0004	-0.0068	6.6013
5	214.8	269.8	183.3	173.5	112.1	232.2	367.3	367.1	314.2	219.7	-255.2	-134.9	527.20	552.54	-0.0160	-0.0243	6.5657
6	212.0	287.3	180.0	167.9	112.0	233.2	372.5	372.0	316.7	217.9	-260.5	-138.8	511.99	528.73	-0.0233	-0.0327	6.5397
.7	199.8	277.3	164.8	146.6	112.9	235.4	377.7	377.0	311.9	203.8	-264.8	-141.6	460.44	453.53	-0.0285	-0.0397	6.4288

SL	B-1 DEGREE	B-2 DEGREE	B'-1 DEGREE	B'-2 DEGREE	M-1	M-2	M'-1	M'-2	INCS DEGREE	INCM DEGREE	DEV DEGREE	TURN DEGREE	D FAC	OMEGA-B TOTAL	LOSS-P TOTAL	PO2/PO1	%EFF-A TOTAL	%EFF-P TOTAL
1	31.4	55.8	54.40	27.92	0.4183	0.6276	0.6133	0.3991	0.0	0.0	0.0	26.48	0.5786	0.0765	0.0316	1.3087	93.80	94.02
2	28.3	51.0	49.18	27.27	0.4938	0.6588	0.6649	0.4659	0.0	0.0	0.0	21.91	0.4922	0.0538	0.0227	1.2928	94.72	94.90
3	28.9	51.0	49.75	29.66	0.4970	0.6529	0.6738	0.4733	0.0	0.0	0.0	20.09	0.4819	0.0450	0.0188	1.2902	94.72	95.59
4	30.4	51.9	52.15	34.34	0.4828	0.6330	0.6789	0.4727	0.0	0.0	0.0	17.81	0.4826	0.0381	0.0156	1.2880	96.03	96.16
5	31.4	53.2	54.32	37.88	0.4668	0.6161	0.6828	0.4672	0.0	0.0	0.0	16.44	0.4954	0.0442	0.0178	1.2892	95.38	95.54
6	31.9	54.2	55.36	39.59	0.4577	0.6064	0.6836	0.4598	0.0	0.0	0.0	15.76	0.5083	0.0516	0.0205	1.2885	94.65	94.84
7	34.4	58.1	58.10	44.02	0.4271	0.5793	0.6667	0.4258	0.0	0.0	0.0	14.08	0.5496	0.0632	0.0238	1.2886	93.80	94.01

SL	V-1 FT/SEC	V-2 FT/SEC	VM-1 FT/SEC	VM-2 FT/SEC	VO-1 FT/SEC	VO-2 FT/SEC	U-1 FT/SEC	U-2 FT/SEC	V'-1 FT/SEC	V'-2 FT/SEC	VO'-1 FT/SEC	VO'-2 FT/SEC	RHOVM-1 LBM/FT2SEC	RHOVM-2 LBM/FT2SEC	EPSI-1 DEGREE	EPSI-2 DEGREE	PCT TE SPAN
1	643.7	983.7	549.5	552.7	335.3	813.8	1102.7	1106.7	943.9	625.5	-767.4	-292.9	93.58	103.29	1.972	1.538	0.1000
2	749.7	1019.2	659.8	640.7	355.9	792.7	1119.8	1123.0	1009.4	720.8	-763.8	-330.3	115.84	123.81	1.456	1.044	0.2000
3	749.2	1003.3	656.1	632.0	361.6	779.2	1136.8	1139.3	1015.6	727.3	-775.2	-360.0	117.16	124.53	0.988	0.586	0.3000
4	724.6	969.5	625.1	597.7	366.4	763.4	1171.0	1171.8	1018.8	723.9	-804.5	-408.4	113.15	119.76	0.021	-0.390	0.5000
5	704.8	950.9	601.3	569.1	367.7	761.7	1205.1	1204.3	1030.9	721.0	-837.4	-442.6	107.98	113.16	-0.915	-1.394	0.7000
6	695.6	942.8	590.7	551.0	367.4	765.0	1222.2	1220.6	1039.0	714.9	-854.8	-455.5	104.86	108.29	-1.333	-1.875	0.8000
7	655.5	909.7	540.7	481.0	370.5	772.2	1239.2	1236.8	1023.2	668.8	-868.7	-464.6	94.30	92.89	-1.631	-2.276	0.9000

WC1/A1 LBM/SEC SQFT	WC1/A1 KG/SEC SQM	TO/TO INLET	PO/PO INLET	EFF-AD INLET %	EFF-P INLET %	T02/T01	P02/P01	EFF-AD ROTOR %	EFF-P ROTOR %
9.33	45.51	1.7785	6.5478	89.12	91.52	1.0769	1.2922	94.88	95.05

193

STATOR 11

AIRFOIL AERODYNAMIC SUMMARY

SL	V-1 M/SEC	V-2 M/SEC	VM-1 M/SEC	VM-2 M/SEC	VO-1 M/SEC	VO-2 M/SEC	RHOVM-1 KG/M2 SEC	RHOVM-2 KG/M2 SEC	PO/PO INLET	TO/TO INLET	%EFF-A TOT-INLET	%EFF-P TOT-INLET	EPSI-1 RADIAN	EPSI-2 RADIAN
1	302.9	191.9	174.4	156.7	247.7	110.7	519.92	514.66	6.3148	1.8276	81.66	85.61	0.0310	0.0265
2	313.9	219.6	200.6	188.7	241.4	112.4	617.98	640.25	6.5537	1.7902	87.83	90.51	0.0242	0.0202
3	309.5	218.7	198.6	187.6	237.5	112.4	623.37	648.24	6.5747	1.7630	91.24	93.19	0.0172	0.0134
4	299.8	210.8	188.9	179.2	232.8	111.0	602.82	627.74	6.5423	1.7412	93.66	95.07	0.0027	-0.0008
5	294.3	205.2	180.7	173.1	232.3	110.1	572.44	600.24	6.5054	1.7598	90.96	92.95	-0.0131	-0.0161
6	292.2	202.4	175.8	170.1	233.4	109.7	550.67	581.83	6.4798	1.7830	87.96	90.61	-0.0218	-0.0245
7	282.3	188.4	156.2	152.1	235.7	111.2	480.86	510.29	6.3714	1.8108	83.88	87.38	-0.0314	-0.0336

SL	B-1 DEGREE	B-2 DEGREE	M-1	M-2	INCS DEGREE	INCM DEGREE	DEV DEGREE	TURN DEGREE	D-FAC	OMEGA-B TOTAL	LOSS-P TOTAL	PO2/ PO1	PO/PO STAGE	TO/TO STAGE	%EFF-A TOT-STG	%EFF-P TOT-STG
1	54.9	35.3	0.6346	0.3932	0.0	0.0	0.0	19.61	0.5792	0.0693	0.0267	0.9840	1.2899	1.0821	87.94	88.35
2	50.3	30.8	0.6662	0.4566	0.0	0.0	0.0	19.48	0.4967	0.0476	0.0196	0.9879	1.2776	1.0772	90.02	90.35
3	50.1	30.9	0.6614	0.4582	0.0	0.0	0.0	19.17	0.4899	0.0429	0.0179	0.9892	1.2764	1.0761	91.17	91.46
4	50.9	31.8	0.6428	0.4437	0.0	0.0	0.0	19.17	0.4997	0.0385	0.0163	0.9908	1.2762	1.0751	92.37	92.62
5	52.1	32.5	0.6266	0.4291	0.0	0.0	0.0	19.67	0.5156	0.0412	0.0178	0.9905	1.2759	1.0755	91.74	92.01
6	53.0	32.8	0.6176	0.4204	0.0	0.0	0.0	20.20	0.5276	0.0453	0.0197	0.9898	1.2755	1.0761	90.78	91.08
7	56.5	36.2	0.5917	0.3876	0.0	0.0	0.0	20.31	0.5660	0.0515	0.0218	0.9892	1.2745	1.0766	89.72	90.05

SL	V-1 FT/SEC	V-2 FT/SEC	VM-1 FT/SEC	VM-2 FT/SEC	VO-1 FT/SEC	VO-2 FT/SEC	RHOVM-1 LBM/FT2SEC	RHOVM-2 LBM/FT2SEC	PCT TE SPAN	TO/TO INLET	%EFF-A TOT-INLET	%EFF-P TOT-INLET	EPSI-1 DEGREE	EPSI-2 DEGREE
1	993.9	629.5	572.2	514.1	812.7	363.3	106.48	105.41	0.1000	1.8276	81.66	85.61	1.775	1.516
2	1029.9	720.6	658.2	619.0	792.1	368.9	126.57	131.13	0.2000	1.7902	87.83	90.51	1.385	1.155
3	1015.6	717.7	651.5	615.6	779.1	368.9	127.67	132.77	0.3000	1.7630	91.24	93.19	0.986	0.766
4	983.6	691.6	619.8	588.0	763.7	364.2	123.46	128.57	0.5000	1.7412	93.66	95.07	0.154	-0.047
5	965.6	673.1	592.7	568.0	762.3	361.2	117.24	122.94	0.7000	1.7598	90.96	92.95	-0.749	-0.925
6	958.7	663.9	576.7	558.0	765.8	359.8	112.78	119.16	0.8000	1.7830	87.96	90.61	-1.248	-1.403
7	927.8	618.1	512.5	499.1	773.5	364.8	98.48	104.51	0.9000	1.8108	83.88	87.38	-1.800	-1.922

NCORR INLET RPM	WCORR INLET LBM/SEC	WCORR INLET KG/SEC	TO/TO INLET	PO/PO INLET	EFF-AD INLET %	EFF-P INLET %	TO/TO STAGE	PO2/PO1	PO/PO STAGE	EFF-AD STAGE %	EFF-P STAGE %
12136.50	77.52	35.16	1.7785	6.4755	88.44	90.98	1.0769	0.9890	1.2779	90.63	90.93

ROTOR 12

AIRFOIL AERODYNAMIC SUMMARY

SL	V-1 M/SEC	V-2 M/SEC	VM-1 M/SEC	VM-2 M/SEC	VO-1 M/SEC	VO-2 M/SEC	U-1 M/SEC	U-2 M/SEC	V'-1 M/SEC	V'-2 M/SEC	VO'-1 M/SEC	VO'-2 M/SEC	RHOVM-1 KG/M2 SEC	RHOVM-2 KG/M2 SEC	EPSI-1 RADIAN	EPSI-2 RADIAN	PO/PO INLET
1	197.6	292.8	163.7	151.9	110.7	250.3	338.8	339.1	280.8	175.9	-228.1	-88.7	535.68	539.77	0.0149	0.0006	8.0381
2	224.5	308.1	194.4	185.8	112.4	245.8	343.2	343.4	301.8	209.9	-230.8	-97.6	656.73	684.22	0.0081	-0.0039	8.3305
3	224.1	303.3	193.8	185.0	112.4	240.4	347.7	347.7	304.8	213.8	-235.3	-107.3	666.21	695.44	0.0010	-0.0096	8.3396
4	216.8	292.6	186.2	176.9	111.1	233.0	356.5	356.3	308.1	215.6	-245.5	-123.3	648.51	677.09	-0.0148	-0.0228	8.2858
5	211.3	286.6	180.2	169.0	110.2	231.4	365.4	364.9	312.4	215.4	-255.2	-133.5	621.56	641.29	-0.0315	-0.0372	8.2377
6	208.5	283.8	177.3	163.1	109.8	232.2	369.9	369.2	314.7	213.0	-260.1	-137.0	603.49	611.03	-0.0393	-0.0438	8.2011
7	195.0	272.9	160.0	138.3	111.4	235.3	374.3	373.5	307.8	195.6	-262.9	-138.3	534.38	508.51	-0.0456	-0.0478	8.0606

SL	B-1 DEGREE	B-2 DEGREE	B'-1 DEGREE	B'-2 DEGREE	M-1	M-2	M'-1	M'-2	INCS DEGREE	INCM DEGREE	DEV DEGREE	TURN DEGREE	D FAC	OMEGA-B TOTAL	LOSS-P TOTAL	PO2/ PO1	%EFF-A TOTAL	%EFF-P TOTAL
1	34.1	58.8	54.34	30.29	0.4053	0.5900	0.5759	0.3545	0.0	0.0	0.0	24.05	0.6082	0.0796	0.0323	1.2730	93.67	93.87
2	30.0	52.9	49.90	27.72	0.4672	0.6297	0.6280	0.4290	0.0	0.0	0.0	22.18	0.5148	0.0597	0.0251	1.2709	94.36	94.54
3	30.1	52.4	50.51	30.11	0.4698	0.6246	0.6391	0.4403	0.0	0.0	0.0	20.40	0.5005	0.0514	0.0214	1.2685	94.93	95.09
4	30.8	52.8	52.82	34.87	0.4568	0.6050	0.6492	0.4458	0.0	0.0	0.0	17.95	0.4954	0.0431	0.0174	1.2667	95.59	95.72
5	31.5	53.9	54.78	38.32	0.4424	0.5880	0.6542	0.4420	0.0	0.0	0.0	16.46	0.5063	0.0465	0.0184	1.2668	95.19	95.34
6	31.8	54.9	55.73	40.04	0.4337	0.5780	0.6545	0.4338	0.0	0.0	0.0	15.69	0.5202	0.0522	0.0204	1.2674	94.66	94.82
7	34.9	59.6	58.69	45.01	0.4015	0.5501	0.6339	0.3943	0.0	0.0	0.0	13.68	0.5695	0.0609	0.0223	1.2685	94.18	94.35

SL	V-1 FT/SEC	V-2 FT/SEC	VM-1 FT/SEC	VM-2 FT/SEC	VO-1 FT/SEC	VO-2 FT/SEC	U-1 FT/SEC	U-2 FT/SEC	V'-1 FT/SEC	V'-2 FT/SEC	VO'-1 FT/SEC	VO'-2 FT/SEC	RHOVM-1 LBM/FT2SEC	RHOVM-2 LBM/FT2SEC	EPSI-1 DEGREE	EPSI-2 DEGREE	PCT TE SPAN
1	648.3	960.7	537.1	498.4	363.1	821.4	1111.5	1112.4	921.1	577.1	-748.4	-291.1	109.71	110.55	0.856	0.037	0.1000
2	736.7	1010.8	637.8	609.5	368.7	806.3	1126.1	1126.6	990.2	688.5	-757.4	-320.3	134.50	140.13	0.466	-0.222	0.2000
3	735.2	995.2	636.0	606.9	368.8	788.8	1140.7	1140.7	1000.2	701.6	-771.9	-352.0	136.45	142.43	0.057	-0.549	0.3000
4	711.3	960.0	610.9	580.5	364.4	764.6	1169.8	1169.0	1010.9	707.4	-805.5	-404.4	132.82	138.67	-0.850	-1.307	0.5000
5	693.2	940.2	591.3	554.6	361.7	759.2	1199.0	1197.3	1025.0	706.7	-837.3	-438.1	127.30	131.34	-1.802	-2.130	0.7000
6	684.1	931.2	581.6	535.3	360.3	762.0	1213.6	1211.5	1032.6	699.0	-853.3	-449.5	123.60	125.14	-2.250	-2.511	0.8000
7	639.6	895.4	525.0	453.9	365.4	771.9	1228.2	1225.6	1009.9	641.8	-862.7	-453.7	109.45	104.15	-2.611	-2.739	0.9000

WC1/A1 LBM/SEC SQFT	WC1/A1 KG/SEC SQM	TO/TO INLET	PO/PO INLET	EFF-AD INLET %	EFF-P INLET %		T02/T01	P02/P01	EFF-AD ROTOR %	EFF-P ROTOR %
7.57	36.95	1.9039	8.2155	88.69	91.41		1.0705	1.2687	94.77	94.93

STATOR 12

AIRFOIL AERODYNAMIC SUMMARY

SL	V-1 M/SEC	V-2 M/SEC	VM-1 M/SEC	VM-2 M/SEC	VO-1 M/SEC	VO-2 M/SEC	RHOVM-1 KG/M2 SEC	RHOVM-2 KG/M2 SEC	PO/PO INLET	TO/TO INLET	%EFF-A TOT-INLET	%EFF-P TOT-INLET	EPSI-1 RADIAN	EPSI-2 RADIAN
1	299.2	187.1	164.1	150.3	250.2	111.5	584.93	586.23	7.9595	1.9547	82.20	86.39	-0.0031	-0.0033
2	310.9	215.5	190.6	183.2	245.6	113.5	701.12	737.00	8.2309	1.9153	87.65	90.62	-0.0071	-0.0080
3	306.0	214.0	189.2	181.6	240.4	113.2	709.58	743.37	8.2446	1.8852	90.83	93.04	-0.0116	-0.0129
4	296.2	206.6	182.2	173.7	233.5	111.9	694.09	720.43	8.2052	1.8622	93.03	94.71	-0.0194	-0.0223
5	290.7	201.0	175.1	167.7	232.1	110.8	660.92	687.31	8.1573	1.8842	90.33	92.65	-0.0270	-0.0318
6	288.2	197.5	169.8	163.9	232.9	110.3	632.92	662.06	8.1206	1.9097	87.47	90.46	-0.0313	-0.0370
7	273.0	181.9	146.8	143.8	236.1	111.3	537.26	569.68	7.9839	1.9401	83.65	87.52	-0.0365	-0.0432

SL	B-1 DEGREE	B-2 DEGREE	M-1	M-2	INCS DEGREE	INCM DEGREE	DEV DEGREE	TURN DEGREE	D-FAC	OMEGA-B TOTAL	LOSS-P TOTAL	PO2/ PO1	PO/PO STAGE	TO/TO STAGE	%EFF-A TOT-STG	%EFF-P TOT-STG
1	56.7	36.6	0.6048	0.3708	0.0	0.0	0.0	20.18	0.5949	0.0686	0.0263	0.9855	1.2544	1.0719	87.94	88.29
2	52.2	31.8	0.6364	0.4330	0.0	0.0	0.0	20.41	0.5121	0.0534	0.0219	0.9874	1.2547	1.0712	89.27	89.58
3	51.8	32.0	0.6307	0.4332	0.0	0.0	0.0	19.84	0.5043	0.0466	0.0201	0.9887	1.2541	1.0704	90.29	90.58
4	52.0	32.8	0.6128	0.4204	0.0	0.0	0.0	19.26	0.5082	0.0440	0.0185	0.9903	1.2544	1.0697	91.51	91.76
5	53.0	33.5	0.5970	0.4063	0.0	0.0	0.0	19.51	0.5221	0.0468	0.0200	0.9901	1.2542	1.0698	91.09	91.35
6	53.9	33.9	0.5876	0.3964	0.0	0.0	0.0	19.96	0.5353	0.0508	0.0218	0.9895	1.2541	1.0702	90.36	90.64
7	58.1	37.7	0.5610	0.3614	0.0	0.0	0.0	20.39	0.5818	0.0576	0.0238	0.9890	1.2545	1.0706	89.72	90.01

SL	V-1 FT/SEC	V-2 FT/SEC	VM-1 FT/SEC	VM-2 FT/SEC	VO-1 FT/SEC	VO-2 FT/SEC	RHOVM-1 LBM/FT2SEC	RHOVM-2 LBM/FT2SEC	PCT TE SPAN	TO/TO INLET	%EFF-A TOT-INLET	%EFF-P TOT-INLET	EPSI-1 DEGREE	EPSI-2 DEGREE
1	981.6	613.9	538.3	493.1	820.8	365.7	119.80	120.07	0.1000	1.9547	82.20	86.39	-0.179	-0.191
2	1019.9	707.1	625.2	601.1	805.8	372.4	143.60	150.94	0.2000	1.9153	87.65	90.62	-0.407	-0.461
3	1003.8	702.1	620.9	595.7	738.8	371.5	145.33	152.25	0.3000	1.8852	90.83	93.04	-0.663	-0.741
4	971.7	677.9	597.7	570.0	766.1	367.0	142.16	147.55	0.5000	1.8622	93.03	94.71	-1.114	-1.279
5	953.7	659.6	574.3	550.3	761.4	363.6	135.36	-140.77	0.7000	1.8842	90.33	92.65	-1.549	-1.823
6	945.7	648.1	557.1	537.7	764.2	361.9	129.63	135.60	0.8000	1.9097	87.47	90.46	-1.794	-2.120
7	912.1	596.7	481.7	472.0	774.5	365.0	110.03	116.68	0.9000	1.9401	83.65	87.52	-2.091	-2.475

NCORR INLET RPM	WCORR INLET LBM/SEC	WCORR INLET KG/SEC	TO/TO INLET	PO/PO INLET	EFF-AD INLET %	EFF-P INLET %	TO/TO STAGE	PO2/PO1	PO/PO STAGE	EFF-AD STAGE %	EFF-P STAGE %
12136.50	77.52	35.16	1.9030	8.1269	88.17	91.01	1.0705	0.9888	1.2545	90.96	91.03

ROTOR 13

AIRFOIL AERODYNAMIC SUMMARY

SL	V-1 M/SEC	V-2 M/SEC	VM-1 M/SEC	VM-2 M/SEC	VO-1 M/SEC	VO-2 M/SEC	U-1 M/SEC	U-2 M/SEC	V'-1 M/SEC	V'-2 M/SEC	VO'-1 M/SEC	VO'-2 M/SEC	RHOVM-1 KG/M2 SEC	RHOVM-2 KG/M2 SEC	EPSI-1 RADIAN	EPSI-2 RADIAN	PO/PO INLET
1	190.7	284.7	154.7	146.0	111.6	244.4	339.0	338.9	275.0	173.9	-227.4	-94.5	602.24	612.93	-0.0071	-0.0064	9.8820
2	218.6	296.1	186.8	176.9	113.6	237.4	342.9	342.7	295.8	205.9	-229.3	-105.3	749.45	766.64	-0.0111	-0.0100	10.1348
3	217.5	292.0	185.7	176.1	113.3	233.0	346.7	346.5	298.3	209.5	-233.4	-113.5	757.68	778.07	-0.0155	-0.0139	10.1458
4	210.8	283.9	178.6	169.6	112.0	227.6	354.5	354.1	301.1	211.6	-242.5	-126.5	737.89	761.28	-0.0260	-0.0230	10.1081
5	205.7	279.9	173.1	163.2	111.0	227.4	362.3	361.7	305.1	211.4	-251.2	-134.3	707.02	724.89	-0.0379	-0.0333	10.0714
6	202.7	278.2	169.9	158.0	110.5	228.9	366.2	365.5	306.9	208.9	-255.6	-136.6	684.15	692.23	-0.0439	-0.0383	10.0388
7	188.2	268.8	151.5	133.9	111.6	233.0	370.0	369.4	299.6	191.1	-258.5	-136.3	598.09	575.65	-0.0492	-0.0417	9.8954

SL	B-1 DEGREE	B-2 DEGREE	B'-1 DEGREE	B'-2 DEGREE	M-1	M-2	M'-1	M'-2	INCS DEGREE	INCM DEGREE	DEV DEGREE	TURN DEGREE	D FAC	OMEGA-B TOTAL	LOSS-P TOTAL	PO2/ PO1	%EFF-A TOTAL	%EFF-P TOTAL
1	35.8	59.1	55.77	32.90	0.3782	0.5561	0.5454	0.3397	0.0	0.0	0.0	22.87	0.6011	0.0782	0.0313	1.2398	93.64	93.82
2	31.3	53.3	50.83	30.77	0.4395	0.5860	0.5945	0.4075	0.0	0.0	0.0	20.06	0.5059	0.0612	0.0254	1.2311	93.98	94.15
3	31.4	52.9	51.50	32.81	0.4406	0.5823	0.6041	0.4178	0.0	0.0	0.0	18.69	0.4928	0.0536	0.0220	1.2306	94.55	94.70
4	32.1	53.3	53.64	36.72	0.4291	0.5685	0.6131	0.4237	0.0	0.0	0.0	16.92	0.4886	0.0459	0.0184	1.2320	95.21	95.33
5	32.7	54.3	55.44	39.47	0.4161	0.5564	0.6172	0.4202	0.0	0.0	0.0	15.98	0.5011	0.0492	0.0193	1.2349	94.87	95.01
6	33.1	55.4	56.41	40.86	0.4072	0.5488	0.6166	0.4120	0.0	0.0	0.0	15.55	0.5168	0.0545	0.0212	1.2372	94.41	94.57
7	36.4	60.1	59.64	45.51	0.3743	0.5248	0.5961	0.3732	0.0	0.0	0.0	14.13	0.5706	0.0633	0.0231	1.2415	94.03	94.21

SL	V-1 FT/SEC	V-2 FT/SEC	VM-1 FT/SEC	VM-2 FT/SEC	VO-1 FT/SEC	VO-2 FT/SEC	U-1 FT/SEC	U-2 FT/SEC	V'-1 FT/SEC	V'-2 FT/SEC	VO'-1 FT/SEC	VO'-2 FT/SEC	RHOVM-1 LBM/FT2SEC	RHOVM-2 LBM/FT2SEC	EPSI-1 DEGREE	EPSI-2 DEGREE	PCT TE SPAN
1	625.8	934.2	507.6	479.1	366.1	802.0	1112.2	1111.9	902.4	570.7	-746.1	-310.0	123.34	125.53	-0.404	-0.364	0.1000
2	717.3	971.4	612.9	580.4	372.6	778.9	1124.9	1124.4	970.4	675.5	-752.3	-345.5	153.49	157.01	-0.636	-0.571	0.2000
3	713.7	958.2	609.2	577.8	371.9	764.4	1137.7	1136.9	978.6	687.5	-765.8	-372.6	155.18	159.35	-0.888	-0.794	0.3000
4	691.6	931.4	585.9	556.5	367.5	746.8	1163.2	1161.9	988.1	694.2	-795.6	-415.1	151.13	155.92	-1.491	-1.319	0.5000
5	674.8	918.4	568.0	535.5	364.4	746.1	1188.6	1186.9	1001.0	693.6	-824.3	-440.8	144.80	148.46	-2.174	-1.908	0.7000
6	665.0	912.6	557.4	518.4	362.6	751.1	1201.4	1199.4	1007.1	685.3	-838.7	-448.2	140.12	141.78	-2.515	-2.193	0.8000
7	617.3	881.9	497.1	439.5	366.0	764.6	1214.1	1211.9	983.0	627.1	-848.1	-447.3	122.49	117.90	-2.816	-2.389	0.9000

WC1/A1 LBM/SEC SQFT	WC1/A1 KG/SEC SQM	TO/TO INLET	PO/PO INLET	EFF-AD INLET %	EFF-P INLET %		TO2/TO1	PO2/PO1	EFF-AD ROTOR %	EFF-P ROTOR %
6.18	30.15	2.0208	10.0388	88.32	91.32		1.0619	1.2353	94.40	94.55

197

STATOR 13

AIRFOIL AERODYNAMIC SUMMARY

SL	V-1 M/SEC	V-2 M/SEC	VM-1 M/SEC	VM-2 M/SEC	VO-1 M/SEC	VO-2 M/SEC	RHOVM-1 KG/M2 SEC	RHOVM-2 KG/M2 SEC	PQ/PO INLET	TO/TO INLET	%EFF-A TOT-INLET	%EFF-P TOT-INLET	EPSI-1 RADIAN	EPSI-2 RADIAN
1	287.1	177.1	150.6	142.5	244.4	105.1	631.04	647.35	9.7431	2.0778	82.06	86.59	-0.0041	-0.0045
2	293.1	203.7	180.1	172.3	237.5	108.7	778.73	806.81	10.0202	2.0324	87.20	90.48	-0.0077	-0.0086
3	294.1	203.2	179.3	171.6	233.2	108.8	790.07	817.72	10.0433	2.0001	90.24	92.75	-0.0109	-0.0123
4	296.0	197.8	172.9	165.5	227.9	108.2	773.96	799.25	10.0182	1.9756	92.45	94.39	-0.0168	-0.0194
5	282.1	193.8	166.6	161.0	227.7	107.9	738.24	767.97	9.9808	1.9995	89.96	92.54	-0.0231	-0.0269
6	280.5	191.3	161.7	158.1	229.3	107.8	706.85	743.47	9.9493	2.0279	87.23	90.49	-0.0268	-0.0312
7	271.5	177.5	138.6	139.9	233.4	109.2	594.32	644.94	9.8117	2.0626	83.59	87.75	-0.0320	-0.0370

SL	B-1 DEGREE	B-2 DEGREE	M-1	M-2	INCS DEGREE	INCM DEGREE	DEV DEGREE	TURN DEGREE	D-FAC	OMEGA-B TOTAL	LOSS-P TOTAL	PO2/PO1	PO/PO STAGE	TO/TO STAGE	%EFF-A TOT-STG	%EFF-P TOT-STG
1	58.4	36.4	0.5611	0.3403	0.0	0.0	0.0	21.96	0.6113	0.0726	0.0273	0.9864	1.2233	1.0633	87.54	87.88
2	52.8	32.2	0.5902	0.3969	0.0	0.0	0.0	20.59	0.5211	0.0538	0.0215	0.9889	1.2174	1.0611	88.78	89.08
3	52.4	32.4	0.5866	0.3989	0.0	0.0	0.0	20.07	0.5117	0.0495	0.0200	0.9698	1.2181	1.0608	89.76	90.02
4	52.8	33.2	0.5731	0.3904	0.0	0.0	0.0	19.64	0.5134	0.0456	0.0186	0.9910	1.2209	1.0608	90.97	91.19
5	53.8	33.8	0.5612	0.3801	0.0	0.0	0.0	19.97	0.5249	0.0483	0.0200	0.9908	1.2234	1.0615	90.66	90.90
6	54.8	34.3	0.5538	0.3726	0.0	0.0	0.0	20.52	0.5364	0.0521	0.0216	0.9903	1.2249	1.0622	90.02	90.28
7	59.3	38.0	0.5304	0.3423	0.0	0.0	0.0	21.34	0.5802	0.0586	0.0235	0.9899	1.2286	1.0633	89.54	89.83

SL	V-1 FT/SEC	V-2 FT/SEC	VM-1 FT/SEC	VM-2 FT/SEC	VO-1 FT/SEC	VO-2 FT/SEC	RHOVM-1 LBM/FT2SEC	RHOVM-2 LBM/FT2SEC	PCT TE SPAN	TO/TO INLET	%EFF-A TOT-INLET	%EFF-P TOT-INLET	EPSI-1 DEGREE	EPSI-2 DEGREE
1	942.0	581.0	494.2	467.6	801.9	344.8	129.24	132.58	0.1000	2.0778	82.06	86.59	-0.235	-0.255
2	977.9	668.3	590.9	565.3	779.3	356.6	159.49	165.24	0.2000	2.0324	87.20	90.48	-0.442	-0.492
3	964.9	666.6	588.2	563.0	765.0	357.0	161.81	167.48	0.3000	2.0001	90.24	92.75	-0.624	-0.704
4	938.5	648.8	567.1	543.1	747.8	355.1	158.51	163.69	0.5000	1.9756	92.45	94.39	-0.961	-1.110
5	925.7	635.8	546.5	528.1	747.2	354.1	151.20	157.29	0.7000	1.9995	89.96	92.54	-1.321	-1.540
6	920.4	627.8	530.4	518.7	752.3	353.7	144.77	152.27	0.8000	2.0279	87.23	90.49	-1.538	-1.790
7	890.7	582.4	454.6	459.2	765.9	358.3	121.72	132.09	0.9000	2.0626	83.59	87.75	-1.836	-2.118

NCORR INLET RPM	WCORR INLET LBM/SEC	WCORR INLET KG/SEC	TO/TO INLET	PO/PO INLET	EFF-AD INLET %	EFF-P INLET %	TO/TO STAGE	PO2/PO1	PO/PO STAGE	EFF-AD STAGE %	EFF-P STAGE %
12136.50	77.52	35.16	2.0208	9.9355	87.79	90.91	1.0619	0.9897	1.2226	89.65	89.93

STATOR 14

AIRFOIL AERODYNAMIC SUMMARY

SL	V-1 M/SEC	V-2 M/SEC	VM-1 M/SEC	VM-2 M/SEC	VO-1 M/SEC	VO-2 M/SEC	RHOVM-1 KG/M2 SEC	RHOVM-2 KG/M2 SEC	PO/PO INLET	TO/TO INLET	%EFF-A TOT-INLET	%EFF-P TOT-INLET	EPSI-1 RADIAN	EPSI-2 RADIAN
1	279.7	166.5	148.6	136.9	236.9	94.8	721.56	714.32	11.7401	2.2003	81.66	86.59	-0.0023	-0.0017
2	288.9	192.3	172.6	166.8	231.8	95.7	864.43	898.20	12.0251	2.1479	86.66	90.29	-0.0061	-0.0055
3	285.1	192.1	172.0	166.4	227.4	96.0	877.64	911.76	12.0508	2.1127	89.62	92.45	-0.0097	-0.0094
4	273.0	187.6	166.8	161.1	222.4	96.0	864.10	895.08	12.0305	2.0856	91.85	94.08	-0.0164	-0.0169
5	275.2	184.8	161.5	157.7	222.9	96.4	827.38	865.52	11.9994	2.1109	89.55	92.40	-0.0237	-0.0252
6	274.3	183.3	157.2	155.7	224.8	96.7	794.31	842.06	11.9724	2.1420	86.91	90.47	-0.0280	-0.0301
7	266.7	171.3	136.0	139.7	229.5	99.1	673.71	740.05	11.8375	2.1806	83.42	87.90	-0.0337	-0.0364

SL	B-1 DEGREE	B-2 DEGREE	M-1	M-2	INCS DEGREE	INCM DEGREE	DEV DEGREE	TURN DEGREE	D-FAC	OMEGA-B TOTAL	LOSS-P TOTAL	P02/P01	PO/PO STAGE	TO/TO STAGE	%EFF-A TOT-STG	%EFF-P TOT-STG
1	57.9	34.7	0.5308	0.3110	0.0	0.0	0.0	23.20	0.6199	0.0752	0.0263	0.9874	1.2058	1.0585	87.21	87.53
2	53.3	29.8	0.5556	0.3643	0.0	0.0	0.0	23.49	0.5373	0.0598	0.0223	0.9889	1.2003	1.0566	88.11	88.41
3	52.9	30.0	0.5523	0.3667	0.0	0.0	0.0	22.92	0.5274	0.0554	0.0208	0.9898	1.1999	1.0560	89.01	89.28
4	53.1	30.8	0.5412	0.3602	0.0	0.0	0.0	22.34	0.5271	0.0514	0.0195	0.9909	1.2008	1.0556	90.14	90.38
5	54.1	31.4	0.5319	0.3528	0.0	0.0	0.0	22.64	0.5356	0.0540	0.0208	0.9907	1.2022	1.0561	89.83	90.08
6	55.0	31.8	0.5261	0.3473	0.0	0.0	0.0	23.21	0.5448	0.0578	0.0224	0.9902	1.2031	1.0566	89.19	89.46
7	59.3	35.3	0.5065	0.3214	0.0	0.0	0.0	24.01	0.5834	0.0644	0.0241	0.9898	1.2060	1.0576	88.74	89.02

SL	V-1 FT/SEC	V-2 FT/SEC	VM-1 FT/SEC	VM-2 FT/SEC	VO-1 FT/SEC	VO-2 FT/SEC	RHOVM-1 LBM/FT2SEC	RHOVM-2 LBM/FT2SEC	PCT TE SPAN	TO/TO INLET	%EFF-A TOT-INLET	%EFF-P TOT-INLET	EPSI-1 DEGREE	EPSI-2 DEGREE
1	917.6	546.4	487.5	449.2	777.4	311.1	147.78	146.30	0.1000	2.2003	81.66	86.59	-0.132	-0.095
2	948.0	631.1	566.2	547.4	760.4	313.9	177.04	183.96	0.2000	2.1479	86.66	90.29	-0.348	-0.313
3	935.4	630.2	564.3	545.9	746.0	314.9	179.75	186.74	0.3000	2.1127	89.62	92.45	-0.554	-0.536
4	912.1	615.5	547.2	528.7	729.7	315.1	176.98	183.32	0.5000	2.0856	91.85	94.08	-0.942	-0.969
5	902.9	606.5	529.7	517.5	731.2	316.3	169.46	177.27	0.7000	2.1109	89.55	92.40	-1.355	-1.442
6	899.9	601.4	515.7	511.0	737.5	317.2	162.68	172.46	0.8000	2.1420	86.91	90.47	-1.604	-1.725
7	875.1	562.1	446.1	458.5	752.9	325.2	137.98	151.57	0.9000	2.1806	83.42	87.90	-1.932	-2.088

NCORR INLET RPM	WCORR INLET LBM/SEC	WCORR INLET KG/SEC	TO/TO INLET	PO/PO INLET	EFF-AD INLET %	EFF-P INLET %	TO/TO STAGE	P02/P01	PO/PO STAGE	EFF-AD STAGE %	EFF-P STAGE %
12136.50	77.52	35.16	2.1352	11.9473	87.34	90.78	1.0567	0.9898	1.2025	88.97	89.24

ROTOR 15
AIRFOIL AERODYNAMIC SUMMARY

SL	V-1 M/SEC	V-2 M/SEC	VM-1 M/SEC	VM-2 M/SEC	VO-1 M/SEC	VO-2 M/SEC	U-1 M/SEC	U-2 M/SEC	V'-1 M/SEC	V'-2 M/SEC	VO'-1 M/SEC	VO'-2 M/SEC	RHOVM-1 KG/M2 SEC	RHOVM-2 KG/M2 SEC	EPSI-1 RADIAN	EPSI-2 RADIAN	PO/PO INLET
1	170.9	257.9	142.0	135.9	95.0	219.2	338.2	338.2	281.7	180.6	-243.3	-119.0	739.98	756.80	-0.0047	-0.0163	14.0288
2	195.7	267.5	170.6	163.6	95.8	211.6	341.4	341.3	299.1	208.7	-245.7	-129.6	916.69	941.20	-0.0083	-0.0133	14.2806
3	195.6	264.7	170.4	163.2	96.0	208.4	344.6	344.3	301.3	212.4	-248.5	-135.9	931.41	957.08	-0.0119	-0.0127	14.3039
4	191.6	259.7	165.7	158.9	96.2	205.4	350.9	350.5	303.9	215.2	-254.7	-145.1	917.88	946.48	-0.0201	-0.0144	14.2976
5	189.2	259.6	162.7	156.3	96.6	207.2	357.2	356.7	307.2	216.2	-260.6	-149.4	890.57	920.76	-0.0296	-0.0193	14.3037
6	188.0	260.5	161.1	154.5	96.8	209.7	360.3	359.8	308.9	215.4	-263.5	-150.1	868.91	897.00	-0.0349	-0.0227	14.3004
7	176.8	254.6	146.3	136.5	99.3	215.0	363.5	362.9	302.0	201.3	-264.2	-147.9	772.95	776.54	-0.0400	-0.0257	14.1738

SL	B-1 DEGREE	B-2 DEGREE	B'-1 DEGREE	B'-2 DEGREE	M-1	M-2	M'-1	M'-2	INCS DEGREE	INCM DEGREE	DEV DEGREE	TURN DEGREE	D FAC	OMEGA-B TOTAL	LOSS-P TOTAL	PO2/PO1	%EFF-A TOTAL	%EFF-P TOTAL
1	33.8	58.2	59.72	41.22	0.3193	0.4753	0.5264	0.3329	0.0	0.0	0.0	18.50	0.5698	0.0788	0.0282	1.1945	92.92	93.08
2	29.3	52.3	55.21	38.40	0.3708	0.4999	0.5668	0.3901	0.0	0.0	0.0	16.82	0.4881	0.0636	0.0239	1.1875	93.18	93.34
3	29.4	51.9	55.56	39.79	0.3736	0.4986	0.5755	0.4001	0.0	0.0	0.0	15.77	0.4755	0.0589	0.0219	1.1870	93.48	93.62
4	30.1	52.3	56.95	42.39	0.3681	0.4919	0.5838	0.4076	0.0	0.0	0.0	14.56	0.4689	0.0536	0.0195	1.1884	93.93	94.06
5	30.7	53.0	58.02	43.71	0.3613	0.4885	0.5867	0.4069	0.0	0.0	0.0	14.31	0.4767	0.0539	0.0195	1.1920	93.95	94.09
6	31.0	53.6	58.56	44.15	0.3564	0.4866	0.5856	0.4023	0.0	0.0	0.0	14.41	0.4871	0.0561	0.0204	1.1945	93.81	93.96
7	34.2	57.6	61.03	47.28	0.3319	0.4709	0.5671	0.3722	0.0	0.0	0.0	13.75	0.5277	0.0601	0.0208	1.1977	93.83	93.99

SL	V-1 FT/SEC	V-2 FT/SEC	VM-1 FT/SEC	VM-2 FT/SEC	VO-1 FT/SEC	VO-2 FT/SEC	U-1 FT/SEC	U-2 FT/SEC	V'-1 FT/SEC	V'-2 FT/SEC	VO'-1 FT/SEC	VO'-2 FT/SEC	RHOVM-1 LBM/FT2SEC	RHOVM-2 LBM/FT2SEC	EPSI-1 DEGREE	EPSI-2 DEGREE	PCT TE SPAN
1	560.6	846.0	466.1	445.8	311.6	719.1	1109.8	1109.6	924.3	592.6	-798.2	-390.5	151.55	155.00	-0.270	-0.934	0.1000
2	642.0	877.6	559.9	536.7	314.2	694.4	1120.1	1119.7	981.4	684.8	-806.0	-425.3	187.75	192.77	-0.476	-0.764	0.2000
3	641.8	868.5	559.1	535.5	315.1	683.8	1130.5	1129.8	997.0	697.0	-815.4	-446.0	190.76	196.02	-0.682	-0.730	0.3000
4	628.6	852.2	543.7	521.5	315.5	674.0	1151.2	1150.0	997.0	706.1	-835.7	-476.1	187.99	193.85	-1.150	-0.824	0.5000
5	620.8	851.6	533.9	512.8	316.8	679.9	1171.9	1170.3	1008.1	709.5	-855.1	-490.0	182.40	188.58	-1.698	-1.103	0.7000
6	616.8	854.7	528.7	507.0	317.7	688.1	1182.2	1180.4	1013.4	706.7	-864.6	-492.3	177.96	183.71	-1.999	-1.298	0.8000
7	580.1	835.5	480.0	447.9	325.6	705.3	1192.6	1190.5	991.0	660.4	-867.0	-485.3	158.31	159.04	-2.290	-1.473	0.9000

WC1/A1 LBM/SEC SQFT	WC1/A1 KG/SEC SQM	TO/TO INLET	PO/PO INLET	EFF-AD INLET %	EFF-P INLET %
4.45	21.72	2.2435	14.2359	87.35	90.97

TO2/TO1	PO2/PO1	EFF-AD ROTOR %	EFF-P ROTOR %
1.0507	1.1916	93.60	93.75

STATOR 15 (E.V.)

AIRFOIL AERODYNAMIC SUMMARY

SL	V-1 M/SEC	V-2 M/SEC	VM-1 M/SEC	VM-2 M/SEC	VO-1 M/SEC	VO-2 M/SEC	RHOVM-1 KG/M2 SEC	RHOVM-2 KG/M2 SEC	PO/PO INLET	TO/TO INLET	%EFF-A TOT-INLET	%EFF-P TOT-INLET	EPSI-1 RADIAN	EPSI-2 RADIAN
1	260.9	145.7	146.8	145.5	215.7	8.7	837.13	885.70	14.0056	2.2796	84.05	88.58	0.0065	0.0982
2	263.5	154.8	158.4	154.8	210.5	1.2	922.59	960.69	14.1048	2.2400	87.19	90.85	0.0111	0.0972
3	260.5	154.8	157.3	154.8	207.7	0.5	929.25	974.50	14.1156	2.2097	89.50	90.85	0.0111	0.0972
3	260.5	154.8	157.3	154.8	207.7	0.5	929.25	974.50	14.1156	2.2097	89.50	92.51	0.0146	0.0961
4	257.6	154.9	155.3	154.9	205.5	0.4	926.30	983.94	14.1200	2.1895	91.10	93.66	0.0191	0.0929
5	258.5	156.5	154.1	156.5	207.6	0.4	906.91	981.28	14.1198	2.2177	88.90	92.08	0.0209	0.0876
6	259.3	157.4	152.0	157.4	210.1	0.6	881.42	972.05	14.1122	2.2500	86.47	90.34	0.0209	0.0840
7	253.3	148.1	133.2	147.9	215.5	8.3	756.71	894.97	14.0026	2.2908	83.27	88.02	0.0203	0.0792

SL	B-1 DEGREE	B-2 DEGREE	M-1	M-2	INCS DEGREE	INCM DEGREE	DEV DEGREE	TURN DEGREE	D-FAC	OMEGA-B TOTAL	LOSS-P TOTAL	PO2/PO1	PO/PO STAGE	TO/TO STAGE	%EFF-A TOT-STG	%EFF-P TOT-STG
1	55.7	3.4	0.4846	0.2670	0.0	0.0	0.0	52.25	0.5930	0.0943	0.0182	0.9863	1.1737	1.0503	85.74	86.03
2	52.9	0.5	0.4938	0.2861	0.0	0.0	0.0	52.48	0.5659	0.0935	0.0182	0.9860	1.1703	1.0498	85.42	85.72
3	52.8	0.2	0.4914	0.2881	0.0	0.0	0.0	52.60	0.5607	0.0881	0.0173	0.9869	1.1714	1.0497	86.21	86.49
4	52.9	0.1	0.4876	0.2896	0.0	0.0	0.0	52.72	0.5560	0.0846	0.0169	0.9876	1.1738	1.0500	87.01	87.28
5	53.4	0.1	0.4859	0.2909	0.0	0.0	0.0	53.23	0.5550	0.0883	0.0179	0.9871	1.1767	1.0507	86.87	87.16
6	54.1	0.2	0.4833	0.2905	0.0	0.0	0.0	53.86	0.5571	0.0928	0.0190	0.9865	1.1783	1.0513	86.51	86.78
7	58.2	3.2	0.4680	0.2708	0.0	0.0	0.0	55.04	0.5837	0.0946	0.0195	0.9870	1.1817	1.0518	86.88	87.15

SL	V-1 FT/SEC	V-2 FT/SEC	VM-1 FT/SEC	VM-2 FT/SEC	VO-1 FT/SEC	VO-2 FT/SEC	RHOVM-1 LBM/FT2SEC	RHOVM-2 LBM/FT2SEC	PCT TE SPAN	TO/TO INLET	%EFF-A TOT-INLET	%EFF-P TOT-INLET	EPSI-1 DEGREE	EPSI-2 DEGREE
1	856.1	478.2	481.8	477.3	707.7	28.4	171.45	181.40	0.1000	2.2796	84.05	88.58	0.370	5.627
2	864.4	507.8	519.9	507.7	690.6	4.1	188.95	196.76	0.2000	2.2400	87.19	90.85	0.637	5.568
3	854.8	508.0	516.0	508.0	681.5	1.6	190.32	199.59	0.3000	2.2097	89.50	92.51	0.837	5.505
4	845.1	508.2	509.5	508.2	674.3	1.2	189.72	201.52	0.5000	2.1895	91.10	93.66	1.093	5.320
5	848.2	513.6	505.5	513.6	681.2	1.2	185.74	200.97	0.7000	2.2177	88.90	92.08	1.196	5.022
6	850.7	516.4	498.6	516.4	689.2	1.9	180.52	199.08	0.8000	2.2500	86.47	90.34	1.200	4.815
7	831.1	486.0	436.9	485.3	707.0	27.2	154.98	183.30	0.9000	2.2908	83.27	88.02	1.162	4.537

HCORR INLET RPM	WCORR INLET LBM/SEC	WCORR INLET KG/SEC	TO/TO INLET	PO/PO INLET	EFF-AD INLET %	EFF-P INLET %	TO/TO STAGE	PO2/PO1	PO/PO STAGE	EFF-AD STAGE %	EFF-P STAGE %
12136.50	77.52	35.16	2.2387	14.0678	87.16	90.82	1.0507	0.9870	1.1761	91.22	90.60

APPENDIX A.2

AIRFOIL AERODYNAMIC DATA
FOR THE DESIGN UPDATE

AIRFOIL AERODYNAMIC SUMMARY

Corrected Speed   =   12,135 rpm

Corrected Flow   =   35.2 kg/sec (77.5 lb/sec)

Inlet Pressure   =   101.32 kN/m^2 (2116.2 lb/ft^2)

Inlet Temperature   =   14.8°C (518.7°R)

ROTOR 6

AIRFOIL AERODYNAMIC SUMMARY PRINT

RUN NO 100 SPEED CODE 10 POINT NO 3

SL	V-1 M/SEC	V-2 M/SEC	VM-1 M/SEC	VM-2 M/SEC	VO-1 M/SEC	VO-2 M/SEC	U-1 M/SEC	U-2 M/SEC	V'-1 M/SEC	V'-2 M/SEC	VO'-1 M/SEC	VO'-2 M/SEC	RHOVM-1 KG/M2 SEC	RHOVM-2 KG/M2 SEC	EPSI-1 RADIAN	EPSI-2 RADIAN	PO/PO INLET
1	162.1	280.3	157.5	186.2	38.3	209.5	229.1	244.4	247.5	189.4	-190.8	-34.8	163.39	215.48	0.0793	0.1676	1.4902
2	177.9	274.9	171.1	185.6	48.8	202.8	245.8	258.9	260.9	193.9	-197.0	-56.1	178.67	221.68	0.0408	0.1334	1.5061
3	186.8	267.1	178.1	182.4	56.2	195.2	262.5	273.4	272.5	198.5	-206.3	-78.2	186.54	222.93	0.0119	0.1023	1.5031
4	194.5	255.6	183.0	174.2	65.7	187.1	295.8	302.5	294.0	209.0	-230.1	-115.4	191.41	219.48	-0.0332	0.0454	1.5003
5	197.1	247.9	183.8	165.8	71.2	184.3	329.2	331.5	316.9	221.7	-258.1	-147.2	190.93	212.11	-0.0657	-0.0044	1.5035
6	196.0	243.9	182.2	160.6	72.3	183.6	345.9	346.0	328.7	228.4	-273.6	-162.4	187.96	205.96	-0.0780	-0.0267	1.5025
7	189.6	230.4	175.8	146.7	71.2	177.7	362.6	360.6	340.3	234.5	-291.4	-182.9	179.22	187.50	-0.0877	-0.0474	1.4639

SL	B-1 DEGREE	B-2 DEGREE	B'-1 DEGREE	B'-2 DEGREE	M-1	M-2	M'-1	M'-2	INCS DEGREE	INCM DEGREE	DEV DEGREE	TURN DEGREE	D FAC	OMEGA-B TOTAL	LOSS-P TOTAL	PO2/PO1	%EFF-A TOTAL	%EFF-P TOTAL
1	13.5	48.3	50.08	10.57	0.4847	0.8165	0.7399	0.5517	0.0	0.0	0.0	39.52	0.4579	0.1099	0.0329	1.5412	92.31	92.76
2	15.7	47.4	48.69	16.76	0.5362	0.8041	0.7865	0.5672	0.0	0.0	0.0	31.93	0.4577	0.0819	0.0252	1.5194	93.35	93.73
3	17.4	46.8	48.92	23.13	0.5662	0.7831	0.8260	0.5818	0.0	0.0	0.0	25.79	0.4520	0.0592	0.0183	1.5019	94.63	94.93
4	19.7	46.9	51.41	33.45	0.5930	0.7491	0.8967	0.6125	0.0	0.0	0.0	17.97	0.4459	0.0375	0.0113	1.4921	96.01	96.23
5	21.2	48.0	54.58	41.59	0.6015	0.7223	0.9667	0.6460	0.0	0.0	0.0	12.99	0.4419	0.0411	0.0118	1.4990	95.19	95.46
6	21.7	48.8	56.42	45.34	0.5967	0.7069	1.0005	0.6620	0.0	0.0	0.0	11.08	0.4405	0.0460	0.0126	1.5085	94.49	94.80
7	22.1	50.5	58.99	51.29	0.5742	0.6622	1.0304	0.6739	0.0	0.0	0.0	7.70	0.4366	0.0529	0.0131	1.4994	93.40	93.77

SL	V-1 FT/SEC	V-2 FT/SEC	VM-1 FT/SEC	VM-2 FT/SEC	VO-1 FT/SEC	VO-2 FT/SEC	U-1 FT/SEC	U-2 FT/SEC	V'-1 FT/SEC	V'-2 FT/SEC	VO'-1 FT/SEC	VO'-2 FT/SEC	RHOVM-1 LBM/FT2SEC	RHOVM-2 LBM/FT2SEC	EPSI-1 DEGREE	EPSI-2 DEGREE	PCT TE SPAN
1	531.9	919.7	516.9	610.9	125.5	687.5	751.6	801.7	811.9	621.5	-626.1	-114.2	33.46	44.13	4.543	9.605	0.1000
2	583.7	901.9	561.4	608.9	160.0	665.4	806.4	849.4	856.2	636.1	-646.4	-184.1	36.59	45.40	2.338	7.643	0.2000
3	612.9	876.5	584.5	598.5	184.4	640.3	861.2	897.1	894.2	651.3	-676.7	-256.7	38.20	45.66	0.681	5.860	0.3000
4	638.0	838.7	600.5	571.7	215.6	613.7	970.7	992.4	964.7	685.7	-755.0	-378.7	39.20	44.95	-1.905	2.600	0.5000
5	646.8	813.4	603.2	544.0	233.5	604.7	1080.2	1087.7	1039.6	727.5	-846.7	-483.0	39.10	43.44	-3.763	-0.252	0.7000
6	643.2	800.3	597.8	526.9	237.4	602.4	1134.9	1135.4	1078.4	749.5	-897.6	-533.0	38.50	42.18	-4.468	-1.530	0.8000
7	622.2	755.9	576.8	481.2	233.5	582.9	1189.7	1183.0	1116.7	769.2	-956.2	-600.1	36.71	38.40	-5.026	-2.718	0.9000

WC1/A1 LBM/SEC SQFT	WC1/A1 KG/SEC SQM	TO/TO INLET	PO/PO INLET	EFF-AD INLET %	EFF-P INLET %		T02/T01	P02/P01	EFF-AD ROTOR %	EFF-P ROTOR %
37.72	184.17	1.1314	1.4912	92.03	92.47		1.1315	1.5053	94.30	94.62

STATOR 6

AIRFOIL AERODYNAMIC SUMMARY PRINT

SL	V-1 M/SEC	V-2 M/SEC	VM-1 M/SEC	VM-2 M/SEC	VO-1 M/SEC	VO-2 M/SEC	RHOVM-1 KG/M2 SEC	RHOVM-2 KG/M2 SEC	PO/PO INLET	TO/TO INLET	%EFF-A TOT-INLET	%EFF-P TOT-INLET	EPSI-1 RADIAN	EPSI-2 RADIAN
1	284.1	196.5	196.5	178.6	205.2	82.0	225.31	234.73	1.4373	1.1543	70.94	72.37	0.1967	0.2052
2	280.5	204.9	197.3	187.8	199.5	82.1	232.47	252.79	1.4767	1.1401	84.17	85.01	0.1655	0.1761
3	273.9	203.0	194.7	184.9	192.7	83.9	234.18	252.47	1.4803	1.1285	92.47	92.87	0.1347	0.1462
4	263.5	199.7	186.8	179.8	185.8	86.8	231.16	249.36	1.4838	1.1184	100.87	100.83	0.0776	0.0893
5	256.0	197.3	177.9	176.5	184.1	88.2	223.70	245.00	1.4850	1.1234	96.99	97.16	0.0234	0.0357
6	252.0	195.6	172.4	174.4	183.8	88.6	217.44	240.65	1.4812	1.1311	90.64	91.15	-0.0033	0.0105
7	239.1	181.1	159.1	157.5	178.4	89.4	200.14	214.79	1.4381	1.1370	79.85	80.86	-0.0295	-0.0131

SL	B-1 DEGREE	B-2 DEGREE	M-1	M-2	INCS DEGREE	INCM DEGREE	DEV DEGREE	TURN DEGREE	D-FAC	OMEGA-B TOTAL	LOSS-P TOTAL	PO2/ PO1	PO/PO STAGE	TO/TO STAGE	%EFF-A TOT-STG	%EFF-P TOT-STG
1	46.2	24.6	0.8291	0.5535	0.0	0.0	0.0	21.54	0.4572	0.0956	0.0312	0.9653	1.4887	1.1428	84.32	85.18
2	45.2	23.6	0.8228	0.5830	0.0	0.0	0.0	21.64	0.4175	0.0545	0.0183	0.9804	1.4906	1.1363	88.65	89.27
3	44.6	24.4	0.8054	0.5803	0.0	0.0	0.0	20.26	0.4029	0.0438	0.0149	0.9847	1.4792	1.1304	90.83	91.33
4	44.8	25.8	0.7748	0.5729	0.0	0.0	0.0	19.06	0.3851	0.0336	0.0118	0.9890	1.4757	1.1262	93.20	93.56
5	46.0	26.5	0.7485	0.5643	0.0	0.0	0.0	19.42	0.3789	0.0396	0.0143	0.9877	1.4805	1.1288	92.12	92.55
6	46.8	26.9	0.7328	0.5570	0.0	0.0	0.0	19.90	0.3784	0.0472	0.0173	0.9858	1.4873	1.1320	91.01	91.50
7	48.3	29.6	0.6895	0.5122	0.0	0.0	0.0	18.72	0.3955	0.0613	0.0222	0.9834	1.4739	1.1313	89.30	89.87

SL	V-1 FT/SEC	V-2 FT/SEC	VM-1 FT/SEC	VM-2 FT/SEC	VO-1 FT/SEC	VO-2 FT/SEC	RHOVM-1 LBM/FT2SEC	RHOVM-2 LBM/FT2SEC	PCT TE SPAN	TO/TO INLET	%EFF-A TOT-INLET	%EFF-P TOT-INLET	EPSI-1 DEGREE	EPSI-2 DEGREE
1	932.2	644.8	644.7	586.0	673.4	268.9	46.14	48.07	0.1000	1.1543	70.94	72.37	11.271	11.759
2	920.4	672.4	647.2	616.1	654.4	269.4	47.61	51.77	0.2000	1.1401	84.17	85.01	9.485	10.088
3	898.7	666.2	638.7	606.7	632.2	275.1	47.96	51.71	0.3000	1.1285	92.47	92.87	7.720	8.379
4	864.4	655.2	612.7	590.1	609.8	284.8	47.34	51.07	0.5000	1.1184	100.87	100.83	4.444	5.115
5	839.9	647.4	583.7	579.2	603.9	289.3	45.82	50.18	0.7000	1.1234	96.99	97.16	1.338	2.045
6	826.8	641.7	565.7	572.1	603.0	290.6	44.53	49.29	0.8000	1.1311	90.64	91.15	-0.190	0.599
7	784.3	594.3	521.9	516.9	585.5	293.3	40.99	43.99	0.9000	1.1370	79.85	80.86	-1.691	-0.750

NCORR INLET RPM	WCORR INLET LBM/SEC	WCORR INLET KG/SEC		TO/TO INLET	PO/PO INLET	EFF-AD INLET %	EFF-P INLET %		TO/TO STAGE	PO2/PO1	PO/PO STAGE	EFF-AD STAGE %	EFF-P STAGE %
12136.50	77.44	35.13		1.1314	1.4657	87.83	88.47		1.1315	0.9829	1.4795	90.08	90.62

ROTOR 7

AIRFOIL AERODYNAMIC SUMMARY PRINT

RUN NO 100 SPEED CODE 10 POINT NO 3

SL	V-1 M/SEC	V-2 M/SEC	VM-1 M/SEC	VM-2 M/SEC	VO-1 M/SEC	VO-2 M/SEC	U-1 M/SEC	U-2 M/SEC	V'-1 M/SEC	V'-2 M/SEC	VO'-1 M/SEC	VO'-2 M/SEC	RHOVM-1 KG/M2 SEC	RHOVM-2 KG/M2 SEC	EPSI-1 RADIAN	EPSI-2 RADIAN	PO/PO INLET
1	203.2	285.0	186.5	180.3	80.6	220.7	263.1	272.5	261.0	187.7	-182.5	-51.9	242.45	266.34	0.1962	0.1820	2.0725
2	213.5	287.6	197.5	189.3	80.9	216.4	275.0	283.3	276.9	200.8	-194.1	-66.9	262.07	289.86	0.1673	0.1540	2.1429
3	212.8	280.1	196.0	184.1	82.9	211.1	286.9	294.1	282.9	202.0	-204.0	-83.0	263.18	288.97	0.1376	0.1264	2.1440
4	210.4	267.7	191.9	174.4	86.2	203.1	310.7	315.6	295.3	207.5	-224.5	-112.4	261.30	282.31	0.0796	0.0739	2.1393
5	207.5	260.3	187.9	166.7	87.9	199.9	334.5	337.1	310.0	215.8	-246.6	-137.1	256.44	272.76	0.0270	0.0264	2.1413
6	204.8	257.2	184.7	161.1	88.5	200.4	346.4	347.8	317.2	218.4	-257.9	-147.4	251.13	263.17	0.0039	0.0050	2.1393
7	189.8	248.2	167.4	139.4	89.5	205.3	358.3	358.6	316.7	207.2	-268.8	-153.3	225.45	225.94	-0.0167	-0.0144	2.1054

SL	B-1 DEGREE	B-2 DEGREE	B'-1 DEGREE	B'-2 DEGREE	M-1	M-2	M'-1	M'-2	INCS DEGREE	INCM DEGREE	DEV DEGREE	TURN DEGREE	D FAC	OMEGA-B TOTAL	LOSS-P TOTAL	PO2/ PO1	%EFF-A TOTAL	%EFF-P TOTAL
1	23.3	50.6	44.29	15.97	0.5739	0.7821	0.7370	0.5150	0.0	0.0	0.0	28.33	0.4692	0.0729	0.0234	1.4389	94.01	94.32
2	22.2	48.6	44.37	19.33	0.6090	0.7951	0.7899	0.5552	0.0	0.0	0.0	25.03	0.4493	0.0564	0.0183	1.4505	94.90	95.16
3	22.8	48.7	46.00	24.13	0.6102	0.7770	0.8113	0.5603	0.0	0.0	0.0	21.88	0.4506	0.0453	0.0146	1.4481	95.67	95.90
4	24.1	49.2	49.34	32.68	0.6057	0.7429	0.8502	0.5758	0.0	0.0	0.0	16.66	0.4476	0.0360	0.0112	1.4415	96.21	96.41
5	25.0	50.1	52.63	39.39	0.5953	0.7174	0:8895	0.5949	0.0	0.0	0.0	13.24	0.4458	0.0452	0.0134	1.4419	94.95	95.21
6	25.6	51.2	54.36	42.43	0.5851	0.7043	0.9061	0.5981	0.0	0.0	0.0	11.94	0.4510	0.0541	0.0157	1.4474	93.92	94.23
7	28.1	55.8	58.09	47.72	0.5382	0.6734	0.8979	0.5622	0.0	0.0	0.0	10.37	0.4903	0.0710	0.0191	1.4714	92.56	92.96

SL	V-1 FT/SEC	V-2 FT/SEC	VM-1 FT/SEC	VM-2 FT/SEC	VO-1 FT/SEC	VO-2 FT/SEC	U-1 FT/SEC	U-2 FT/SEC	V'-1 FT/SEC	V'-2 FT/SEC	VO'-1 FT/SEC	VO'-2 FT/SEC	RHOVM-1 LBM/FT2SEC	RHOVM-2 LBM/FT2SEC	EPSI-1 DEGREE	EPSI-2 DEGREE	PCT TE SPAN
1	666.7	935.0	612.0	591.7	264.4	724.0	863.2	894.2	856.2	615.7	-598.8	-170.2	49.66	54.55	11.241	10.427	0.1000
2	700.4	943.5	648.1	621.1	265.6	710.2	902.3	929.5	908.6	658.7	-636.7	-219.3	53.68	59.37	9.586	8.823	0.2000
3	698.2	918.9	643.1	604.1	271.9	692.5	941.3	964.8	928.3	662.6	-669.4	-272.3	53.90	59.18	7.886	7.244	0.3000
4	690.2	878.3	629.6	572.1	282.9	666.4	1019.4	1035.4	968.9	680.8	-736.5	-368.9	53.52	57.82	4.560	4.232	0.5000
5	680.7	854.0	616.5	546.8	288.5	656.0	1097.5	1106.0	1017.1	708.2	-809.0	-450.0	52.52	55.86	1.549	1.512	0.7000
6	672.0	843.8	606.0	528.6	290.4	657.6	1136.5	1141.3	1040.8	716.5	-846.1	-483.6	51.43	53.90	0.221	0.287	0.8000
7	622.8	814.2	549.3	457.3	293.5	673.7	1175.5	1176.5	1039.1	679.7	-882.1	-502.9	46.18	46.27	-0.955	-0.826	0.9000

WC1/A1 LBM/SEC SQFT	WC1/A1 KG/SEC SQM	TO/TO INLET	PO/PO INLET	EFF-AD INLET %	EFF-P INLET %
36.56	178.49	1.2646	2.1227	90.56	91.50

TO2/TO1	PO2/PO1	EFF-AD ROTOR %	EFF-P ROTOR %
1.1177	1.4483	94.58	94.86

STATOR 7

AIRFOIL AERODYNAMIC SUMMARY PRINT

RUN NO 100 SPEED CODE 10 POINT NO 3

SL	V-1 M/SEC	V-2 M/SEC	VM-1 M/SEC	VM-2 M/SEC	VO-1 M/SEC	VO-2 M/SEC	RHOVM-1 KG/M2 SEC	RHOVM-2 KG/M2 SEC	PO/PO INLET	TO/TO INLET	%EFF-A TOT-INLET	%EFF-P TOT-INLET	EPSI-1 RADIAN	EPSI-2 RADIAN
1	288.6	192.8	189.7	168.3	217.4	93.9	278.14	284.07	2.0180	1.2884	76.95	79.08	0.1729	0.1577
2	292.2	209.9	199.1	186.2	213.8	96.8	301.81	322.61	2.1020	1.2741	86.18	87.54	0.1498	0.1345
3	285.5	208.5	194.6	183.8	208.9	98.6	301.87	323.80	2.1126	1.2592	91.87	92.68	0.1265	0.1120
4	273.9	203.4	185.1	176.7	201.9	100.6	295.87	317.23	2.1163	1.2459	97.03	97.33	0.0815	0.0689
5	266.4	198.7	176.7	171.1	199.4	100.9	285.65	307.44	2.1149	1.2538	93.92	94.52	0.0397	0.0291
6	263.1	196.0	170.8	168.2	200.1	100.6	275.88	300.39	2.1101	1.2649	89.66	90.68	0.0198	0.0105
7	254.1	185.2	149.9	154.4	205.2	102.2	240.42	272.19	2.0718	1.2787	82.90	84.55	-0.0020	-0.0085

SL	B-1 DEGREE	B-2 DEGREE	M-1	M-2	INCS DEGREE	INCM DEGREE	DEV. DEGREE	TURN DEGREE	D-FAC	OMEGA-B TOTAL	LOSS-P TOTAL	PO2/ PO1	PO/PO STAGE	TO/TO STAGE	%EFF-A TOT-STG	%EFF-P TOT-STG
1	49.0	29.2	0.7932	0.5123	0.0	0.0	0.0	19.82	0.5014	0.0668	0.0239	0.9775	1.4052	1.1159	87.79	88.37
2	47.1	27.5	0.8095	0.5637	0.0	0.0	0.0	19.64	0.4444	0.0527	0.0193	0.9815	1.4233	1.1178	89.81	90.32
3	47.1	28.2	0.7940	0.5634	0.0	0.0	0.0	18.87	0.4293	0.0433	0.0160	0.9852	1.4271	1.1165	91.58	91.99
4	47.5	29.7	0.7621	0.5517	0.0	0.0	0.0	17.85	0.4139	0.0336	0.0124	0.9893	1.4262	1.1142	93.23	93.56
5	48.5	30.5	0.7361	0.5365	0.0	0.0	0.0	17.93	0.4139	0.0403	0.0151	0.9878	1.4242	1.1157	91.67	92.08
6	49.5	30.9	0.7223	0.5265	0.0	0.0	0.0	18.63	0.4202	0.0493	0.0185	0.9855	1.4249	1.1178	90.09	90.58
7	53.9	33.5	0.6911	0.4931	0.0	0.0	0.0	20.37	0.4508	0.0652	0.0240	0.9821	1.4420	1.1246	88.21	88.81

SL	V-1 FT/SEC	V-2 FT/SEC	VM-1 FT/SEC	VM-2 FT/SEC	VO-1 FT/SEC	VO-2 FT/SEC	RHOVM-1 LBM/FT2SEC	RHOVM-2 LBM/FT2SEC	PCT TE SPAN	TO/TO INLET	%EFF-A TOT-INLET	%EFF-P TOT-INLET	EPSI-1 DEGREE	EPSI-2 DEGREE
1	946.8	632.4	622.5	552.3	713.4	308.0	56.97	58.18	0.1000	1.2884	76.95	79.08	9.906	9.037
2	958.6	688.6	653.4	611.0	701.4	317.5	61.81	66.07	0.2000	1.2741	86.18	87.54	8.585	7.706
3	936.8	684.2	638.6	602.9	685.5	323.5	61.83	66.32	0.3000	1.2592	91.87	92.68	7.245	6.416
4	898.7	667.2	607.5	579.8	662.4	330.1	60.60	64.97	0.5000	1.2459	97.03	97.33	4.669	3.948
5	874.1	651.9	579.7	561.5	654.2	331.2	58.50	62.97	0.7000	1.2538	93.92	94.52	2.273	1.666
6	863.2	643.2	560.4	551.9	656.6	330.2	56.50	61.52	0.8000	1.2649	89.66	90.68	1.134	0.602
7	833.7	607.6	491.7	506.7	673.3	335.2	49.24	55.75	0.9000	1.2787	82.90	84.55	-0.112	-0.490

NCORR INLET RPM	WCORR INLET LBM/SEC	WCORR INLET KG/SEC	TO/TO INLET	PO/PO INLET	EFF-AD INLET %	EFF-P INLET %		TO/TO STAGE	PO2/PO1	PO/PO STAGE	EFF-AD STAGE %	EFF-P STAGE %
12136.50	77.44	35.13	1.2646	2.0897	88.47	89.60		1.1177	0.9845	1.4258	90.38	90.86

ROTOR 8

AIRFOIL AERODYNAMIC SUMMARY PRINT

RUN NO 100 SPEED CODE 10 POINT NO 3

SL	V-1 M/SEC	V-2 M/SEC	VM-1 M/SEC	VM-2 M/SEC	VO-1 M/SEC	VO-2 M/SEC	U-1 M/SEC	U-2 M/SEC	V'-1 M/SEC	V'-2 M/SEC	VO'-1 M/SEC	VO'-2 M/SEC	RHOVM-1 KG/M2 SEC	RHOVM-2 KG/M2 SEC	EPSI-1 RADIAN	EPSI-2 RADIAN	PO/PO INLET
1	200.7	289.6	177.8	171.4	93.1	233.4	284.7	290.0	261.5	180.5	-191.7	-56.5	297.02	321.01	0.1425	0.1104	2.8571
2	217.3	295.6	194.9	186.6	96.0	229.3	293.8	298.4	277.7	199.0	-197.8	-69.1	333.86	362.16	0.1177	0.0926	2.9665
3	216.3	288.6	192.9	182.0	98.0	223.9	302.9	306.7	281.4	200.0	-204.9	-82.9	335.78	362.11	0.0945	0.0737	2.9679
4	211.6	275.9	186.3	172.3	100.2	215.4	321.0	323.5	288.9	203.4	-220.8	-108.1	330.28	352.59	0.0488	0.0344	2.9522
5	206.7	268.7	180.4	164.2	100.8	212.8	339.2	340.3	298.9	207.9	-238.3	-127.5	320.28	337.72	0.0055	-0.0045	2.9476
6	203.5	265.5	176.9	158.7	100.6	212.9	348.2	348.7	304.3	208.8	-247.6	-135.8	312.46	324.68	-0.0148	-0.0232	2.9392
7	192.1	256.0	162.7	138.1	102.2	215.6	357.3	357.1	302.5	197.7	-255.1	-141.5	284.13	279.39	-0.0325	-0.0386	2.8863

SL	B-1 DEGREE	B-2 DEGREE	B'-1 DEGREE	B'-2 DEGREE	M-1	M-2	M'-1	M'-2	INCS DEGREE	INCM DEGREE	DEV DEGREE	TURN DEGREE	D FAC	OMEGA-B TOTAL	LOSS-P TOTAL	PO2/ PO1	%EFF-A TOTAL	%EFF-P TOTAL
1	27.7	53.6	47.18	18.21	0.5346	0.7517	0.6965	0.4684	0.0	0.0	0.0	28.98	0.4998	0.0793	0.0258	1.4113	93.72	94.02
2	26.2	50.8	45.40	20.26	0.5850	0.7746	0.7476	0.5214	0.0	0.0	0.0	25.14	0.4576	0.0583	0.0194	1.4095	94.74	94.99
3	26.9	50.8	46.69	24.41	0.5859	0.7598	0.7621	0.5267	0.0	0.0	0.0	22.28	0.4564	0.0468	0.0157	1.4046	95.57	95.78
4	28.2	51.3	49.78	32.04	0.5754	0.7277	0.7857	0.5365	0.0	0.0	0.0	17.75	0.4555	0.0358	0.0120	1.3948	96.32	96.50
5	29.2	52.3	52.86	37.82	0.5593	0.7036	0.8090	0.5443	0.0	0.0	0.0	15.04	0.4636	0.0462	0.0153	1.3941	95.07	95.30
6	29.6	53.3	54.46	40.56	0.5477	0.6904	0.8189	0.5430	0.0	0.0	0.0	13.90	0.4731	0.0560	0.0184	1.3958	94.02	94.30
7	32.2	57.4	57.48	45.71	0.5126	0.6592	0.8071	0.5091	0.0	0.0	0.0	11.77	0.5100	0.0715	0.0222	1.3980	92.69	93.02

SL	V-1 FT/SEC	V-2 FT/SEC	VM-1 FT/SEC	VM-2 FT/SEC	VO-1 FT/SEC	VO-2 FT/SEC	U-1 FT/SEC	U-2 FT/SEC	V'-1 FT/SEC	V'-2 FT/SEC	VO'-1 FT/SEC	VO'-2 FT/SEC	RHOVM-1 LBM/FT2SEC	RHOVM-2 LBM/FT2SEC	EPSI-1 DEGREE	EPSI-2 DEGREE	PCT TE SPAN
1	658.5	950.2	583.5	562.3	305.3	765.9	934.1	951.4	857.8	592.1	-628.8	-185.5	60.83	65.75	8.163	6.326	0.1000
2	712.9	969.8	639.5	612.2	315.1	752.2	963.9	978.9	911.0	652.8	-648.8	-226.7	68.38	74.17	6.744	5.305	0.2000
3	709.8	946.7	632.9	597.3	321.4	734.6	993.7	1006.4	923.3	656.3	-672.3	-271.9	68.77	74.16	5.415	4.224	0.3000
4	694.2	905.1	611.4	565.3	328.8	706.9	1053.2	1061.5	947.9	667.3	-724.4	-354.6	67.64	72.21	2.796	1.970	0.5000
5	678.0	881.8	591.9	538.7	330.8	698.1	1112.8	1116.5	980.7	682.1	-782.0	-418.5	65.60	69.17	0.315	-0.256	0.7000
6	667.7	871.2	580.3	520.6	330.2	698.5	1142.5	1144.1	998.4	685.2	-812.4	-445.6	63.99	66.50	-0.850	-1.327	0.8000
7	630.4	840.1	533.8	453.2	335.5	707.3	1172.3	1171.6	992.6	648.8	-836.9	-464.2	58.19	57.22	-1.860	-2.210	0.9000

WC1/A1 LBM/SEC SQFT	WC1/A1 KG/SEC SQM	TO/TO INLET	PO/PO INLET	EFF-AD INLET %	EFF-P INLET %		T02/T01	P02/P01	EFF-AD ROTOR %	EFF-P ROTOR %
34.31	167.54	1.3986	2.9258	89.79	91.20		1.1060	1.4001	94.64	94.89

STATOR 8

AIRFOIL AERODYNAMIC SUMMARY PRINT

RUN NO 100 SPEED CODE 10 POINT NO 3

SL	V-1 M/SEC	V-2 M/SEC	VM-1 M/SEC	VM-2 M/SEC	VO-1 M/SEC	VO-2 M/SEC	RHOVM-1 KG/M2 SEC	RHOVM-2 KG/M2 SEC	PO/PO INLET	TO/TO INLET	%EFF-A TOT-INLET	%EFF-P TOT-INLET	EPSI-1 RADIAN	EPSI-2 RADIAN
1	291.7	177.8	177.2	152.4	231.7	91.5	330.31	326.02	2.7573	1.4307	77.79	80.67	0.1116	0.1071
2	299.4	205.1	194.2	181.4	227.9	95.6	373.73	399.89	2.9021	1.4130	85.90	87.82	0.0957	0.0893
3	293.7	205.0	191.3	180.4	222.9	97.5	376.44	405.13	2.9212	1.3932	90.92	92.17	0.0783	0.0714
4	282.1	199.4	182.7	173.1	214.9	99.0	369.41	396.06	2.9184	1.3742	95.41	96.05	0.0431	0.0370
5	275.0	194.8	174.3	167.7	212.6	99.2	354.57	381.79	2.9066	1.3847	92.38	93.43	0.0089	0.0047
6	271.6	191.9	168.5	164.5	212.9	98.7	341.37	370.92	2.8934	1.3993	88.55	90.11	-0.0077	-0.0108
7	262.0	178.7	148.5	148.5	215.9	99.5	297.68	328.89	2.8315	1.4173	82.74	85.04	-0.0251	-0.0269

SL	B-1 DEGREE	B-2 DEGREE	M-1	M-2	INCS DEGREE	INCM DEGREE	DEV DEGREE	TURN DEGREE	D-FAC	OMEGA-B TOTAL	LOSS-P TOTAL	PO2/ PO1	PO/PO STAGE	TO/TO STAGE	%EFF-A TOT-STG	%EFF-P TOT-STG
1	52.6	31.0	0.7577	0.4461	0.0	0.0	0.0	21.61	0.5905	0.0864	0.0317	0.9732	1.3729	1.1096	85.84	86.45
2	49.6	27.8	0.7856	0.5212	0.0	0.0	0.0	21.79	0.5026	0.0599	0.0227	0.9800	1.3815	1.1083	88.75	89.25
3	49.4	28.4	0.7747	0.5249	0.0	0.0	0.0	20.98	0.4847	0.0491	0.0185	0.9839	1.3827	1.1063	90.70	91.11
4	49.6	29.8	0.7459	0.5135	0.0	0.0	0.0	19.86	0.4700	0.0378	0.0142	0.9883	1.3789	1.1031	92.76	93.08
5	50.7	30.6	0.7217	0.4990	0.0	0.0	0.0	20.04	0.4702	0.0479	0.0178	0.9860	1.3744	1.1040	90.94	91.34
6	51.6	31.0	0.7078	0.4885	0.0	0.0	0.0	20.67	0.4763	0.0581	0.0216	0.9835	1.3723	1.1054	89.22	89.69
7	55.5	33.8	0.6761	0.4507	0.0	0.0	0.0	21.64	0.5122	0.0789	0.0284	0.9792	1.3688	1.1075	86.67	87.24

SL	V-1 FT/SEC	V-2 FT/SEC	VM-1 FT/SEC	VM-2 FT/SEC	VO-1 FT/SEC	VO-2 FT/SEC	RHOVM-1 LBM/FT2SEC	RHOVM-2 LBM/FT2SEC	PCT TE SPAN	TO/TO INLET	%EFF-A TOT-INLET	%EFF-P TOT-INLET	EPSI-1 DEGREE	EPSI-2 DEGREE
1	957.1	583.3	581.6	500.0	760.2	300.4	67.65	66.77	0.1000	1.4307	77.79	80.67	6.392	6.134
2	982.3	672.9	637.0	595.2	747.7	313.8	76.54	81.90	0.2000	1.4130	85.90	87.82	5.484	5.119
3	963.6	672.7	627.6	591.8	731.2	320.0	77.10	82.97	0.3000	1.3932	90.92	92.17	4.484	4.092
4	925.6	654.4	599.5	568.0	705.2	325.0	75.66	81.12	0.5000	1.3742	95.41	96.05	2.467	2.120
5	902.2	639.2	572.0	550.1	697.7	325.5	72.62	78.19	0.7000	1.3847	92.38	93.43	0.510	0.267
6	891.0	629.6	553.0	539.9	698.6	323.9	69.92	75.97	0.8000	1.3993	88.55	90.11	-0.439	-0.621
7	859.7	586.4	487.3	487.1	708.2	326.5	60.97	67.36	0.9000	1.4173	82.74	85.04	-1.440	-1.544

NCORR INLET RPM	WCORR INLET LBM/SEC	WCORR INLET KG/SEC	TO/TO INLET	PO/PO INLET	EFF-AD INLET %	EFF-P INLET %		TO/TO STAGE	PO2/PO1	PO/PO STAGE	EFF-AD STAGE %	EFF-P STAGE %
12136.50	77.44	35.13	1.3986	2.8746	88.08	89.70		1.1060	0.9825	1.3756	89.45	89.92

ROTOR 9

AIRFOIL AERODYNAMIC SUMMARY PRINT

RUN NO 100 SPEED CODE 10 POINT NO 3

SL	V-1 M/SEC	V-2 M/SEC	VM-1 M/SEC	VM-2 M/SEC	VO-1 M/SEC	VO-2 M/SEC	U-1 M/SEC	U-2 M/SEC	V'-1 M/SEC	V'-2 M/SEC	VO'-1 M/SEC	VO'-2 M/SEC	RHOVM-1 KG/M2 SEC	RHOVM-2 KG/M2 SEC	EPSI-1 RADIAN	EPSI-2 RADIAN	PO/PO INLET
1	189.0	283.6	165.6	158.5	91.1	235.2	297.8	300.6	264.8	171.4	-206.7	-65.4	350.83	374.33	0.0850	0.0722	3.8381
2	214.1	292.3	191.7	183.8	95.2	227.3	304.9	307.2	284.1	200.4	-209.7	-79.9	417.96	450.05	0.0678	0.0581	3.9818
3	214.1	286.5	190.8	181.2	97.1	221.9	311.9	313.8	287.3	203.2	-214.8	-91.9	423.49	454.10	0.0514	0.0438	3.9848
4	208.9	275.0	184.1	172.6	98.8	214.1	326.0	327.0	292.4	206.2	-227.2	-112.9	415.76	443.19	0.0183	0.0138	3.9578
5	203.8	269.2	178.1	165.0	99.2	212.8	340.1	340.3	299.6	208.5	-240.9	-127.5	400.71	422.90	-0.0141	-0.0164	3.9442
6	200.4	266.6	174.3	159.7	98.8	213.6	347.1	346.9	303.4	208.0	-248.3	-133.3	388.71	405.75	-0.0296	-0.0311	3.9306
7	187.0	257.8	158.2	139.1	99.7	217.1	354.2	353.5	299.7	194.8	-254.5	-136.4	347.27	347.97	-0.0435	-0.0441	3.8626

SL	B-1 DEGREE	B-2 DEGREE	B'-1 DEGREE	B'-2 DEGREE	M-1	M-2	M'-1	M'-2	INCS DEGREE	INCM DEGREE	DEV DEGREE	TURN DEGREE	D FAC	OMEGA-B TOTAL	LOSS-P TOTAL	PO2/ PO1	%EFF-A TOTAL	%EFF-P TOTAL
1	28.8	56.0	51.31	22.41	0.4756	0.6959	0.6664	0.4207	0.0	0.0	0.0	28.90	0.5612	0.0973	0.0335	1.3834	92.51	92.86
2	26.4	51.0	47.55	23.48	0.5455	0.7264	0.7240	0.4981	0.0	0.0	0.0	24.08	0.4744	0.0615	0.0216	1.3696	94.26	94.52
3	27.0	50.7	48.36	26.86	0.5497	0.7168	0.7376	0.5084	0.0	0.0	0.0	21.50	0.4644	0.0503	0.0176	1.3640	95.08	95.29
4	28.2	51.1	50.97	33.17	0.5393	0.6909	0.7547	0.5180	0.0	0.0	0.0	17.80	0.4584	0.0395	0.0136	1.3564	95.88	96.06
5	29.1	52.2	53.53	37.71	0.5233	0.6711	0.7691	0.5198	0.0	0.0	0.0	15.82	0.4686	0.0482	0.0165	1.3577	94.87	95.09
6	29.6	53.2	54.94	39.88	0.5112	0.6598	0.7740	0.5147	0.0	0.0	0.0	15.07	0.4806	0.0565	0.0191	1.3609	94.04	94.30
7	32.2	57.4	58.14	44.46	0.4725	0.6313	0.7571	0.4769	0.0	0.0	0.0	13.68	0.5245	0.0708	0.0228	1.3680	92.98	93.30

SL	V-1 FT/SEC	V-2 FT/SEC	VM-1 FT/SEC	VM-2 FT/SEC	VO-1 FT/SEC	VO-2 FT/SEC	U-1 FT/SEC	U-2 FT/SEC	V'-1 FT/SEC	V'-2 FT/SEC	VO'-1 FT/SEC	VO'-2 FT/SEC	RHOVM-1 LBM/FT2SEC	RHOVM-2 LBM/FT2SEC	EPSI-1 DEGREE	EPSI-2 DEGREE	PCT TE SPAN
1	620.1	930.4	543.3	520.0	299.0	771.6	977.2	986.1	869.0	562.5	-678.2	-214.6	71.85	76.67	4.868	4.139	0.1000
2	702.3	959.0	629.1	603.1	312.3	745.6	1000.3	1007.8	932.2	657.7	-687.9	-262.2	85.60	92.17	3.883	3.329	0.2000
3	702.6	940.1	626.2	594.7	318.6	728.1	1023.4	1029.6	942.7	666.7	-704.7	-301.5	86.74	93.00	2.945	2.510	0.3000
4	685.5	902.4	603.9	566.3	324.3	702.6	1069.6	1073.0	959.3	676.6	-745.3	-370.4	85.15	90.77	1.049	0.789	0.5000
5	668.8	883.3	584.2	541.2	325.5	698.1	1115.8	1116.4	982.8	684.1	-790.4	-418.4	82.07	86.61	-0.805	-0.938	0.7000
6	657.4	874.9	571.8	523.8	324.2	700.7	1138.9	1138.1	995.4	682.5	-814.7	-437.4	79.61	83.10	-1.695	-1.782	0.8000
7	613.6	846.0	519.2	456.2	327.1	712.4	1162.0	1159.8	983.2	639.0	-835.0	-447.4	71.12	71.27	-2.492	-2.526	0.9000

WC1/A1 LBM/SEC SQFT	WC1/A1 KG/SEC SQM	TO/TO INLET	PO/PO INLET	EFF-AD INLET %	EFF-P INLET %
33.12	161.70	1.5352	3.9252	88.83	90.73

T02/T01	P02/P01	EFF-AD ROTOR %	EFF-P ROTOR %
1.0976	1.3655	94.17	94.43

STATOR 9

AIRFOIL AERODYNAMIC SUMMARY PRINT

RUN NO 100 SPEED CODE 10 POINT NO 3

SL	V-1 M/SEC	V-2 M/SEC	VM-1 M/SEC	VM-2 M/SEC	VO-1 M/SEC	VO-2 M/SEC	RHOVM-1 KG/M2 SEC	RHOVM-2 KG/M2 SEC	PO/PO INLET	TO/TO INLET	%EFF-A TOT-INLET	%EFF-P TOT-INLET	EPSI-1 RADIAN	EPSI-2 RADIAN
1	286.0	171.6	163.8	147.2	234.5	.88.1	385.15	388.79	3.7027	1.5798	77.78	81.38	0.0783	0.0735
2	295.6	203.2	189.7	180.0	226.7	94.4	461.33	492.24	3.8987	1.5517	85.65	88.08	0.0651	0.0607
3	290.8	203.0	188.3	178.9	221.6	96.0	467.96	499.29	3.9203	1.5266	90.23	91.89	0.0516	0.0476
4	280.1	196.7	180.7	171.2	214.0	96.9	459.82	486.61	3.9096	1.5029	94.24	95.22	0.0244	0.0212
5	274.3	191.6	173.1	165.4	212.8	96.6	440.25	466.40	3.8879	1.5175	91.13	92.63	-0.0022	-0.0046
6	271.8	188.2	168.0	161.8	213.6	96.1	423.68	450.55	3.8673	1.5358	87.58	89.67	-0.0155	-0.0171
7	263.1	174.0	148.2	144.2	217.4	97.4	368.35	393.79	3.7865	1.5591	82.33	85.25	-0.0297	-0.0300

SL	B-1 DEGREE	B-2 DEGREE	M-1	M-2	INCS DEGREE	INCM DEGREE	DEV DEGREE	TURN DEGREE	D-FAC	OMEGA-B TOTAL	LOSS-P TOTAL	PO2/PO1	PO/PO STAGE	TO/TO STAGE	%EFF-A TOT-STG	%EFF-P TOT-STG
1	55.1	30.9	0.7025	0.4089	0.0	0.0	0.0	24.16	0.6263	0.1143	0.0436	0.9685	1.3414	1.1044	82.83	83.54
2	50.1	27.7	0.7353	0.4919	0.0	0.0	0.0	22.42	0.5142	0.0664	0.0266	0.9800	1.3427	1.0987	87.89	88.40
3	49.6	28.2	0.7283	0.4956	0.0	0.0	0.0	22.44	0.5006	0.0552	0.0225	0.9836	1.3420	1.0965	89.75	90.18
4	49.8	29.5	0.7047	0.4833	0.0	0.0	0.0	20.32	0.4981	0.0438	0.0183	0.9876	1.3397	1.0939	91.80	92.14
5	50.9	30.3	0.6852	0.4678	0.0	0.0	0.0	20.58	0.5130	0.0536	0.0231	0.9856	1.3380	1.0951	90.22	90.62
6	51.8	30.7	0.6738	0.4563	0.0	0.0	0.0	21.10	0.5275	0.0635	0.0277	0.9834	1.3379	1.0965	88.76	89.22
7	55.7	34.0	0.6455	0.4177	0.0	0.0	0.0	21.69	0.5754	0.0854	0.0366	0.9792	1.3393	1.0993	86.51	87.07

SL	V-1 FT/SEC	V-2 FT/SEC	VM-1 FT/SEC	VM-2 FT/SEC	VO-1 FT/SEC	VO-2 FT/SEC	RHOVM-1 LBM/FT2SEC	RHOVM-2 LBM/FT2SEC	PCT TE SPAN	TO/TO INLET	%EFF-A TOT-INLET	%EFF-P TOT-INLET	EPSI-1 DEGREE	EPSI-2 DEGREE
1	938.5	563.0	537.5	483.0	769.3	289.1	78.88	79.63	0.1000	1.5798	77.78	81.38	4.488	4.212
2	969.9	666.8	622.4	590.6	743.9	309.6	94.48	100.82	0.2000	1.5517	85.65	88.08	3.729	3.477
3	954.0	666.2	617.8	587.1	726.9	314.8	95.84	102.26	0.3000	1.5266	90.23	91.89	2.955	2.728
4	918.9	645.4	592.7	561.7	702.2	317.9	94.18	99.66	0.5000	1.5029	94.24	95.22	1.400	1.213
5	900.1	628.5	568.0	542.7	698.2	317.0	90.17	95.52	0.7000	1.5175	91.13	92.63	-0.127	-0.265
6	891.6	617.4	551.1	530.7	700.9	315.5	86.77	92.28	0.8000	1.5358	87.58	89.67	-0.889	-0.982
7	863.3	571.0	486.3	473.2	713.3	319.5	75.44	80.65	0.9000	1.5591	82.33	85.25	-1.699	-1.720

NCORR INLET RPM	WCORR INLET LBM/SEC	WCORR INLET KG/SEC		TO/TO INLET	PO/PO INLET	EFF-AD INLET %	EFF-P INLET %		TO/TO STAGE	PO2/PO1	PO/PO STAGE	EFF-AD STAGE %	EFF-P STAGE %
12136.50	77.44	35.13		1.5352	3.8541	87.40	89.52		1.0976	0.9819	1.3407	88.41	88.89

ROTOR 10

AIRFOIL AERODYNAMIC SUMMARY PRINT

RUN NO 100 SPEED CODE 10 POINT NO 3

SL	V-1 M/SEC	V-2 M/SEC	VM-1 M/SEC	VM-2 M/SEC	VO-1 M/SEC	VO-2 M/SEC	U-1 M/SEC	U-2 M/SEC	V'-1 M/SEC	V'-2 M/SEC	VO'-1 M/SEC	VO'-2 M/SEC	RHOVM-1 KG/M2 SEC	RHOVM-2 KG/M2 SEC	EPSI-1 RADIAN	EPSI-2 RADIAN	PO/PO INLET
1	176.8	276.3	153.3	146.6	88.0	234.3	304.7	306.6	265.5	163.4	-216.7	-72.4	403.25	425.31	0.0635	0.0537	5.0125
2	208.0	286.3	185.5	177.1	94.1	224.9	310.5	312.1	285.0	197.5	-216.4	-87.2	504.30	535.31	0.0509	0.0430	5.1934
3	208.5	281.2	185.2	175.7	95.8	219.6	316.3	317.6	288.0	201.2	-220.6	-98.0	513.18	543.84	0.0382	0.0318	5.2024
4	202.8	270.5	178.2	167.7	96.8	212.2	328.0	328.6	291.9	204.2	-231.1	-116.4	502.81	531.88	0.0109	0.0073	5.1712
5	197.4	266.1	172.1	160.5	96.7	212.2	339.6	339.6	297.7	205.0	-242.9	-127.4	482.17	505.79	-0.0166	-0.0185	5.1571
6	193.7	264.1	168.1	154.8	96.2	214.0	345.4	345.1	300.5	202.9	-249.2	-131.1	465.37	482.10	-0.0297	-0.0313	5.1409
7	179.3	255.3	150.5	131.2	97.5	219.0	351.2	350.6	295.0	185.8	-253.7	-131.6	408.85	400.81	-0.0410	-0.0424	5.0546

SL	B-1 DEGREE	B-2 DEGREE	B'-1 DEGREE	B'-2 DEGREE	M-1	M-2	M'-1	M'-2	INCS DEGREE	INCM DEGREE	DEV DEGREE	TURN DEGREE	D FAC	OMEGA-B TOTAL	LOSS-P TOTAL	PO2/ PO1	%EFF-A TOTAL	%EFF-P TOTAL
1	29.8	57.9	54.72	26.26	0.4218	0.6441	0.6334	0.3810	0.0	0.0	0.0	28.46	0.6451	0.1211	0.0505	1.3494	90.95	91.33
2	26.9	51.8	49.39	26.20	0.5040	0.6778	0.6906	0.4675	0.0	0.0	0.0	23.19	0.5257	0.0716	0.0304	1.3309	93.30	93.57
3	27.3	51.3	49.98	29.15	0.5094	0.6712	0.7038	0.4802	0.0	0.0	0.0	20.83	0.5092	0.0577	0.0243	1.3270	94.32	94.55
4	28.5	51.7	52.36	34.76	0.4989	0.6492	0.7180	0.4901	0.0	0.0	0.0	17.61	0.4982	0.0435	0.0178	1.3229	95.47	95.65
5	29.3	52.9	54.68	38.45	0.4828	0.6334	0.7280	0.4880	0.0	0.0	0.0	16.23	0.5123	0.0532	0.0215	1.3271	94.45	94.67
6	29.8	54.1	56.01	40.27	0.4702	0.6238	0.7298	0.4792	0.0	0.0	0.0	15.74	0.5294	0.0626	0.0251	1.3314	93.59	93.85
7	33.0	59.1	59.34	45.10	0.4308	0.5962	0.7087	0.4338	0.0	0.0	0.0	14.23	0.5871	0.0797	0.0300	1.3388	92.46	92.77

SL	V-1 FT/SEC	V-2 FT/SEC	VM-1 FT/SEC	VM-2 FT/SEC	VO-1 FT/SEC	VO-2 FT/SEC	U-1 FT/SEC	U-2 FT/SEC	V'-1 FT/SEC	V'-2 FT/SEC	VO'-1 FT/SEC	VO'-2 FT/SEC	RHOVM-1 LBM/FT2SEC	RHOVM-2 LBM/FT2SEC	EPSI-1 DEGREE	EPSI-2 DEGREE	PCT TE SPAN
1	580.0	906.6	503.1	480.8	288.7	768.6	999.8	1006.0	871.1	536.3	-711.1	-237.4	82.59	87.11	3.641	3.078	0.1000
2	682.4	939.2	608.5	581.2	308.9	737.8	1018.9	1024.0	935.0	647.8	-710.0	-286.2	103.29	109.64	2.919	2.464	0.2000
3	684.0	922.7	607.5	576.5	314.2	720.4	1037.9	1042.1	944.9	660.1	-723.7	-321.7	105.10	111.38	2.191	1.823	0.3000
4	665.4	887.4	584.7	550.3	317.7	696.2	1076.1	1078.2	957.6	669.9	-758.4	-382.0	102.98	108.93	0.627	0.418	0.5000
5	647.8	872.9	564.8	526.7	317.2	696.2	1114.2	1114.3	976.9	672.5	-797.0	-418.1	98.75	103.59	-0.953	-1.059	0.7000
6	635.4	866.6	551.4	508.0	315.7	702.1	1133.2	1132.3	986.1	665.7	-817.5	-430.2	95.31	98.74	-1.704	-1.794	0.8000
7	588.3	837.7	493.7	430.3	319.9	718.7	1152.3	1150.4	967.8	609.6	-832.4	-431.7	83.74	82.09	-2.350	-2.427	0.9000

WC1/A1 LBM/SEC SQFT	WC1/A1 KG/SEC SQM	TO/TO INLET	PO/PO INLET	EFF-AD INLET %	EFF-P INLET %		T02/T01	P02/P01	EFF-AD ROTOR %	EFF-P ROTOR %
31.15	152.07	1.6726	5.1326	87.83	90.24		1.0895	1.3317	93.54	93.80

STATOR 10

AIRFOIL AERODYNAMIC SUMMARY PRINT

RUN NO 100 SPEED CODE 10 POINT NO 3

SL	V-1 M/SEC	V-2 M/SEC	VM-1 M/SEC	VM-2 M/SEC	VO-1 M/SEC	VO-2 M/SEC	RHOVM-1 KG/M2 SEC	RHOVM-2 KG/M2 SEC	PO/PO INLET	TO/TO INLET	%EFF-A TOT-INLET	%EFF-P TOT-INLET	EPSI-1 RADIAN	EPSI-2 RADIAN
1	278.4	154.4	151.2	131.7	233.8	80.7	437.20	421.54	4.8263	1.7359	76.51	80.95	0.0555	0.0509
2	288.9	192.8	181.8	171.5	224.5	88.1	546.72	572.27	5.0825	1.6927	84.63	87.64	0.0464	0.0429
3	284.7	194.4	181.4	172.4	219.4	89.9	558.15	587.92	5.1188	1.6619	89.12	91.27	0.0367	0.0337
4	274.7	188.9	174.5	165.5	212.2	91.1	549.64	576.01	5.1094	1.6321	93.22	94.57	0.0165	0.0158
5	270.5	184.6	167.7	160.4	212.2	91.3	525.11	552.50	5.0840	1.6503	90.24	92.17	-0.0042	-0.0018
6	268.7	181.6	162.5	157.1	214.0	91.2	503.22	533.39	5.0596	1.6729	86.85	89.43	-0.0151	-0.0109
7	260.4	166.8	140.6	138.8	219.2	92.5	427.18	460.64	4.9586	1.7028	81.83	85.34	-0.0277	-0.0210

SL	B-1 DEGREE	B-2 DEGREE	M-1	M-2	INCS DEGREE	INCM DEGREE	DEV DEGREE	TURN DEGREE	D-FAC	OMEGA-B TOTAL	LOSS-P TOTAL	PO2/ PO1	PO/PO STAGE	TO/TO STAGE	%EFF-A TOT-STG	%EFF-P TOT-STG
1	57.1	31.5	0.6492	0.3501	0.0	0.0	0.0	25.63	0.7033	0.1346	0.0537	0.9676	1.3091	1.0977	80.31	81.03
2	51.0	27.2	0.6845	0.4455	0.0	0.0	0.0	23.84	0.5570	0.0747	0.0316	0.9800	1.3049	1.0898	86.35	86.85
3	50.4	27.6	0.6800	0.4535	0.0	0.0	0.0	22.87	0.5375	0.0614	0.0264	0.9837	1.3057	1.0879	88.54	88.96
4	50.6	28.8	0.6601	0.4442	0.0	0.0	0.0	21.73	0.5328	0.0482	0.0211	0.9878	1.3069	1.0858	91.09	91.43
5	51.7	29.6	0.6450	0.4313	0.0	0.0	0.0	22.04	0.5480	0.0589	0.0264	0.9857	1.3077	1.0875	89.53	89.92
6	52.8	30.1	0.6357	0.4213	0.0	0.0	0.0	22.66	0.5632	0.0701	0.0317	0.9833	1.3085	1.0891	88.00	88.44
7	57.3	33.7	0.6092	0.3825	0.0	0.0	0.0	23.67	0.6191	0.0955	0.0422	0.9789	1.3100	1.0920	85.51	86.05

SL	V-1 FT/SEC	V-2 FT/SEC	VM-1 FT/SEC	VM-2 FT/SEC	VO-1 FT/SEC	VO-2 FT/SEC	RHOVM-1 LBM/FT2SEC	RHOVM-2 LBM/FT2SEC	PCT TE SPAN	TO/TO INLET	%EFF-A TOT-INLET	%EFF-P TOT-INLET	EPSI-1 DEGREE	EPSI-2 DEGREE
1	913.3	506.7	496.0	432.1	767.0	264.7	89.54	86.34	0.1000	1.7359	76.51	80.95	3.179	2.918
2	947.9	632.6	596.5	562.8	736.7	288.9	111.97	117.21	0.2000	1.6927	84.63	87.64	2.661	2.457
3	934.0	637.9	595.2	565.5	719.8	295.1	114.31	120.41	0.3000	1.6619	89.12	91.27	2.101	1.931
4	901.3	619.7	572.5	542.9	696.1	298.9	112.57	117.97	0.5000	1.6321	93.22	94.57	0.948	0.905
5	887.4	605.6	550.1	526.3	696.3	299.5	107.55	113.16	0.7000	1.6503	90.24	92.17	-0.242	-0.102
6	881.5	596.0	533.2	515.5	702.0	299.1	103.06	109.24	0.8000	1.6729	86.85	89.43	-0.866	-0.623
7	854.4	547.3	461.2	455.5	719.3	303.5	87.49	94.34	0.9000	1.7028	81.83	85.34	-1.584	-1.203

NCORR INLET RPM	WCORR INLET LBM/SEC	WCORR INLET KG/SEC	TO/TO INLET	PO/PO INLET	EFF-AD INLET %	EFF-P INLET %	TO/TO STAGE	PO2/PO1	PO/PO STAGE	EFF-AD STAGE %	EFF-P STAGE %
12136.50	77.44	35.13	1.6726	5.0405	86.62	89.24	1.0895	0.9821	1.3078	87.41	87.88

213

ROTOR 11

AIRFOIL AERODYNAMIC SUMMARY PRINT

RUN NO 100 SPEED CODE 10 POINT NO 3

SL	V-1 M/SEC	V-2 M/SEC	VM-1 M/SEC	VM-2 M/SEC	VO-1 M/SEC	VO-2 M/SEC	U-1 M/SEC	U-2 M/SEC	V'-1 M/SEC	V'-2 M/SEC	VO'-1 M/SEC	VO'-2 M/SEC	RHOVM-1 KG/M2 SEC	RHOVM-2 KG/M2 SEC	EPSI-1 RADIAN	EPSI-2 RADIAN	PO/PO INLET
1	162.1	270.5	140.6	140.1	80.7	231.4	309.5	310.6	268.6	161.0	-228.8	-79.3	448.01	490.44	0.0333	0.0257	6.4357
2	198.4	278.1	177.9	172.6	87.9	218.0	314.3	315.2	288.0	198.1	-226.5	-97.2	590.17	631.84	0.0242	0.0170	6.6172
3	200.4	273.2	179.2	172.6	89.7	211.7	319.1	319.8	291.1	203.6	-229.4	-108.0	607.03	647.38	0.0157	0.0090	6.6241
4	195.2	262.3	172.7	165.0	91.0	203.8	328.7	328.9	293.8	207.0	-237.7	-125.1	597.06	634.03	-0.0022	-0.0082	6.5761
5	190.4	257.9	167.0	157.5	91.3	204.3	338.3	338.0	298.1	206.6	-246.9	-133.8	572.61	599.86	-0.0198	-0.0256	6.5501
6	187.7	256.3	164.0	152.2	91.1	206.2	343.0	342.6	300.6	204.4	-251.9	-136.4	555.68	572.44	-0.0278	-0.0339	6.5301
7	175.2	248.5	148.7	130.7	92.5	211.3	347.8	347.2	295.5	188.5	-255.3	-135.8	493.50	481.48	-0.0338	-0.0406	6.4364

SL	B-1 DEGREE	B-2 DEGREE	B'-1 DEGREE	B'-2 DEGREE	M-1	M-2	M'-1	M'-2	INCS DEGREE	INCM DEGREE	DEV DEGREE	TURN DEGREE	D FAC	OMEGA-B TOTAL	LOSS-P TOTAL	PO2/ PO1	%EFF-A TOTAL	%EFF-P TOTAL
1	29.8	58.8	58.44	29.49	0.3680	0.6014	0.6098	0.3579	0.0	0.0	0.0	28.95	0.6624	0.1318	0.0527	1.3262	90.23	90.62
2	26.3	51.6	51.84	29.37	0.4590	0.6300	0.6662	0.4487	0.0	0.0	0.0	22.47	0.5240	0.0767	0.0312	1.3002	92.68	92.95
3	26.6	50.8	52.00	32.04	0.4680	0.6246	0.6797	0.4655	0.0	0.0	0.0	19.96	0.4990	0.0601	0.0241	1.2940	93.91	94.13
4	27.8	51.0	54.00	37.16	0.4596	0.6040	0.6917	0.4768	0.0	0.0	0.0	16.84	0.4825	0.0454	0.0176	1.2872	95.08	95.28
5	28.7	52.4	55.93	40.35	0.4456	0.5894	0.6978	0.4722	0.0	0.0	0.0	15.58	0.4968	0.0558	0.0213	1.2885	93.99	94.20
6	29.1	53.6	56.93	41.88	0.4362	0.5810	0.6989	0.4635	0.0	0.0	0.0	15.06	0.5130	0.0655	0.0248	1.2908	93.06	93.31
7	31.9	58.3	59.78	46.12	0.4028	0.5569	0.6794	0.4225	0.0	0.0	0.0	13.66	0.5664	0.0827	0.0295	1.2961	91.89	92.19

SL	V-1 FT/SEC	V-2 FT/SEC	VM-1 FT/SEC	VM-2 FT/SEC	VO-1 FT/SEC	VO-2 FT/SEC	U-1 FT/SEC	U-2 FT/SEC	V'-1 FT/SEC	V'-2 FT/SEC	VO'-1 FT/SEC	VO'-2 FT/SEC	RHOVM-1 LBM/FT2SEC	RHOVM-2 LBM/FT2SEC	EPSI-1 DEGREE	EPSI-2 DEGREE	PCT TE SPAN
1	531.8	887.5	461.2	459.7	264.7	759.2	1015.5	1019.2	881.2	528.1	-750.8	-260.1	91.76	100.45	1.905	1.475	0.1000
2	651.1	912.5	583.8	566.4	288.2	715.4	1031.2	1034.2	944.9	649.9	-743.0	-318.8	120.87	129.41	1.388	0.976	0.2000
3	657.5	896.2	587.9	566.2	294.4	694.7	1047.0	1049.2	954.9	668.0	-752.5	-354.5	124.33	132.59	0.899	0.513	0.3000
4	640.4	860.4	566.5	541.4	298.6	668.8	1078.4	1079.1	963.9	679.3	-779.8	-410.3	122.28	129.86	-0.129	-0.470	0.5000
5	624.5	846.2	547.9	516.7	299.7	670.2	1109.8	1109.1	978.1	678.0	-810.2	-438.9	117.28	122.86	-1.136	-1.467	0.7000
6	615.7	840.8	538.2	499.5	298.9	676.4	1125.5	1124.1	986.4	670.7	-826.6	-447.7	113.81	117.24	-1.592	-1.941	0.8000
7	574.7	815.2	488.0	428.8	303.6	693.4	1141.3	1139.0	969.5	618.4	-837.7	-445.7	101.07	98.61	-1.935	-2.326	0.9000

WC1/A1 LBM/SEC SQFT	WC1/A1 KG/SEC SQM	TO/TO INLET	PO/PO INLET	EFF-AD INLET %	EFF-P INLET %	T02/T01	P02/P01	EFF-AD ROTOR %	EFF-P ROTOR %
29.64	144.73	1.8066	6.5373	87.00	89.87	1.0806	1.2964	92.99	93.24

STATOR 11

AIRFOIL AERODYNAMIC SUMMARY PRINT

SL	V-1 M/SEC	V-2 M/SEC	VM-1 M/SEC	VM-2 M/SEC	VO-1 M/SEC	VO-2 M/SEC	RHOVM-1 KG/M2 SEC	RHOVM-2 KG/M2 SEC	PO/PO INLET	TO/TO INLET	%EFF-A TOT-INLET	%EFF-P TOT-INLET	EPSI-1 RADIAN	EPSI-2 RADIAN
1	273.3	160.9	146.1	135.9	231.0	86.2	509.76	516.00	6.2396	1.8919	76.14	81.24	0.0283	0.0244
2	280.9	191.9	177.3	169.9	217.9	89.2	646.34	675.79	6.4964	1.8301	84.14	87.62	0.0206	0.0173
3	276.4	192.2	177.7	170.3	211.7	89.1	663.26	692.91	6.5268	1.7933	88.42	90.97	0.0137	0.0106
4	266.0	185.5	170.7	163.4	204.0	87.9	652.49	679.04	6.5043	1.7575	92.41	94.09	0.0004	-0.0025
5	261.8	180.5	163.6	158.2	204.4	87.0	620.31	649.98	6.4684	1.7775	89.66	91.93	-0.0134	-0.0161
6	260.4	177.8	159.0	155.4	206.3	86.4	595.17	629.51	6.4427	1.8024	86.60	89.54	-0.0211	-0.0236
7	253.2	165.2	139.1	138.9	211.6	89.5	510.10	549.83	6.3415	1.8371	82.04	85.94	-0.0306	-0.0325

SL	B-1 DEGREE	B-2 DEGREE	M-1	M-2	INCS DEGREE	INCM DEGREE	DEV DEGREE	TURN DEGREE	D-FAC	OMEGA-B TOTAL	LOSS-P TOTAL	PO2/PO1	PO/PO STAGE	TO/TO STAGE	%EFF-A TOT-STG	%EFF-P TOT-STG
1	57.7	32.4	0.6082	0.3500	0.0	0.0	0.0	25.28	0.6626	0.1338	0.0534	0.9710	1.2894	1.0910	80.47	81.16
2	50.9	27.7	0.6368	0.4263	0.0	0.0	0.0	23.18	0.5363	0.0749	0.0318	0.9822	1.2775	1.0819	86.06	86.54
3	50.0	27.6	0.6324	0.4314	0.0	0.0	0.0	22.39	0.5204	0.0631	0.0272	0.9851	1.2750	1.0794	88.21	88.62
4	50.1	28.3	0.6131	0.4201	0.0	0.0	0.0	21.79	0.5203	0.0500	0.0220	0.9888	1.2730	1.0768	90.70	91.03
5	51.3	28.8	0.5991	0.4061	0.0	0.0	0.0	22.50	0.5400	0.0589	0.0264	0.9873	1.2721	1.0778	89.18	89.54
6	52.4	29.1	0.5913	0.3970	0.0	0.0	0.0	23.30	0.5560	0.0677	0.0306	0.9858	1.2721	1.0790	87.77	88.18
7	56.7	32.8	0.5683	0.3648	0.0	0.0	0.0	23.88	0.6014	0.0840	0.0371	0.9835	1.2742	1.0812	85.86	86.34

SL	V-1 FT/SEC	V-2 FT/SEC	VM-1 FT/SEC	VM-2 FT/SEC	VO-1 FT/SEC	VO-2 FT/SEC	RHOVM-1 LBM/FT2SEC	RHOVM-2 LBM/FT2SEC	PCT TE SPAN	TO/TO INLET	%EFF-A TOT-INLET	%EFF-P TOT-INLET	EPSI-1 DEGREE	EPSI-2 DEGREE
1	896.6	528.0	479.3	445.7	757.8	283.0	104.40	105.68	0.1000	1.8919	76.14	81.24	1.623	1.400
2	921.7	629.7	581.8	557.6	714.9	292.5	132.38	138.41	0.2000	1.8301	84.14	87.62	1.180	0.989
3	906.9	630.6	583.0	558.8	694.7	292.3	135.84	141.91	0.3000	1.7933	88.42	90.97	0.786	0.607
4	872.6	608.7	560.1	536.1	669.2	288.5	133.64	139.07	0.5000	1.7575	92.41	94.09	0.023	-0.145
5	859.0	592.3	536.9	518.9	670.6	285.5	127.04	133.12	0.7000	1.7775	89.66	91.93	-0.768	-0.924
6	854.4	583.3	521.6	509.8	676.7	283.4	121.90	128.93	0.8000	1.8024	86.60	89.54	-1.210	-1.352
7	830.7	542.1	456.3	455.6	694.2	293.7	104.47	112.61	0.9000	1.8371	82.04	85.94	-1.750	-1.860

NCORR INLET RPM	WCORR INLET LBM/SEC	WCORR INLET KG/SEC	TO/TO INLET	PO/PO INLET	EFF-AD INLET %	EFF-P INLET %	TO/TO STAGE	PO2/PO1	PO/PO STAGE	EFF-AD STAGE %	EFF-P STAGE %
12136.50	77.44	35.13	1.8066	6.4339	86.05	89.11	1.0806	0.9842	1.2759	87.08	87.54

ROTOR 12

AIRFOIL AERODYNAMIC SUMMARY PRINT

RUN NO 100 SPEED CODE 10 POINT NO 3

SL	V-1 M/SEC	V-2 M/SEC	VM-1 M/SEC	VM-2 M/SEC	VO-1 M/SEC	VO-2 M/SEC	U-1 M/SEC	U-2 M/SEC	V'-1 M/SEC	V'-2 M/SEC	VO'-1 M/SEC	VO'-2 M/SEC	RHOVM-1 KG/M2 SEC	RHOVM-2 KG/M2 SEC	EPSI-1 RADIAN	EPSI-2 RADIAN	PO/PO INLET
1	166.7	263.5	142.6	127.1	86.3	230.9	312.0	312.2	266.9	150.9	-225.6	-81.4	540.19	522.85	0.0165	0.0035	8.0159
2	196.4	275.1	175.0	165.4	89.1	219.8	316.1	316.2	286.6	191.5	-227.0	-96.4	693.25	716.76	0.0100	-0.0005	8.2861
3	197.1	269.6	175.8	166.9	89.1	211.8	320.2	320.2	290.4	199.0	-231.1	-108.4	711.73	742.57	0.0026	-0.0068	8.2919
4	191.1	257.4	169.6	160.8	88.0	201.1	328.4	328.1	294.2	204.9	-240.4	-127.1	701.12	734.70	-0.0144	-0.0217	8.2255
5	186.2	253.0	164.5	153.8	87.1	200.9	336.5	336.1	298.8	204.7	-249.4	-135.2	672.70	695.25	-0.0326	-0.0385	8.1896
6	183.4	251.3	161.8	148.2	86.5	203.0	340.6	340.0	301.2	201.8	-254.1	-137.0	652.34	659.88	-0.0413	-0.0465	8.1616
7	171.3	243.1	146.0	122.0	89.6	210.2	344.7	344.0	293.9	181.1	-255.1	-133.8	575.62	531.50	-0.0481	-0.0505	8.0454

SL	B-1 DEGREE	B-2 DEGREE	B'-1 DEGREE	B'-2 DEGREE	M-1	M-2	M'-1	M'-2	INCS DEGREE	INCM DEGREE	DEV DEGREE	TURN DEGREE	D FAC	OMEGA-B TOTAL	LOSS-P TOTAL	PO2/PO1	%EFF-A TOTAL	%EFF-P TOTAL
1	31.2	61.2	57.71	32.63	0.3630	0.5615	0.5813	0.3214	0.0	0.0	0.0	25.08	0.6905	0.1251	0.0494	1.2878	90.64	90.96
2	27.0	53.0	52.36	30.23	0.4367	0.5991	0.6373	0.4170	0.0	0.0	0.0	22.13	0.5484	0.0817	0.0335	1.2759	92.33	92.59
3	26.9	51.8	52.74	33.01	0.4426	0.5933	0.6522	0.4380	0.0	0.0	0.0	19.73	0.5175	0.0655	0.0264	1.2704	93.41	93.63
4	27.4	51.4	54.80	38.33	0.4330	0.5715	0.6668	0.4550	0.0	0.0	0.0	16.47	0.4888	0.0456	0.0173	1.2648	95.06	95.22
5	27.9	52.6	56.60	41.33	0.4192	0.5571	0.6728	0.4508	0.0	0.0	0.0	15.27	0.4947	0.0538	0.0191	1.2666	94.17	94.36
6	28.1	53.9	57.54	42.78	0.4101	0.5487	0.6735	0.4406	0.0	0.0	0.0	14.76	0.5090	0.0635	0.0218	1.2687	93.25	93.47
7	31.6	59.9	60.23	47.65	0.3786	0.5244	0.6496	0.3907	0.0	0.0	0.0	12.58	0.5708	0.0800	0.0252	1.2726	92.26	92.51

SL	V-1 FT/SEC	V-2 FT/SEC	VM-1 FT/SEC	VM-2 FT/SEC	VO-1 FT/SEC	VO-2 FT/SEC	U-1 FT/SEC	U-2 FT/SEC	V'-1 FT/SEC	V'-2 FT/SEC	VO'-1 FT/SEC	VO'-2 FT/SEC	RHOVM-1 LBM/FT2SEC	RHOVM-2 LBM/FT2SEC	EPSI-1 DEGREE	EPSI-2 DEGREE	PCT TE SPAN
1	547.0	864.7	467.9	416.9	283.3	757.6	1023.6	1024.5	875.8	495.0	-740.3	-266.9	110.64	107.09	0.948	0.200	0.1000
2	644.5	902.7	574.3	542.8	292.4	721.2	1037.0	1037.5	940.4	628.2	-744.6	-316.3	141.98	146.80	0.574	-0.031	0.2000
3	646.5	884.6	576.8	547.5	292.2	694.8	1050.5	1050.5	952.7	653.0	-758.3	-355.7	145.77	152.09	0.147	-0.387	0.3000
4	626.9	844.6	556.5	527.5	288.6	659.7	1077.3	1076.6	965.2	672.4	-788.7	-416.9	143.60	150.47	-0.822	-1.246	0.5000
5	610.8	830.1	539.8	504.6	285.9	659.2	1104.2	1102.6	980.3	671.8	-818.3	-443.5	137.77	142.39	-1.867	-2.206	0.7000
6	601.8	824.7	530.7	486.1	283.8	666.1	1117.6	1115.7	988.4	662.1	-833.8	-449.5	133.61	135.15	-2.369	-2.663	0.8000
7	562.0	797.5	479.0	400.4	294.1	689.7	1131.0	1128.7	964.3	594.2	-837.0	-439.0	117.89	108.86	-2.754	-2.894	0.9000

WC1/A1 LBM/SEC SQFT	WC1/A1 KG/SEC SQM	TO/TO INLET	PO/PO INLET	EFF-AD INLET %	EFF-P INLET %		TO2/TO1	PO2/PO1	EFF-AD ROTOR %	EFF-P ROTOR %
28.28	138.08	1.9398	8.1800	86.24	89.58		1.0737	1.2714	93.17	93.39

STATOR 12

AIRFOIL AERODYNAMIC SUMMARY PRINT

RUN NO 100 SPEED CODE 10 POINT NO 3

SL	V-1 M/SEC	V-2 M/SEC	VM-1 M/SEC	VM-2 M/SEC	VO-1 M/SEC	VO-2 M/SEC	RHOVM-1 KG/M2 SEC	RHOVM-2 KG/M2 SEC	PO/PO INLET	TO/TO INLET	%EFF-A TOT-INLET	%EFF-P TOT-INLET	EPSI-1 RADIAN	EPSI-2 RADIAN
1	268.6	163.1	139.1	137.2	229.8	88.2	576.57	616.51	7.8982	2.0290	76.97	82.42	-0.0095	-0.0074
2	277.3	189.0	169.9	166.9	219.2	88.8	736.08	782.67	8.1478	1.9629	83.93	87.82	-0.0134	-0.0122
3	271.8	188.3	170.7	166.2	211.5	88.6	758.02	797.41	8.1675	1.9210	87.98	90.90	-0.0167	-0.0163
4	260.6	181.8	165.3	159.3	201.4	87.5	752.53	780.74	8.1349	1.8814	91.77	93.77	-0.0215	-0.0236
5	256.6	177.0	159.0	154.2	201.5	86.8	715.50	745.11	8.0890	1.9068	88.83	91.53	-0.0253	-0.0307
6	255.2	173.9	153.9	151.0	203.6	86.2	682.50	718.32	8.0549	1.9355	85.81	89.23	-0.0278	-0.0346
7	247.4	160.2	129.6	133.3	210.8	88.9	562.00	619.09	7.9321	1.9749	81.47	85.89	-0.0324	-0.0403

SL	B-1 DEGREE	B-2 DEGREE	M-1	M-2	INCS DEGREE	INCM DEGREE	DEV DEGREE	TURN DEGREE	D-FAC	OMEGA-B TOTAL	LOSS-P TOTAL	PO2/ PO1	PO/PO STAGE	TO/TO STAGE	%EFF-A TOT-STG	%EFF-P TOT-STG
1	58.8	32.7	0.5751	0.3429	0.0	0.0	0.0	26.07	0.6462	0.1146	0.0460	0.9773	1.2559	1.0786	82.53	83.08
2	52.2	28.0	0.6052	0.4054	0.0	0.0	0.0	24.20	0.5451	0.0816	0.0347	0.9823	1.2524	1.0751	85.45	85.90
3	51.1	28.1	0.5990	0.4081	0.0	0.0	0.0	23.04	0.5279	0.0685	0.0295	0.9854	1.2514	1.0732	87.56	87.95
4	50.6	28.8	0.5790	0.3977	0.0	0.0	0.0	21.83	0.5211	0.0543	0.0238	0.9890	1.2509	1.0708	90.47	90.77
5	51.7	29.4	0.5656	0.3843	0.0	0.0	0.0	22.34	0.5391	0.0640	0.0285	0.9876	1.2508	1.0718	89.08	89.42
6	52.9	29.7	0.5577	0.3746	0.0	0.0	0.0	23.19	0.5566	0.0732	0.0329	0.9861	1.2509	1.0729	87.71	88.09
7	58.4	33.7	0.5343	0.3411	0.0	0.0	0.0	24.72	0.6108	0.0910	0.0395	0.9840	1.2517	1.0745	85.92	86.35

SL	V-1 FT/SEC	V-2 FT/SEC	VM-1 FT/SEC	VM-2 FT/SEC	VO-1 FT/SEC	VO-2 FT/SEC	RHOVM-1 LBM/FT2SEC	RHOVM-2 LBM/FT2SEC	PCT TE SPAN	TO/TO INLET	%EFF-A TOT-INLET	%EFF-P TOT-INLET	EPSI-1 DEGREE	EPSI-2 DEGREE
1	881.4	535.1	456.5	450.1	753.9	289.3	118.09	126.27	0.1000	2.0290	76.97	82.42	-0.544	-0.426
2	909.9	620.3	557.3	547.5	719.3	291.5	150.76	160.30	0.2000	1.9629	83.93	87.82	-0.770	-0.699
3	891.8	617.8	560.0	545.2	694.1	290.6	155.25	163.32	0.3000	1.9210	87.98	90.90	-0.959	-0.934
4	854.9	596.5	542.5	522.8	660.8	287.2	154.12	159.90	0.5000	1.8814	91.77	93.77	-1.230	-1.353
5	842.0	580.6	521.6	505.9	661.0	284.9	146.54	152.60	0.7000	1.9068	88.83	91.53	-1.451	-1.757
6	837.2	570.4	504.9	495.4	667.9	282.8	139.78	147.12	0.8000	1.9355	85.81	89.23	-1.591	-1.983
7	811.8	525.6	425.1	437.3	691.6	291.6	115.10	126.80	0.9000	1.9749	81.47	85.89	-1.858	-2.309

NCORR INLET RPM	WCORR INLET LBM/SEC	WCORR INLET KG/SEC	TO/TO INLET	PO/PO INLET	EFF-AD INLET %	EFF-P INLET %	TO/TO STAGE	PO2/PO1	PO/PO STAGE	EFF-AD STAGE %	EFF-P STAGE %
12136.50	77.44	35.13	1.9384	8.0606	85.57	89.05	1.0737	0.9851	1.2525	87.19	87.59

ROTOR 13

AIRFOIL AERODYNAMIC SUMMARY PRINT

RUN NO 100 SPEED CODE 10 POINT NO 3

SL	V-1 M/SEC	V-2 M/SEC	VM-1 M/SEC	VM-2 M/SEC	VO-1 M/SEC	VO-2 M/SEC	U-1 M/SEC	U-2 M/SEC	V'-1 M/SEC	V'-2 M/SEC	VO'-1 M/SEC	VO'-2 M/SEC	RHOVM-1 KG/M2 SEC	RHOVM-2 KG/M2 SEC	EPSI-1 RADIAN	EPSI-2 RADIAN	PO/PO INLET
1	166.3	255.8	141.0	122.5	88.2	224.5	312.2	312.1	264.6	150.6	-223.9	-87.6	632.39	589.22	-0.0006	-0.0006	9.8054
2	191.9	266.4	170.1	160.5	88.9	212.6	315.8	315.6	283.6	190.7	-226.9	-103.0	795.72	811.17	-0.0050	-0.00391	0.0757
3	191.7	261.3	169.9	161.3	88.7	205.5	319.3	319.1	286.5	197.3	-230.7	-113.6	812.73	837.70	-0.0106	-0.00871	0.0820
4	185.8	250.9	163.8	155.3	87.7	197.1	326.5	326.1	289.6	201.9	-238.8	-129.1	799.82	827.76	-0.0237	-0.02041	0.0256
5	181.4	248.4	159.2	149.4	87.0	198.5	333.6	333.1	293.6	201.1	-246.6	-134.7	766.89	785.94	-0.0384	-0.03381	0.0031
6	178.8	247.8	156.6	144.9	86.3	201.0	337.2	336.6	295.7	198.5	-250.9	-135.7	742.68	750.34	-0.0459	-0.0405	9.9815
7	166.2	240.4	140.4	119.8	89.0	208.4	340.8	340.1	288.3	178.0	-251.8	-131.7	650.10	605.52	-0.0522	-0.0447	9.8572

SL	B-1 DEGREE	B-2 DEGREE	B'-1 DEGREE	B'-2 DEGREE	M-1	M-2	M'-1	M'-2	INCS DEGREE	INCM DEGREE	DEV DEGREE	TURN DEGREE	D FAC	OMEGA-B TOTAL	LOSS-P TOTAL	PO2/ PO1	%EFF-A TOTAL	%EFF-P TOTAL
1	32.0	61.4	57.81	35.57	0.3499	0.5269	0.5566	0.3103	0.0	0.0	0.0	22.24	0.6748	0.1301	0.0499	1.2477	89.98	90.27
2	27.6	53.0	53.13	32.68	0.4118	0.5608	0.6083	0.4014	0.0	0.0	0.0	20.45	0.5324	0.0869	0.0344	1.2377	91.54	91.79
3	27.6	51.9	53.62	35.15	0.4155	0.5561	0.6212	0.4200	0.0	0.0	0.0	18.48	0.5029	0.0716	0.0276	1.2344	92.58	92.79
4	28.2	51.8	55.55	39.74	0.4067	0.5391	0.6339	0.4339	0.0	0.0	0.0	15.82	0.4798	0.0546	0.0197	1.2324	94.00	94.17
5	28.7	53.0	57.16	42.05	0.3943	0.5292	0.6380	0.4285	0.0	0.0	0.0	15.12	0.4927	0.0619	0.0215	1.2369	93.29	93.48
6	28.9	54.2	58.04	43.12	0.3857	0.5233	0.6378	0.4193	0.0	0.0	0.0	14.93	0.5086	0.0696	0.0238	1.2404	92.63	92.85
7	32.4	60.1	60.88	47.72	0.3543	0.5016	0.6145	0.3714	0.0	0.0	0.0	13.15	0.5718	0.0853	0.0268	1.2455	91.83	92.07

SL	V-1 FT/SEC	V-2 FT/SEC	VM-1 FT/SEC	VM-2 FT/SEC	VO-1 FT/SEC	VO-2 FT/SEC	U-1 FT/SEC	U-2 FT/SEC	V'-1 FT/SEC	V'-2 FT/SEC	VO'-1 FT/SEC	VO'-2 FT/SEC	RHOVM-1 LBM/FT2SEC	RHOVM-2 LBM/FT2SEC	EPSI-1 DEGREE	EPSI-2 DEGREE	PCT TE SPAN
1	545.7	839.1	462.6	402.0	289.5	736.6	1024.2	1024.0	868.2	494.2	-734.7	-287.4	129.52	120.68	-0.037	-0.036	0.1000
2	629.8	874.1	558.2	526.6	291.7	697.7	1036.0	1035.5	930.4	625.6	-744.3	-337.8	162.97	166.14	-0.286	-0.223	0.2000
3	628.8	857.3	557.5	529.4	290.9	674.3	1047.7	1047.0	940.0	647.4	-756.8	-372.7	166.45	171.57	-0.607	-0.498	0.3000
4	609.6	823.1	537.5	509.4	287.6	646.5	1071.2	1070.0	950.2	662.5	-783.5	-423.5	163.81	169.53	-1.361	-1.170	0.5000
5	595.3	815.0	522.4	490.0	285.5	651.2	1094.7	1093.0	963.1	659.8	-809.2	-441.8	157.07	160.97	-2.201	-1.936	0.7000
6	586.7	813.0	513.8	475.5	283.3	659.4	1106.4	1104.5	970.3	651.3	-823.1	-445.1	152.11	153.68	-2.630	-2.322	0.8000
7	545.4	788.8	460.7	393.1	291.9	683.9	1118.1	1116.0	946.0	584.1	-826.2	-432.1	133.15	124.01	-2.988	-2.558	0.9000

WC1/A1 LBM/SEC SQFT	WC1/A1 KG/SEC SQM	TO/TO INLET	PO/PO INLET	EFF-AD INLET %	EFF-P INLET %		T02/T01	P02/P01	EFF-AD ROTOR %	EFF-P ROTOR %
26.68	130.27	2.0653	9.9807	85.62	89.37		1.0655	1.2382	92.41	92.64

STATOR 13

AIRFOIL AERODYNAMIC SUMMARY PRINT

RUN NO 100 SPEED CODE 10 POINT NO 3

SL	V-1 M/SEC	V-2 M/SEC	VM-1 M/SEC	VM-2 M/SEC	VO-1 M/SEC	VO-2 M/SEC	RHOVM-1 KG/M2 SEC	RHOVM-2 KG/M2 SEC	PO/PO INLET	TO/TO INLET	%EFF-A TOT-INLET	%EFF-P TOT-INLET	EPSI-1 RADIAN	EPSI-2 RADIAN
1	257.7	146.6	126.8	123.3	224.4	79.3	609.69	638.04	9.6081	2.1732	75.91	82.03	-0.0085	-0.0086
2	267.9	178.7	162.9	157.9	212.7	83.6	821.98	856.27	9.9212	2.0947	82.98	87.40	-0.0114	-0.0124
3	263.0	178.8	163.8	158.1	205.7	83.6	848.90	878.57	9.9523	2.0468	87.06	90.43	-0.0137	-0.0155
4	252.9	173.4	158.2	152.3	197.3	83.0	841.19	866.58	9.9307	2.0005	91.05	93.39	-0.0176	-0.0209
5	250.5	170.1	152.5	148.5	198.7	82.9	800.62	832.86	9.8949	2.0291	88.27	91.33	-0.0221	-0.0267
6	250.0	168.1	148.3	146.3	201.2	82.7	766.51	807.27	9.8665	2.0620	85.32	89.13	-0.0250	-0.0301
7	242.8	154.8	124.2	128.9	208.7	85.8	626.80	693.15	9.7321	2.1079	81.03	85.91	-0.0300	-0.0353

SL	B-1 DEGREE	B-2 DEGREE	M-1	M-2	INCS DEGREE	INCM DEGREE	DEV DEGREE	TURN DEGREE	D-FAC	OMEGA-B TOTAL	LOSS-P TOTAL	PO2/ PO1	PO/PO STAGE	TO/TO STAGE	%EFF-A TOT-STG	%EFF-P TOT-STG
1	60.5	32.8	0.5315	0.2975	0.0	0.0	0.0	27.77	0.6973	0.1294	0.0509	0.9778	1.2192	1.0689	80.77	81.26
2	52.6	27.9	0.5642	0.3705	0.0	0.0	0.0	24.66	0.5607	0.0811	0.0339	0.9844	1.2183	1.0658	84.66	85.07
3	51.5	27.9	0.5599	0.3751	0.0	0.0	0.0	23.60	0.5419	0.0678	0.0286	0.9872	1.2185	1.0644	86.75	87.10
4	51.3	28.6	0.5436	0.3676	0.0	0.0	0.0	22.71	0.5353	0.0531	0.0228	0.9904	1.2206	1.0631	89.54	89.83
5	52.5	29.2	0.5340	0.3578	0.0	0.0	0.0	23.33	0.5513	0.0625	0.0272	0.9891	1.2231	1.0645	88.38	88.70
6	53.6	29.5	0.5283	0.3507	0.0	0.0	0.0	24.14	0.5660	0.0714	0.0313	0.9878	1.2247	1.0657	87.27	87.62
7	59.2	33.6	0.5070	0.3191	0.0	0.0	0.0	25.59	0.6201	0.0901	0.0381	0.9856	1.2269	1.0674	85.63	86.02

SL	V-1 FT/SEC	V-2 FT/SEC	VM-1 FT/SEC	VM-2 FT/SEC	VO-1 FT/SEC	VO-2 FT/SEC	RHOVM-1 LBM/FT2SEC	RHOVM-2 LBM/FT2SEC	PCT TE SPAN	TO/TO INLET	%EFF-A TOT-INLET	%EFF-P TOT-INLET	EPSI-1 DEGREE	EPSI-2 DEGREE
1	845.6	480.9	416.1	404.5	736.2	260.2	124.87	130.68	0.1000	2.1732	75.91	82.03	-0.485	-0.491
2	878.9	586.2	534.3	518.1	697.9	274.3	168.35	175.37	0.2000	2.0947	82.98	87.40	-0.654	-0.713
3	862.7	586.7	537.5	518.7	674.9	274.2	173.86	179.94	0.3000	2.0468	87.06	90.43	-0.785	-0.888
4	829.7	569.1	518.9	499.8	647.4	272.2	172.28	177.48	0.5000	2.0005	91.05	93.39	-1.009	-1.197
5	821.8	558.0	500.2	487.2	652.0	272.0	163.97	170.58	0.7000	2.0291	88.27	91.33	-1.265	-1.527
6	820.1	551.4	486.6	480.1	660.1	271.2	156.99	165.34	0.8000	2.0620	85.32	89.13	-1.435	-1.726
7	796.8	508.0	407.6	422.9	684.7	281.4	128.37	141.96	0.9000	2.1079	81.03	85.91	-1.719	-2.022

NCORR INLET RPM	WCORR INLET LBM/SEC	WCORR INLET KG/SEC	TO/TO INLET	PO/PO INLET	EFF-AD INLET %	EFF-P INLET %	TO/TO STAGE	PO2/PO1	PO/PO STAGE	EFF-AD STAGE %	EFF-P STAGE %
12136.50	77.44	35.13	2.0653	9.8477	84.94	88.85	1.0655	0.9867	1.2217	86.44	86.82

ROTOR 14

AIRFOIL AERODYNAMIC SUMMARY PRINT

RUN NO 100 SPEED CODE 10 POINT NO 3

SL	V-1 M/SEC	V-2 M/SEC	VM-1 M/SEC	VM-2 M/SEC	VO-1 M/SEC	VO-2 M/SEC	U-1 M/SEC	U-2 M/SEC	V'-1 M/SEC	V'-2 M/SEC	VO'-1 M/SEC	VO'-2 M/SEC	RHOVM-1 KG/M2 SEC	RHOVM-2 KG/M2 SEC	EPSI-1 RADIAN	EPSI-2 RADIAN	PO/PO INLET
1	152.0	251.2	129.4	120.5	79.7	220.4	311.8	311.8	265.7	151.2	-232.1	-91.4	669.12	667.30	-0.0041	-0.0047	11.8632
2	182.2	256.6	161.8	154.1	83.7	205.2	315.1	314.9	282.4	189.2	-231.4	-109.7	875.76	898.04	-0.0088	-0.0090	12.0758
3	182.4	251.4	162.0	155.0	83.7	197.8	318.3	318.1	285.2	196.2	-234.6	-120.2	898.23	928.47	-0.0143	-0.0138	12.0738
4	177.3	241.5	156.7	150.1	83.1	189.2	324.8	324.4	288.0	202.0	-241.7	-135.2	888.64	923.35	-0.0269	-0.0251	12.0122
5	174.1	240.7	153.0	145.3	83.1	191.9	331.2	330.7	291.6	201.0	-248.2	-138.9	855.84	880.42	-0.0404	-0.0376	12.0043
6	172.2	241.1	151.0	141.3	82.8	195.3	334.5	333.9	293.5	197.9	-251.7	-138.6	830.96	840.91	-0.0470	-0.0437	11.9910
7	159.6	234.8	134.6	115.8	85.9	204.2	337.7	337.1	285.5	176.3	-251.8	-132.9	721.86	671.89	-0.0516	-0.0470	11.8666

SL	B-1 DEGREE	B-2 DEGREE	B'-1 DEGREE	B'-2 DEGREE	M-1	M-2	M'-1	M'-2	INCS DEGREE	INCM DEGREE	DEV DEGREE	TURN DEGREE	D FAC	OMEGA-B TOTAL	LOSS-P TOTAL	PO2/ PO1	%EFF-A TOTAL	%EFF-P TOTAL
1	31.6	61.3	60.86	37.17	0.3088	0.5012	0.5399	0.3018	0.0	0.0	0.0	23.69	0.6856	0.1437	0.0545	1.2358	89.08	89.38
2	27.3	53.1	55.03	35.45	0.3781	0.5237	0.5860	0.3860	0.0	0.0	0.0	19.58	0.5368	0.0868	0.0340	1.2172	91.45	91.66
3	27.3	51.9	55.37	37.80	0.3827	0.5189	0.5985	0.4050	0.0	0.0	0.0	17.58	0.5062	0.0704	0.0270	1.2132	92.59	92.78
4	27.9	51.6	57.05	42.02	0.3761	0.5038	0.6108	0.4214	0.0	0.0	0.0	15.04	0.4810	0.0523	0.0193	1.2097	94.11	94.26
5	28.5	52.9	58.35	43.71	0.3666	0.4976	0.6138	0.4156	0.0	0.0	0.0	14.64	0.4992	0.0631	0.0230	1.2135	93.03	93.21
6	28.8	54.1	59.05	44.46	0.3597	0.4939	0.6129	0.4054	0.0	0.0	0.0	14.59	0.5197	0.0740	0.0270	1.2166	92.06	92.26
7	32.6	60.4	61.89	48.93	0.3293	0.4749	0.5889	0.3565	0.0	0.0	0.0	12.96	0.5919	0.0947	0.0320	1.2223	90.94	91.17

SL	V-1 FT/SEC	V-2 FT/SEC	VM-1 FT/SEC	VM-2 FT/SEC	VO-1 FT/SEC	VO-2 FT/SEC	U-1 FT/SEC	U-2 FT/SEC	V'-1 FT/SEC	V'-2 FT/SEC	VO'-1 FT/SEC	VO'-2 FT/SEC	RHOVM-1 LBM/FT2SEC	RHOVM-2 LBM/FT2SEC	EPSI-1 DEGREE	EPSI-2 DEGREE	PCT TE SPAN
1	498.7	824.2	424.6	395.4	261.6	723.1	1023.1	1022.9	871.9	496.2	-761.5	-299.8	137.04	136.67	-0.232	-0.270	0.1000
2	597.8	842.0	531.0	505.6	274.6	673.3	1033.7	1033.3	926.4	620.7	-759.2	-360.0	179.36	183.93	-0.505	-0.516	0.2000
3	598.3	824.7	531.7	508.7	274.5	649.1	1044.3	1043.6	935.6	643.7	-769.9	-394.5	183.97	190.16	-0.817	-0.789	0.3000
4	581.8	792.4	514.1	492.5	272.6	620.8	1065.6	1064.4	945.1	662.9	-793.0	-443.6	182.00	189.11	-1.539	-1.437	0.5000
5	571.3	789.7	502.1	476.8	272.5	629.6	1086.8	1085.2	956.6	659.5	-814.3	-455.6	175.28	180.32	-2.316	-2.153	0.7000
6	565.1	790.9	495.5	463.6	271.7	640.9	1097.4	1095.5	963.0	649.3	-825.7	-454.7	170.19	172.23	-2.690	-2.501	0.8000
7	523.8	770.3	441.5	380.0	281.9	670.0	1108.0	1105.9	936.7	578.3	-826.2	-435.9	147.84	137.61	-2.957	-2.691	0.9000

WC1/A1 LBM/SEC SQFT	WC1/A1 KG/SEC SQM	TO/TO INLET	PO/PO INLET	EFF-AD INLET %	EFF-P INLET %		T02/T01	P02/P01	EFF-AD ROTOR %	EFF-P ROTOR %
25.07	122.41	2.1887	11.9830	84.96	89.11		1.0597	1.2168	92.02	92.23

STATOR 14

AIRFOIL AERODYNAMIC SUMMARY PRINT

RUN NO 100 SPEED CODE 10 POINT NO 3

SL	V-1 M/SEC	V-2 M/SEC	VM-1 M/SEC	VM-2 M/SEC	VO-1 M/SEC	VO-2 M/SEC	RHOVM-1 KG/M2 SEC	RHOVM-2 KG/M2 SEC	PO/PO INLET	TO/TO INLET	%EFF-A TOT-INLET	%EFF-P TOT-INLET	EPSI-1 RADIAN	EPSI-2 RADIAN
1	253.5	152.2	125.7	130.5	220.1	78.3	696.10	771.26	11.6508	2.3076	75.91	82.40	-0.0099	-0.0088
2	258.3	173.7	156.9	155.0	205.2	78.3	913.34	960.08	11.9065	2.2166	82.66	87.42	-0.0141	-0.0131
3	253.0	173.2	157.6	154.4	197.9	78.4	942.07	980.25	11.9308	2.1643	86.61	90.30	-0.0163	-0.0157
4	243.3	168.3	152.6	149.0	189.4	78.3	937.19	968.74	11.9087	2.1141	90.51	93.14	-0.0197	-0.0203
5	242.5	166.3	147.9	146.4	192.1	78.9	894.61	937.07	11.8797	2.1474	87.69	91.09	-0.0235	-0.0254
6	242.9	165.1	144.0	145.0	195.5	78.9	856.03	912.01	11.8543	2.1844	84.76	88.95	-0.0261	-0.0286
7	236.8	153.0	119.5	129.2	204.4	81.9	692.34	791.18	11.7130	2.2369	80.51	85.82	-0.0311	-0.0339

SL	B-1 DEGREE	B-2 DEGREE	M-1	M-2	INCS DEGREE	INCM DEGREE	DEV DEGREE	TURN DEGREE	D-FAC	OMEGA-B TOTAL	LOSS-P TOTAL	PO2/PO1	PO/PO STAGE	TO/TO STAGE	%EFF-A TOT-STG	%EFF-P TOT-STG
1	60.3	31.0	0.5064	0.3003	0.0	0.0	0.0	29.30	0.6386	0.1265	0.0462	0.9800	1.2086	1.0652	80.72	81.19
2	52.6	26.8	0.5275	0.3502	0.0	0.0	0.0	25.78	0.5384	0.0846	0.0325	0.9856	1.1994	1.0599	84.61	84.97
3	51.5	26.9	0.5225	0.3532	0.0	0.0	0.0	24.55	0.5204	0.0702	0.0272	0.9882	1.1988	1.0585	86.83	87.14
4	51.1	27.7	0.5076	0.3470	0.0	0.0	0.0	23.41	0.5109	0.0546	0.0214	0.9913	1.1992	1.0569	89.68	89.93
5	52.4	28.3	0.5015	0.3402	0.0	0.0	0.0	24.08	0.5242	0.0667	0.0265	0.9896	1.2006	1.0583	87.96	88.25
6	53.6	28.6	0.4978	0.3349	0.0	0.0	0.0	25.06	0.5380	0.0780	0.0312	0.9880	1.2014	1.0594	86.38	86.70
7	59.7	32.4	0.4792	0.3064	0.0	0.0	0.0	27.32	0.5919	0.1013	0.0393	0.9854	1.2034	1.0613	84.17	84.55

SL	V-1 FT/SEC	V-2 FT/SEC	VM-1 FT/SEC	VM-2 FT/SEC	VO-1 FT/SEC	VO-2 FT/SEC	RHOVM-1 LBM/FT2SEC	RHOVM-2 LBM/FT2SEC	PCT TE SPAN	TO/TO INLET	%EFF-A TOT-INLET	%EFF-P TOT-INLET	EPSI-1 DEGREE	EPSI-2 DEGREE
1	831.7	499.4	412.5	428.2	722.1	256.9	142.57	157.96	0.1000	2.3076	75.91	82.40	-0.566	-0.504
2	847.6	569.9	514.9	508.6	673.2	257.0	187.06	196.63	0.2000	2.2166	82.66	87.42	-0.806	-0.748
3	830.1	568.1	516.9	506.5	649.5	257.4	192.94	200.76	0.3000	2.1643	86.61	90.30	-0.935	-0.902
4	798.2	552.2	500.8	488.8	621.5	256.9	191.95	198.41	0.5000	2.1141	90.51	93.14	-1.131	-1.164
5	795.5	545.7	485.3	480.4	630.4	259.0	183.22	191.92	0.7000	2.1474	87.69	91.09	-1.346	-1.453
6	796.8	541.7	472.5	475.8	641.6	259.0	175.32	186.79	0.8000	2.1844	84.76	88.95	-1.497	-1.641
7	776.9	502.0	392.1	424.0	670.7	268.8	141.80	162.04	0.9000	2.2369	80.51	85.82	-1.785	-1.943

NCORR INLET RPM	WCORR INLET LBM/SEC	WCORR INLET KG/SEC	TO/TO INLET	PO/PO INLET	EFF-AD INLET %	EFF-P INLET %	TO/TO STAGE	PO2/PO1	PO/PO STAGE	EFF-AD STAGE %	EFF-P STAGE %
12136.50	77.44	35.13	2.1887	11.8316	84.35	88.65	1.0597	0.9874	1.2015	85.92	86.26

ROTOR 15

AIRFOIL AERODYNAMIC SUMMARY PRINT

RUN NO 100 SPEED CODE 10 POINT NO 3

SL	V-1 M/SEC	V-2 M/SEC	VM-1 M/SEC	VM-2 M/SEC	VO-1 M/SEC	VO-2 M/SEC	U-1 M/SEC	U-2 M/SEC	V'-1 M/SEC	V'-2 M/SEC	VO'-1 M/SEC	VO'-2 M/SEC	RHOVM-1 KG/M2 SEC	RHOVM-2 KG/M2 SEC	EPSI-1 RADIAN	EPSI-2 RADIAN	PO/PO INLET
1	157.0	236.9	135.9	125.0	78.5	201.3	311.5	311.4	269.8	166.6	-233.0	-110.1	802.37	786.93	-0.0017	-0.0098	13.9126
2	177.2	244.1	158.9	151.5	78.4	191.4	314.4	314.3	284.5	195.1	-236.0	-122.9	982.18	1003.40	-0.0058	-0.0063	14.1611
3	176.6	239.3	158.2	151.1	78.5	185.5	317.3	317.1	286.5	200.4	-238.8	-131.6	1002.38	1028.27	-0.0104	-0.0067	14.1594
4	172.1	231.7	153.1	146.7	78.4	179.3	323.1	322.8	288.7	205.2	-244.7	-143.5	993.13	1025.20	-0.0207	-0.0112	14.1202
5	170.3	233.8	150.8	144.4	79.1	183.9	328.9	328.5	291.9	204.3	-249.9	-144.6	962.96	992.76	-0.0325	-0.0198	14.1505
6	169.3	236.4	149.7	142.7	79.1	188.5	331.8	331.3	293.8	201.9	-252.8	-142.8	939.15	962.72	-0.0386	-0.0248	14.1668
7	157.9	233.7	135.0	122.3	82.0	199.1	334.7	334.2	286.5	182.2	-252.7	-135.0	824.30	802.63	-0.0437	-0.0284	14.0775

SL	B-1 DEGREE	B-2 DEGREE	B'-1 DEGREE	B'-2 DEGREE	M-1	M-2	M'-1	M'-2	INCS DEGREE	INCM DEGREE	DEV DEGREE	TURN DEGREE	D FAC	OMEGA-B TOTAL	LOSS-P TOTAL	PO2/ PO1	%EFF-A TOTAL	%EFF-P TOTAL
1	30.0	58.2	59.74	41.39	0.3099	0.4601	0.5327	0.3235	0.0	0.0	0.0	18.36	0.5978	0.0980	0.0347	1.1958	91.17	91.38
2	26.3	51.6	56.04	39.05	0.3575	0.4847	0.5740	0.3875	0.0	0.0	0.0	17.00	0.5017	0.0770	0.0283	1.1897	91.74	91.92
3	26.4	50.8	56.47	41.05	0.3604	0.4807	0.5846	0.4027	0.0	0.0	0.0	15.42	0.4770	0.0664	0.0237	1.1868	92.49	92.65
4	27.1	50.7	57.96	44.35	0.3549	0.4707	0.5954	0.4169	0.0	0.0	0.0	13.61	0.4549	0.0532	0.0181	1.1857	93.66	93.80
5	27.7	51.9	58.89	45.03	0.3486	0.4709	0.5974	0.4115	0.0	0.0	0.0	13.86	0.4707	0.0647	0.0218	1.1912	92.54	92.70
6	27.9	52.9	59.37	45.03	0.3436	0.4717	0.5962	0.4029	0.0	0.0	0.0	14.34	0.4895	0.0770	0.0260	1.1955	91.42	91.62
7	31.3	58.4	61.90	47.83	0.3165	0.4601	0.5741	0.3587	0.0	0.0	0.0	14.07	0.5577	0.1009	0.0325	1.2033	90.04	90.28

SL	V-1 FT/SEC	V-2 FT/SEC	VM-1 FT/SEC	VM-2 FT/SEC	VO-1 FT/SEC	VO-2 FT/SEC	U-1 FT/SEC	U-2 FT/SEC	V'-1 FT/SEC	V'-2 FT/SEC	VO'-1 FT/SEC	VO'-2 FT/SEC	RHOVM-1 LBM/FT2SEC	RHOVM-2 LBM/FT2SEC	EPSI-1 DEGREE	EPSI-2 DEGREE	PCT TE SPAN
1	515.0	777.4	446.0	410.0	257.5	660.5	1022.0	1021.8	885.1	546.5	-764.6	-361.3	164.33	161.17	-0.099	-0.559	0.1000
2	581.4	800.9	521.4	497.2	257.2	627.9	1031.6	1031.1	933.5	640.2	-774.3	-403.3	201.16	205.50	-0.330	-0.360	0.2000
3	579.6	785.1	519.2	495.5	257.6	608.6	1041.1	1040.5	939.9	657.6	-783.5	-431.9	205.30	210.60	-0.594	-0.383	0.3000
4	564.5	760.3	502.5	481.4	257.3	588.4	1060.2	1059.1	947.2	673.3	-802.9	-470.7	203.40	209.97	-1.186	-0.642	0.5000
5	558.8	767.2	494.9	473.8	259.4	603.4	1079.2	1077.7	957.6	670.4	-819.8	-474.4	197.22	203.33	-1.863	-1.133	0.7000
6	555.4	775.5	491.1	468.0	259.4	618.4	1088.8	1087.1	963.8	662.4	-829.3	-468.7	192.35	197.17	-2.210	-1.421	0.8000
7	518.2	766.7	442.8	401.2	269.1	653.3	1098.3	1096.4	940.0	597.7	-829.2	-443.1	168.82	164.39	-2.502	-1.628	0.9000

WC1/A1 LBM/SEC SQFT	WC1/A1 KG/SEC SQM	TO/TO INLET	PO/PO INLET	EFF-AD INLET %	EFF-P INLET %	T02/T01	P02/P01	EFF-AD ROTOR %	EFF-P ROTOR %
24.05	117.43	2.3041	14.0996	84.37	88.87	1.0528	1.1917	91.93	92.10

EXIT VANE 1

AIRFOIL AERODYNAMIC SUMMARY PRINT

RUN NO 100 SPEED CODE 10 POINT NO 3

SL	V-1 M/SEC	V-2 M/SEC	VM-1 M/SEC	VM-2 M/SEC	VO-1 M/SEC	VO-2 M/SEC	RHOVM-1 KG/M2 SEC	RHOVM-2 KG/M2 SEC	PO/PO INLET	TO/TO INLET	%EFF-A TOT-INLET	%EFF-P TOT-INLET	EPSI-1 RADIAN	EPSI-2 RADIAN
1	238.7	190.5	133.3	137.6	198.0	131.8	868.67	927.76	14.0036	2.3750	79.59	85.41	0.0279	0.0869
2	239.5	193.3	146.9	147.0	189.1	125.4	987.06	1021.40	14.0914	2.3116	83.86	88.50	0.0313	0.0843
3	235.0	189.4	146.0	147.8	184.2	118.4	1001.98	1048.40	14.0734	2.2638	87.08	90.81	0.0335	0.0824
4	230.2	184.8	144.4	148.2	179.3	110.4	1009.99	1072.48	14.0465	2.2207	90.17	93.02	0.0344	0.0790
5	233.7	188.3	143.8	149.5	184.3	114.6	987.36	1062.22	14.0737	2.2615	87.25	90.93	0.0310	0.0738
6	236.4	191.0	142.0	146.8	189.0	122.2	956.50	1024.60	14.0862	2.3029	84.42	88.91	0.0289	0.0702
7	233.5	187.6	121.3	135.0	199.5	130.2	795.38	916.94	14.0021	2.3623	80.35	85.96	0.0252	0.0644

SL	B-1 DEGREE	B-2 DEGREE	M-1	M-2	INCS DEGREE	INCM DEGREE	DEV DEGREE	TURN DEGREE	D-FAC	OMEGA-B TOTAL	LOSS-P TOTAL	PO2/ PO1	PO/PO STAGE	TO/TO STAGE	%EFF-A TOT-STG	%EFF-P TOT-STG
1	56.0	43.8	0.4694	0.3722	0.0	0.0	0.0	12.18	0.3011	0.0462	0.0121	0.9936	1.1856	1.0531	88.08	88.35
2	52.1	40.5	0.4776	0.3827	0.0	0.0	0.0	11.61	0.2891	0.0426	0.0119	0.9939	1.1810	1.0518	88.68	88.93
3	51.5	38.7	0.4732	0.3786	0.0	0.0	0.0	12.81	0.2967	0.0400	0.0115	0.9944	1.1797	1.0511	89.56	89.78
4	51.1	36.7	0.4675	0.3729	0.0	0.0	0.0	14.41	0.3081	0.0378	0.0114	0.9948	1.1797	1.0506	90.77	90.96
5	52.0	37.5	0.4703	0.3767	0.0	0.0	0.0	14.49	0.3055	0.0393	0.0119	0.9946	1.1848	1.0525	89.59	89.81
6	53.1	39.8	0.4713	0.3789	0.0	0.0	0.0	13.24	0.2978	0.0415	0.0123	0.9942	1.1884	1.0539	88.45	88.70
7	58.7	44.0	0.4596	0.3673	0.0	0.0	0.0	14.68	0.3118	0.0467	0.0130	0.9938	1.1950	1.0564	86.97	87.28

SL	V-1 FT/SEC	V-2 FT/SEC	VM-1 FT/SEC	VM-2 FT/SEC	VO-1 FT/SEC	VO-2 FT/SEC	RHOVM-1 LBM/FT2SEC	RHOVM-2 LBM/FT2SEC	PCT TE SPAN	TO/TO INLET	%EFF-A TOT-INLET	%EFF-P TOT-INLET	EPSI-1 DEGREE	EPSI-2 DEGREE
1	783.2	625.1	437.5	451.4	649.7	432.5	177.91	190.01	0.1000	2.3750	79.59	85.41	1.596	4.980
2	785.8	634.1	482.1	482.5	620.5	411.5	202.16	209.19	0.2000	2.3116	83.86	88.50	1.794	4.827
3	771.0	621.3	478.9	484.8	604.2	388.5	205.21	214.72	0.3000	2.2638	87.08	90.81	1.921	4.723
4	755.4	606.5	473.7	486.4	588.4	362.3	206.86	219.65	0.5000	2.2207	90.17	93.02	1.970	4.527
5	766.9	617.9	471.8	490.4	604.6	376.0	202.22	217.55	0.7000	2.2615	87.25	90.93	1.777	4.227
6	775.5	626.8	465.8	481.6	620.1	401.1	195.90	209.85	0.8000	2.3029	84.42	88.91	1.655	4.020
7	766.2	615.5	398.0	443.0	654.7	427.3	162.90	187.80	0.9000	2.3623	80.35	85.96	1.442	3.690

NCORR INLET RPM	WCORR INLET LBM/SEC	WCORR INLET KG/SEC	TO/TO INLET	PO/PO INLET	EFF-AD INLET %	EFF-P INLET %		TO/TO STAGE	PO2/PO1	PO/PO STAGE	EFF-AD STAGE %	EFF-P STAGE %
12136.50	77.44	35.13	2.2957	14.0273	84.71	89.11		1.0528	0.9939	1.1844	88.71	88.95

EXIT VANE 2

AIRFOIL AERODYNAMIC SUMMARY PRINT

RUN NO 100 SPEED CODE 10 POINT NO 3

SL	V-1 M/SEC	V-2 M/SEC	VM-1 M/SEC	VM-2 M/SEC	VO-1 M/SEC	VO-2 M/SEC	RHOVM-1 KG/M2 SEC	RHOVM-2 KG/M2 SEC	PO/PO INLET	TO/TO INLET	%EFF-A TOT-INLET	%EFF-P TOT-INLET	EPSI-1 RADIAN	EPSI-2 RADIAN
1	190.5	138.8	137.6	138.4	131.8	9.9	927.76	953.05	13.8896	2.3841	78.69	84.75	0.0869	0.1019
2	193.3	148.0	147.0	148.0	125.4	1.1	1021.40	1051.32	14.0093	2.3166	83.26	88.06	0.0843	0.1000
3	189.4	146.1	147.8	146.1	118.4	-1.5	1048.40	1059.94	14.0055	2.2672	86.61	90.47	0.0824	0.0985
4	184.8	143.1	148.2	143.0	110.4	-4.3	1072.48	1059.31	13.9879	2.2209	89.95	92.86	0.0790	0.0963
5	188.3	146.4	149.5	146.4	114.6	-4.2	1062.22	1066.95	14.0084	2.2571	87.34	91.00	0.0738	0.0930
6	191.0	148.9	146.8	148.9	122.2	-2.2	1024.60	1066.39	14.0189	2.2964	84.63	89.05	0.0702	0.0897
7	187.6	143.3	135.0	143.1	130.2	6.2	916.94	996.96	13.9344	2.3576	80.42	86.01	0.0644	0.0844

SL	B-1 DEGREE	B-2 DEGREE	M-1	M-2	INCS DEGREE	INCM DEGREE	DEV DEGREE	TURN DEGREE	D-FAC	OMEGA-B TOTAL	LOSS-P TOTAL	PO2/ PO1	PO/PO STAGE	TO/TO STAGE	%EFF-A TOT-STG	%EFF-P TOT-STG
1	43.8	4.1	0.3722	0.2691	0.0	0.0	0.0	39.67	0.5194	0.0767	0.0301	0.9932	1.1784	1.0533	84.46	84.80
2	40.5	0.4	0.3827	0.2913	0.0	0.0	0.0	40.03	0.4888	0.0616	0.0244	0.9942	1.1743	1.0519	85.42	85.73
3	38.7	-0.6	0.3786	0.2903	0.0	0.0	0.0	39.28	0.4812	0.0531	0.0212	0.9951	1.1739	1.0512	86.75	87.03
4	36.7	-1.7	0.3729	0.2872	0.0	0.0	0.0	38.41	0.4764	0.0466	0.0189	0.9958	1.1746	1.0506	88.39	88.63
5	37.5	-1.6	0.3767	0.2918	0.0	0.0	0.0	39.09	0.4776	0.0489	0.0202	0.9955	1.1791	1.0523	87.29	87.56
6	39.8	-0.8	0.3789	0.2942	0.0	0.0	0.0	40.59	0.4868	0.0542	0.0225	0.9950	1.1818	1.0537	85.96	86.26
7	43.9	2.5	0.3673	0.2794	0.0	0.0	0.0	41.45	0.5131	0.0674	0.0282	0.9940	1.1874	1.0562	84.14	84.49

SL	V-1 FT/SEC	V-2 FT/SEC	VM-1 FT/SEC	VM-2 FT/SEC	VO-1 FT/SEC	VO-2 FT/SEC	RHOVM-1 LBM/FT2SEC	RHOVM-2 LBM/FT2SEC	PCT TE SPAN	TO/TO INLET	%EFF-A TOT-INLET	%EFF-P TOT-INLET	EPSI-1 DEGREE	EPSI-2 DEGREE
1	625.1	455.4	451.4	454.2	432.5	32.6	190.01	195.19	0.1000	2.3841	78.69	84.75	4.980	5.841
2	634.1	485.7	482.5	485.7	411.5	3.7	209.19	215.32	0.2000	2.3166	83.26	88.06	4.827	.5.729
3	621.3	479.2	484.8	479.2	388.5	-4.9	214.72	217.08	0.3000	2.2672	86.61	90.47	4.723	5.646
4	606.5	469.5	486.4	469.3	362.3	-14.2	219.65	216.96	0.5000	2.2209	89.95	92.86	4.527	5.515
5	617.9	480.5	490.4	480.3	376.0	-13.6	217.55	218.52	0.7000	2.2571	87.34	91.00	4.227	5.326
6	626.8	488.5	481.6	488.4	401.1	-7.1	209.85	218.41	0.8000	2.2964	84.63	89.05	4.020	5.137
7	615.5	470.1	443.0	469.7	427.3	20.4	187.80	204.19	0.9000	2.3576	80.42	86.01	3.690	4.835

NCORR INLET RPM	WCORR INLET LBM/SEC	WCORR INLET KG/SEC	TO/TO INLET	PO/PO INLET	EFF-AD INLET %	EFF-P INLET %	TO/TO STAGE	PO2/PO1	PO/PO STAGE	EFF-AD STAGE %	EFF-P STAGE %
12136.50	77.44	35.13	2.2957	13.9543	84.47	88.93	1.0528	0.9948	1.1780	85.90	86.20

TRANSLATION OF COMPUTER SYMBOLS TO ENGINEERING SYMBOLS (ROTOR)

SL	V-1 M/SEC	V-2 M/SEC	VM-1 M/SEC	VM-2 M/SEC	VØ-1 M/SEC	VØ-2 M/SEC	U-1 M/SEC	U-2 M/SEC	V'-1 M/SEC	V'-2 M/SEC	VØ'-1 M/SEC	VØ'-2 M/SEC	RHOVM-1 KG/M2 SEC	RHOVM-2 KG/M2 SEC	EPSI-1 RADIAN	EPSI-2 RADIAN	PO/PO INLET
	V_{LE}	V_{TE}	V_{MLE}	V_{MTE}	$V_{\theta LE}$	$V_{\theta TE}$	U_{LE}	U_{TE}	V'_{LE}	V'_{TE}	$V'_{\theta LE}$	$V'_{\theta TE}$	ρV_{MLE}	ρV_{MTE}	ϵ_{LE}	ϵ_{TE}	$\dfrac{P_{oTE}}{P_{oin}}$

SL	B-1 DEGREE	B-2 DEGREE	B'-1 DEGREE	B'-2 DEGREE	M-1	M-2	M'-1	M'-2	INCH DEGREE	DEV DEGREE	TURN DEGREE	D FAC	OMEGA-B TOTAL	LOSS-P TOTAL	PO2/ PO1	XEFF-A TOTAL	XEFF-P TOTAL
	β_{LE}	β_{TE}	β'_{LE}	β'_{TE}	M_{LE}	M_{TE}	M'_{LE}	M'_{TE}	i_m	δ°	$\Delta\beta$	D	$\bar{\omega}$	$\dfrac{\bar{\omega}\cos\beta_{TE}}{2\sigma}$	$\dfrac{P_{oLE}}{P_{oTE}}$	η_{ad} LE→TE	η_p LE→TE

SL	V-1 FT/SEC	V-2 FT/SEC	VM-1 FT/SEC	VM-2 FT/SEC	VØ-1 FT/SEC	VØ-2 FT/SEC	U-1 FT/SEC	U-2 FT/SEC	V'-1 FT/SEC	V'-2 FT/SEC	VØ'-1 FT/SEC	VØ'-2 FT/SEC	RHOVM-1 LBM/FT2SEC	RHOVM-2 LBM/FT2SEC	EPSI-1 DEGREE	EPSI-2 DEGREE	PCT TE SPAN
	V_{LE}	V_{TE}	V_{mLE}	V_{mTE}	$V_{\theta LE}$	$V_{\theta TE}$	U_{LE}	U_{TE}	V'_{LE}	V'_{TE}	$V'_{\theta LE}$	$V'_{\theta TE}$	ρV_{mLE}	ρV_{mTE}	ϵ_{LE}	ϵ_{TE}	$\dfrac{\%Span}{TE}$

WC1/A1 LBM/SEC SQFT	WC1/A1 KG/SEC SQM		TO/TO INLET	PO/PO INLET	EFF-AD INLET %	EFF-P INLET %		T02/T01 ROTOR %	P02/P01	EFF-AD ROTOR %	EFF-P ROTOR %
$\left(\dfrac{W\sqrt{\theta}}{\delta A}\right)_{LE}$	$\left(\dfrac{W\sqrt{\theta}}{\delta A}\right)_{LE}$		$\dfrac{T_{oTE}}{T_{oin}}$	$\dfrac{P_{oTE}}{P_{oin}}$	η_{ad} in→TE	η_p in→TE		$\dfrac{T_{oTE}}{T_{oLE}}$	$\dfrac{P_{oTE}}{P_{oLE}}$	η_{ad} LE→TE	η_p LE→TE

TRANSLATION OF COMPUTER SYMBOLS TO ENGINEERING SYMBOLS (STATOR OR IGV)

SL	V-1 M/SEC	V-2 M/SEC	VM-1 M/SEC	VM-2 M/SEC	VØ-1 M/SEC	VØ-2 M/SEC	RHOVM-1 KG/M2 SEC	RHOVM-2 KG/M2 SEC	PO/PO INLET	TO/TO INLET	%EFF-A TOT-INLET	%EFF-P TOT-INLET	EPSI-1 RADIAN	EPSI-2 RADIAN
	V_{LE}	V_{TE}	V_{mLE}	V_{mTE}	$V_{\theta LE}$	$V_{\theta TE}$	ρV_{mLE}	ρV_{mTE}	$\dfrac{P_{oTE}}{P_{oin}}$	$\dfrac{T_{oTE}}{T_{oin}}$	η_{ad} in→TE	η_p in→TE	ϵ_{LE}	ϵ_{TE}

SL	B-1 DEGREE	B-2 DEGREE	M-1	M-2	INCM DEGREE	DEV DEGREE	TURN DEGREE	D-FAC	OMEGA-B TOTAL	LOSS-P TOTAL	PO2/ PO1	PO/PO STAGE	TO/TO STAGE	%EFF-A TOT-STG	%EFF-P TOT-STG
	β_{LE}	β_{TE}	M_{LE}	M_{TE}	i_m	δ^o	$\Delta\beta$	D	$\bar\omega$	$\dfrac{\bar\omega \cos\beta_{TE}}{2\sigma}$	$\dfrac{P_{oTE}}{P_{oLE}}$	$\dfrac{P_{o3}}{P_{o1}}$	$\dfrac{T_{o3}}{T_{o1}}$	$\eta_{ad1\to3}$	$\eta_{p1\to3}$

SL	V-1 FT/SEC	V-2 FT/SEC	VM-1 FT/SEC	VM-2 FT/SEC	VØ-1 FT/SEC	VØ-2 FT/SEC	RHOVM-1 LBM/FT2SEC	RHOVM-2 LBM/FT2SEC	PCT TE SPAN	TO/TO INLET	%EFF-A TOT-INLET	%EFF-P TOT-INLET	EPSI-1 DEGREE	EPSI-2 DEGREE
	V_{LE}	V_{TE}	V_{mLE}	V_{mTE}	$V_{\theta LE}$	$V_{\theta TE}$	ρV_{mLE}	ρV_{mTE}	% Span TE	$\dfrac{T_{oTE}}{T_{oin}}$	η_{ad} in→TE	η_p in→TE	ϵ_{LE}	ϵ_{TE}

NCORR INLET RPM	WCORR INLET LBM/SEC	WCORR INLET KG/SEC		TO/TO INLET	PO/PO INLET	EFF-AD INLET %	EFF-P INLET %		TO/TO STAGE	PO2/PO1	PO/PO STAGE	EFF-AD STAGE %	EFF-P STAGE %
$\dfrac{N}{\sqrt{\theta_1}}$	$\dfrac{W\sqrt{\theta_1}}{\delta_1}$	$\dfrac{W\sqrt{\theta_1}}{\delta_1}$		$\dfrac{T_{oTE}}{T_{oin}}$	$\dfrac{P_{oTE}}{P_{oin}}$	η_{ad} in→TE	η_p in→TE		$\dfrac{T_{o3}}{T_{o1}}$	$\dfrac{P_{oTE}}{P_{oLE}}$	$\dfrac{P_{o3}}{P_{o1}}$	$\eta_{ad1\to3}$	$\eta_{p1\to3}$

APPENDIX B

MATERIAL EQUIVALENCY

APPENDIX B

MATERIAL EQUIVALENCY

PWA 92   Waspalloy (AMS 7471)

PWA 96   Inconel 718

PWA 1003   Incoloy 901 (AMS 5660, 5661)

PWA 1010   Inconel 718 (AMS 5663)

PWA 1099   Modified IN-100 Alloy (formerly MERL 76)

PWA 1202   Titanium (8AL-1MO-1V), (AMS 4933)

PWA 1209   Titanium (6AL-2SN-4ZR-2MO), (AMS 4976)

PWA 1214   Titanium (6AL-2SN-4ZR-2MO)
                High Creep Strength

PWA 1224   Titanium (6AL-2SN-4ZR-2MO)
                Forged Below Beta Transus

PWA 1225   Titanium (6AL-2SN-4ZR-2MO)
                Forged Above Beta Transus

PWA 1226   Titanium (6AL-2SN-4ZR-2MO)
                Forged, Beta Annealed, Precipitation Heat-Treated

PWA 1262   Titanium (6AL-4V), (AMS 4935)
                Cast

MERL 76   Now PWA 1099 (see above)

MERL 80   Modified IN-100 (Improved form of PWA 1099)

REFERENCES

1. "Energy Efficient Engine - Flight Propulsion System Preliminary Analysis and Design Report," NASA CR-159487, April, 1979.

2. "Energy Efficient Engine - Fan Component Detailed Design Report," NASA CR-165466, September, 1981.

3. "Energy Efficient Engine - Combustor Test Hardware, Detailed Design Report," NASA CR-167945, March, 1982.

NASA Scientific and Technical
   Information Facility
P. O. Box 8757
B.W.I. Airport, MD 21240

NASA Headquarters
Attn: R/R. Rosen
600 Independence Avenue, S.W.
Washington, D.C. 20564

NASA Headquarters
Attn: RJ/C. Rosen
600 Independence Avenue, S.W.
Washington, D.C. 20564

NASA Headquarters
Attn: RP/E. Gabris
600 Independence Avenue, S.W.
Washington, D.C. 20564

NASA Headquarters
Attn: RP/J. Facey
600 Independence Avenue, S.W.
Washington, D.C. 20564

NASA-Lewis Research Center
Attn: Werner R. Britsch, MS 86-4
21000 Brookpark Road
Cleveland, OH 44135   (10 copies)

NASA-Lewis Research Center
Attn: J. A. Ziemianski, MS 86-1
21000 Brookpark Road
Cleveland, OH 44135

NASA-Lewis Research Center
Attn: J. H. Rohde, MS 77-10
21000 Brookpark Road
Cleveland, OH 44135

NASA-Lewis Research Center
Attn: P. G. Batterton, MS 86-4
21000 Brookpark Road
Cleveland, OH 44135

NASA-Lewis Research Center
Attn: G. K. Sievers, MS 86-7
21000 Brookpark Road
Cleveland, OH 44135

NASA-Lewis Research Center
Attn: E. T. Meleason, MS 77-10
21000 Brookpark Road
Cleveland, OH 44135

NASA-Lewis Research Center
Attn: Report Control, MS 60-1
21000 Brookpark Road
Cleveland, OH 44135

NASA-Lewis Research Center
Attn: N. T. Saunders, MS 3-8
21000 Brookpark Road
Cleveland, OH 44135

NASA-Lewis Research Center
Attn: M. J. Hartmann, MS 3-7
21000 Brookpark Road
Cleveland, OH 44135

NASA-Lewis Research Center
Attn: J. C. Williams, MS 500-211
21000 Brookpark Road
Cleveland, OH 44135

NASA-Lewis Research Center
Attn: L. J. Kiraly, MS 23-3
21000 Brookpark Road
Cleveland, OH 44135

NASA-Lewis Research Center
Attn: D. C. Mikkelson, MS 6-12
21000 Brookpark Road
Cleveland, OH 44135

NASA-Lewis Research Center
Attn: R. Paginton, MS 500-305
21000 Brookpark Road
Cleveland, OH 44135

NASA-Lewis Research Center
Attn: R. H. Johns, MS 49-8
21000 Brookpark Road
Cleveland, OH 44135

NASA-Lewis Research Center
Attn: J. R. Mihaloew, MS 86-4
21000 Brookpark Road
Cleveland, OH 44135

NASA-Lewis Research Center
Attn: L. Reid, MS 5-3
21000 Brookpark Road
Cleveland, OH 44135

NASA-Lewis Research Center
Attn: R. W. Niedzwiecki, MS 77-6
21000 Brookpark Road
Cleveland, OH 44135

NASA-Lewis Research Center
Attn: AFSC Liaison Office, MS 501-3
21000 Brookpark Road
Cleveland, OH 44135

NASA-Lewis Research Center
Attn: Army R&T Propulsion, MS 77-12
21000 Brookpark Road
Cleveland, OH 44135

NASA Ames Research Center
Attn: M. H. Waters, MS 202-7
      (2 copies)
Moffett Field, CA 94035

NASA Dryden Flight Research Center
Attn: J. A. Albers
P. O. Box 273
Edwards, CA 93523

NASA Langley Research Center
Attn: Bob James, MS 258
      (2 copies)
Hampton, VA 23665-5225

Department of Defense
Attn: D. M. Dix
      3D1089/Pentagon
Washington, D.C. 20301-3080

Wright-Patterson Air Force Base
Attn: APL Chief Scientist, AFWAL/PS
Dayton, OH 45433

Wright-Patterson Air Force Base
Attn: E. E. Abell, ASD/YZE
Dayton, OH 45433

Wright-Patterson Air Force Base
Attn: H. I. Bush, AFWAL/POT
Dayton, OH 45433

Wright-Patterson Air Force Base
Attn: R. P. Carmichael, ASD/XRHI
Dayton, OH 45433

Wright-Patterson Air Force Base
Attn: R. Ellis, ASD/YZN
Dayton, OH 45433

Wright-Patterson Air Force Base
Attn: W. H. Austin, Jr., ASD/ENF
Dayton, OH 45433

Eustis Directorate
U.S. Army Air Mobility, R&D Lab.
Attn: J. Lane, SAVDL-EU-Tapp
Fort Eustis, VA 23604

Navy Department
Naval Air Systems Command
Attn: W. Koven, AIR-03E
Washington, D.C. 20361

Navy Department
Naval Air Systems Command
Attn: J. L. Byers, AIR-53602
Washington, D.C. 20361

Navy Department
Naval Air Systems Command
Attn: E. A. Lichtman, AIR-330E
Washington, D.C. 20361

Navy Department
Naval Air Systems Command
Attn: G. Derderian, AIR-5362C
Washington, D.C. 20361

Naval Air Propulsion Test Center
Attn: J. J. Curry
Trenton, NJ 08628

Naval Air Propulsion Test Center
Attn: A. Cifone
Trenton, NJ 08628

USAVRAD Command
Attn: Robert M. Titus (ASTIO)
P. O. Box 209
St. Louis, MO 63166

Department of Transportation
NASA/DOT Joint Office of Noise Abatement
Attn: C. Foster
Washington, D.C.   20590

Federal Aviation Administration
Noise Abatement Division
Attn: E. Sellman, AEE-120
Washington, D.C.   20590

Federal Aviation Administration
Attn: Jack A. Sain, ANE-200
12 New England Executive Park
Burlington, MA 18083

Curtiss Wright Corporation
Attn: S. Lombardo
Woodridge, NJ   07075

Curtiss Wright Corporation
Attn: S. Moskowitz
Woodridge, NJ   07075

Detroit Diesel, Allison Div., GMC
Attn: D. Quick
P. O. Box 894
Indianapolis, IN   46206

AVCO/Lycoming
Attn: H. Moellmann
550 S. Main Street
Stratford, CT   06497

The Garrett Corporation
AiResearch Manufacturing Co.
Attn: F. E. Faulkner
Torrance, CA   90509

The Garrett Corporation
AiResearch Manufacturing Co.
Attn: M. L. Early
402 South 36 Street
Phoeniz, AZ   85034

AiResearch Manufacturing Co.
Attn: C. E. Corrigan (93-120/503-4F)
111 South 34th Street
P. O. Box 5217
Phoeniz, AZ   85010

UTC/Pratt & Whitney
Attn: B. A. Jones, MS 713-11
P. O. Box 109600
West Palm Beach, FL   23410-9600

UTC/Pratt & Whitney
Attn: D. Gray, MS 118-26
Main Street
East Hartford, CT   06108

Williams Research Co.
Attn: Library
2280 W. Maple Road
Walled Lake, MI   48088

Lockheed-California Co.
Attn: R. Tullis, Dept. 75-21
Burbank, CA   91502

Lockheed-California Co.
Attn: J. F. Stroud, Dept. 75-42
Burbank, CA   91502

Williams Research Co.
Attn: R. Van Nimwegen
2280 W. Maple Road
Walled Lake, MI   48088

Williams Research Co.
Attn: R. Horn
2280 W. Maple Road
Walled Lake, MI   48088

General Electric Company/AEG
Attn: R. E. Neitzel
1000 Western Avenue
Lynn, MA   01910

General Electric Company/AEG
Attn: R. W. Bucy   (3 copies)
One Neumann Way
P. O. Box 15631
Cincinnati, OH   45215

General Electric Company/AEG
Attn: T. F. Donahue
One Neumann Way
P. O. Box 15631
Cincinnati, OH   45215

232

Douglas Aircraft Company
McDonnell Douglas Corporation
Attn: R. T. Kawai, Code 36-41
3855 Lakewood Blvd.
Long Beach, CA 90846

Boeing Commercial Airplane Co.
Attn: P. E. Johnson, MS 9H-46
P. O. Box 3707
Seattle, WA 98124

Teledyne CAE, Turbine Engines
Attn: E. Benstein
1330 Laskey Road
Toledo, OH 43612

Drexel University
College of Engineering
Attn: A. M. Mellor
Philadelphia, PA 19104

Douglas Aircraft Company
McDonnell Douglas Corporation
Attn: M. Klotzsche
3855 Lakewood Blvd.
Long Beach, CA 90846

Boeing Commercial Airplane Co.
Attn: D. C. Nordstrom, MS 73-4F
P. O. Box 3707
Seattle, WA 98124

Brunswick Corporation
Attn: A. Erickson
2000 Brunswick Lane
Deland, FL 32720